

SKIN EFFECT IN LARGE BI-MEDIA POWER CONDUCTORS

by

Cory James Liu

A dissertation submitted to the faculty of
The University of North Carolina at Charlotte
in partial fulfillment of the requirements
for the degree of Doctor of Philosophy in
Electrical Engineering

Charlotte

2016

Approved by:

Dr. Valentina Cecchi

Dr. Sherif Kamel

Dr. Zia Salami

Dr. Deborah Sharer

ABSTRACT

CORY JAMES LIU. Skin effect in large bi-media power conductors (Under the direction of DR. VALENTINA CECCHI and DR. SHERIF KAMEL)

This dissertation work presents the development of a novel closed-form mathematical solution for calculating AC resistance in conductors of two different media using current density. Current density is non-uniform under AC current, and is directly responsible for the increase in AC over DC resistance of a conductor. Therefore, a solution is presented using the current density distribution under AC operation. This solution is then expanded to a conductor using two different media. Results using the obtained closed-form solution are validated against the solution using multiphysics finite element analysis (FEA). These theoretical results are then confirmed with laboratory measurements. Optimized bi-media conductor designs are determined by solving the AC current density equations and selecting the appropriate media proportion to minimize conductor AC resistance. These optimized designs are evaluated against all types of existing large segmented copper power conductors of equal AC resistance and shown to reduce cost and weight. Additionally, an extensive analysis is presented such that cost ratios of the two media can be used to determine cost effectiveness. Finally, given the complexity of the analytical solution, simplified calculation methods are proposed that demonstrate the practicality of their implementation.

DEDICATION

This work is dedicated to my loving parents and wife, whose own desires to spread knowledge has inspired me and shaped my life. I hope the research herein is able to teach others some small fraction of what your guidance has helped me learn in life. You have always been the greatest supporters of my academic pursuits, and your nurturing of my scientific spirit made this research possible. Thank you, with all my heart.

ACKNOWLEDGEMENTS

I would like to thank all my committee members for their dedication of time and the invaluable feedback provided that helped guide the content of this material. This body of work has been made possible thanks to my co-advisors, Dr. Valentina Cecchi and Dr. Sherif Kamel, whom I am honored to have been working under and will be eternally grateful to have learned so much from. I would also like to thank Copperweld® for their donation of a copper-clad aluminum conductor for laboratory measurements. Finally, a very special thank you goes to Southwire® management for their moral and financial support, as well as all employees involved in production of both test samples, which would not have been possible without their dedication and support to the development of this technology.

TABLE OF CONTENTS

LIST OF FIGURES	ix
LIST OF TABLES	xv
LIST OF SYMBOLS	xix
LIST OF ABBREVIATIONS	xxiv
CHAPTER 1: INTRODUCTION	1
1.1 Overview	1
1.2 Background and Motivation	1
1.3 Prior Work	7
1.3.1 Historical Overview	7
1.3.2 Current Research	8
1.4 Dissertation Overview and Organization	11
CHAPTER 2: BACKGROUND	14
2.1 Overview	14
2.2 Vector Calculus	14
2.3 Field Theory	18
2.4 Maxwell's Equations	21
2.5 Bessel Functions	24
2.6 DC & AC Resistance	28
2.7 Industry Practices	39
CHAPTER 3: PROBLEM STATEMENT	49
3.1 Overview	49
3.2 Research Questions and Hypothesis	49

3.3 Modeling Assumptions	56
3.4 Research/Verification	58
CHAPTER 4: PROPOSED MODEL DEVELOPMENT	72
4.1 Overview	72
4.2 AC Resistance Analytical Solution	72
4.3 Theoretical Validation and Analysis	80
CHAPTER 5: EXPERIMENTAL VALIDATION	94
5.1 Overview	94
5.2 AC Resistance Laboratory Testing	94
5.2.1 Test Setup	99
5.2.2 Cable Samples	104
5.2.3 Experiment Results	121
5.2.4 Summary of Results and Observations	134
CHAPTER 6: INDUSTRY APPLICATION	138
6.1 Overview	138
6.2 Standardized Sizes	141
6.3 Replacement of Segmented Conductors	165
6.4 Simplified Equations	237
6.5 Selection Methodology	250
CHAPTER 7: CONCLUSIONS	267
7.1 Overview	267
7.2 Summary of Contributions	267
7.3 Future Vision	269

REFERENCES	273
APPENDIX A: MATLAB CODE	283

LIST OF FIGURES

FIGURE 1-1: Stranded (left) and segmented (right) conductors	9
FIGURE 2-1: Cylindrical coordinates	15
FIGURE 2-2: 2D (left) and 3D (right) surfaces	16
FIGURE 2-3: Gradient (left), curl (middle), and divergence (right)	17
FIGURE 2-4: Bessel function (first kind, zero order)	25
FIGURE 2-5: Proximity effect	29
FIGURE 2-6: Skin effect	31
FIGURE 2-7: Skin depth vs frequency	35
FIGURE 2-8: EM wave in single medium	36
FIGURE 2-9: Conductor type by diameter and area	46
FIGURE 2-10: AC/DC resistance ratios	47
FIGURE 3-1: Separated Bessel functions of the first kind	59
FIGURE 3-2: Separated Kelvin functions of the first kind	60
FIGURE 3-3: Comparison of zero order Bessel functions (1 st and 2 nd kinds)	61
FIGURE 3-4: Comparison of zero order Bessel functions (3 rd kind)	61
FIGURE 3-5: Comparison of first order Bessel functions (1 st and 2 nd kinds)	62
FIGURE 3-6: Comparison of first order Bessel functions (3 rd kind)	63
FIGURE 3-7: Scaled current density magnitudes	64
FIGURE 3-8: Bessel function input argument vs conductor radius	66
FIGURE 3-9: AC/DC resistance using Bessel input argument	67
FIGURE 3-10: AC/DC inductance using Bessel input argument	67
FIGURE 3-11: Actual vs approximated resistance ratios (solid round)	68

FIGURE 3-12: Actual vs approximated resistance ratios (solid round tube)	69
FIGURE 4-1: Suppressed vs unsuppressed current density	73
FIGURE 4-2: Bi-media EM wave boundary condition	76
FIGURE 4-3: Bi-media suppress vs unsuppressed volume	78
FIGURE 4-4: Current density in various solid copper conductor sizes	80
FIGURE 4-5: Current density in bi-media conductors	82
FIGURE 4-6: Resistance in bi-media conductors	83
FIGURE 4-7: Skin effect in bi-media conductors	84
FIGURE 4-8: Inductance ratio in bi-media conductors	85
FIGURE 4-9: Current density in optimal bi-media conductors	87
FIGURE 4-10: DC Resistance in various radii AL / CU conductors	88
FIGURE 4-11: AC Resistance in various radii AL / CU conductors	89
FIGURE 4-12: Skin effect in various radii AL / CU conductors	90
FIGURE 4-13: DC resistance in various radii CU / AL conductors	91
FIGURE 4-14: AC resistance in various radii CU / AL conductors	92
FIGURE 4-15: Skin effect in various radii CU / AL conductors	93
FIGURE 5-1: General AC resistance measurement test setup	97
FIGURE 5-2: Detailed AC resistance measurement test setup	100
FIGURE 5-3: Picture of AC resistance measurement test setup	101
FIGURE 5-4: Circuit diagram of AC resistance measurement test setup	101
FIGURE 5-5: Sampling rate versus frequency	103
FIGURE 5-6: Sampling rate versus frequency (zoomed view)	104
FIGURE 5-7: Picture of CCA test sample	107

FIGURE 5-8: Calculated current density in CCA conductor	108
FIGURE 5-9: AC/DC resistance ratio in CCA conductor	109
FIGURE 5-10: AC/DC resistance ratio in CCA vs all AL conductor	111
FIGURE 5-11: AC resistance in CCA conductor	112
FIGURE 5-12: Picture of post-stranding DC resistance measurement setup	115
FIGURE 5-13: Picture of 2570 mm ² bi-media conductor	116
FIGURE 5-14: Calculated current density in 2570 mm ² bi-media conductor	117
FIGURE 5-15: AC/DC resistance ratio in 2570 mm ² bi-media conductor	118
FIGURE 5-16: R_{ac} / R_{dc} in 2570 mm ² bi-media vs all AL conductor	119
FIGURE 5-17: AC resistance in 2570 mm ² bi-media conductor	120
FIGURE 5-18: Equipment test setup of CCA conductor	122
FIGURE 5-19: Cable test setup of CCA conductor	123
FIGURE 5-20: AC/DC resistance ratios measured on CCA conductor	125
FIGURE 5-21: AC resistance measured on CCA conductor	126
FIGURE 5-22: Equipment test setup of 2570 mm ² conductor (steel reel)	128
FIGURE 5-23: AC/DC resistance ratios of 2570 mm ² conductor (steel reel)	129
FIGURE 5-24: AC resistance measured on 2570 mm ² conductor (steel reel)	130
FIGURE 5-25: Equipment test setup of 2570 mm ² conductor (wood reel)	131
FIGURE 5-26: AC/DC resistance ratios of 2570 mm ² conductor (wood reel)	132
FIGURE 5-27: AC resistance measured on 2570 mm ² conductor (wood reel)	134
FIGURE 6-1: Optimal radii (90°C, 60 Hz)	142
FIGURE 6-2: Optimal area (90°C, 60 Hz)	143
FIGURE 6-3: AC and DC resistance of optimal Air / CU conductors (90°C, 60 Hz)	144

FIGURE 6-4: AC and DC resistance of optimal AL / CU conductors (90°C, 60 Hz)	145
FIGURE 6-5: Optimal radii (105°C, 60 Hz)	146
FIGURE 6-6: Optimal area (105°C, 60 Hz)	147
FIGURE 6-7: AC and DC resistance of optimal Air / CU conductors (105°C, 60 Hz)	148
FIGURE 6-8: AC and DC resistance of optimal AL / CU conductors (105°C, 60 Hz)	149
FIGURE 6-9: Optimal radii (90°C, 50 Hz)	150
FIGURE 6-10: Optimal area (90°C, 50 Hz)	151
FIGURE 6-11: AC and DC resistance of optimal Air / CU conductors (90°C, 50 Hz)	152
FIGURE 6-12: AC and DC resistance of optimal AL / CU conductors (90°C, 50 Hz)	153
FIGURE 6-13: Optimal radii (105°C, 50 Hz)	154
FIGURE 6-14: Optimal area (105°C, 50 Hz)	155
FIGURE 6-15: AC and DC resistance of optimal Air / CU conductors (105°C, 50 Hz)	156
FIGURE 6-16: AC and DC resistance of optimal AL / CU conductors (105°C, 50 Hz)	157
FIGURE 6-17: Compaction Ratio of Stranded Conductors	163
FIGURE 6-18: Weight of Air / CU ($k_s=0.8$) vs segmented CU	169
FIGURE 6-19: Weight of Air / CU vs segmented CU (enamel = 0%)	170
FIGURE 6-20: “Effective” weight of Air / CU vs segmented CU (enamel = 30%)	172
FIGURE 6-21: Weight of Air / CU vs segmented CU ($k_s=0.8$)	173
FIGURE 6-22: “Effective” weight of Air / CU vs enameled CU ($k_s=0.35$)	174
FIGURE 6-23: “Effective” weight of AL / CU vs segmented CU (enamel = 0%)	176
FIGURE 6-24: “Effective” weight of AL / CU vs segmented CU (enamel = 30%)	177
FIGURE 6-25: “Effective” weight of AL / CU vs segmented CU ($k_s=0.8$)	178
FIGURE 6-26: “Effective” weight of AL / CU vs enameled CU ($k_s=0.35$)	179

FIGURE 6-27: Areas and weights of Air / CU conductors ($k_s=0.8$, 90°C, 60 Hz)	180
FIGURE 6-28: Areas and weights of Air / CU conductors ($k_s=0.8$, 105°C, 60 Hz)	181
FIGURE 6-29: Areas and weights of Air / CU conductors ($k_s=0.8$, 90°C, 50 Hz)	181
FIGURE 6-30: Areas and weights of Air / CU conductors ($k_s=0.8$, 105°C, 50 Hz)	182
FIGURE 6-31: Areas and weights of Air / CU conductors ($k_s=0.62$, 90°C, 60 Hz)	182
FIGURE 6-32: Areas and weights of Air / CU conductors ($k_s=0.62$, 105°C, 60 Hz)	183
FIGURE 6-33: Areas and weights of Air / CU conductors ($k_s=0.62$, 90°C, 50 Hz)	183
FIGURE 6-34: Areas and weights of Air / CU conductors ($k_s=0.62$, 105°C, 50 Hz)	184
FIGURE 6-35: Areas and weights of Air / CU conductors ($k_s=0.435$, 90°C, 60 Hz)	184
FIGURE 6-36: Areas and weights of Air / CU conductors ($k_s=0.435$, 105°C, 60 Hz)	185
FIGURE 6-37: Areas and weights of Air / CU conductors ($k_s=0.435$, 90°C, 50 Hz)	186
FIGURE 6-38: Areas and weights of Air / CU conductors ($k_s=0.435$, 105°C, 50 Hz)	186
FIGURE 6-39: Areas and weights of Air / CU conductors ($k_s=0.35$, 90°C, 60 Hz)	187
FIGURE 6-40: Areas and weights of Air / CU conductors ($k_s=0.35$, 105°C, 60 Hz)	188
FIGURE 6-41: Areas and weights of Air / CU conductors ($k_s=0.35$, 90°C, 50 Hz)	188
FIGURE 6-42: Areas and weights of Air / CU conductors ($k_s=0.35$, 105°C, 50 Hz)	189
FIGURE 6-43: Areas and weights of AL / CU conductors ($k_s=0.8$, 90°C, 60 Hz)	190
FIGURE 6-44: Areas and weights of AL / CU conductors ($k_s=0.8$, 105°C, 60 Hz)	191
FIGURE 6-45: Areas and weights of AL / CU conductors ($k_s=0.8$, 90°C, 50 Hz)	191
FIGURE 6-46: Areas and weights of AL / CU conductors ($k_s=0.8$, 105°C, 50 Hz)	192
FIGURE 6-47: Areas and weights of AL / CU conductors ($k_s=0.62$, 90°C, 60 Hz)	192
FIGURE 6-48: Areas and weights of AL / CU conductors ($k_s=0.62$, 105°C, 60 Hz)	193
FIGURE 6-49: Areas and weights of AL / CU conductors ($k_s=0.62$, 90°C, 50 Hz)	193

FIGURE 6-50: Areas and weights of AL / CU conductors ($k_s=0.62$, 105°C, 50 Hz)	194
FIGURE 6-51: Areas and weights of AL / CU conductors ($k_s=0.435$, 90°C, 60 Hz)	194
FIGURE 6-52: Areas and weights of AL / CU conductors ($k_s=0.435$, 105°C, 60 Hz)	195
FIGURE 6-53: Areas and weights of AL / CU conductors ($k_s=0.435$, 90°C, 50 Hz)	196
FIGURE 6-54: Areas and weights of AL / CU conductors ($k_s=0.435$, 105°C, 50 Hz)	196
FIGURE 6-55: Areas and weights of AL / CU conductors ($k_s=0.35$, 90°C, 60 Hz)	197
FIGURE 6-56: Areas and weights of AL / CU conductors ($k_s=0.35$, 105°C, 60 Hz)	198
FIGURE 6-57: Areas and weights of AL / CU conductors ($k_s=0.35$, 90°C, 50 Hz)	198
FIGURE 6-58: Areas and weights of AL / CU conductors ($k_s=0.35$, 105°C, 50 Hz)	199
FIGURE 6-59: Average Change in Radius for Stranded Segmented vs Bi-Media	237
FIGURE 6-60: Input argument cross-sectional area vs temperature	241
FIGURE 6-61: Skin effect in bi-media conductors (90°C, 60 Hz)	243
FIGURE 6-62: Skin effect in bi-media conductors (105°C, 60 Hz)	243
FIGURE 6-63: Skin effect in bi-media conductors (90°C, 50 Hz)	244
FIGURE 6-64: Skin effect in bi-media conductors (105°C, 50 Hz)	244
FIGURE 6-65: Error in Air / CU area estimation	247
FIGURE 6-66: Error in AL / CU area estimation	249

LIST OF TABLES

TABLE 2-1: Field theory parameters	20
TABLE 2-2: Circuit theory parameters	21
TABLE 2-3: Maxwell's equations	24
TABLE 2-4: Boundary conditions	24
TABLE 2-5: Comparison of copper and aluminum	40
TABLE 2-6: Nominal vs actual conductor areas	41
TABLE 2-7: IEC 60287-1-1 k_s and k_p factors	42
TABLE 3-1: Skin depth at various frequencies	65
TABLE 5-1: CCA conductor certificate of compliance	106
TABLE 5-2: CCA conductor data	106
TABLE 5-3: Skin effect in CCA conductor	110
TABLE 5-4: 2570 mm ² bi-media conductor dimensions	114
TABLE 5-5: Skin effect in 2570 mm ² bi-media conductor	118
TABLE 5-6: Error in AC/DC resistance ratios measured on CCA conductor	126
TABLE 5-7: Error in AC/DC resistance ratios of 2570 mm ² conductor (steel reel)	130
TABLE 5-8: Error in AC/DC resistance ratios of 2570 mm ² conductor (wood reel)	133
TABLE 6-1: Standardized designs (90°C, 60 Hz)	158
TABLE 6-2: Standardized designs (105°C, 60 Hz)	159
TABLE 6-3: Standardized designs (90°C, 50 Hz)	160
TABLE 6-4: Standardized designs (105°C, 50 Hz)	161
TABLE 6-5: Compaction Ratio of Stranded Conductors	162
TABLE 6-6: Stranded Radii and AC Resistance of Standardized Bi-Media (60 Hz)	164

TABLE 6-7: Stranded Radii and AC Resistance of Standardized Bi-Media (50 Hz)	165
TABLE 6-8: Percent of enameled wires in segmented conductors	166
TABLE 6-9: Conductor data of equal R_{ac} conductors ($k_s=0.8$, 90°C, 60 Hz)	202
TABLE 6-10: Conductor data of equal R_{ac} conductors ($k_s=0.8$, 105°C, 60 Hz)	203
TABLE 6-11: Conductor data of equal R_{ac} conductors ($k_s=0.8$, 90°C, 50 Hz)	204
TABLE 6-12: Conductor data of equal R_{ac} conductors ($k_s=0.8$, 105°C, 50 Hz)	205
TABLE 6-13: Conductor data of equal R_{ac} conductors ($k_s=0.62$, 90°C, 60 Hz)	206
TABLE 6-14: Conductor data of equal R_{ac} conductors ($k_s=0.62$, 105°C, 60 Hz)	207
TABLE 6-15: Conductor data of equal R_{ac} conductors ($k_s=0.62$, 90°C, 50 Hz)	208
TABLE 6-16: Conductor data of equal R_{ac} conductors ($k_s=0.62$, 105°C, 50 Hz)	209
TABLE 6-17: Conductor data of equal R_{ac} conductors ($k_s=0.435$, 90°C, 60 Hz)	210
TABLE 6-18: Conductor data of equal R_{ac} conductors ($k_s=0.435$, 105°C, 60 Hz)	211
TABLE 6-19: Conductor data of equal R_{ac} conductors ($k_s=0.435$, 90°C, 50 Hz)	212
TABLE 6-20: Conductor data of equal R_{ac} conductors ($k_s=0.435$, 105°C, 50 Hz)	213
TABLE 6-21: Conductor data of equal R_{ac} conductors ($k_s=0.35$, 90°C, 60 Hz)	214
TABLE 6-22: Conductor data of equal R_{ac} conductors ($k_s=0.35$, 105°C, 60 Hz)	215
TABLE 6-23: Conductor data of equal R_{ac} conductors ($k_s=0.35$, 90°C, 50 Hz)	216
TABLE 6-24: Conductor data of equal R_{ac} conductors ($k_s=0.35$, 105°C, 50 Hz)	217
TABLE 6-25: Cost effectiveness ($k_s=0.35$, 90°C, 60 Hz): enamel = 12–22%	218
TABLE 6-26: Cost effectiveness ($k_s=0.35$, 90°C, 60 Hz): enamel = 23–33%	219
TABLE 6-27: Cost effectiveness ($k_s=0.35$, 90°C, 60 Hz): enamel = 34–44%	220
TABLE 6-28: Cost effectiveness ($k_s=0.35$, 105°C, 60 Hz): enamel = 12–22%	221
TABLE 6-29: Cost effectiveness ($k_s=0.35$, 105°C, 60 Hz): enamel = 23–33%	222

TABLE 6-30: Cost effectiveness ($k_s=0.35$, 105°C, 60 Hz): enamel = 34–44%	223
TABLE 6-31: Cost effectiveness ($k_s=0.35$, 90°C, 50 Hz): enamel = 12–22%	224
TABLE 6-32: Cost effectiveness ($k_s=0.35$, 90°C, 50 Hz): enamel = 23–33%	225
TABLE 6-33: Cost effectiveness ($k_s=0.35$, 90°C, 50 Hz): enamel = 34–44%	226
TABLE 6-34: Cost effectiveness ($k_s=0.35$, 105°C, 50 Hz): enamel = 12–22%	227
TABLE 6-35: Cost effectiveness ($k_s=0.35$, 105°C, 50 Hz): enamel = 23–33%	228
TABLE 6-36: Cost effectiveness ($k_s=0.35$, 105°C, 50 Hz): enamel = 34–44%	229
TABLE 6-37: Stranded Radii of Bi-Media Conductors ($k_s=0.8$)	232
TABLE 6-38: Stranded Radii of Bi-Media Conductors ($k_s=0.62$)	233
TABLE 6-39: Stranded Radii of Bi-Media Conductors ($k_s=0.435$)	234
TABLE 6-40: Stranded Radii of Bi-Media Conductors ($k_s=0.35$)	235
TABLE 6-41: Average Change in Radius for Stranded Segmented vs Bi-Media	236
TABLE 6-42: Input argument cross-sectional area vs temperature	241
TABLE 6-43: Minimum recommended area for AL / CU polynomial equations	247
TABLE 6-44: Minimum recommended area for Air / CU polynomial equations	250
TABLE 6-45: Cost deltas of bi-media designs (60 Hz, 90°C, $k_s=0.8$)	251
TABLE 6-46: Cost deltas of bi-media designs (60 Hz, 105°C, $k_s=0.8$)	251
TABLE 6-47: Cost deltas of bi-media designs (50 Hz, 90°C, $k_s=0.8$)	252
TABLE 6-48: Cost deltas of bi-media designs (50 Hz, 105°C, $k_s=0.8$)	252
TABLE 6-49: Cost deltas of bi-media designs (60 Hz, 90°C, $k_s=0.62$)	252
TABLE 6-50: Cost deltas of bi-media designs (60 Hz, 105°C, $k_s=0.62$)	253
TABLE 6-51: Cost deltas of bi-media designs (50 Hz, 90°C, $k_s=0.62$)	253
TABLE 6-52: Cost deltas of bi-media designs (50 Hz, 105°C, $k_s=0.62$)	253

TABLE 6-53: Cost deltas of bi-media designs (60 Hz, 90°C, $k_s=0.435$)	254
TABLE 6-54: Cost deltas of bi-media designs (60 Hz, 105°C, $k_s=0.435$)	255
TABLE 6-55: Cost deltas of bi-media designs (50 Hz, 90°C, $k_s=0.435$)	255
TABLE 6-56: Cost deltas of bi-media designs (50 Hz, 105°C, $k_s=0.435$)	255
TABLE 6-57: Cost deltas of bi-media designs (60 Hz, 90°C, $k_s=0.35$)	256
TABLE 6-58: Cost deltas of bi-media designs (60 Hz, 105°C, $k_s=0.35$)	256
TABLE 6-59: Cost deltas of bi-media designs (50 Hz, 90°C, $k_s=0.35$)	257
TABLE 6-60: Cost deltas of bi-media designs (50 Hz, 105°C, $k_s=0.35$)	257
TABLE 6-61: Cost deltas summary table	258

LIST OF SYMBOLS

Symbol	Unit	Description
$\$Al$	\$/kg	Cost of aluminum
$\$Cu$	\$/kg	Cost of copper
α	-	Order of Bessel function
α_{20}	1/K	Temperature coefficient of electrical resistivity at 20°C (copper = 0.00403, aluminum = 0.00393)
A	m ²	Area
A_{Air}	mm ²	Air area in bi-media conductor
A_{AL}	mm ²	AL area in bi-media conductor
A_{CU}	mm ²	CU area in bi-media conductor
A_T	mm ²	Total area in bi-media conductor
B	T=Wb/m ²	Magnetic flux density
B_n	T=Wb/m ²	Normal magnetic flux density
ber	-	Real part of Bessel function
bei	-	Imaginary part of Bessel function
C	F	Capacitance
δ	m	Skin depth
d	-	Reflected wave factor
d_c	m	Conductor diameter
d'_c	m	OD of equal area solid tube with ID d_i
d_i	m	Inside diameter of conductor
D	C/m ²	Electric flux density

D_n	C/m ²	Normal electric flux density
ε	F/m	Permittivity
ε_0	F/m	Permittivity of free space (8.854187817 x 10 ⁻¹²)
ε_r	F/m	Relative permittivity
E	V/m	Electric field
E_t	V/m	Tangential electric field
E_r	V/m	Electric field, r-component
E_{r2}	V/m	Electric field at radius r ₂
E_φ	V/m	Electric field, φ -component
E_z	V/m	Electric field, z-component
f	Hz	Frequency
Γ	-	Gamma function
H	A/m	Magnetic field
H_t	A/m	Tangential magnetic field
H_α	-	Bessel function (first kind, α order)
i	-	Imaginary operator = $\sqrt{-1}$
I	A	Electric current
I_i	A	Electric current (instantaneous)
I_{ac}	A	AC electric current
I_{dc}	A	DC electric current
I_{enc}	A	Enclosed electric current
I_e	A	Electric current
I_m	V	Magnetic current

\mathbf{J}	A/m^2	Electric current density
\mathbf{J}_c	A/m^2	Conducting electric current density
\mathbf{J}_d	A/m^2	Displacement electric current density
\mathbf{J}_{dc}	A/m^2	DC electric current density
\mathbf{J}_r	A/m^2	Electric current density at radius r
\mathbf{J}_{r1}	A/m^2	Electric current density at radius r_1
\mathbf{J}_{r2}	A/m^2	Electric current density at radius r_2
J_α	-	Bessel function (first kind, α order)
ker	-	Real part of Kelvin function
kei	-	Imaginary part of Kelvin function
k_p	-	Proximity effect coefficient
k_s	-	Skin effect coefficient
l	m	Length
L	H	Inductance
L_{ac}	H	Inductance
m	m^{-1}	Bessel function argument
m_1	m^{-1}	Bessel function argument, medium 1
m_2	m^{-1}	Bessel function argument, medium 2
\mathbf{M}	V/m^2	Magnetic current density
\mathbf{M}_d	V/m^2	Displaced magnetic current density
ω	rad/s	Angular frequency ($2\pi f$)
P	W	Real power
φ	-	Angle around conductor

ψ	Wb	Flux of an inductor
q	C	Electric charge
r	m	Radius
r_1	m	Radius of inner medium (medium 1)
r_2	m	Radius of outer medium (medium 2)
R	Ω	Electrical resistance
R_0	Ω	DC electrical resistance @ 20°C
R_{dc}	Ω	DC electrical resistance
R_{ac}	Ω	AC electrical resistance
ρ	$\Omega \cdot m$	Electrical resistivity
ρ_e	C/m^3	Electric charge density
ρ_m	Wb/m^2	Magnetic charge density
s	m	Conductor spacing
σ	S/m	Electric conductivity
σ_1	S/m	Electric conductivity, medium 1
σ_2	S/m	Electric conductivity, medium 2
θ	°C	Operating temperature
t	s	Time
T	s	Time step
μ	H/m	Permeability
μ_1	H/m	Permeability, medium 1
μ_2	H/m	Permeability, medium 2
μ_0	H/m	Permeability of free space ($4\pi \times 10^{-7}$)

μ_r	H/m	Relative permeability
V	V	Voltage
V_i	V	Voltage (instantaneous)
V_{dc}	V	DC voltage
V_{ac}	V	AC voltage
W_{AlCu_Al}	kg/m	AL weight in AL / CU conductor per unit length
W_{AlCu_Cu}	kg/m	CU weight in AL / CU conductor per unit length
W_{S_Cu}	kg/m	CU weight in segmented copper conductor per unit length
x	-	x-coordinate
x_p	-	Bessel function argument to calculate proximity effect
x_s	-	Bessel function argument to calculate skin effect
X_{ac}	Ω	AC reactance
y	-	y-coordinate
y_p	-	Proximity effect factor
y_s	-	Skin effect factor
Y_α	-	Kelvin function (second kind, α order)
z	-	z-coordinate
Z_{ac}	Ω	AC impedance

LIST OF ABBREVIATIONS

AC	Alternating current
ACSR	Aluminum-conductor steel-reinforced
AL	Aluminum
AWG	American wire gauge
CBV	Copper by volume
CCA	Copper-clad aluminum
CD	Cost differential
CU	Copper
DC	Direct current
ECI	Enameling cost increase
EM	Electromagnetic
EMF	Electromotive force
FEA	Finite element analysis
ID	Inner diameter
KCL	Kirchhoff's current law
KVL	Kirchhoff's voltage law
OD	Outer diameter
OH	Overhead
PC	Personal computer
PDE	Partial differential equation
RMS	Root mean square
SCFF	Self-contained fluid-filled

CHAPTER 1: INTRODUCTION

1.1 Overview

This chapter introduces the phenomenon of increased resistance of a conductor operating under AC current as opposed to DC current. Although this phenomenon, referred to as skin effect, has long been understood for a few simple constructions, namely solid round conductors [1] and solid tube conductors [2], a mathematical solution for bi-media does not currently exist. Therefore, the background and motivation for development of an analytical solution using bi-media is discussed, a historical overview of the development of the two existing solutions is reviewed, and the research that followed these mathematical solutions is examined. During this literature review commentary is made on how the focus of past research and development has changed, up to current day ongoing research on this topic. The chapter concludes with an overview of the remaining body of this dissertation and how it is organized.

1.2 Background and Motivation

Currently, conductors rely on a single metal to carry the bulk of the current/power. Some special bi-media designs are used, however the intention is only to use one metal as the current carrying material and the other for desirable application driven properties. For example, in the power industry ACSR conductors use aluminum for its electrical conductivity and low weight in conjunction with steel for its mechanical strength [3]. Copper-clad aluminum (CCA) conductors use an aluminum layer over copper for its

corrosion resistance and electrical contact [4]. In fact, for ACSR conductors it can be assumed that all current is distributed solely in the aluminum part [5]. At higher frequencies, practically all of the current travels on a thin layer just below the surface of the conductor [6], and thus hollow conductors are typically used to reduce cost and weight in applications such as antenna design in microwave engineering. In power engineering some special hollow conductor designs exist. However, as discussed in later sections such designs use the hollow conductor core for application purposes and are not optimized to minimize AC resistance. Since the current travels mostly on the skin of the conductor the term “skin effect” is used to describe the effect of AC current [7]. Skin depth is a related characterizing term, which refers to the depth at which the current density is reduced to $1/e$, or approximately 37%, of the surface value [8]. Stated practically, this means that skin depth is the depth at which the uniform DC current density is equal to the exponentially distributed AC current density [9]. It also means that AC resistance can be found approximately using skin depth, since the AC resistance of a solid conductor is approximately equal to the DC resistance of an equivalent cross-sectional area solid tube conductor with thickness equal to the skin depth [10]. If the skin depth is greater than the conductor radius then AC and DC resistance are approximately equal. At 60 Hz, a 240 mm² copper conductor has a radius that is approximately equal to the skin depth; as a result, the increase in AC resistance from DC resistance is only about 1%. Although the AC current density in a conductor cannot be physically measured, it can be verified by the effects it produces, namely the excitation of external magnetic field [11]. Additionally, the magnetic field inside the conductor can also not be measured, however it is calculable outside the conductor using the Biot-Savart law [11].

At high frequencies the conductor diameter is typically orders of magnitude larger than the skin depth. This allows for the core to be removed at a certain point with negligible effect on AC resistance. For power frequencies, although removing the core causes a more uniform distribution of current density, the resulting AC resistance is still usually greater than a conductor with the core intact [12]. Even for applications at power frequencies, skin effect on small conductors cannot be ignored since mathematical models of intermittent earth faults must include the more pronounced skin effect occurring in the high frequency content found in real world disturbance recordings [13]. In fact, even DC cable conductors experience high frequency ripple currents from converters resulting in increased resistances due to the skin effect [14].

The power industry constantly pushes the boundaries of conductor sizes for higher power transmission capacity, resulting in higher AC/DC resistance ratios. This causes a decreasing return in conductor load capacity although more of the costly metal is being used. The increased resistance ratios at power frequencies over the range of conductor sizes can lead to as much as a twofold increase in effective resistance [15].

The key to formulating the mathematical solution for AC resistance is in understanding the current density behavior. DC current uniformly distributes current density over the entire cross-section of a conductor. Alternating current, however, increases the current density towards the surface of the conductor while reducing it away from the surface, due to the skin effect phenomenon [16]. This uneven current distribution reduces the effective cross-sectional area of the conductor, and thus increases resistance. Large power conductors are usually circular in shape, which facilitates the manufacturing process. Additionally, a circular conductor is ideal for having the lowest AC resistance

when compared to other solid shapes of equal cross-sectional area [17]. Since the current density under AC current is highest at the conductor surface and decreases exponentially with radial distance from the surface, it is more pronounced on larger diameter conductors. Skin depth decreases more rapidly for higher conductivity materials, higher permeability materials, and higher operating frequencies [8].

There are only two conductor shapes that have analytical solutions published in the literature: solid round conductors [1] and solid round hollow tubes [18]. It can further be shown that the solid round conductor is a special case of the solid round hollow tube conductor derivation [19]. However, conductors of any other shapes only have approximate solutions based on measurements and empirically derived equations. Previously, an attempt at deriving the skin effect in a laminated conductor (the application of a high conductivity material on a lower conductivity material, such that nearly all the current flows in the outer higher conductivity material) had been shown in [20], but results were incorrect due to the omission of the behavior of the electromagnetic (EM) wave between the two different media [21]. Besides studies resulting in simplified equations, researchers have also studied simplified mathematical models for skin effect. The simplified equations present polynomial formulas based on curve fitting that mimic the true solution but do not require Bessel functions and imaginary numbers. The simplified mathematical models use modelling techniques to approximate the skin effect phenomenon. Some such methods include modeling the conductor using lumped circuit parameters for an equivalent circuit [19] or solving the equations using Fourier transforms [22] [23]. Still, the Bessel function solution is the only true analytical solution. The

problem with the simplified equations and simplified mathematical models is that the accuracy of both of these approaches only holds true over a certain frequency range.

Aside from the more common method of solving for skin effect using Maxwell's equations in differential form, it has been shown that skin effect may also be solved in integral form [6]. Generally, Bessel functions in integral form are only used for solving boundary conditions, and have limited applications [24]. These solutions require the conducting medium be linear, isotropic, homogeneous, isothermal and non-ferrous. Although there can be a small radial temperature gradient that creates non-uniform radial current density, it is usually negligible [25]. However, this radial temperature gradient should be kept in mind for applications involving stranded conductors with large temperature gradients, such as overhead transmission, since radial thermal conductivity is only about one-hundredth the axial thermal conductivity [26]. It has been reported that in the most extreme conditions the conductor radial temperature gradient may be as high as 40°C at a core temperature of 200°C. However, a task force was formed to address this concern and it was found that while conductors routinely experience temperature gradients around 10% of their rating, the impact on AC resistance estimates is negligible [27]. The media must be assumed non-ferrous, otherwise they would become magnetized and hence not be independent of current [28]. It should be kept in mind that current may indirectly influence the skin effect due to heating, as the resistivity of metals is temperature dependent. Increased temperature increases material resistivity, which in turn increases the skin depth. This means that at higher temperature the skin effect of a conductor is lower [29].

The non-uniform AC current density distribution and resulting AC resistance is difficult to calculate even for symmetrical shapes due to the complexity of Bessel functions involved in the solution [30]. Bessel functions are the solutions of second-order differential equations governing the current density distribution in the conductor. Large conductors are often stranded to increase flexibility, which distorts the current density due to the reactance of the spirals [31]. However, it is only a small fraction of the skin effect and considered negligible [32]. Stranding conductors introduces more difficulties in finding analytical solutions, such as the asymmetric shape of the conductor, non-regular strand distribution and elliptical shape of the strands [33]. Because of the complexity of calculating AC/DC resistance ratios using Bessel functions in analytical solutions, much literature has focused on proposing simplified equations [34] [35] [2] [36] [18] [37] [38] [5] [23] or using PCs to iteratively solve the problem [39]. The simplified equations often either focus on low or high frequencies, as the skin effect becomes asymptotic. At low frequencies, such as power frequencies, the skin effect is inversely proportional to the square of the radius; at high frequencies, it becomes inversely proportional to the radius alone [6]. Because analytical solutions do not exist for non-symmetric shapes, including stranded designs, some researchers have focused on proposing test methodologies [40] [41] [42] [43] and verifying the results [44] [45] [46]. Experimental data has shown that the AC/DC resistance ratio of a stranded conductor is approximately equal to that of a solid conductor having the same cross-sectional area, with negligible error [31] [32].

Before delving into the physics of why AC resistance is greater than DC resistance it is important to understand the history of how the existing closed-form solutions for the solid round conductor and solid round hollow tube conductor were derived. Studies of skin

effect go back over a century and mathematics for all but these two most simple geometries remains a mystery.

1.3 Prior Work

The first part of this section reviews the historical development of the two existing closed-form solutions: a solid round conductor and a solid tube conductor. This includes the work done by others to verify these solutions. The second part of this section discusses the work done after these solutions were developed and verified, all the way up to current-day ongoing research activities.

1.3.1 Historical Overview

There are many good resources that detail the historical development of the closed-form solution of AC resistance in a solid round wire [6] [16]. James Clerk Maxwell was the first to begin investigation on why resistance and inductance varied on a wire due to a change in the frequency of the applied voltage and current. Dating back to 1873, Maxwell understood that the current density was not uniform under AC conditions, as it was under DC conditions. In his treatise [1] he detailed this effect in writing “when the current in a wire is of varying intensity (time dependent), the electromotive force arising from the induction of the current on itself is different in different parts of the section of a wire, being in general a function of the distance from the axis of the wire as well as of time...the current will not be the same at different distances from the axis of the cylinder.” Maxwell’s treatise in its current form underwent two posthumous reviews, which is why it now presents a fully developed solution in terms of Bessel functions [47]. However, Maxwell did not fully understand the mathematics of the phenomena at the time of the original authorship.

A group of British scientists, known as the Maxwellians, were responsible for the development of the solution as we know it today. In particular, George Francis Fitzgerald, Oliver Lodge, and Oliver Heaviside formulated the solution by the end of the 19th century [48] [49] [50] [51] [52] [53]. Also involved, was Lord Rayleigh who refined Maxwell's model for time-harmonic sources [54]. Lord Rayleigh also produced equations approximating AC resistance and internal inductance at high frequencies. These results were confirmed through work by Heaviside [55] [56] and solved in terms of Bessel functions by Lord Kelvin across all frequencies [57]. Additionally, Heaviside first developed the solution for solid round tube conductors [58] [59]. Due to the impracticality of solving complex valued Bessel functions by hand, tabulated values were commonly used at the time. The values were given by Lord Kelvin for the real and imaginary parts of the Bessel function [57] [60] [61]. Due to equipment limitations, these results could not be accurately verified until sources of high-frequency AC current became available. This was first done at the Massachusetts Institute of Technology (MIT) in 1915 by Arthur Kennelly [31]. Using rotating machines to generate AC currents up to 100 kHz and a Heaviside bridge, the professor of electrical engineering was able to confirm the closed-form solution of both the solid round and solid round tube conductors. The work of Kennelly was also able to confirm that stranded conductors manufactured with strands that were not twisted had the same AC/DC resistance ratios as solid conductors having the same cross-sectional areas. Additionally, if the conductors were stranded with helically applied strands, the same is approximately true with negligible error. These results of helically stranded conductors were later verified by John Zaborszky in 1953 [32].

1.3.2 Current Research

Following the development of the closed-form solutions for AC resistance of solid round and solid round tube conductors, the research activities have encompassed three main areas: design, measurement, and approximation. The goal in design of conductors is to mitigate skin effect. How this is done is dependent on the frequency range of the application. At low/power frequencies, special designs have not always been necessary. However, throughout history power demands have continuously increased, giving rise to larger and larger cross-sectional area conductors. When the conductors became sufficiently large ($> 1000 \text{ mm}^2$) the skin effect so negatively impacted AC resistance that the solution of using segmented conductors was developed. Segmented conductors are also known as Milliken conductors, as they were developed and patented by Henry Milliken [62] [63]. These conductors consist of multiple pie-shaped segments that are twisted together around a round conductor, form, or air gap. Typical stranded and segmented copper and aluminum conductor designs are shown in FIGURE 1-1:

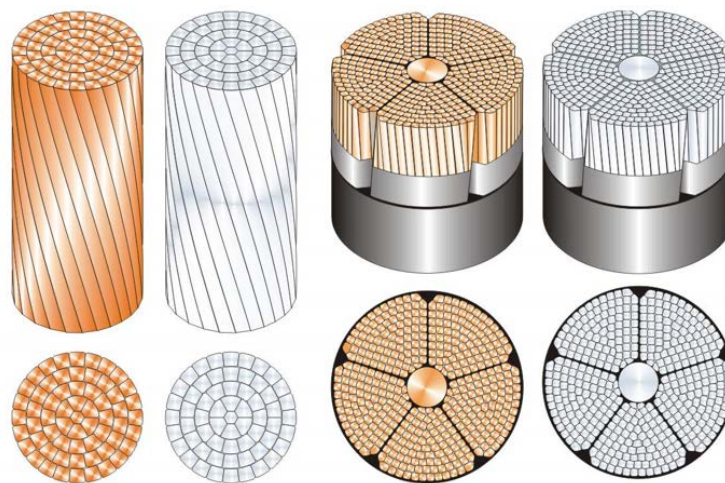


FIGURE 1-1: Stranded (left) and segmented (right) conductors

The effectiveness of this design is dependent on the current's inability to pass between segments, effectively making this a larger cross-section conductor composed of

smaller individual conductors not as susceptible to the skin effect as a single large conductor would be. With segmented conductors being the typical design for large conductors in power frequency applications a lot of work is also being done to examine different design properties, such as construction and number of the individual segments [64]. A similar theoretical technique of dividing the conductor into multiple parts is used at mid-frequency ranges (above power frequencies but less than tens or hundreds of kHz) in a design known as Litz wires [65]. In Litz wires, individual wires of the conductor are fully separated and insulated from each other. However, for high current applications (such as at power frequencies where the current is typically over a few hundred amperes), this type of conductor is not recommended since current would be unequal between individual conductors. At high frequencies, the depth at which the current flows is so small that the technique of plating is more commonly deployed. Plating involves the application of a highly conductive metal on top of another medium, such that all but a negligible amount of current under AC conditions travels within the outer plated metal.

Laboratory work has been a critical component in the development of designs to reduce skin effect. The two main areas of laboratory work include test equipment and testing methodology, as well as verification of theoretical results. The accuracy of test equipment has historically driven the refinement of analytical solutions in many fields. There are a couple of different techniques for measuring DC resistance. These include a Kelvin bridge, a DC potentiometer, or a precision digital voltmeter with a standard resistor. Measurement of AC resistance is much more difficult and has been developed over the years. After the Heaviside bridge was initially used at MIT in 1915, the Arnold bridge was later developed in 1935 [41]. Later, the AC coordinate potentiometer was used in 1948

[40]. These remained the preferred methods until voltage and current probe techniques [42] and later a high precision Kelvin bridge modified for measuring AC resistance was used in 1978 [66]. Finally, the four-terminal impedance current transformer bridge was later used in 1979 [67] [68] [43]. Because of the lack of a closed-form solution for segmented conductors a lot of research into the measurement of their AC resistance is still ongoing in the industry [44] [46]. Kouichi Sugiyama is currently credited for having developed the closest model for segmented conductors to date [69], although others have recommended modifications to the formulas due to the enormous amount of manufacturing variability [70].

With the development of new designs and verification of theoretical work through laboratory measurements, the final challenge is to make it possible to implement the work. The complexity in solving Bessel functions was overcome by Lord Kelvin by using tabulated values, however this was still very tedious and time consuming. A lot of work has been done in the 20th century to address this [35] [2] [36] [18] [37] [38] [5] [23]. Most of these works include simplified polynomial equations, which are applicable over a certain frequency range. This is because the skin effect, for a smaller Bessel function input argument (typical at low frequencies) has a different behavior than a large input argument (typical at high frequencies). With the advent of PCs, the calculation of Bessel functions no longer poses the same problems. However, PCs also have had their limitations in implementing Bessel functions using numerical methods throughout the years, so research was also done to reduce such constraints [39]. Particularly, software errors can occur when Bessel functions require large input arguments [71].

1.4 Dissertation Overview and Organization

This dissertation provides a complete solution within the context of research activities related to skin effect. From a design point of view, skin effect in bi-media conductors is formulated. Then, from a measurement perspective, the theory is experimentally validated. Finally, from an approximation standpoint, simplified equations for the design of bi-media conductors are presented, accompanied by a selection methodology and cost analysis for implementation.

First, the closed-form mathematical solution for calculating AC resistance in conductors of two different media is presented. Current density is non-uniform under AC current, and is directly related to the increase in AC over DC resistance of a conductor. Therefore, a solution is first presented using the current density under AC operation as opposed to its operation under DC current for a single medium. This method differs from that used in existing literature, which solves for AC resistance using solely Bessel functions. It is shown that identical results are obtained using the method of current density that is proposed. This solution is then expanded to a conductor using two different media. Following the mathematical solutions, a comparison of results using the obtained closed-form solution is compared to the solution using finite element analysis (FEA). Finally, these theoretical results are compared to laboratory measured AC resistances on two designs manufactured with bi-media. Results all show that the derived solution is consistent with FEA calculations and measured values.

Using the theoretical solutions verified with laboratory measurements, the development of standardized sizes for usage within the power industry is presented. For equivalent cost comparison, it is of interest to see how bi-media designs compare to current

design technologies. Analysis is presented detailing cost savings for these designs and a methodology for choosing the most cost effective solution.

Finally, due the complexity of the solution, simplified equations are presented to aid in the design of bi-media conductors. These only require simple mathematical equations and calculation methods known to current industry practitioners, as opposed to requiring knowledge of Bessel functions and advance modeling tools.

Considerations made on the application of bi-media designs are focused on large conductors operating at power frequencies (50 and 60 Hz). However, as the increase in resistance is a function of frequency the solution also is applicable to smaller conductors operating at higher frequencies [36]. This point is made clearer through the derivation of the skin effect. To follow the derivation a background of EM theory is required, and is therefore presented next. The theory discussed is catered to the formulation of AC resistance, and is therefore not meant to be comprehensive. For the interested reader references are provided that discuss the mathematical background in its entirety.

CHAPTER 2: BACKGROUND

2.1 Overview

This chapter provides the theoretical background for calculating skin effect solely with Bessel functions, which is required to understand the closed-form solution developed for calculation of skin effect using current density in single and bi-media conductors. The topics discussed are focused on the application within this dissertation, and therefore are not meant to be exhaustive. Skin effect calculations require working knowledge of vector calculus and field theory. Using these, Maxwell's equations are presented, as the starting point for the derivation of skin effect. Because Bessel functions are involved in the derivation, these are discussed, as well. Next, DC resistance is presented, followed by a full derivation of AC resistance in a solid round conductor. Finally, an overview of how this solution is implemented in the industry through simplified polynomial equations is explained.

2.2 Vector Calculus

For the derivations provided in this dissertation all mathematical solutions are performed in cylindrical coordinates. This greatly simplifies the mathematics, and is the reason closed-form solutions only exist for symmetrically round shapes. Rectangular coordinates (x, y, z) are mapped to cylindrical coordinates (r, φ, z) using:

$$r = \sqrt{x^2 + y^2} \tag{1}$$

$$\varphi = \tan^{-1}\left(\frac{y}{x}\right) \quad (2)$$

$$z = z \quad (3)$$

And shown graphically in FIGURE 2-1:

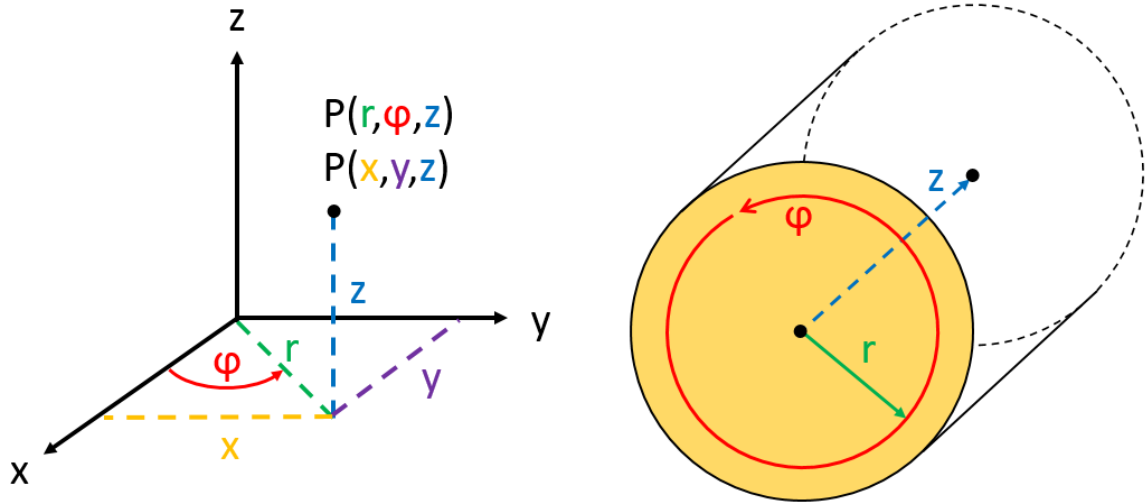


FIGURE 2-1: Cylindrical coordinates

Certain line, surface and volume integrals are also used, particularly as they relate to cylinders:

$$2D \text{ Line Integral} = \oint_L d\mathbf{L} \quad (4)$$

$$2D \text{ Surface Integral} = \int_S d\mathbf{S} \quad (5)$$

$$3D \text{ Surface Integral} = \oint_S d\mathbf{S} \quad (6)$$

$$3D \text{ Volume Integral} = \int_V dv \quad (7)$$

Note that bold font throughout the dissertation always denotes vectors. These equations are used to work with the material in integral form. The corresponding graphics for these equations are shown in FIGURE 2-2:

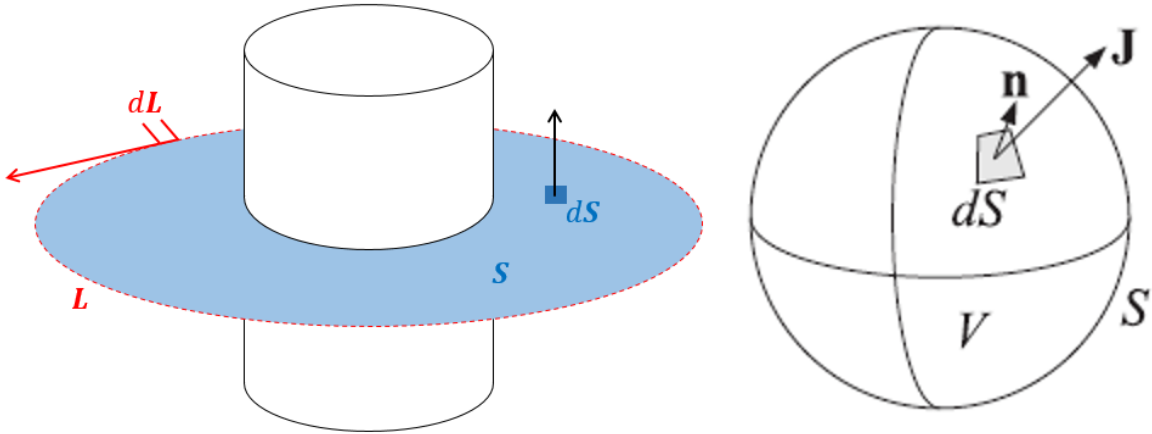


FIGURE 2-2: 2D (left) and 3D (right) surfaces

Maxwell's equations, along with the derivation of skin effect, are more easily represented in differential, or point, form. These forms utilize differential operators known as the gradient, curl, divergence, and Laplacian, which are represented by the del operator (∇). The gradient (generalization of the derivative concept), curl (characterizes rotation at a point), divergence (characterizes outward flux at a point), and Laplacian (divergence of the gradient) formulas, respectively, are:

$$\nabla V = \frac{\partial V}{\partial r} \hat{\mathbf{r}} + \frac{1}{r} \frac{\partial V}{\partial \phi} \hat{\boldsymbol{\phi}} + \frac{\partial V}{\partial z} \hat{\mathbf{z}} \quad (8)$$

$$\nabla \times V = \left(\frac{1}{r} \frac{\partial \mathcal{N}_z}{\partial \phi} - \frac{\partial \mathcal{N}_\phi}{\partial z} \right) \hat{\mathbf{r}} + \left(\frac{\partial \mathcal{N}_r}{\partial z} - \frac{\partial \mathcal{N}_z}{\partial r} \right) \hat{\boldsymbol{\phi}} + \frac{1}{r} \left(\frac{\partial (r \mathcal{N}_\phi)}{\partial r} - \frac{\partial \mathcal{N}_r}{\partial \phi} \right) \hat{\mathbf{z}} \quad (9)$$

$$\nabla \cdot V = \frac{1}{r} \frac{\partial}{\partial r} (r \mathcal{N}_r) + \frac{1}{r} \frac{\partial \mathcal{N}_\phi}{\partial \phi} + \frac{\partial \mathcal{N}_z}{\partial z} \quad (10)$$

$$\nabla^2 V = \frac{1}{r} \frac{\partial}{\partial r} \left(r \frac{\partial V}{\partial r} \right) + \frac{1}{r^2} \frac{\partial^2 V}{\partial \phi^2} + \frac{\partial^2 V}{\partial z^2} \quad (11)$$

The vector fields of the gradient, curl, and divergence can be shown graphically in FIGURE 2-3:

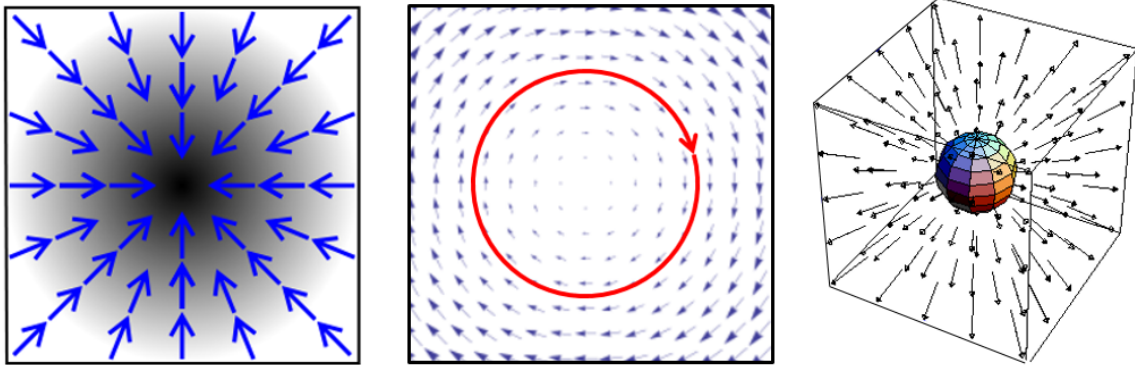


FIGURE 2-3: Gradient (left), curl (middle), and divergence (right)

Finally, there are two important theorems that are introduced [24]. These two theorems are used to convert Maxwell's Equations between integral and differential forms. First is the divergence theorem (also known as Gauss's theorem) that relates the 3D volume and surface integrals. This means it relates the flux through a volumetric surface to the behavior inside. This theorem is shown here:

$$\int_V \nabla \cdot \mathbf{A} \, dV = \oint_S \mathbf{A} \cdot d\mathbf{S} \quad (12)$$

Second is Stokes' theorem that relates the 2D surface integral of the curl and line integral over its boundary. This theorem is shown here:

$$\int_S (\nabla \times \mathbf{A}) \cdot d\mathbf{S} = \oint_L \mathbf{A} \cdot d\mathbf{L} \quad (13)$$

2.3 Field Theory

To work with Maxwell's equations, and eventually derive skin effect, field theory needs to be fully understood. Electric field is a vector representing the electrical force on a unit charge at a given distance:

$$\mathbf{E} = \frac{q}{4\pi r^2 \epsilon} \quad (14)$$

This is a measurement of intensity, which decreases with the square of the distance. Electric flux is a scalar field originating from a charge. Electric flux can be expanded to electric flux density, which is a measure of electric flux through a surface:

$$\mathbf{D} = \epsilon \mathbf{E} \quad (15)$$

Note that electric field and electric flux are related through the permittivity of the medium, ϵ . The permittivity measures the polarization, or ability of the body to store an electric charge. Equation (15) is the first of the constitutive equations, which characterizes the response of a material to an applied electric field. The permittivity is commonly written in terms of the permittivity of free space (i.e. in a vacuum) times the relative (to that of free space) permittivity of a given medium:

$$\epsilon = \epsilon_0 \epsilon_r \quad (16)$$

Therefore, the higher the relative permittivity the more easily the medium stores an electric charge.

Magnetic field is a vector representing the magnetic force on a unit charge at a given distance, which due to an enclosed current:

$$\mathbf{H} = \frac{I_{enc}}{2\pi r} \quad (17)$$

Magnetic field, like electric field, is also a measurement of intensity, which decreases with distance. It can be observed, as to be discussed later, that this is Ampère's law [24]. Maxwell was the first to show the relationship between electric and magnetic forces, being that they are an interrelated part of electromagnetism [72]. Magnetic flux is a scalar measurement of magnetic field passing through a surface. This can be expanded to magnetic flux density, which is a measure of magnetic flux through a surface:

$$\mathbf{B} = \mu\mathbf{H} \quad (18)$$

Note that magnetic field and magnetic flux density are related through the permeability of the medium. The permeability measures the magnetization, or ability of the body to support the formation of a magnetic field. Equation (18) is the second of the constitutive equations, which characterizes the response of a material to an applied magnetic field. Like permittivity, permeability is also commonly written in terms of the permeability of free space (i.e. in a vacuum) times the relative (to that of free space) permeability of a given medium:

$$\mu = \mu_0\mu_r \quad (19)$$

Therefore, the higher the relative permeability the more easily the medium stores a magnetic charge.

The third and final constitutive equation is:

$$\mathbf{J}_c = \sigma\mathbf{E} \quad (20)$$

Equation (20) shows the relationship between the conducting current density and the electric field, as related through the material conductivity. The conductivity represents how readily the material allows the flow of electric current. It can be observed that this is Ohm's law in circuit theory, which is later discussed in more detail. In general, materials

are classified into three categories: dielectrics, magnetics, and conductors. These represent, respectively, the predominant phenomena of the material being either polarization, magnetization, or conduction [24]. However, these properties are not mutually exclusive. A good conductor is defined as a material where the conducting current density is much greater than the displacement current density.

Note that circuit theory is a special case of the more general field theory equations. Many textbooks cover the relationships between the two, one from which a summary of notable parameters is given on TABLE 2-1 [24]:

TABLE 2-1: Field theory parameters

Field Theory		
Row	Symbol	Description
1	\mathbf{E}	electric field
2	\mathbf{H}	magnetic field
3	\mathbf{D}	electric flux density
4	\mathbf{B}	magnetic flux density
5	\mathbf{J}	electric current density
6	\mathbf{M}	magnetic current density
7	$J_d = \epsilon \frac{\partial \mathbf{E}}{\partial t}$	electric displacement current density
8	$M_d = \mu \frac{\partial \mathbf{H}}{\partial t}$	magnetic displacement current density
9	$J_c = \sigma \mathbf{E}$	electric conduction current density
10	$\mathbf{D} = \epsilon \mathbf{E}$	dielectric material
11	$\mathbf{B} = \mu \mathbf{H}$	magnetic material
12	$\nabla \times \mathbf{E} = -\frac{\partial \mathbf{B}}{\partial t}$	Maxwell's 3 rd equation
13	$\nabla \cdot \mathbf{B} = 0$	Maxwell's 2 nd equation

The equivalent circuit theory variables and equations are shown on TABLE 2-2:

TABLE 2-2: Circuit theory parameters

Circuit Theory		
Row	Symbol	Description
1	V	voltage
2	I	current
3	ρ_e	electric charge density
4	ρ_m	magnetic charge density
5	I_e	electric current
6	I_m	magnetic current
7	$I = C \frac{dV}{dt}$	current through a capacitor
8	$V = L \frac{dI}{dt}$	voltage across an inductor
9	$I = \frac{V}{R}$	Ohm's law
10	$q = CV$	charge in a capacitor
11	$\psi = LI$	flux of an inductor
12	$\sum V = 0$	Kirchhoff's voltage law
13	$\sum I = 0$	Kirchhoff's current law

2.4 Maxwell's Equations

Maxwell's equations are four equations presented by Maxwell that form the basis of electromagnetic theory. The first three of Maxwell's equations had already existed in their present or alternate form, whereas the fourth equation is an existing equation modified by Maxwell. The first equation, known as Gauss's law states that the total flux out of a closed surface is equal to the net charge enclosed within the surface. Mathematically it is represented in integral and point forms, respectively, as:

$$\oint_S \mathbf{D} \cdot d\mathbf{S} = \int_V \rho_e dv \quad (21)$$

$$\nabla \cdot \mathbf{D} = \rho_e \quad (22)$$

This law states that an electric charge will act as a source or a sink for an electric field.

Maxwell's second equation, known as Gauss's law for magnetism, states that the total magnetic flux out of a closed surface is equal to the net magnetic charge enclosed within the surface, which always must be zero. Mathematically it is represented in integral and point forms, respectively, as:

$$\oint_S \mathbf{B} \cdot d\mathbf{S} = 0 \quad (23)$$

$$\nabla \cdot \mathbf{B} = 0 \quad (24)$$

This law implies that magnetic charge does not exist, and therefore every magnetic object is a dipole. This is to be expected, as this is the counterpart of KCL.

Maxwell's 3rd equation is the generalization of Faraday's law. It states that the induced electromotive force in any closed circuit is equal to the rate of change of the magnetic flux through the circuit. Mathematically it is represented in integral and point forms, respectively, as:

$$\oint_L \mathbf{E} \cdot d\mathbf{L} = - \int_S \frac{\partial \mathbf{B}}{\partial t} \cdot d\mathbf{S} \quad (25)$$

$$\nabla \times \mathbf{E} = - \frac{\partial \mathbf{B}}{\partial t} \quad (26)$$

This equation shows that a changing magnetic field creates an electric field. Faraday was able to show this time dependence experimentally by winding the wires attached to a DC source around a toroid and measuring the voltage between another set of wires around the same toroid. When closing the circuit he observed a momentary spike in voltage with

opposite polarity to the battery. Had he had an AC source he would've observed a constantly fluctuating voltage measurement.

Maxwell's fourth equation is his most important contribution, aside from collecting the equations into a single unified theory. Maxwell's fourth equation is Ampère's law plus displacement current, which was his contribution. Ampère's law states that the line integral of the tangential component of the magnetic field strength around a closed path is equal to the current enclosed by the path, represented mathematically by:

$$\oint_L \mathbf{H} \cdot d\mathbf{L} = I_{enc} \quad (27)$$

This equation only considers conducting current, and is therefore only valid for DC conditions. It shows that a magnetic field can be created by an electric current. Maxwell added displacement current to this equation, making it universal to both DC and AC currents. Mathematically it is represented in integral and point forms, respectively, as:

$$\oint_L \mathbf{H} \cdot d\mathbf{L} = \int_S \left(\mathbf{J}_c + \frac{\partial \mathbf{D}}{\partial t} \right) \cdot d\mathbf{S} \quad (28)$$

$$\nabla \times \mathbf{H} = \mathbf{J}_c + \frac{\partial \mathbf{D}}{\partial t} \quad (29)$$

In addition to what is shown by the part of this equation representing Ampère's law, this equation also shows that a magnetic field can be created by a time-varying electric flux.

The forms of Maxwell's equations given are general, in that they apply to static, dynamic, and time-harmonic fields. The derivations for skin effect utilize the time-varying forms of the equations, but all three can be summarized in point form as shown on TABLE 2-3:

TABLE 2-3: Maxwell's equations

Static Fields	Dynamic Fields	Time-Harmonic Fields
$\nabla \cdot \mathbf{D} = \rho_e$	$\nabla \cdot \mathbf{D} = \rho_e$	$\nabla \cdot \mathbf{D} = \rho_e$
$\nabla \cdot \mathbf{B} = 0$	$\nabla \cdot \mathbf{B} = 0$	$\nabla \cdot \mathbf{B} = 0$
$\nabla \times \mathbf{E} = 0$	$\nabla \times \mathbf{E} = -\frac{\partial \mathbf{B}}{\partial t}$	$\nabla \times \mathbf{E} = -j\omega \mathbf{B}$
$\nabla \times \mathbf{H} = \mathbf{J}_c$	$\nabla \times \mathbf{H} = \mathbf{J}_c + \frac{\partial \mathbf{D}}{\partial t}$	$\nabla \times \mathbf{H} = \mathbf{J}_c + j\omega \mathbf{D}$

Since this dissertation focuses on two-medium conductors, it is also critical to understand boundary conditions of electric and magnetic fields between the two dissimilar media. Boundary conditions of the electric field are derived from Maxwell's 1st and 3rd equations, whereas the boundary conditions of the magnetic field are derived from Maxwell's 2nd and 4th equations. These equations allow for the relation of the tangential and normal components of the fields. A summary from one of many available resources giving detailed derivations of these properties is as shown on TABLE 2-4 [24]:

TABLE 2-4: Boundary conditions

Field/Flux Parameter	General	Finite Conductivity Media
\mathbf{E}_t	$\hat{n} \times (\mathbf{E}_2 - \mathbf{E}_1) = -\mathbf{M}_s$	$\hat{n} \times (\mathbf{E}_2 - \mathbf{E}_1) = 0$
\mathbf{H}_t	$\hat{n} \times (\mathbf{H}_2 - \mathbf{H}_1) = \mathbf{J}_s$	$\hat{n} \times (\mathbf{H}_2 - \mathbf{H}_1) = 0$
\mathbf{D}_n	$\hat{n} \cdot (\mathbf{D}_2 - \mathbf{D}_1) = \rho_e$	$\hat{n} \cdot (\mathbf{D}_2 - \mathbf{D}_1) = 0$
\mathbf{B}_n	$\hat{n} \cdot (\mathbf{B}_2 - \mathbf{B}_1) = \rho_m$	$\hat{n} \cdot (\mathbf{B}_2 - \mathbf{B}_1) = 0$

2.5 Bessel Functions

An intermediate step within the derivation of skin effect results in a second-order partial differential equation, which relates current density to the radius. The form of the equation encountered is that of the well-known Bessel function [73]. Therefore, employing these functions will allow for the representation of current density as a function of the radius. There are three kinds of Bessel functions: the first kind, second kind, and third kind. Bessel functions of all kinds are related and derived from that of the first kind. However, as shown in the derivation for skin effect, it is advantageous to represent the

functions in these separate forms since they are mathematically more compact and also have physical meanings. The Bessel function also has a related order, which can be seen in the form of the equation it solves here:

$$x^2 \frac{d^2 y}{dx^2} + x \frac{dy}{dx} + (x^2 + \alpha^2)y = 0 \quad (30)$$

In the context of current density in a solid round wire the order is zero. The general solution of the Bessel function of the first kind is:

$$J_\alpha(x) = \sum_{m=0}^{\infty} \frac{(-1)^m}{m! \Gamma(m + \alpha + 1)} \left(\frac{x}{2}\right)^{2m+\alpha} \quad (31)$$

This has the corresponding plot shown in FIGURE 2-4:

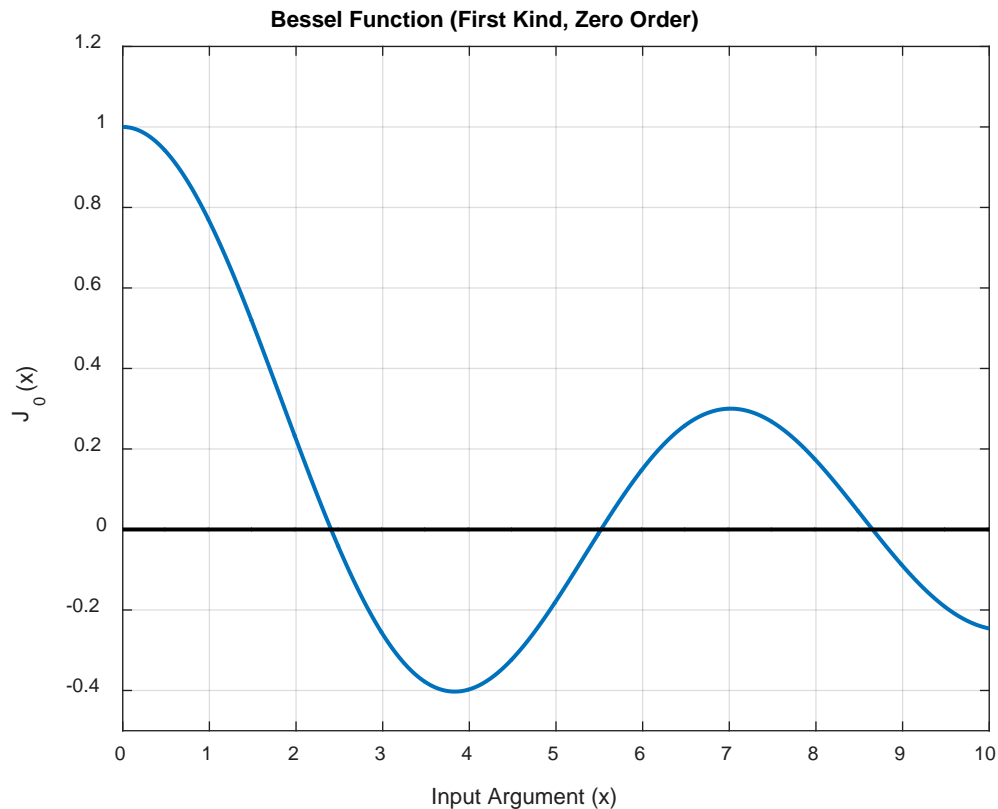


FIGURE 2-4: Bessel function (first kind, zero order)

As is shown in the derivation for skin effect, the Bessel function of the first kind and zero order fully defines the attenuation of an electromagnetic wave penetrating the conductor from its surface. Note that for copper conductors larger than 800 mm^2 the input argument is larger than 2.4, which is where the function becomes negative. This is the reason segmented conductors are used on sufficiently large conductors, as introducing additional metal has the counterintuitive effect of increasing AC resistance [12]. At power frequencies the input argument would not be expected to exceed 4.5, which would correspond to a 3000 mm^2 copper conductor.

The Bessel function accepts complex inputs, which current density is. Because this is a second-order partial differential equation there are two unique solutions. In cases where there is a singularity at zero (which exists in the solution for solid round tube conductors) a Bessel function of the second kind is used (also known as the Kelvin function), whose general solution is shown here:

$$Y_{\alpha}(x) = \frac{J_{\alpha}(x) \cos(\alpha\pi) - J_{-\alpha}(x)}{\sin(\alpha\pi)} \quad (32)$$

The final Bessel function is that of the third kind, which is also known as the Hankel function after Hermann Hankel. It is a combination of Bessel functions of the first and second kinds, and is used to express inward-propagating or outward-propagating cylindrical wave solutions. Mathematically, the general solution for the Hankel function of the first kind is:

$$H_{\alpha}(x) = J_{\alpha}(x) + iY_{\alpha}(x) = \frac{J_{-\alpha}(x) - e^{-\alpha\pi i} J_{\alpha}(x)}{i \sin(\alpha\pi)} \quad (33)$$

The Bessel functions of the first kind is important because it maintains regularity at the origin, and the Bessel function of the third kind is important because it maintains

regularity at infinity [74]. Before the advent of PCs, these functions all had to be calculated by hand. Therefore, it was common practice to use tabulated value to speed up work [30]. Now that PCs are used care must be taken such that non-regularities that arise from certain Bessel function input arguments do not result in errors [39]. Because the functions consist of a real and imaginary part, tables included solutions for both the real and imaginary parts.

Some derivations also require the derivatives of the Bessel function, which are denoted with a prime. Note that when using separated real and imaginary Bessel functions there is no imaginary component of the input. The Bessel function of the first kind separated into real and imaginary parts is as follows:

$$J_{\alpha}\left(xe^{\frac{3\pi i}{4}}\right) = ber_{\alpha}(x) + bei_{\alpha}(x) \quad (34)$$

$$J'_{\alpha}\left(xe^{\frac{3\pi i}{4}}\right) = ber'_{\alpha}(x) + bei'_{\alpha}(x) \quad (35)$$

Likewise, the Bessel function of the second kind (Kelvin function) separated into real and imaginary parts is:

$$Y_{\alpha}\left(xe^{\frac{\pi i}{4}}\right) = ker_{\alpha}(x) + kei_{\alpha}(x) \quad (36)$$

$$Y'_{\alpha}\left(xe^{\frac{\pi i}{4}}\right) = ker'_{\alpha}(x) + kei'_{\alpha}(x) \quad (37)$$

There are many more properties of Bessel functions, including their usage in spherical coordinates, derivatives and integrals, alternate forms / modified types, and theorems and identities. These are outside the scope of this dissertation; the reader interested in engineering applications of Bessel functions is encouraged to refer to [73].

2.6 DC & AC Resistance

Although there can be a small radial temperature gradient that creates non-uniform radial DC current density, it is usually negligible [25]. Therefore, the current density at any point of the conductor can be calculated by:

$$J_{dc} = \frac{I_{dc}}{A} \quad (38)$$

The DC resistance of a conductor is calculated by:

$$R_{dc} = \frac{\rho l}{A} \quad (39)$$

Note that electrical resistivity ρ is a temperature dependent value, and thus R_{dc} will be as well. The DC resistance for aluminum and copper increases approximately 4% for every 10°C rise in the temperature of the conductor [33]. Additionally, stranding conductors increases DC resistance since the spiraled strands are longer than the conductor itself [75]. This increase in resistance is commonly estimated at 2% [76]. However, today larger designs have more layers of stranded wires on the outside. This has led to an increased DC resistance as high as 4% on large conductor sizes [77].

Alternating Current (AC) density, unlike DC, is not uniform throughout a conductor due to the skin and proximity effects. Both phenomena are caused by the changing magnetic field of AC current. Specifically, the skin effect is caused by the time-varying magnetic field created by the AC current flowing within the conductor itself, whereas the proximity effect is the influence of this same magnetic field on an external conductor [78]. Stranded conductors also have an additional increase in AC resistance from the spirality effect. This is caused by the wires being helically twisted, which slightly changes the direction of the magnetic field in the conductor. This superimposes with the

skin effect, of which it only adds a small fraction for non-ferrous materials and is therefore negligible [31].

The time-varying magnetic field created by a conductor carrying AC current decreases exponentially with the distance from the conductor. Another conductor in the presence of this field has a resulting voltage induced on it. Because the magnetic fields are superimposed, the effective AC resistance of both conductors is increased [79]. In the case where the current is in the same direction on both conductors, the eddy current circulates such that the conducting current is reinforced on the far side of the conductor and opposed on the near side [79]. Conversely, if current were flowing in opposite directions, the current density distribution would be higher on the inner sides of both conductors. For example, in a coaxial conductor carrying both the go and return currents, the current density is higher towards the nearer side of the conductors and lower towards the outsides [9]. A graphical representation of the proximity effect of conductors with AC current flowing in the same direction is shown FIGURE 2-5:

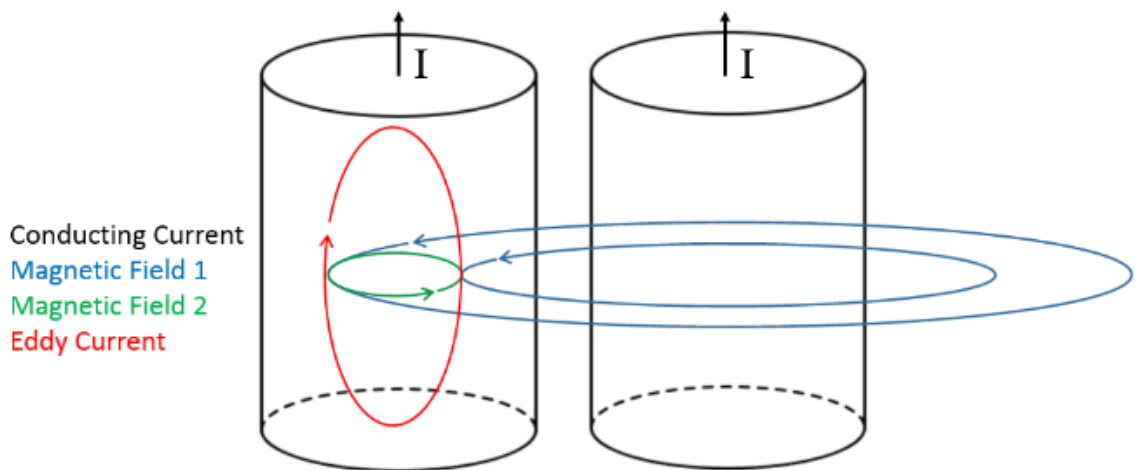


FIGURE 2-5: Proximity effect

Proximity effect is proportional to the magnitude of the currents and inversely proportional to the distance between the conductors [29]. Until reports in the early 1930s

proved otherwise, it was believed the proximity effect for stranded conductors would be zero [80] [81]. The rationale for having no proximity effect in stranded conductors was due to the belief the longitudinal electrical conductivity was so much better than radial conductivity. If so, the current would only follow the path of the each strand and not move between strands. Therefore, there would be a zero net induced voltage on each strand since the strands were helically wound around the central point of the conductor [28]. If the strands were perfectly insulated this would be true, since each strand would alternate position around the center of the conductor and therefore the net induced voltage would be zero. However, experimental results indicate radial strand conductivity is around 45-80% longitudinal conductivity, depending on factors such as compression and core impregnation [28]. When a conducting current flows through a conductor it generates a magnetic field, as shown by Maxwell's 4th equation (Ampère's law). By Maxwell's 3rd equation (Faraday's law), this time-varying magnetic field generated by the conducting current induces an electric field. The electric field results in an eddy current flowing in the direction of the conducting current towards the outside of the conductor and in the opposite direction in the inside, as shown in FIGURE 2-6:

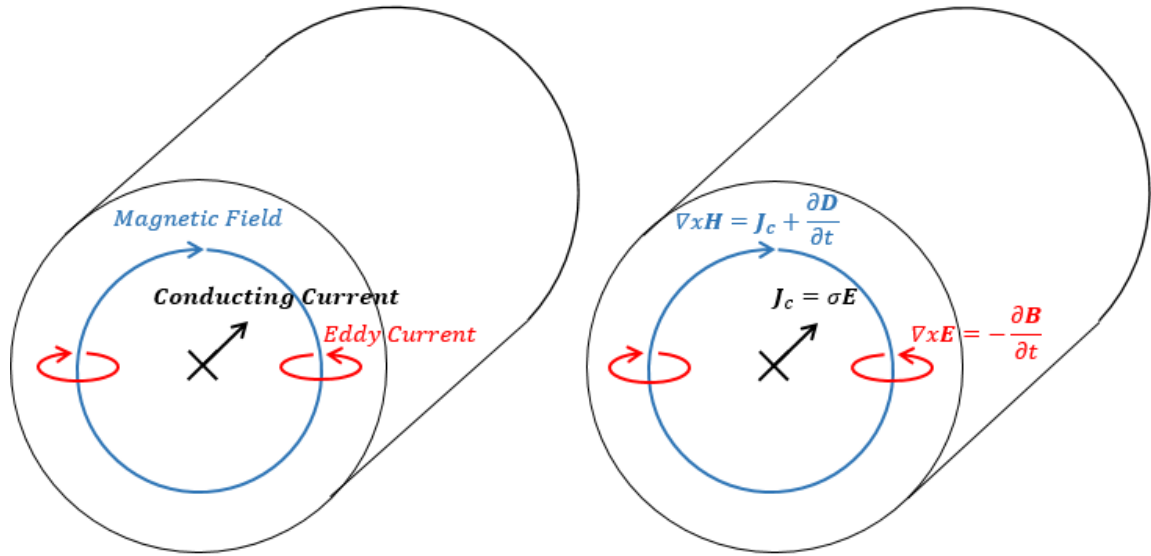


FIGURE 2-6: Skin effect

In a good conductor electron density is approximately uniform. The non-uniform distribution of current density is truly due to non-uniform charge carrier velocity as opposed to charge carrier density [24].

The derivation of skin effect begins by taking the curl of both sides of Maxwell's 3rd equation for time harmonic fields:

$$\nabla \times (\nabla \times \mathbf{E}) = -j\omega (\nabla \times \mathbf{B}) \quad (40)$$

Next, making use of the following vector calculus identity:

$$\nabla \times (\nabla \times \mathbf{E}) = \nabla (\nabla \cdot \mathbf{E}) - \nabla^2 \mathbf{E} \quad (41)$$

Equation (40) is rearranged as follows:

$$\nabla (\nabla \cdot \mathbf{E}) - \nabla^2 \mathbf{E} = -j\omega (\nabla \times \mathbf{B}) \quad (42)$$

Maxwell's 4th equation can be rearranged to be written in terms of \mathbf{B} and \mathbf{E} using the constitutive equations as:

$$\nabla \times \mathbf{H} = \mathbf{J}_c + j\omega \mathbf{D} \rightarrow \nabla \times \left(\frac{\mathbf{B}}{\mu} \right) = \sigma \mathbf{E} + j\omega (\epsilon \mathbf{E}) \quad (43)$$

$$\nabla \times \mathbf{B} = \mu \sigma \mathbf{E} + j\omega \mu \varepsilon \mathbf{E} \quad (44)$$

Substituting this into equation (42) and rearranging yields:

$$\nabla(\nabla \cdot \mathbf{E}) - \nabla^2 \mathbf{E} = -j\omega(\mu \sigma \mathbf{E} + j\omega \mu \varepsilon \mathbf{E}) \quad (45)$$

$$\nabla^2 \mathbf{E} - \nabla(\nabla \cdot \mathbf{E}) = j\omega \mu \sigma \mathbf{E} + (j\omega)^2 \mu \varepsilon \mathbf{E} \quad (46)$$

Rearranging Maxwell's first equation in terms of \mathbf{E} using the constitutive equations yields:

$$\nabla \cdot \mathbf{D} = \rho \rightarrow \nabla \cdot (\varepsilon \mathbf{E}) = \rho \rightarrow \nabla \cdot \mathbf{E} = \frac{\rho}{\varepsilon} \quad (47)$$

It is assumed there is no gradient of charge density and material permittivity, since radially the conductor is at uniform voltage potential. Therefore, part of equation (46) can be eliminated:

$$\nabla(\nabla \cdot \mathbf{E}) = \nabla \left(\frac{\rho}{\varepsilon} \right) \approx 0 \quad (48)$$

It can also be assumed that $\omega \sigma \gg \omega^2 \varepsilon$. This assumption is valid since this medium is a good conductor over a large range of frequencies. For example, $\omega \sigma$ for copper at power frequencies is 16 orders of magnitude larger than $\omega^2 \varepsilon$, and at 1 GHz $\omega \sigma$ is still 9 orders of magnitude larger than $\omega^2 \varepsilon$. Therefore:

$$j\omega \mu \sigma \mathbf{E} \gg (j\omega)^2 \mu \varepsilon \mathbf{E} \quad (49)$$

Using equations (48) and (49) into conjunction with equation (46) yields:

$$\nabla^2 \mathbf{E} = j\omega \mu \sigma \mathbf{E} \quad (50)$$

In cylindrical coordinates (r, φ, z) this equation is simplified, due to the circular symmetry of the conductor. Therefore, variations in the r and φ directions are zero and hence all derivatives with respect to these variables are also zero. Additionally, the electric field is

negligible in the r and φ directions in comparison to the z direction since the conductor is assumed to be of infinite length. With that, E_r and E_φ are also zero

The vector field of \mathbf{E} can be written in terms of unit vectors in cylindrical coordinates as:

$$\mathbf{E} = E_r \hat{\mathbf{r}} + E_\varphi \hat{\boldsymbol{\varphi}} + E_z \hat{\mathbf{z}} \quad (51)$$

Since there is no variation in the r and φ direction:

$$\mathbf{E} = E_z \hat{\mathbf{z}} \quad (52)$$

The vector Laplacian of \mathbf{E} in cylindrical coordinates is:

$$\nabla^2 \mathbf{E} = \begin{bmatrix} \frac{\partial^2 E_r}{\partial r^2} + \frac{1}{r^2} \frac{\partial^2 E_r}{\partial \varphi^2} + \frac{\partial^2 E_r}{\partial z^2} + \frac{1}{r} \frac{\partial E_r}{\partial r} - \frac{2}{r^2} \frac{\partial E_\varphi}{\partial \varphi} - \frac{E_r}{r^2} \\ \frac{\partial^2 E_\varphi}{\partial \varphi^2} + \frac{1}{r^2} \frac{\partial^2 E_\varphi}{\partial \varphi^2} + \frac{\partial^2 E_\varphi}{\partial z^2} + \frac{1}{r} \frac{\partial E_\varphi}{\partial r} + \frac{2}{r^2} \frac{\partial E_r}{\partial \varphi} - \frac{E_\varphi}{r^2} \\ \frac{\partial^2 E_z}{\partial r^2} + \frac{1}{r^2} \frac{\partial^2 E_z}{\partial \varphi^2} + \frac{\partial^2 E_z}{\partial z^2} + \frac{1}{r} \frac{\partial E_z}{\partial r} \end{bmatrix} \quad (53)$$

Because there is no variation in the r and φ direction:

$$\nabla^2 \mathbf{E} = \frac{d^2 E_z}{dr^2} + \frac{1}{r} \frac{dE_z}{dr} \quad (54)$$

Therefore, the equation (50) in cylindrical coordinates using equations (52) and (54) becomes:

$$\frac{d^2 E_z}{dr^2} + \frac{1}{r} \frac{dE_z}{dr} = j\omega\mu\sigma E_z \quad (55)$$

Using the constitutive equation for \mathbf{J} to write the equation in terms of current density yields ($0 \leq r < r_2$):

$$\frac{d^2 J_r}{dr^2} + \frac{1}{r} \frac{dJ_r}{dr} = m^2 J_r \quad (56)$$

Where:

$$m = \sqrt{j\omega\mu\sigma} \quad (57)$$

Note that the input argument is a complex value, as is current density. The real part of the current density represents the resistance, whereas the imaginary part represents the internal inductance [16]. Current generates a magnetic field inside and outside the conductor. The internal inductance is the portion of the magnetic energy stored inside the conductor. For simplicity, the subscript 2 is used for the outer radius, since an inner medium is introduced later with subscript 1. At the outer boundary r_2 , the current density is technically zero [82]. However, for notational simplicity:

$$J_{r_2} = \lim_{r \rightarrow r_2} J_r \quad (58)$$

Note that skin depth δ is derived as:

$$m = \sqrt{j\omega\mu\sigma} = (1 + j) \sqrt{\frac{\omega\mu\sigma}{2}} = (1 + j) \frac{1}{\delta} \quad (59)$$

Skin depth is the depth at which a magnetic field can penetrate the conductor, and therefore the point current density is equal for time-varying current in the total conductor and time-invariant current at this depth [8]. Skin depth decreases rapidly as frequency increases, as shown here for copper and aluminum in FIGURE 2-7:

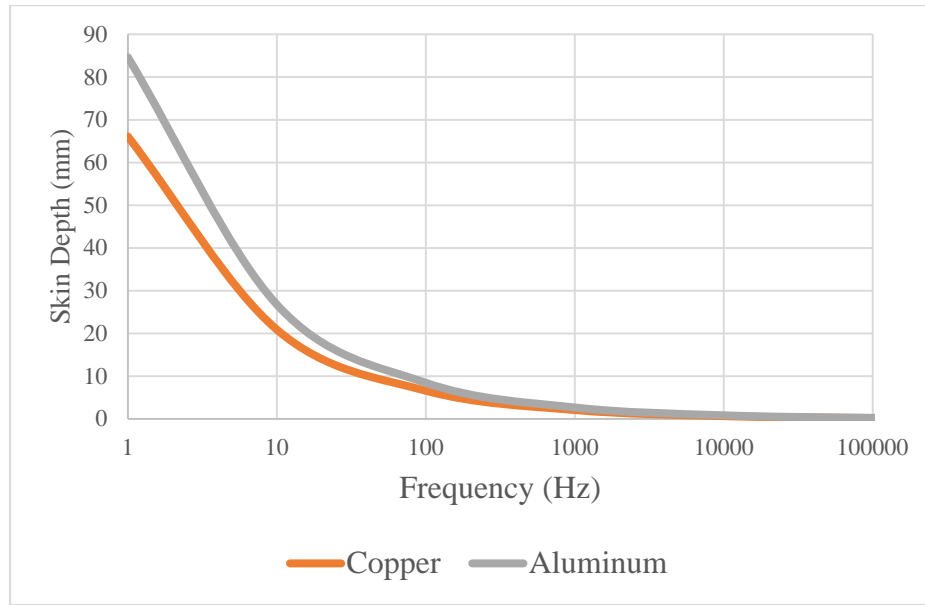


FIGURE 2-7: Skin depth vs frequency

The current penetration into the conductor varies with the square root of the current frequency [83]. The solutions for current density are the well-known Bessel functions, which are the solutions to second-order partial differential equation:

$$J_r = A_1 J_0(mr) + A_2 Y_0(mr) \quad (60)$$

The current density behavior is driven by the changing electromagnetic (EM) fields inside the conductor and appears like an incident EM wave originating from the conductor surface and radially propagating inward. The real part of the current density attenuates exponentially, as depicted in FIGURE 2-8:

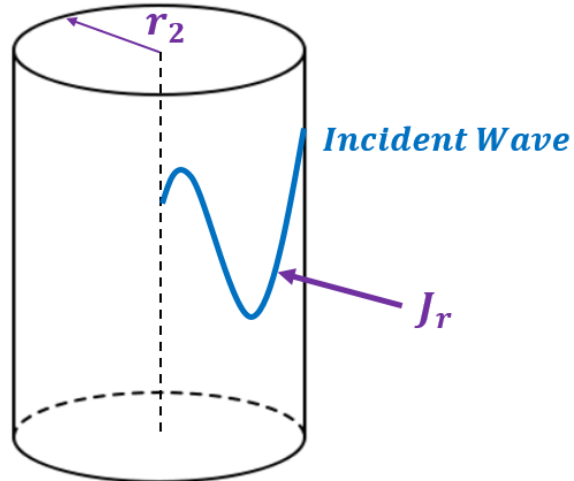


FIGURE 2-8: EM wave in single medium

The constants A_1 and A_2 are arbitrary constants and J_0 and Y_0 represent two independent solutions. Note that:

$$\lim_{r \rightarrow 0} Y_0 = \infty \quad (61)$$

The current density at the center of a solid round conductor (i.e. $r = 0$) cannot be infinite. Therefore, this is a physically impossible solution and the constant A_2 must be zero. Thus the current density is:

$$J_r = A_1 J_0(mr) \quad (62)$$

The constant A_1 can be determined at the surface boundary as:

$$J_{r_2} = A_1 J_0(mr_2) \rightarrow A_1 = \frac{J_{r_2}}{J_0(mr_2)} \quad (63)$$

Substituting equation (63) into equation (62) results in the final current density equation:

$$J_r = \frac{J_{r_2}}{J_0(mr_2)} J_0(mr) \quad (64)$$

The AC current can be obtained with the surface integral of the current density, which reduces to a shell integral:

$$I_{ac} = \iint_S J_r \cdot dS = 2\pi \int_0^{r_2} r J_r \cdot dr \quad (65)$$

Substituting equation (64) into equation (65) yields:

$$I_{ac} = 2\pi \int_0^{r_2} r \left(\frac{J_{r_2}}{J_0(mr_2)} J_0(mr) \right) \cdot dr = \frac{2\pi J_{r_2}}{J_0(mr_2)} \int_0^{r_2} r J_0(mr) \cdot dr \quad (66)$$

Using the following Bessel function identity:

$$\int_0^{r_2} r J_0(mr) dr = \frac{r_2}{m} J_1(mr_2) \quad (67)$$

Reduces equation (66) to:

$$I_{ac} = \frac{2\pi J_{r_2}}{J_0(mr_2)} \frac{r_2}{m} J_1(mr_2) = \frac{2\pi J_{r_2} r_2 J_1(mr_2)}{m J_0(mr_2)} \quad (68)$$

The AC current can now be used to express the AC impedance using Ohm's law:

$$Z_{ac} = \frac{E_{r_2}}{I_{ac}} = \frac{J_{r_2}/\sigma}{I_{ac}} = \frac{m}{2\pi r_2 \sigma} \cdot \frac{J_0(mr_2)}{J_1(mr_2)} \quad (69)$$

Note that the electric field E_{r_2} is the r-component of the cylindrical coordinates of electric field, but the field potential is in the z-direction (i.e. voltage drop down the length of the conductor). The AC resistance and reactance are the real and imaginary parts, respectively:

$$R_{ac} = \operatorname{Re} \left(\frac{m}{2\pi r_2 \sigma} \cdot \frac{J_0(mr_2)}{J_1(mr_2)} \right) \quad (70)$$

$$X_{ac} = \operatorname{Im} \left(\frac{m}{2\pi r_2 \sigma} \cdot \frac{J_0(mr_2)}{J_1(mr_2)} \right) \quad (71)$$

Inductance can be calculated from the reactance as normally done in circuit theory as:

$$L_{ac} = \frac{X_{ac}}{\omega} = \frac{1}{\omega} \operatorname{Im} \left(\frac{m}{2\pi r_2 \sigma} \cdot \frac{J_0(mr_2)}{J_1(mr_2)} \right) \quad (72)$$

The DC resistance for this conductor is:

$$R_{dc} = \frac{\rho l}{A} = \frac{1}{\sigma \pi r_2^2} \quad (73)$$

And thus, the skin effect is:

$$\frac{R_{ac}}{R_{dc}} = Re \left(\frac{mr_2 J_0(mr_2)}{2 J_1(mr_2)} \right) \quad (74)$$

This can also be written in separated real and imaginary parts as [1] [84] [85]:

$$\frac{R_{ac}}{R_{dc}} = \frac{m' r_2}{2} \left(\frac{ber_0(m' r_2) bei'_0(m' r_2) - bei_0(m' r_2) ber'_0(m' r_2)}{(bei'_0(m' r_2))^2 + (ber'_0(m' r_2))^2} \right) \quad (75)$$

Where:

$$m' = Re(m) \quad (76)$$

The internal DC inductance of a round conductor is [86] [87]:

$$L_{dc} = \frac{\mu}{2\pi} \ln \left(\frac{r_2}{GMR} \right) \quad (77)$$

Note that the geometric mean radius (GMR) of a solid round conductor is [85] [88]:

$$GMR = r_2 e^{-1/4} \quad (78)$$

Thus, the DC inductance of a solid round conductor is:

$$L_{dc} = \frac{\mu}{8\pi} \quad (79)$$

And thus, the AC/DC inductance ratio written in separated real and imaginary parts is [89]

[39] [90]:

$$\frac{L_{ac}}{L_{dc}} = \frac{4}{m' r_2} \left(\frac{ber_0(m' r_2) ber'_0(m' r_2) + bei_0(m' r_2) bei'_0(m' r_2)}{(ber'_0(m' r_2))^2 + (bei'_0(m' r_2))^2} \right) \quad (80)$$

The derivation for a tubular conductor is similar, but will not be repeated here. The results for current density and AC resistance from the full derivation [2] are:

$$J_r = J_{r_2} \left[\frac{J_0(mr)Y_0'(mr_1) - J_0'(mr_1)Y_0(mr)}{J_0(mr_2)Y_0'(mr_1) - J_0'(mr_1)Y_0(mr_2)} \right] \quad (81)$$

$$\frac{R_{ac}}{R_{dc}} = Re \left\{ \left[\frac{jmr_2(r_2^2 - r_1^2)}{2r_2^2} \right] x \left[\frac{ber_0(m'r_2) + jbei_0(m'r_2) - C(ker_0(m'r_2) + jkei_0(m'r_2))}{ber_0'(m'r_2) + jbei_0'(m'r_2) - C(ker_0'(m'r_2) + jkei_0'(m'r_2))} \right] \right\} \quad (82)$$

Where:

$$C = \frac{ber_0'(m'r_1) + jbei_0'(m'r_1)}{ker_0'(m'r_1) + jkei_0'(m'r_1)} \quad (83)$$

Formulas exist for the DC current densities and resistance of some asymmetric shapes, such as rectangular, triangular, and elliptical conductors. However, analytical solutions do not exist for the skin effect of any of these shapes. Rectangular conductors suffer from the edge effect, rather than the skin effect. It is the same phenomena, only the current density concentrates more towards the edges of the conductor rather than uniformly around the shell as in a cylindrical conductor. Researchers have worked on formulating mathematical theory for skin effect in rectangular conductors, but the solution remains elusive due to the asymmetry [11]. Elliptical conductors have an approximation of skin effect shown to be accurate within 1% of error [91].

2.7 Industry Practices

Conductor sizes are commercially defined in terms of their cross-sectional area, so conductors made with the same type of metal will have the same DC resistance regardless of the type of design. Metals with higher conductivity (e.g. copper vs aluminum) have lower DC resistances but higher AC/DC resistance ratios for equivalent cross-sectional areas and type of design. Generally, the overall AC resistance is still lower for the higher

conductivity metals, which therefore dominate usage for high capacity applications.

TABLE 2-5 provides a comparison of copper and aluminum, with values relative to copper:

TABLE 2-5: Comparison of copper and aluminum

Attribute	Copper	Aluminum
Cost	100%	33%
Weight	100%	30%
Conductivity	100%	61%
Pulling Strength	100%	75%
Diameter (for Equal R_{dc})	100%	128%
Corrosion	Less	More

Current industry practice for calculating the AC resistance of a power conductor is to first calculate the DC resistance at the desired operating temperature and then multiply it with factors representative of the increased percentage of resistance due to the skin and proximity effects. Calculation of AC resistance is complex, so simplified polynomial equations not requiring Bessel functions and complex numbers have been derived to approximate the true results [38]. To understand the origin of the simplified equations used in the industry it is important to understand the true analytical solution.

It is important to recognize that the commercially defined nominal cross-sectional areas do not exactly match the cross-sectional areas calculated with each conductor size's corresponding DC resistance. The reason for this is that historically, the design standards governing DC resistance had to cover many different design types. These included not only solid and stranded conductors, but also single conductor and three conductor core configurations. Any time helical geometry is introduced, as in stranded conductors and three core configurations, the shape of the strands becomes elliptical and the relative length per unit distance is increased. This results in an increased resistance, as well. Manufacturing practices cannot be standardized, so instead DC resistances are

standardized. Throughout this dissertation when referring to nominal cross-sectional area, “nominal” will specifically be written. Otherwise, it should be assumed that the true cross-sectional area is being referred to. The true cross-sectional areas of copper and aluminum do not match exactly when calculated based on their standardized DC resistances. This is mostly due the standardized DC resistances covering multiple conductor design configurations, but also partly due to rounding error since the DC resistances are set to a fixed precision of decimal points. A comparison of nominal conductor areas and actual areas calculated per the standardized DC resistances [92] is in TABLE 2-6:

TABLE 2-6: Nominal vs actual conductor areas

Area		Difference	Area		Difference
Nominal	True		Nominal	True	
mm ²		%	mm ²		%
Aluminum			Copper		
35	32.6	-7.0%	35	32.9	-6.0%
50	44.1	-11.8%	50	44.6	-10.9%
70	63.8	-8.9%	70	64.3	-8.1%
95	88.3	-7.0%	95	89.3	-6.0%
120	111.7	-6.9%	120	112.7	-6.1%
150	137.2	-8.5%	150	139.0	-7.3%
185	172.3	-6.8%	185	174.0	-6.0%
240	226.1	-5.8%	240	228.7	-4.7%
300	282.6	-5.8%	300	286.9	-4.4%
400	363.3	-9.2%	400	366.8	-8.3%
500	467.2	-6.6%	500	471.1	-5.8%
630	602.6	-4.3%	630	609.2	-3.3%
800	770.1	-3.7%	800	780.1	-2.5%
1000	971.3	-2.9%	1000	979.6	-2.0%
1200	1144.3	-4.6%	1200	1141.8	-4.9%
1400	1333.2	-4.8%	1400	1336.5	-4.5%
1600	1519.6	-5.0%	1600	1525.8	-4.6%
2000	1896.9	-5.2%	2000	1915.7	-4.2%
2500	2375.1	-5.0%	2500	2394.6	-4.2%
3000	2852.1	-4.9%	3000	2873.5	-4.2%

In simplified industry practices, three equations are used for calculating AC resistance [15] that introduce an experimentally derived skin effect coefficient k_s . This coefficient adds flexibility to the equations, as it is changed depending on the material and type of conductor. The same input argument used in the analytical solution of the Bessel functions is also used for the simplified polynomial equations, with the removal of the imaginary component and the addition of k_s . The recommended empirical factors in industry standards for k_s and k_p are shown in TABLE 2-7 [15]:

TABLE 2-7: IEC 60287-1-1 k_s and k_p factors

Type of Conductor	Insulation System	k_s	k_p
Copper			
Round, solid	All	1	1
Round, stranded	Fluid/paper/PPL	1	0.8
Round, stranded	Extruded/Mineral	1	1
Round, Milliken	Fluid/paper/PPL	0.435	0.37
Round, Milliken, insulated wires	Extruded	0.35	0.2
Round, Milliken, bare uni-directional wires	Extruded	0.62	0.37
Round, Milliken, bare bi-directional wires	Extruded	0.8	0.37
Hollow, helical stranded	All	*	0.8
Sector-shaped	Fluid/paper/PPL	1	0.8
Sector-shaped	Extruded/Mineral	1	1
Aluminum			
Round, solid	All	1	1
Round, stranded	All	1	0.8
Round, Milliken	All	0.25	0.15
Hollow, helical stranded	All	*	0.8

* See equation (84)

Note that a k_s of 1 represents no change to the approximated solution of the true analytical solution derived with Bessel functions. Hollow conductors have a special formula to calculate k_s , which is:

$$k_s = \left(\frac{d'_c - d_i}{d'_c + d_i} \right) \left(\frac{d'_c + 2d_i}{d'_c + d_i} \right)^2 \quad (84)$$

The Bessel function input argument is also written in terms of a standardized DC resistance [92], as opposed to conductivity and radius:

$$x_s = \sqrt{\frac{\omega\mu}{\pi R_{dc}}} k_s \quad (85)$$

Using this input argument the skin effect factor is calculated with one of three different formulas, depending on the value of x_s .

For $0 < x_s \leq 2.8$:

$$y_s = \frac{x_s^4}{192 + 0.8x_s^4} \quad (86)$$

For $2.8 < x_s \leq 3.8$:

$$y_s = -0.136 - 0.0177x_s + 0.0563x_s^2 \quad (87)$$

For $x_s > 3.8$:

$$y_s = 0.354x_s - 0.733 \quad (88)$$

These equations have a maximum error of less than 0.6% [70], which is considered negligible. Calculation of the proximity effect also uses empirically-derived equations created based on measurements. Equations have been developed for two conductors carrying single-phase current [38] and three conductors carrying three-phase current [93]. The process to calculate the proximity effect factor is the same as done to calculate the skin effect factor, just using different equations. First is to calculate the proximity effect Bessel function input argument:

$$x_p = \sqrt{\frac{8\pi f}{R_{dc}} 10^{-7} k_p} \quad (89)$$

Then for two conductors carrying single-phase current:

$$y_p = \frac{x_p^4}{192 + 0.8x_p^4} \left(\frac{d_c}{s}\right)^2 \cdot 2.9 \quad (90)$$

Or three conductors carrying three-phase current:

$$y_p = \frac{x_p^4}{192 + 0.8x_p^4} \left(\frac{d_c}{s}\right)^2 \left[0.312 \left(\frac{d_c}{s}\right)^2 + \frac{1.18}{\frac{x_p^4}{192 + 0.8x_p^4} + 0.27} \right] \quad (91)$$

The proximity effect is relatively small compared to the skin effect at power frequencies, as it decreases exponentially with separation of conductors and is considered negligible when axial spacing exceeds about five times the conductor diameter [31]. The proximity effect is independent of the skin effect, and thus beyond the scope of this dissertation and will not be discussed further. The skin and proximity effect factors are finally used to calculate the AC resistance of an extruded dielectric cable conductor:

$$R_{ac} = R_{dc}(1 + y_s + y_p) \quad (92)$$

It can be observed that y_s and y_p are equivalent to a percentage of increase in AC resistance from DC resistance caused by the skin and proximity effects, respectively. The DC resistance given here is the DC resistance at operating temperature. Since the DC resistances are defined at 20°C [92], there is also a formula to convert the table value to the correct operating temperature [15]. This is:

$$R_{dc} = R_0[1 + \alpha_{20}(\theta - 20)] \quad (93)$$

The temperature coefficient is assumed to be a constant value that is specified by standards [15]. This allows for the DC resistance at the operating temperature of the conductor to be calculated using a linear equation. It should be noted, however, that the temperature coefficient is truly a non-linear value. In the temperature range used here for power conductors, using a constant temperature coefficient and a linear equation for DC resistance at operating temperature is extremely accurate. For ACSR conductors the temperature coefficient is commonly calculated based on the aluminum alone, neglecting the effects of steel. Taking the steel into account would result in an error of at most 0.05% [94]. In general, on any two metals as similar as copper and aluminum the error would be negligible even if the temperature coefficient were based on only one metal. However, for complete accuracy when bi-media conductors are used each DC resistance is individually calculated with its linearized temperature coefficient.

Small conductors are generally composed of one solid wire. Large conductors are composed of several smaller wires helically twisted together. Segmented conductors, composed of multiple pie-shaped segments of stranded conductors, are used for very large conductors. Conceptually, segmented conductors aim to reduce inter-wire conduction as much as possible [70]. While this reduces the skin effect, it introduces eddy-currents arising from the proximity effect between the insulated segments. The segmented conductors, unlike stranded conductors, have the individual wires rotating from the inside to outside of the conductor. This causes a partial cancellation of the emf, and thus reduces skin effect as well [75]. Generally, there are 4-6 such segments in addition to an inner solid or stranded core, although designs with nine segments have been made [95]. The switch from solid to stranded conductors depends on the application, and for power transmission

and distribution the largest typical solid conductor outer diameters (ODs) are in the 10-15 mm range. Stranded conductors are then usually used up to an outer diameter in the 35-40 mm range. For conductor diameters exceeding this range, it is common to use segmented conductors. These give additional benefits in reducing the AC/DC resistance ratios, and are then used on conductors with outer diameters up to 70 mm. The switch from stranded to segmented can be seen in terms of diameter and area in FIGURE 2-9:

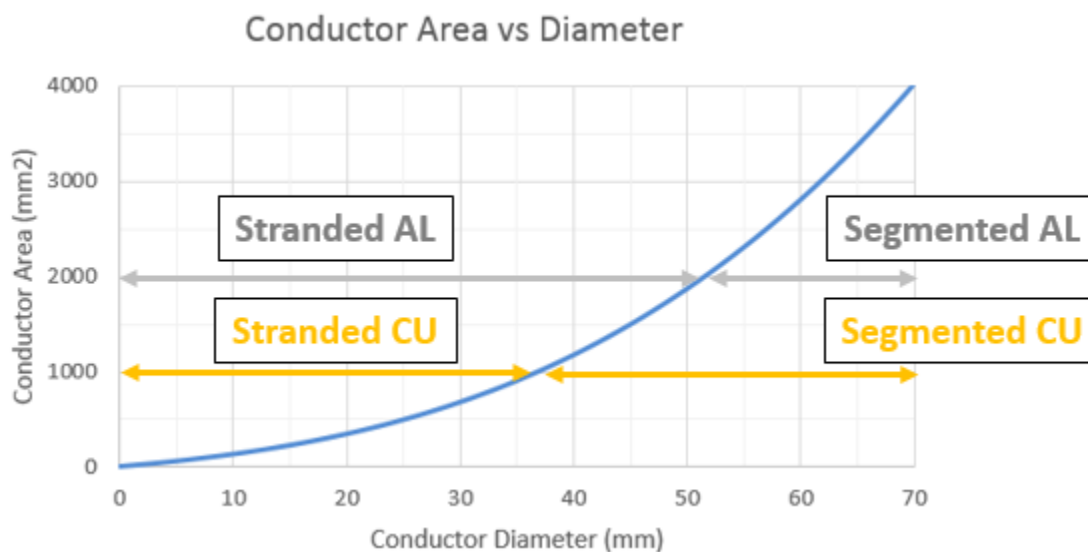


FIGURE 2-9: Conductor type by diameter and area

Whereas the AC/DC resistance ratios for solid and stranded conductors are very accurate and reproducible, segmented conductors have much variability. This is due to many factors, including a lack of explicit solutions for such designs, variability in the number of segments, variability in impregnation of the core, variability in compression of the insulation affecting contact resistance, and different types of barrier tapes used (if at all). To address this variability Cigré working group B1.03 performed analysis of such designs and recommended the revised skin effect factors for segmented copper conductors and segmented aluminum conductors shown on TABLE 2-7 [70]. Segmented conductor designs and manufacturing techniques vary between manufactures, and therefore the AC

resistance of a standardized size segmented conductor will also vary. To address this, Cigré working group B1.03 further recommended that AC resistance be measured during qualification testing. Cigré working group D1.54 is currently working on developing a guide for measurement of AC resistance [96]. Current design standards [15] were recently updated in 2014 taking these recommendations into account. The k_s factor can cause quite a large difference in the AC/DC resistance ratio, shown here calculated per industry standards at 90°C and 60Hz in FIGURE 2-10:

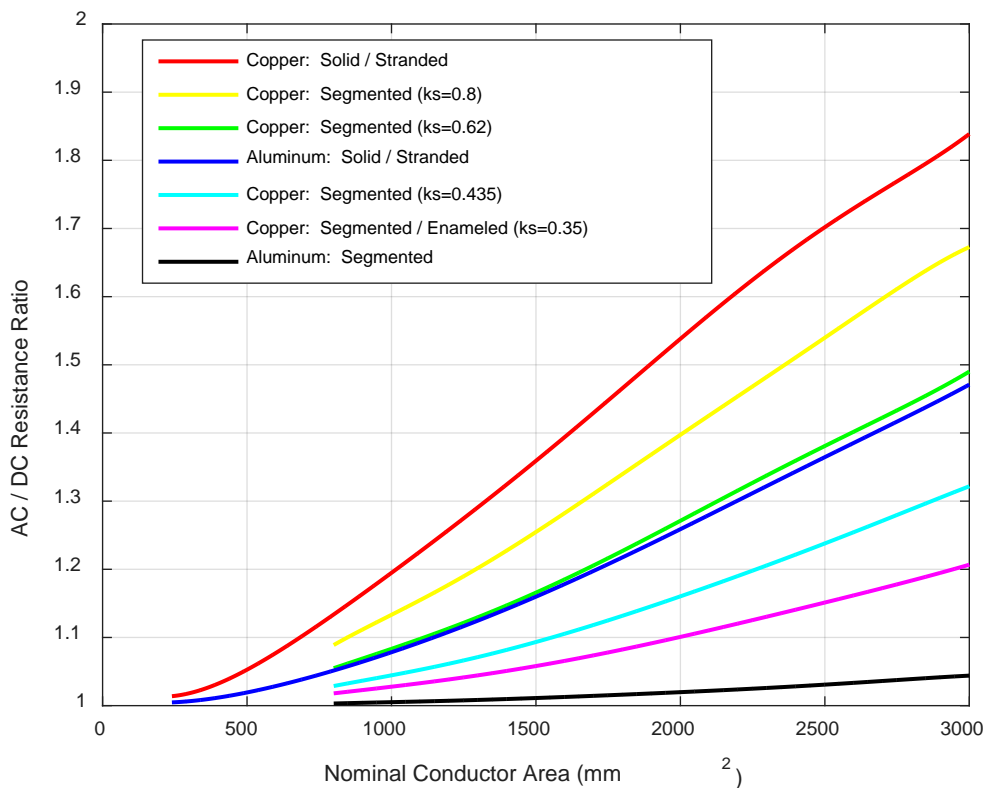


FIGURE 2-10: AC/DC resistance ratios

An additional conductor design technique for reducing AC/DC resistance ratios involves insulating the wires (shown on the chart using $k_s = 0.35$). Although effective, the effectiveness, like for segmented conductors, depends on variables that inherently cannot be controlled and thus such designs suffer from the same issues of inconsistency.

Additionally, such designs introduce new application problems during jointing and terminating cables.

The background knowledge has now been established for the mathematical theory in calculating skin effect of a single medium conductor. It has also been shown how the industry addresses the complexity in implementing the mathematical theory as well as the design techniques used to mitigate the increased skin effect on large power conductors. The next chapter will now discuss the motivation in using bi-media conductors in the power industry. This includes the hypothesis for the formulation of the mathematical theory in addition to an explanation of the value bi-media designs present to the industry.

CHAPTER 3: PROBLEM STATEMENT

3.1 Overview

This chapter covers the framework of what is needed to be done in order for this research to introduce optimized bi-media conductor designs to the power industry. It discusses in detail the thought process behind the proposed work and how the current industry practices and design techniques could be improved upon. In the identification of research gaps, the chapter also addresses pertinent research questions and hypotheses to which this thesis is expected to be a valuable contribution. Also discussed is what modeling assumptions were made in the creation of this dissertation. The mathematical complexity of the problem had to be handled very carefully, and a lot of quality control has been performed. Multiple layers of programming functions were used in handling the Bessel equations. To ensure accuracy along the way, outputs at each step were compared to known results in available published literature. These comparisons are shown to demonstrate the conformity of the outputs of the code written to known solutions when possible, and FEA generated approximated solutions when analytical solutions did not exist.

3.2 Research Questions and Hypothesis

World energy consumption is increasing exponentially, and the demand for lower resistance conductors that can transmit more power is constantly increasing. Low and accurate AC resistance is paramount to conductor ampacity. As described previously, for

copper conductors the power industry generally switches from stranded designs to segmented designs on nominal cross-sectional areas greater than 1000 mm² [12]. However, segmented designs suffer from the problem of uncontrolled variability of AC resistance, due to variability in manufacturing and the fact that very little measurement information exists to confirm empirical factors being used to adjust known solid and stranded AC resistance to expected segmented AC resistance [70]. Besides the solid round conductor the only other design that is mathematically defined is the solid hollow tube conductor [2]. These designs can also be stranded, for which the error of the AC resistance approximation is negligible [32].

Hollow conductors are not currently being used in place of segmented conductors. Additionally, there are no defined dimensions for hollow core conductors. When hollow core conductors are used in the power industry it is for special application driven purposes, such as self-contained fluid-filled (SCFF) cable conductors [75]. Such design has the hollow core for a pressurized dielectric fluid. Hollow core copper conductors have been used on transmission lines as long ago as the early 1930s by General Cable. Designs known as the type HH were composed of interlocking “tongue and groove” sections of copper. The main purpose of these conductors was the reduction of weight coupled with the high conductivity of copper and the ability to pump gas or oil through the center [97]. While it was known these conductors obtained a lower skin effect (AC/DC resistance ratio) than solid core conductors, their development was application driven and the designs were not optimized such that the lowest AC resistance could be achieved. Due to their lower capacity compared to large aluminum conductors, they quickly became obsolete.

Hollow core conductors are most often used at radio frequencies, for which the skin depth is very small. The rule of thumb used in microwave engineering is that there should be at least five skin depths of low-loss conductor. With five skin depths it can be guaranteed that over 99% of the current flows within the area of the low-loss medium. At 1 GHz, skin depth is approximately $2\ \mu\text{m}$; therefore, it is easier to over-engineer the amount of low-loss conductor and use $10\ \mu\text{m}$. However, what about at power frequencies where the skin depth is 8.5 mm for copper and 10.9 mm for aluminum? A $1000\ \text{mm}^2$ conductor has an equivalent solid radius of 17.8 mm, which is only about 2 skin depths. It can also be observed that 100% of the current must travel within this area. The concept of skin depth pertains to a mathematical limit as the depth becomes infinite. When examining a problem where the total size of the conductor is of the same order of magnitude as the skin depth, the solution is not as simple. It can also be observed through the mathematical limit of skin effect that at an infinite depth the current density at one skin depth will be $1/e$, or 37%, of its surface value [8]. For a conductor that is of the same order of magnitude as the skin depth, the current density at one skin depth will be greater than 37% of its surface value. Great care must be taken, as removal of part of the conductor causes a redistribution of the current density, such that 100% of the total current must still flow within the given cross-sectional area [36]. At a point, the center of a conductor could be removed with no noticeable impact on AC resistance, but such is not the case for large conductors at power frequencies. Is there an optimal dimensional point that exists in the design of hollow core conductors in this application? If so, is there a range that exists where a hollow core conductor is more cost effective than a segmented conductor of the same AC resistance? Assume two conductor designs of equal AC resistance were manufactured using the same

metal: one hollow core conductor and one segmented conductor. Ignoring the higher manufacturing costs to produce the segmented conductor, it would only be necessary that the cross-sectional area of the hollow core conductor were less than that of the segmented conductor in order for the material costs of the hollow core conductor to be less than those of the segmented conductor. This would make the hollow core conductor the obvious choice in place of a segmented design.

Bi-media conductors may also have an application window. Hollow core conductors are a subset of bi-media conductors, whereas the inner medium is air [12]. But is there a medium aside from air that would be more ideal? Steel cores are used in the middle of aluminum-conductor steel-reinforced (ACSR) designs, but such conductors get no benefits of lower AC resistance. Steel is important in the application of ACSR, and it has a high tensile strength and allows for long spans of overhead (OH) lines. Can another good conducting metal, such as aluminum, be used in place of air as a way to improve AC resistance? Does adding another metal in the inside of a conductor causes partial redistribution of current density compared to a hollow conductor, resulting in a more favorable solution? Current density starts at its largest value at the surface of a conductor and attenuates moving radially inward. Because copper is more conductive than aluminum and current density is highest on the outside of the conductor, a reasonable assumption is that the ideal combination of a bi-media copper and aluminum conductor would be copper on the outside and aluminum on the inside. This way the more conductive medium is in the same location of the highest current density. Can a mathematical theory be developed, such that a closed-form solution is found to calculate the current density in a bi-media conductor? If a theory is developed, how can it be verified? Copperweld® currently makes

a bi-media conductor known as copper-clad aluminum [4]. As the name implies, it is a solid round aluminum conductor that is clad with a solid layer of copper. The application purpose of this design is to get the low-cost benefits of aluminum and good corrosion resistance and electrical contact benefits of copper. However the conductor design is currently rated as if it were all aluminum [98]. This is deemed acceptable since the largest cross-sectional area of this design is #1/0 AWG (53.5 mm^2), which has a radius of 4.1 mm. This is less than half of the skin depth, and it is therefore unlikely such a small conductor at power frequencies could be optimized to improve AC resistance by adjusting dimensional characteristics. It would be good to have some verification testing done on a large stranded conductor to show the theory is valid on a design of the application for which it was intended. Could such a design be made? Manufacturing and installation of stranded conductors of bi-media designs could prove challenging, as the hardness of each metal is different, which could affect drawing and compression. Finally, after the designs were made, what additional application challenges might be faced? Two media would have two different sets of properties, such as thermal expansion. Could all the required connectors and accessories be found or devised to address any potential issues?

If the mathematical theory can be conceived and validated through laboratory measurements, how can this information be made available to the public in a usable fashion? Even the simplest case of a solid round conductor has a true solution that is very difficult and time consuming to calculate. As is currently the normal industry practice, simplified equations that mimic the true solution are used by engineers working in the power industry [15]. These equations have the advantage of not requiring imaginary numbers and Bessel functions. The simplified equations make it such that the AC

resistance at a given operating temperature and frequency can be calculated with the DC resistance, which is easily measured during routine factory production testing. Therefore, a simplified polynomial equation must first be created for the optimal inner medium area given the total area. This will fully define the optimal conductor design from the dimensional standpoint and DC resistance. Following this, another polynomial equation needs to be developed such that the same Bessel function input argument current industry standards use to produce a skin effect factor can be used to define a skin effect factor for the bi-media conductors. This way AC resistance can be easily calculated. Alternatively, if it is possible to find an adjusted k_s value instead of creating a new polynomial equation that would also be an acceptable solution. However, this is unlikely since the current polynomial equations were designed to match solid/stranded conductors and the k_s factors were selected to match a few measured available data points for segmented designs. Most likely new polynomial equations are to be created. Currently, industry standards use one of three equations for calculating the skin effect factor depending on the size of the Bessel function input argument. These three equations will likely be different, as well. This is to be examined also, and error between the polynomial approximations and the true analytical solution should be evaluated to ensure accuracy over the entire range of temperature and frequency. This would give industry practitioners a simple way of designing a conductor of any cross-sectional area. However, the industry currently uses standardized nominal cross-sectional areas to reduce the number of conductor designs and simplify procurement and installation practices. Therefore, it would also be beneficial to have standardized bi-media designs created with the same nominal cross-sectional areas [92] of existing standardized single medium designs.

The cost effectiveness of a bi-media conductor may not be obvious when comparing a bi-media design to a single medium design. Single medium designs only have a single material price for the medium being used, and therefore material costs difference of single medium designs can be directly compared using only the cross-sectional area of the conductor. In some, or possibly all cases, a larger cross-sectional area bi-media conductor may be required as compared to a segmented copper conductor with an equivalent AC resistance. However, this doesn't mean the bi-media conductor would be a less ideal choice. The price (currently) and density of aluminum are about one-third that of copper. That means that even a bi-media aluminum/copper conductor with a larger cross-section than a segmented copper conductor having the same AC resistance could still potentially be lighter and/or less expensive. Of course, this introduces variables that change with time: the price of copper and aluminum. So how can this be presented such that it is independent of today's prices of the media to be used? For this it is assumed that there exists some ratio of cost between the two media at which point the material costs for both designs would be equal. Note that this ratio would represent the point at which the material cost to manufacture both conductors providing equivalent current carrying capacity would be equal. Therefore, by knowing the current ratio of cost of copper to aluminum one could quickly know if a certain bi-media design would be more cost effective at any point in time. Moreover, the cost analysis is complicated by the fact that there is one special design of segmented copper conductors that has a different material cost than the others. This is a segmented copper conductor where the individual copper wires are enameled. The enamel helps to insulate the strands from each other, thus keeping current density higher in each wire individually. The cost to enamel wires is very high,

currently today causing nearly a 30% increase on the cost of just the copper. So how can the cost of this process be captured to compare to a bi-media conductor? The solution for this is to define the cost of the enameling as a percent cost increase on the copper wire. Therefore, there will be a copper to aluminum cost ratio for each percent cost increase to enamel the copper wires. Tables can be created for each k_s value used in the design standards to show what the equivalent bi-media conductor design at a given operating temperature and frequency would be. Additionally, the cost ratio required to make it a viable solution should be presented. This data should also be summarized at each operating temperature and frequency showing whether the more cost effective solution is the segmented conductor or a bi-media conductor.

3.3 Modeling Assumptions

Modeling of the analytical solutions is done using the MathWorks, Inc. software MATLAB. MATLAB is a discrete implementation of a continuous problem. However, enough points is chosen to obtain accurate solutions. Also, special control statements are used at extreme points that could cause error. For example, zero is a valid point along the radius but must have special statements to avoid errors in coding that manifest themselves in the results. MATLAB was also used to model approximate solutions that exist in the literature. These polynomial equations (i.e. equations (86) to (88)) used in the industry are very accurate to the true Bessel function solutions, and therefore can be used as an accuracy check for the analytical results.

It was mentioned previously that it is assumed the media used in the conductor for the derivation of skin effect in a solid round or solid hollow tube conductor are linear, isotropic, homogeneous, isothermal and non-ferrous. These same assumptions are made

for the media used in the bi-media design. These five assumptions have the following implications:

- the material is linear if the conductivity does not vary with the application of the electric field,
- the material is isotropic if the conductivity does not vary with direction,
- the material is homogeneous if conductivity is the same at all points,
- the material is isothermal if it is the same temperature at all points, and
- the material is non-ferrous if it does not contain appreciable amounts of iron.

Since material conductivity is dependent on temperature, assuming isothermal conductors eliminates any non-uniformity in conductivity throughout the conductor. As previously mentioned, it is possible on bare overhead conductors that there can be a temperature gradient. When conductors have a steel (i.e. ferrous) core, such as ACSR designs, the permeability also changes as a function of temperature and must be accounted for [99]. ACSR conductors have magnetic core losses in the steel resulting from both eddy current losses and hysteresis losses. The high non-linearity of the hysteresis losses makes it impossible to calculate AC resistance in ACSR conductors [27]. Additionally, in ACSR conductors the number of aluminum wires has an impact on the temperature gradient [100], as it also does on permeability of the steel core and current density [101] [102]. Approximate formulas exist to calculate the temperature gradient for solid/stranded designs, as well as solid/stranded tubes with non-ferrous inner media [103]. A lot of work has been done to raise concern over the effects of the temperature gradient on conductors [104] [103] [105]. However, for the application of large conductors the medium is usually copper and there is no need for steel cores providing mechanical tensile strength since the

cable is typically buried underground. Further, the temperature gradient is very small in the conductor, as all the surrounding layers of cable materials and soil dissipate heat much slower than air. Therefore, the assumptions that the conductor is non-ferrous and isothermal is valid for bi-media conductors when used in the application of large underground power conductors. Therefore, it can be assumed that all five assumptions discussed above have negligible impact on all results obtained in this thesis.

An assumption made, and previously verified through laboratory measurements, is that stranded conductors have an approximately equivalent AC resistance to solid conductors of the same cross-sectional area. This is also true for stranded tube conductors, where the stranded tube would have the same AC resistance as a solid tube having the same inner diameter. These assumptions are also expected to hold true for stranded conductors when two media are used. Furthermore, this assumption is to be tested and verified through laboratory measurements on a large stranded bi-media conductor.

3.4 Research/Verification

Extensive recreation of existing functions was required for this work. The first step was the creation of the Bessel functions in MATLAB. MATLAB has built in Bessel functions, but had to be separated into real and imaginary parts for solutions using *ber*, *bei*, *ker*, and *kei*, as well as their derivatives. These functions only take a real value as the input argument, and the complex number is added within the function. Further, many equations use Bessel functions multiple times, making the code very cumbersome to write and follow. Therefore, simplified functions were generated to implement Bessel functions of the first, second, and third kinds. Some of these functions have special statements added to avoid singularity errors with input arguments of zero. Limitations in modeling Bessel functions

with computers has been a research interest for some time. Researchers have done many studies on the errors that can be created implementing Bessel functions in an automated fashion [39]. Bessel functions normally take a complex input, but to simplify the MATLAB Bessel functions code, the imaginary number was added within the functions. The MATLAB code for all customized Bessel functions shown in FIGURE 3-1 through FIGURE 3-5 can be found in Appendix A. Plots showing Bessel functions of the first kind and their derivatives separated into real and imaginary parts from available literature [106] compared to the outputs from the functions written in MATLAB are shown here in FIGURE 3-1:

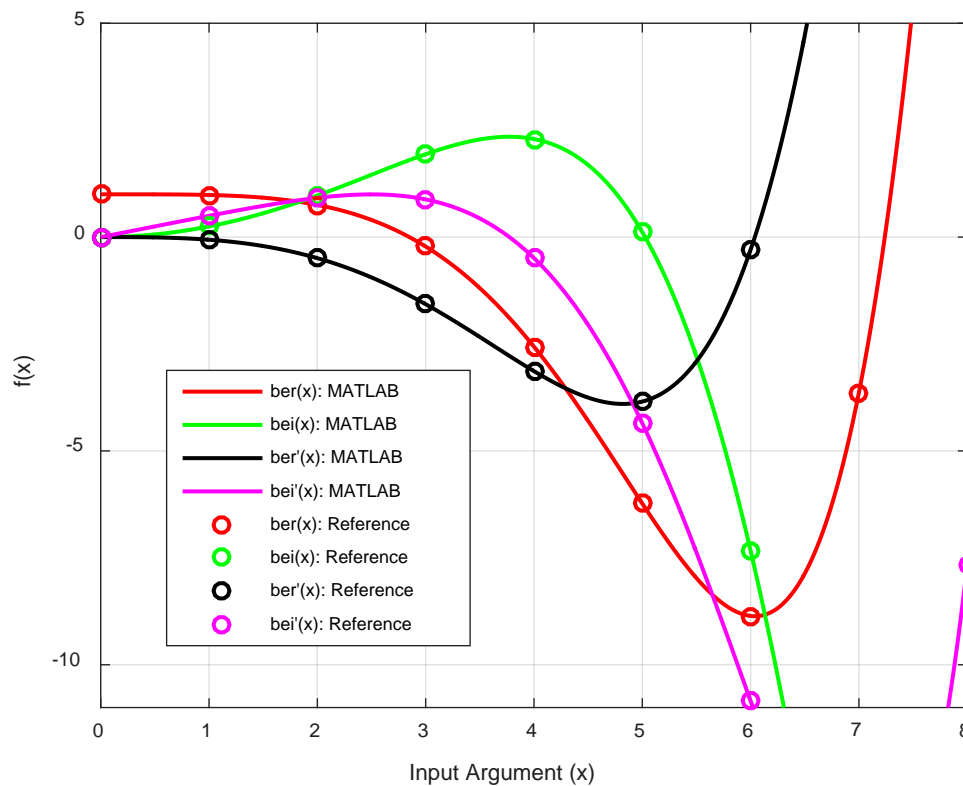


FIGURE 3-1: Separated Bessel functions of the first kind

Plots showing Bessel functions of the second kind and their derivatives separated into real and imaginary parts from available literature [106] compared to the outputs from the functions written in MATLAB are shown here in FIGURE 3-2:

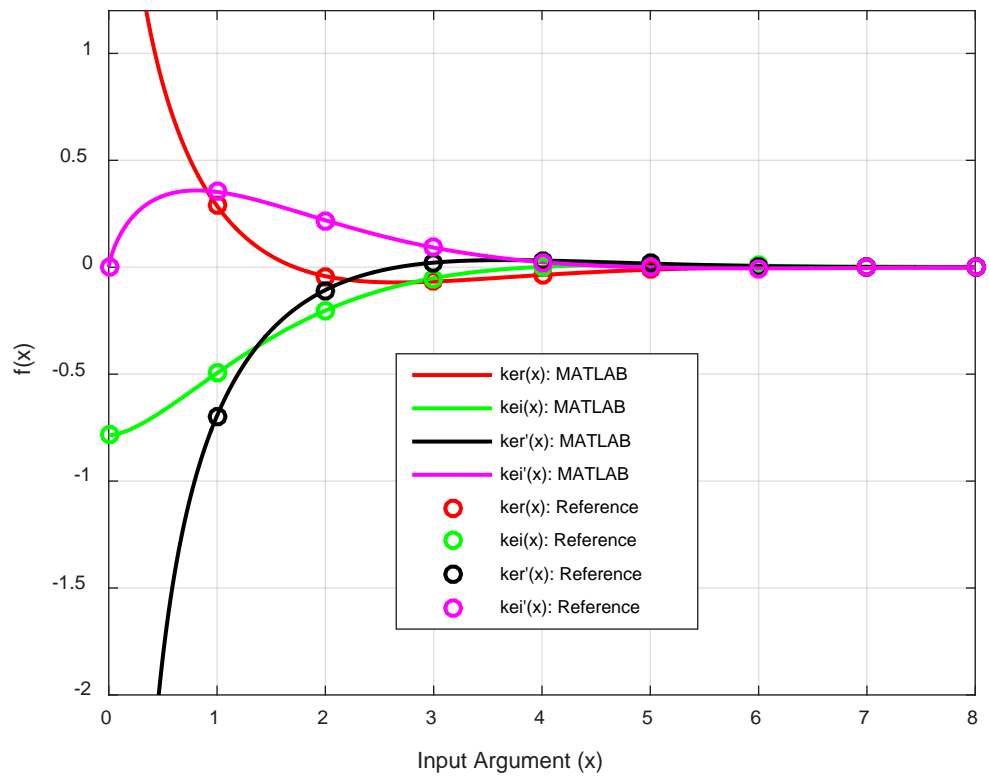


FIGURE 3-2: Separated Kelvin functions of the first kind

The following plots for all three kinds of Bessel functions of zero order were created directly in MATLAB and compared to modified custom functions written in MATLAB for accuracy, shown in FIGURE 3-3 and FIGURE 3-4:

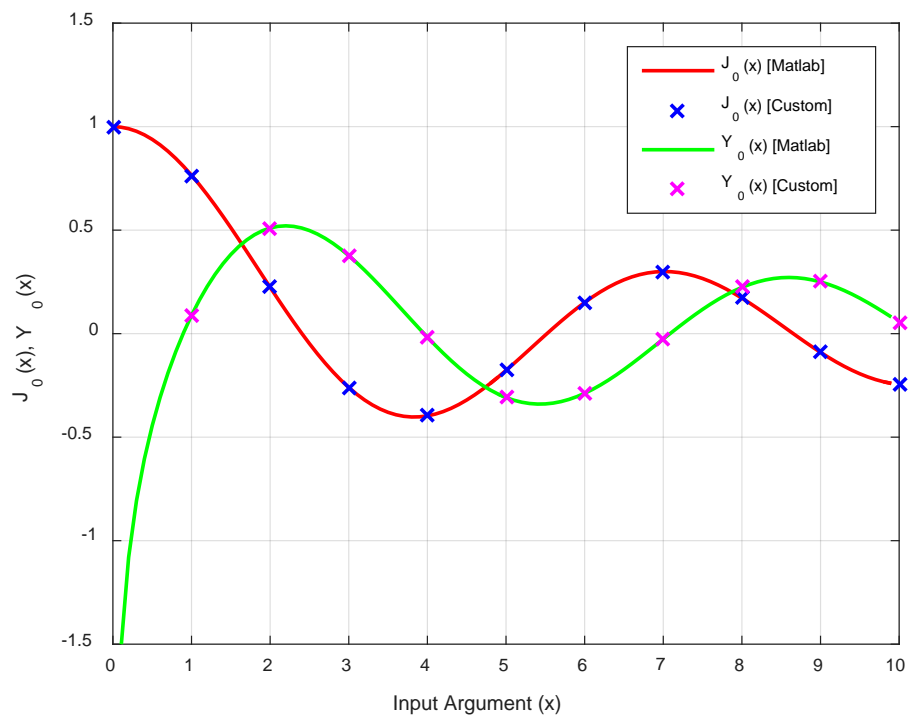


FIGURE 3-3: Comparison of zero order Bessel functions (1st and 2nd kinds)

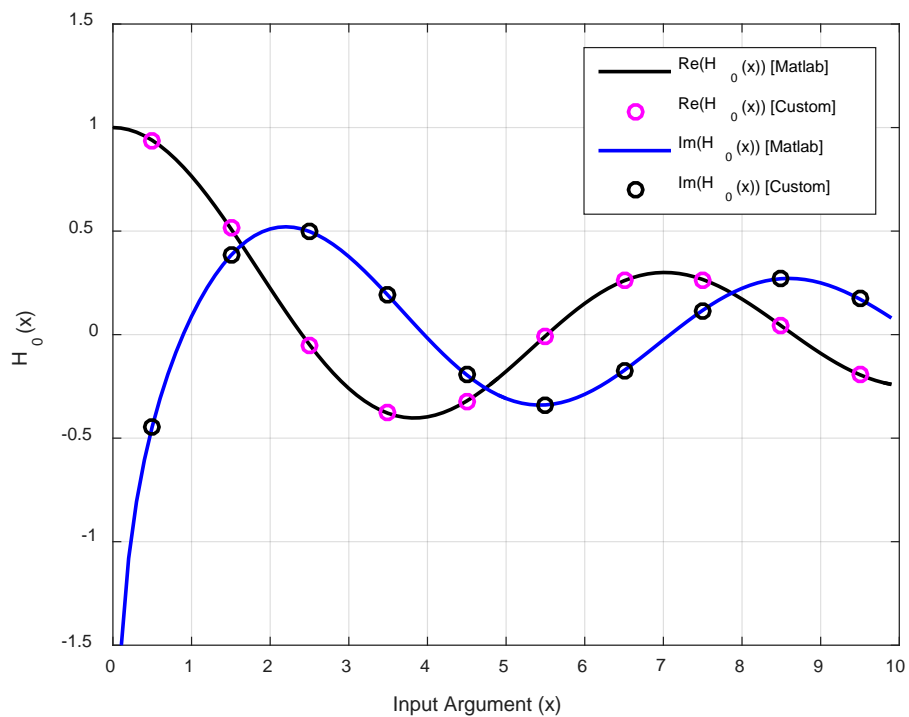


FIGURE 3-4: Comparison of zero order Bessel functions (3rd kind)

Note that since the Bessel function of the third kind is a combination of the first and second kinds for the same inputs of the other two functions, the real part overlaps with J_0 and the imaginary part overlaps with Y_0 (i.e. see equations (31) to (33)). The following plots for all three kinds of Bessel functions of the first order were created directly in MATLAB and compared to the modified custom functions written in MATLAB for accuracy, shown in FIGURE 3-5 and FIGURE 3-6:

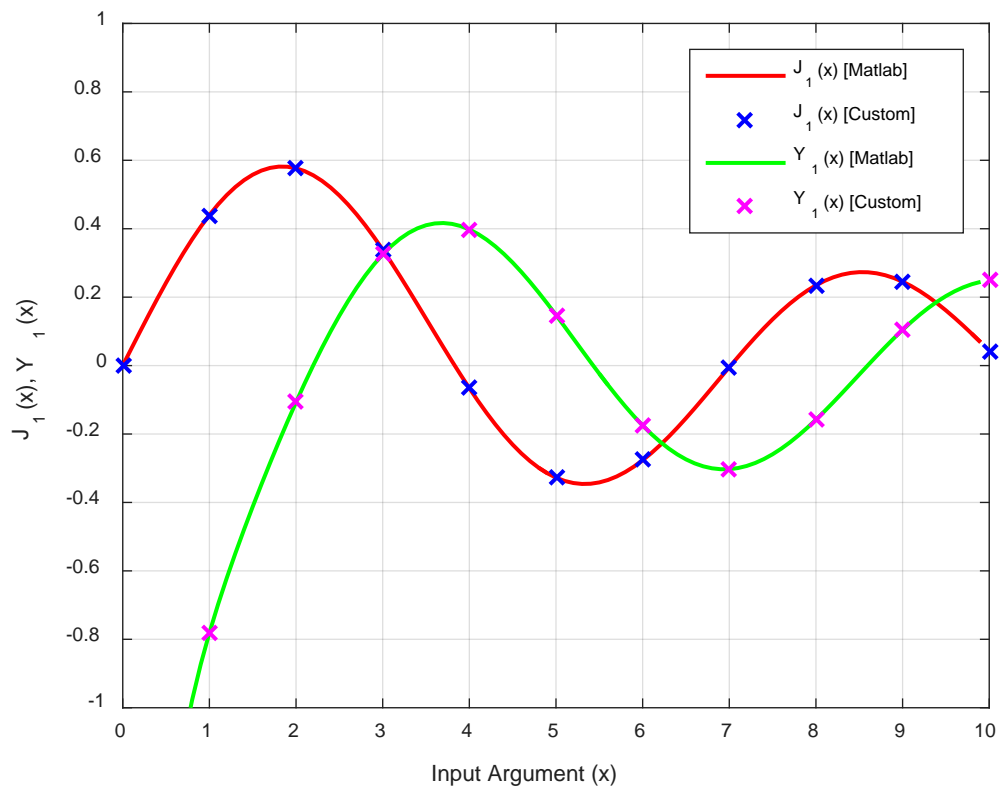


FIGURE 3-5: Comparison of first order Bessel functions (1st and 2nd kinds)

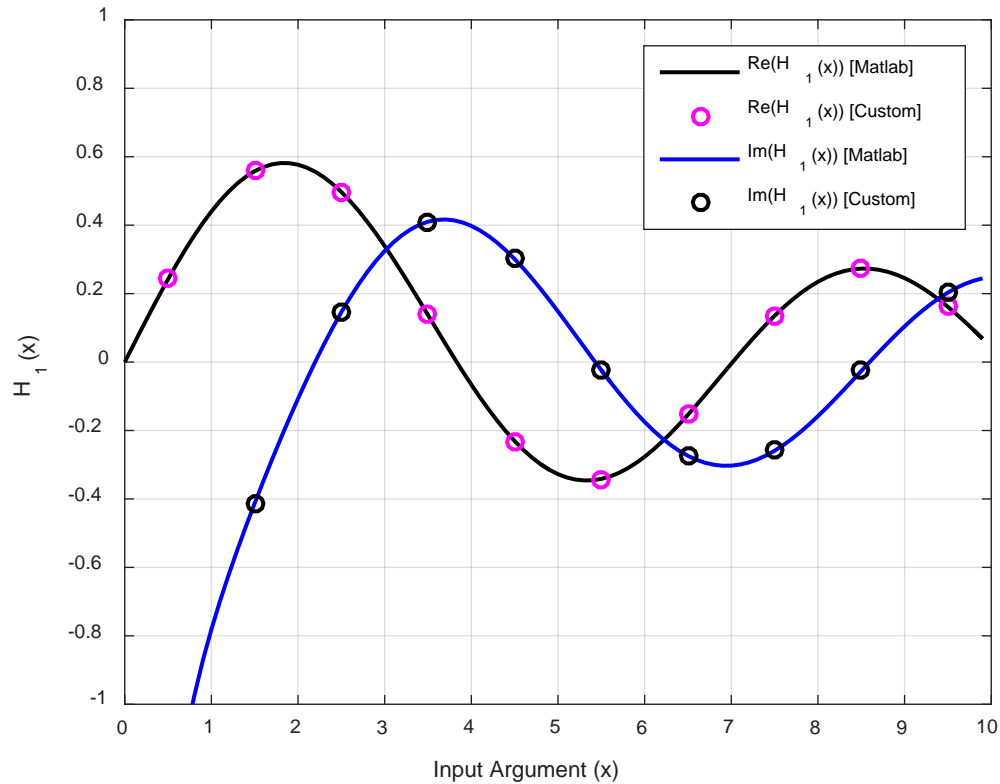


FIGURE 3-6: Comparison of first order Bessel functions (3rd kind)

Note again that since the Bessel function of the third kind is a combination of the first and second kinds for the same inputs of the other two functions, the real part overlaps with J_1 and the imaginary part overlaps with Y_1 (i.e. see equations (31) to (33)).

The next step was to take the custom Bessel functions generated and show that they could be used to generate the current density. Scaled current density is used instead since this makes viewing the current density behavior through the conductor more straightforward (see equation (64) for current density: note that if the surface current density $J_{r2} = 1 \text{ A/m}^2$ then the current density equation is scaled). Both the scaled and non-scaled current density can be used to calculate the skin effect, as the behavior of the current density is the same. The scaled current density can be scaled to the true current density by multiplying all the scaled current density values with the current density at the surface of

the conductor. Available literature has shown the following results on a 1 mm radius copper wire over a range of frequencies from 1 kHz to 1 GHz [107], which were compared to current density values obtained using the custom Bessel functions written in MATLAB shown in FIGURE 3-7:

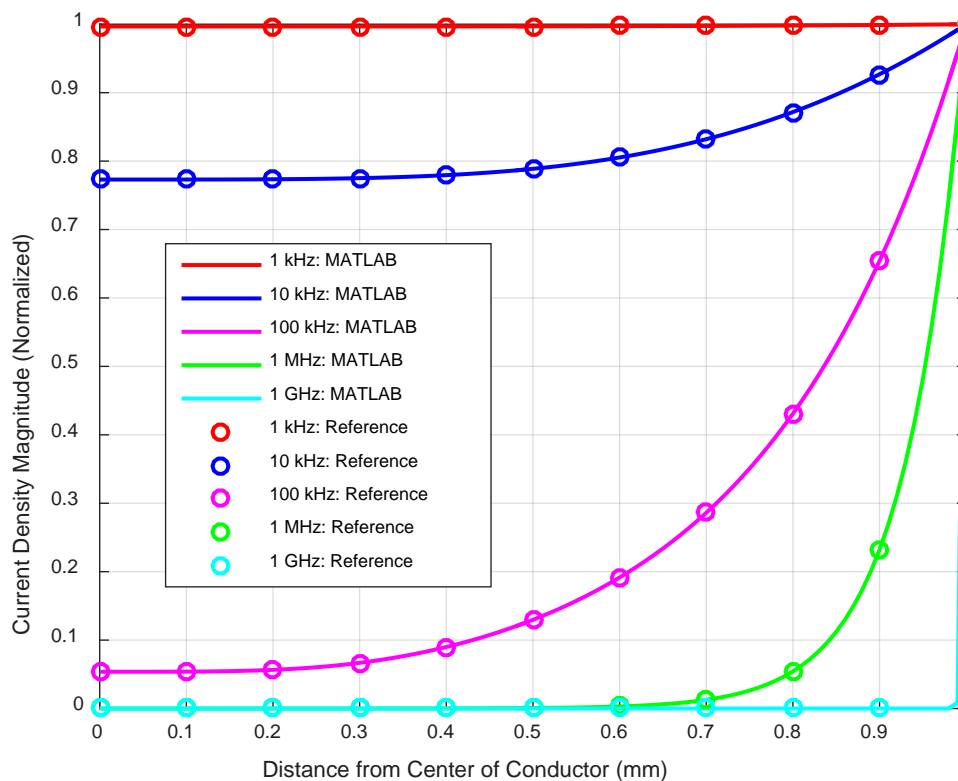


FIGURE 3-7: Scaled current density magnitudes

The current densities plotted throughout this dissertation always refer to the current density within a specific conductor. These results show a perfect match for the expected current density over a wide range of frequencies. It is also interesting, from these plots, to observe what is happening to the current density magnitude for each frequency plotted relative to the skin depth for each corresponding frequency. The skin depths at the different frequencies plotted are shown on TABLE 3-1:

TABLE 3-1: Skin depth at various frequencies

Frequency	Skin Depth	Distance from Center of Conductor
	(mm)	(mm)
1 kHz	2.090	-
10 kHz	0.661	0.339
100 kHz	0.209	0.791
1 MHz	0.066	0.934
1 GHz	0.002	0.998

The skin depth would be measured from the outside of the conductor, or from the right side of the plot. For this reason the distance from the center has also been listed to make it easy to line up on the plot where the skin depth would be for each frequency. It can be observed the higher the frequency the closer the skin depth location is to its mathematical limit of $1/e$, or 37% the current density at the surface. The current density distribution typically seen on large conductors operating at power frequency is most similar in nature to the current density distribution on a 1 mm radius conductor operating between 10 and 100 kHz. Therefore, when the size of conductor and skin depth are of the same order of magnitude, the magnitude of the current density will be larger than 37% of its surface value.

Now that the current density has been obtained the next step is to verify that the correct AC/DC resistance and inductance ratios can also be obtained. Because the Bessel function input argument is a calculated value it is easier to ensure accuracy by first using assumed Bessel function input arguments, rather than ones calculated specific to the conductor being modeled. Using this method also allows for comparison to results available in literature. The Bessel function input argument corresponds directly to a given conductor radius, and by extension cross-sectional area, for both copper and aluminum at a given frequency, as shown in FIGURE 3-8:

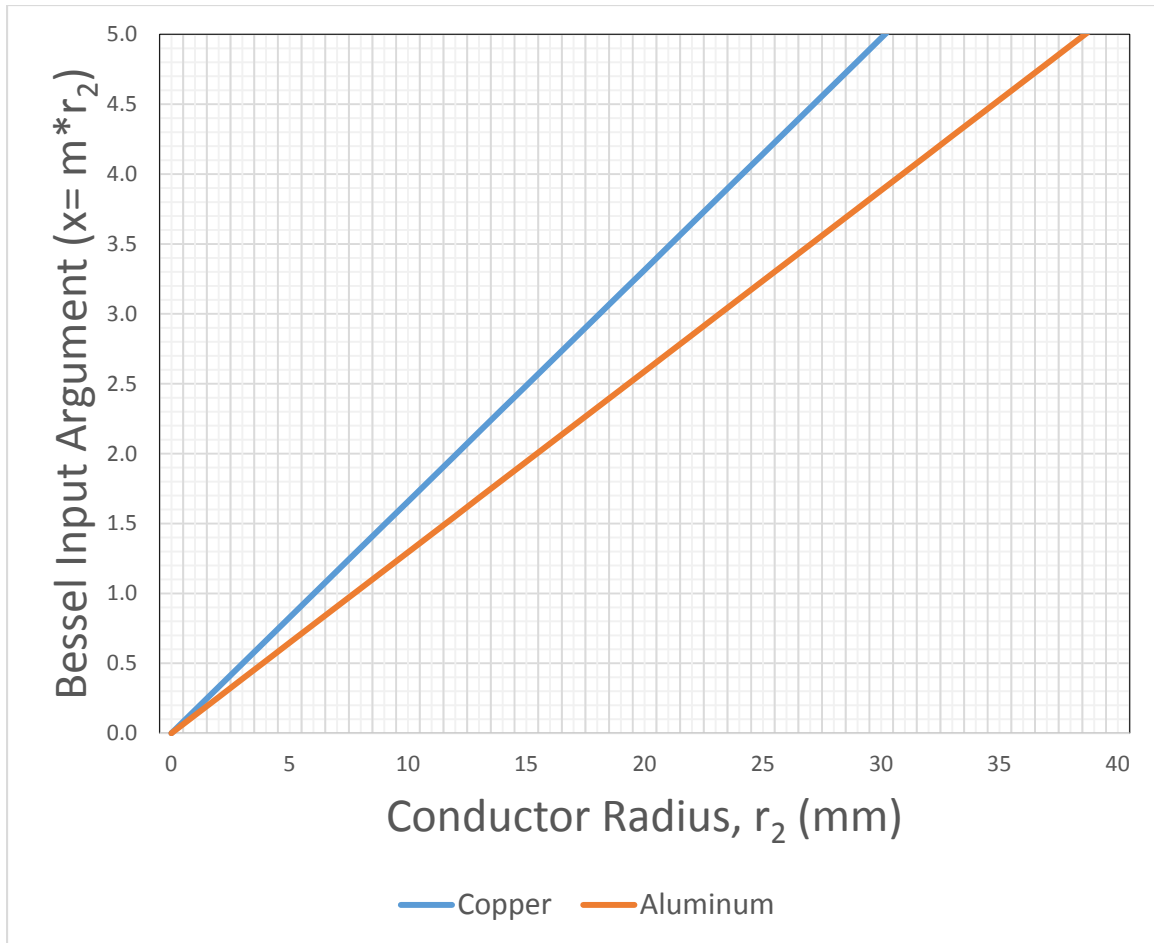


FIGURE 3-8: Bessel function input argument vs conductor radius

It can be noted a conductor radius of 17.8 mm corresponds to 1000 mm², after which copper conductors are generally segmented. Furthermore, a conductor radius of 30.9 mm corresponds to 3000 mm², which is a cross-sectional area still considered experimental and not currently specified in design standards. Therefore, the Bessel function input argument is rarely larger than 5.0 when calculating skin effect in large power conductors and the following plots are for Bessel function input arguments up to 5.0. Using AC/DC resistance and inductance ratios from published literature [108] FIGURE 3-9 and FIGURE 3-10 were created, for AC/DC resistance and inductance, respectively:

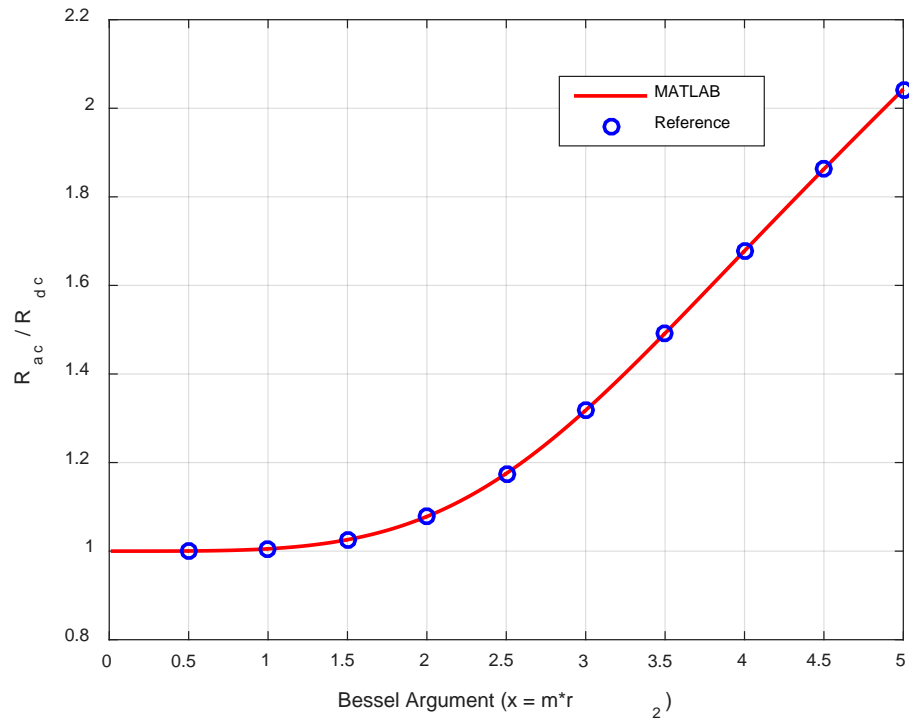


FIGURE 3-9: AC/DC resistance using Bessel input argument

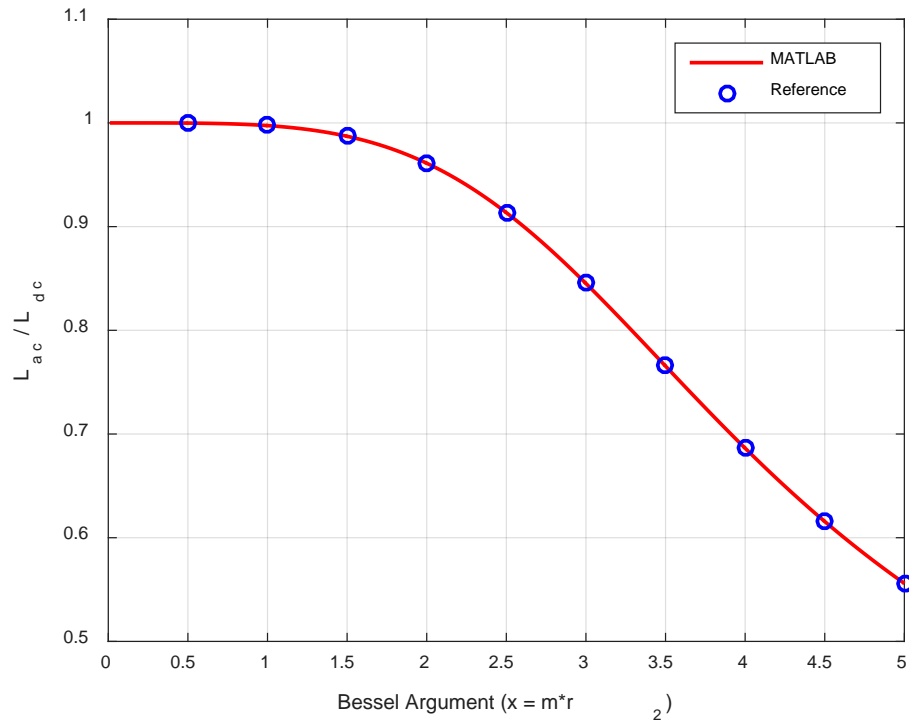


FIGURE 3-10: AC/DC inductance using Bessel input argument

The next step in the recreation and verification of the coding was to check the true analytical solutions using the Bessel functions with calculated input arguments and compare them to the industry published simplified polynomial equations. The results of this are shown in FIGURE 3-11:

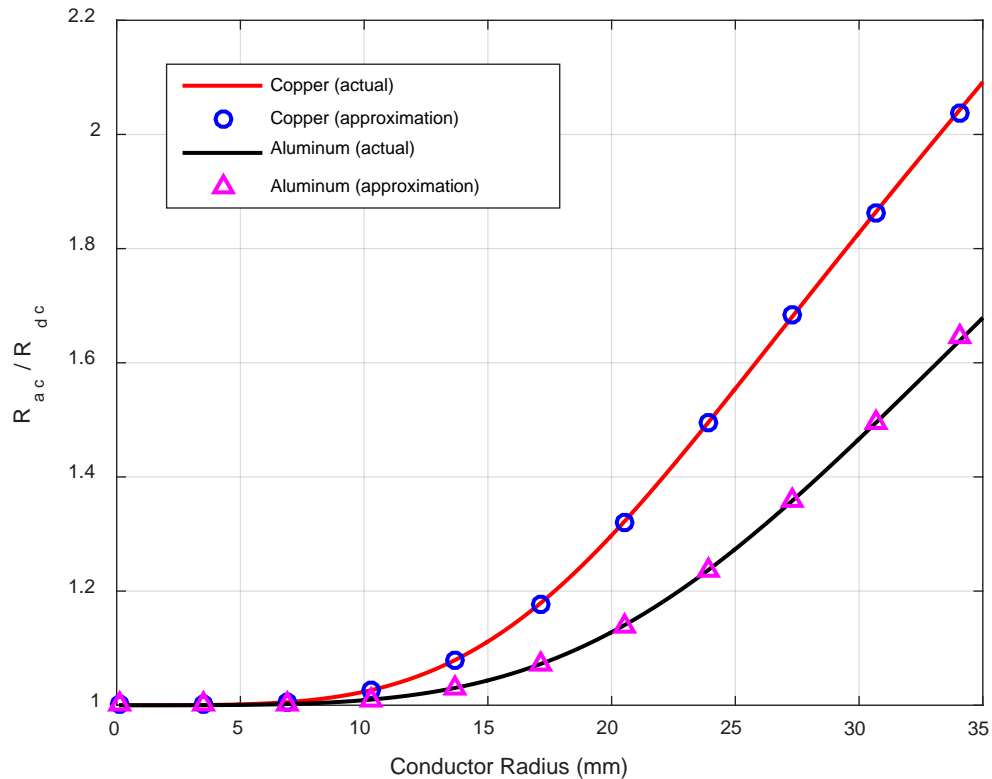


FIGURE 3-11: Actual vs approximated resistance ratios (solid round)

The actual Bessel function solutions were found to match the approximate solutions with a maximum error of 0.6%, as specified in literature [70]. The maximum error occurs when the Bessel function input argument is approximately 3.8, which corresponds to nearly a 27 mm conductor radius for copper and 33 mm conductor radius for aluminum. The reason the error is at a maximum at this point is due to a transition in the approximated equation used (see equation (88)). This was also done for solid hollow tube conductors.

For this plot it was assumed the inner diameter of the tube is always half of the radius. The results are shown in FIGURE 3-12:

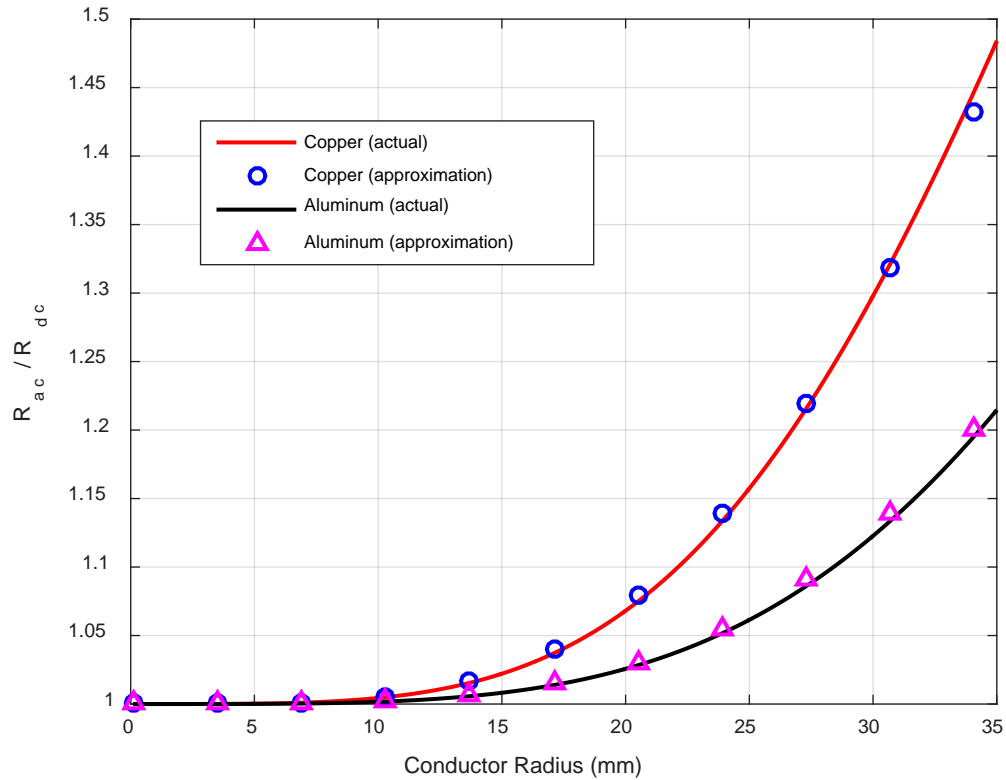


FIGURE 3-12: Actual vs approximated resistance ratios (solid round tube)

The actual Bessel function solutions were found to match the approximate solutions very well, having a maximum error of 2.0% on the test case shown in FIGURE 3-12. Unlike the solid round conductor, the AC/DC resistance ratio equations for solid round tube conductors have stipulations related to the design features. The maximum error of 2.0% found here is specific to a conductor with an inner diameter that is exactly half of the outer diameter. If the ratio of the tube thickness to conductor outer diameter or frequency to DC resistance is outside of a predefined range the error in the approximated equation becomes increasingly large [25]. The results were also plotted for an inner radius of zero,

as a test to ensure there was an exact match to the AC/DC resistance ratios of a solid round conductor. The test proved to be an exact match.

Research objectives:

- Derive a closed-form mathematical solution for bi-media conductors.
- Evaluate if bi-media designs suffer from manufacturing variability like segmented designs.
- Evaluate how will skin depth and conductor radius being within the same order of magnitude effects the redistribution of current within the bi-media conductors.
- Evaluate what materials (or lack thereof) are best to use in bi-media conductors.
- Evaluate what effect the different media have on bi-media conductor designs.
- Manufacture a bi-media conductor.
- Experimentally validate the accuracy of a closed-form solution for bi-media conductors.
- Evaluate the effects of stranding on skin effect for bi-media designs.
- Create optimal designs for bi-media conductors that minimize AC resistance.
- Evaluate how the operating temperature and frequency of bi-media conductors affect their optimal designs.
- Create tables of standardized designs that are comparable to standardized designs in the industry.

- Evaluate the application window (i.e. be cost effective) of bi-media designs compared to segmented conductors.
- Develop method for comparing cost effectiveness of bi-media designs versus segmented conductors that is independent of current metal prices.
- Develop method for comparing cost effectiveness of bi-media designs versus enameled wire segmented conductors that is independent of current metal prices.
- Develop simplified equations for designing bi-media conductors that can be used by industry practitioners.

The first step in answering all these questions begins with deriving a mathematical solution for bi-media conductors. Such a solution opens the doors for many questions to be answered.

CHAPTER 4: PROPOSED MODEL DEVELOPMENT

4.1 Overview

This chapter goes through the derivation of the AC/DC resistance ratio using the current density. This is first done for one medium, and then expanded for two media. Following the derivation, the formulated analytical solution is validated using Comsol Multiphysics®. The data will be taken from the program and plotted in MATLAB alongside the analytical solution to verify the theory. Comsol Multiphysics® is a platform that uses computer simulation for the study of multiple interacting physical properties [109] to produce approximated results using FEA [110]. It works by creating a mesh and solving the governing physics equations at each point of the mesh, made possible through the computational capabilities of computers [111]. The physics in this case are Maxwell's equations. The program iteratively resolves every mesh point until the error between iterations is less than a predefined value. By ensuring Maxwell's equations are fulfilled at every point within the maximum chosen error, the laws of physics are satisfied and an approximately accurate solution is obtained. Comsol Multiphysics® is mainly used for the calculation of nonlinear problems that don't possess analytical solutions. As such, it can be used to verify hypotheses and theories of the expected current density behavior in bi-media conductors, and also the ultimate AC resistance. It can also be used to verify analytical equations developed for bi-media conductors with any two types of media used.

4.2 AC Resistance Analytical Solution

A large part of the derivation begins in the same way as it does using all Bessel functions. However, the difference occurs after I_{ac} has been calculated in equation (65). From here, it is the current density that will be used to complete the new derivation. To do this the concept of “suppressed” and “unsuppressed” current density is introduced. The concept of “unsuppressed” corresponds to the volume of the conductor that would be effectively utilized if the conductor were carrying DC current; this amounts to the volume of the cylinder, or conductor. However, under AC conditions the volume is changed, and the current density is suppressed. By examining the ratio of the real and imaginary parts of the unsuppressed to suppressed volumes, the resistance and reactance ratios, respectively, are calculated. The suppression of the current density under AC current is caused by the eddy current. As seen previously, the eddy current acts to reinforce the current towards the outside of the conductor and to oppose it towards the inside. The currents superimpose, and the resulting net effect is an exponentially decreasing current density from the outside of the conductor radially inwards, as graphically shown in FIGURE 4-1:

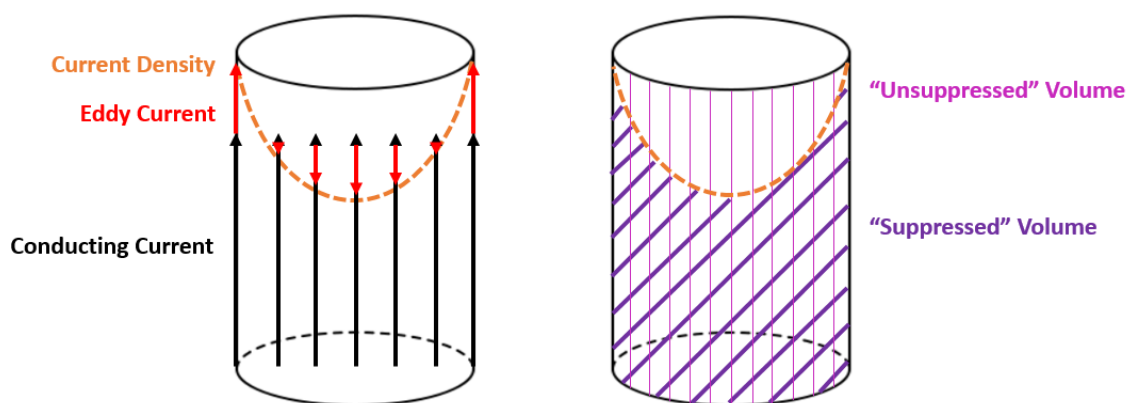


FIGURE 4-1: Suppressed vs unsuppressed current density

Note that the surface current density dictates the magnitude of the current density within the conductor. The AC/DC resistance ratio is a measure of how suppressed the current density is in relation to the uniform DC current density that is unsuppressed. The actual current density in the conductor scales equally at every point of the conductor radius, and therefore the AC/DC resistance ratio is independent of the actual current density. Therefore, the current density is scaled to the current density on the surface of the conductor, J_{r2} . The scaled surface current density J_r then becomes 1 A/m^2 . The Bessel function of the first kind zero order fully defines the behavior of the radially inward propagating EM wave. Therefore, the AC current density in the conductor, scaled to its surface value J_{r2} , is:

$$J_r = \frac{J_0(mr)}{J_{r2}} = \frac{J_0(mr)}{J_0(mr_2)} \quad (94)$$

Note that the Bessel function of the first kind first order always starts at a real value of one and an imaginary value of zero. Proceeding from equation (65), which gives the AC current, the DC current is:

$$I_{dc} = \iint_S J_r \cdot dS = 2\pi \int_0^{r_2} r J_{r2} \cdot dr = \pi r_2^2 \quad (95)$$

Recall that the AC current, previously derived, is:

$$I_{ac} = \iint_S J_r \cdot dS = 2\pi \int_0^{r_2} r J_r \cdot dr \quad (96)$$

To produce a surface current density of 1 A/m^2 the same electric field would be required for both AC and DC current, therefore:

$$V_{dc} = V_{ac} \quad (97)$$

$$I_{dc}R_{dc} = I_{ac}Z_{ac} \quad (98)$$

Note that R_{dc} can be easily measured and also calculated. Recall that the DC resistance previously stated (for uniform length, $l = 1$ m) is:

$$R_{dc} = \frac{\rho l}{A} = \frac{1}{\sigma \pi r_2^2} \quad (99)$$

Thus, solving for AC impedance yields:

$$Z_{ac} = R_{ac} + jX_{ac} = \frac{I_{dc}}{I_{ac}} R_{dc} = \frac{\pi r_2^2}{2\pi \int_0^{r_2} r J_r \cdot dr} R_{dc} \quad (100)$$

Which separating into AC resistance and reactance is:

$$R_{ac} = \frac{\pi r_2^2}{\text{Re}(2\pi \int_0^{r_2} r J_r \cdot dr)} R_{dc} \quad (101)$$

$$X_{ac} = \frac{\pi r_2^2}{\text{Im}(2\pi \int_0^{r_2} r J_r \cdot dr)} R_{dc} \quad (102)$$

AC inductance can be readily obtained as:

$$X_{ac} = \omega L_{ac} \rightarrow L_{ac} = \frac{X_{ac}}{\omega} \quad (103)$$

In bi-media conductors the incident wave has a boundary condition at the interface of the outer medium 2 and inner medium 1. As a result, part of the incident wave is reflected backwards towards the conductor surface and part is transmitted into medium 1, as shown in FIGURE 4-2:

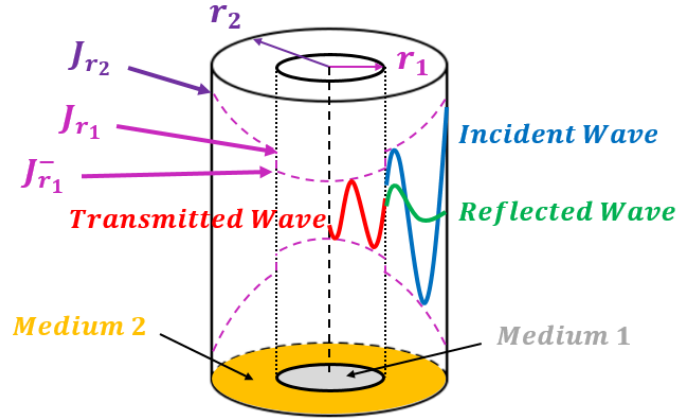


FIGURE 4-2: Bi-media EM wave boundary condition

Note that for $0 \leq r < r_1$:

$$J_{r_1}^- = \lim_{r \rightarrow r_1} J_r \quad (104)$$

This is because there exists a step discontinuity in the current density just inside of J_{r_1} .

For a bi-media conductor the incoming incident EM wave behaves the same as it does for a single medium conductor:

$$J_{incident} = J_0(m_2 r) \quad (105)$$

At the boundary between the metals, the part of the incident wave reflected backwards is [112]:

$$J_{reflected} = d H_0(m_2 r) \quad (106)$$

$$d = - \frac{J_1(m_1 r_1) J_0(m_2 r_1) - (m_2/m_1) J_0(m_1 r_1) J_1(m_2 r_1)}{J_1(m_1 r_1) H_0(m_2 r_1) - (m_2/m_1) J_0(m_1 r_1) H_1(m_2 r_1)} \quad (107)$$

It can be observed that d is a constant, and therefore the magnitude of the reflected wave is dependent on the inner radius and material properties of both media. At the boundary, the part of the incident wave not reflected is transmitted into the inner medium

according to the boundary conditions derived from Maxwell's equations. The boundary conditions state that the normal (perpendicular) component of the magnetic field and tangential component of the electric field of the incident wave must be continuous (i.e. voltage drop only occurs down the length of the conductor) [113], thus for the tangential electric field:

$$E_1^- = \lim_{r \rightarrow r_1} E_r = E_1 \quad (108)$$

Using the constitutive equation for J :

$$\frac{J_{r_1}^-}{\sigma_1} = \frac{J_{r_1}}{\sigma_2} \rightarrow J_{r_1}^- = \frac{\sigma_1}{\sigma_2} J_{r_1} \quad (109)$$

Because the incident and reflected waves superimpose, the total current density in the outer medium ($r_1 \leq r < r_2$) scaled to its surface value J_{r_2} can be calculated as:

$$J_r = \frac{J_0(m_2 r) + dH_0(m_2 r)}{J_{r_2}} = \frac{J_0(m_2 r) + dH_0(m_2 r)}{J_0(m_2 r_2) + dH_0(m_2 r_2)} \quad (110)$$

In the inner medium ($0 \leq r < r_1$) the current density of the transmitted wave behaves as a new incident wave. Its amplitude is that of the incoming incident wave J_{r_1} that is changed relative to the boundary condition (i.e. conductivities of the two media):

$$J_r = \frac{J_0(m_1 r)}{J_{r_1}^-} = \frac{J_0(m_1 r)}{\frac{\sigma_1}{\sigma_2} \left(\frac{J_0(m_2 r_1) + dH_0(m_2 r_1)}{J_0(m_2 r_2) + dH_0(m_2 r_2)} \right)} \quad (111)$$

J_r is scaled to $J_{r_1}^-$. The AC current can again be obtained with the surface integral, which reduces to a shell integral, of the current density for each medium:

$$I_{ac_1} = \iint_S r J_r \cdot dS = 2\pi \int_0^{r_1} r J_r \cdot dr \quad (112)$$

$$I_{ac_2} = \iint_S r J_r \cdot dS = 2\pi \int_{r_1}^{r_2} r J_r \cdot dr \quad (113)$$

DC current for medium 2 is:

$$I_{dc_2} = \iint_S J_r \cdot dS = 2\pi \int_{r_1}^{r_2} r J_{r_2} \cdot dr = \pi(r_2^2 - r_1^2) \quad (114)$$

The surface current density still dictates the magnitude of the current density within the conductor. In a bi-media conductor the suppressed AC current density to unsuppressed DC current density is shown in FIGURE 4-3:

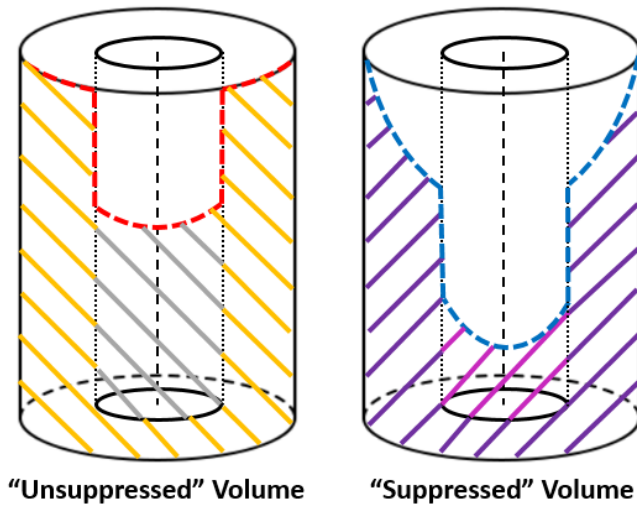


FIGURE 4-3: Bi-media suppress vs unsuppressed volume

For the inner medium, the current density would still be uniform but have a maximum value scaled by the material conductivities, and thus for medium 1:

$$I_{dc_1} = \iint_S J_r \cdot dS = 2\pi \int_0^{r_1} r J_{r_2} \frac{\sigma_1}{\sigma_2} \cdot dr = \pi r_1^2 \frac{\sigma_1}{\sigma_2} \quad (115)$$

To produce a surface current density of 1 A/m² the same electric field would be required for both AC and DC current, therefore:

$$V_{dc} = V_{ac} \quad (116)$$

$$(I_{dc_1} + I_{dc_2})R_{dc} = (I_{ac_1} + I_{ac_2})Z_{ac} \quad (117)$$

Note that R_{dc} can be easily measured and also calculated using (for uniform length, $l = 1$ m):

$$R_{dc} = R_{dc_1} // R_{dc_2} = \frac{1}{\sigma_1 \pi r_1^2 + \sigma_2 \pi (r_2^2 - r_1^2)} \quad (118)$$

Thus, solving for AC impedance yields:

$$Z_{ac} = \frac{I_{dc_1} + I_{dc_2}}{I_{ac_1} + I_{ac_2}} R_{dc} = \frac{\pi r_1^2 \frac{\sigma_1}{\sigma_2} + \pi (r_2^2 - r_1^2)}{2\pi \int_0^{r_1} r J_r dr + 2\pi \int_{r_1}^{r_2} r J_r dr} R_{dc} \quad (119)$$

Which separating into AC resistance and reactance is:

$$R_{ac} = \frac{\pi r_1^2 \frac{\sigma_1}{\sigma_2} + \pi (r_2^2 - r_1^2)}{Re \left(2\pi \int_0^{r_1} r J_r dr + 2\pi \int_{r_1}^{r_2} r J_r dr \right)} R_{dc} \quad (120)$$

$$X_{ac} = \frac{\pi r_1^2 + \pi (r_2^2 - r_1^2)}{Im \left(2\pi \int_0^{r_1} r J_r dr + 2\pi \int_{r_1}^{r_2} r J_r dr \right)} R_{dc} \quad (121)$$

Note that if $r_1 = 0$ then this gives the exact same solution as the single medium derivation of equations (101) and (102). AC inductance can again be readily obtained with:

$$X_{ac} = \omega L_{ac} \rightarrow L_{ac} = \frac{X_{ac}}{\omega} \quad (122)$$

The peak of the current densities always appears on the surface of the conductor when a higher conductivity medium is used on the outside. However, this may not be true if a lower conductivity medium is used on the outside. For practical purposes (i.e. having the higher conductivity medium in the location with the highest possible current density), this is the only configuration that would be desirable to use.

4.3 Theoretical Validation and Analysis

In the power industry it is typical to segment copper conductors greater than 1000 mm². Sometimes copper conductors with cross-sectional areas as low as 800 mm² are segmented. FIGURE 4-4 shows the scaled real part of the current density of some nominal area sized copper conductors:

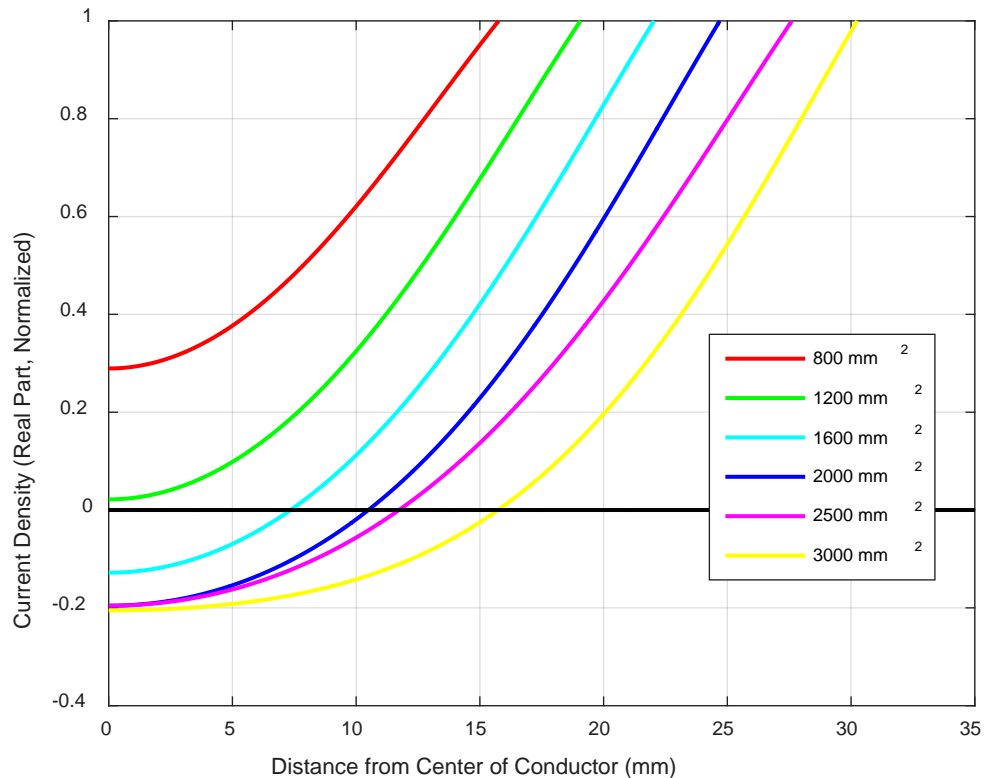


FIGURE 4-4: Current density in various solid copper conductor sizes

It can be observed that at 1200 mm², the first standardized size that is larger than 1000 mm², the current density is nearly zero on the inside of the conductor. Hence, much of the cross-sectional area added to the conductor is not effectively carrying current. This indicates that increasing area would result in less and less of a return on lowering AC resistance. On sizes above 1200 mm², the current density actually goes negative. Because this is a good conductor the electron density is approximately uniform. The negative

density here is truly a negative charge carrier velocity, indicating the current is flowing in the opposite direction. This means that adding copper will actually give a higher AC resistance. This makes it apparent why industry practice is to use segmented conductor designs on cross-sectional areas larger than 1000 mm². The current density is a complex quantity, with real part corresponding to resistance and imaginary part corresponding to reactance. Once the phase angle of current towards the inside of the conductor lags the surface value by more than 90° the current flows backwards, and thus removing this part would improve AC resistance [114]. However, care must be taken when creating such designs, since removing or replacing one of the media with another causes a redistribution of current density [36]. Hence, the point at which the current density becomes negative will shift towards the outside of the conductor. The further apart in conductivity the two media are, the more the crossing point will shift. This makes sense intuitively since most of the current flows within the higher conductivity outer medium, raising the current density in that area.

In order to evaluate the theoretical accuracy of the equations obtained, a test case is performed on a 2000 mm² round copper conductor. The DC resistance value at 20°C is defined as 9x10⁻⁶ ohm/m [92]. The DC resistance at 90°C is:

$$R_{dc} = R_0[1 + \alpha_{20}(\theta - 20)] \quad (123)$$

$$R_{dc} = 9x10^{-6}[1 + 0.00393(90 - 20)] = 1.15x10^{-5} \quad (124)$$

The resistivity of copper at 90°C is:

$$\rho = \rho_0[1 + \alpha_{20}(\theta - 20)] \quad (125)$$

$$\rho = 1.7241x10^{-8}[1 + 0.00393(90 - 20)] = 2.1984x10^{-8} \quad (126)$$

Therefore, the equivalent radius of a solid conductor of this resistance is:

$$r_2 = \sqrt{\frac{\rho}{\pi R_{dc}}} = 0.0247 \text{ m} = 24.7 \text{ mm} \quad (127)$$

Two types of inner media are used: air and aluminum. In both cases it is assumed that the inner radius is 15 mm. This is the current density distribution when having a 15 mm radius air or aluminum core, created with the analytical solution derived and compared to the Comsol Multiphysics® approximation using FEA, shown in FIGURE 4-5:

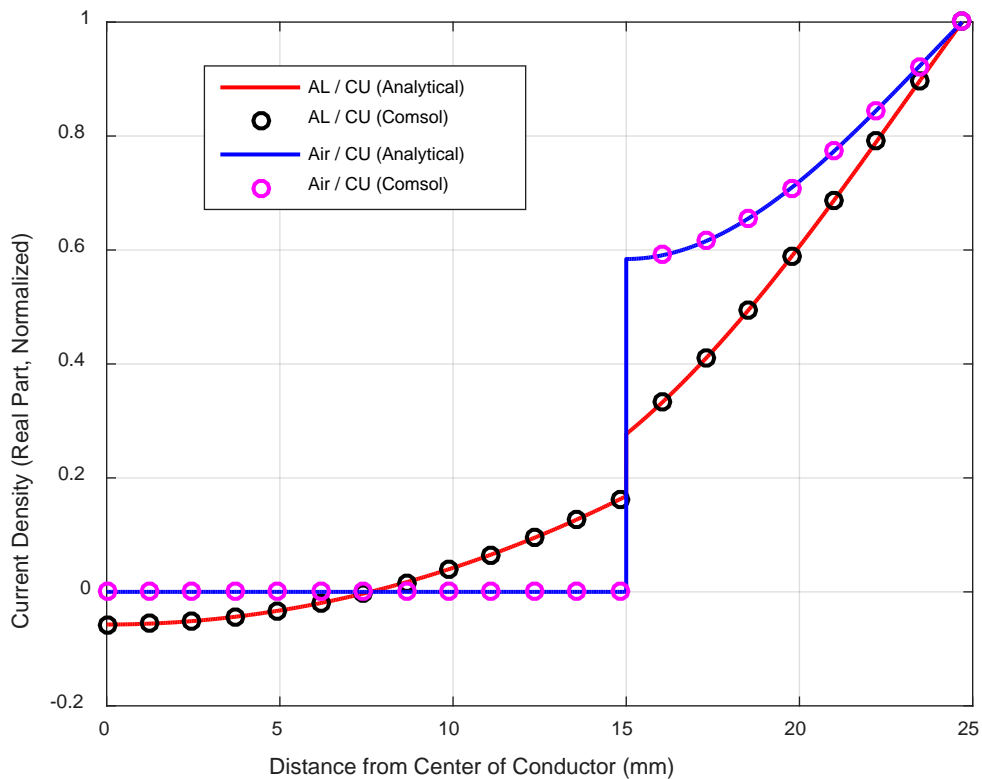


FIGURE 4-5: Current density in bi-media conductors

Note that removing the core and replacing it with a lower conductivity medium always improves current density in the outer medium. However, this is not necessarily an optimal design, as it also increases the DC resistance. The ultimate goal is to have an optimal point where the media are switched, that gives the lowest possible AC resistance.

The point changes depending on the media used (i.e. conductivity), outer radius (or cross-sectional area), frequency, and temperature. Now that the current density distribution has been verified, the AC resistance, inductance and their ratios can be as well. While current density is a calculation taking place on a conductor of fixed inner and outer radii, in order to find the optimal design point, the AC resistance needs to be examined over the entire range of inner radii with a fixed outer radius only. Doing this allows for the observance and analysis of AC resistance when removing the core and replacing it with air or aluminum. FIGURE 4-6 shows the AC and DC resistances of this copper conductor as an inner core is replaced by either air or aluminum:

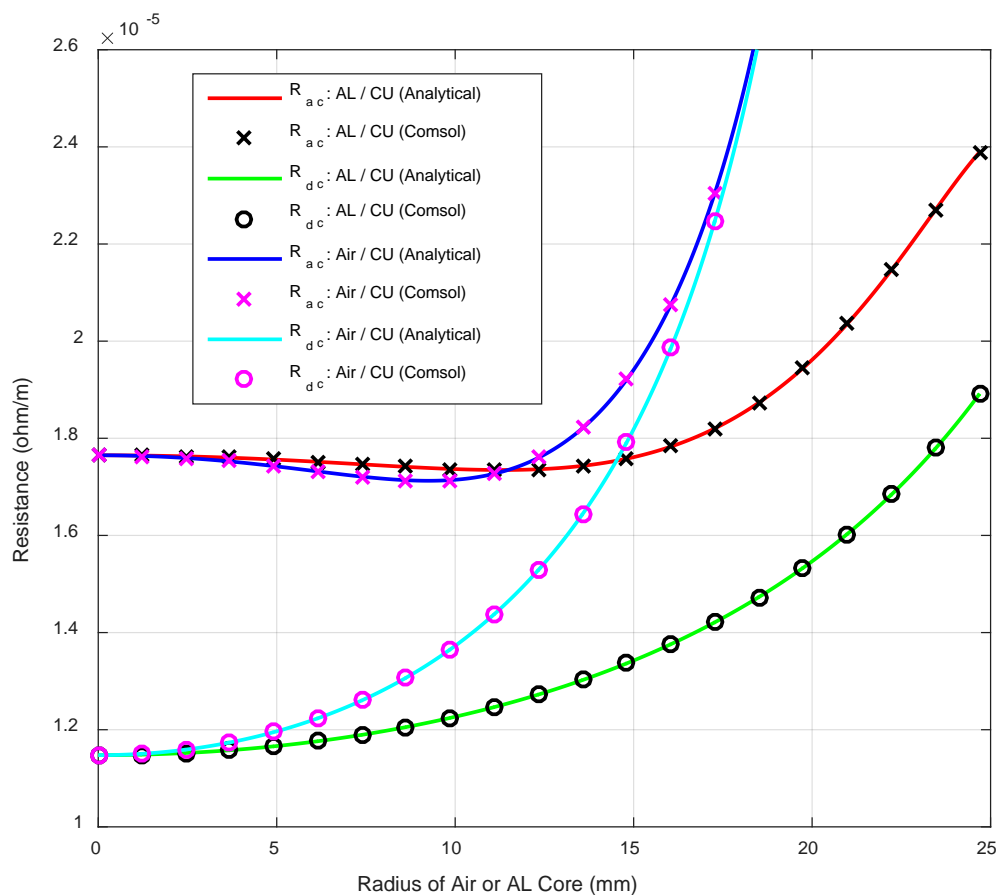


FIGURE 4-6: Resistance in bi-media conductors

The left-most side of this plot shows an all copper conductor, since none of the core has been replaced by air or aluminum. The right-most side of this plot shows an all air or aluminum conductor. This is the reason the Air / CU conductor design goes to infinity although r_2 in both designs is fixed at 24.7 mm. It can also be observed that both the Air / CU and AL / CU conductors start at the same DC and AC resistance values, as they are both all copper at this point. These values have also been verified against methods in existing literature [1] not using a shell integration of current density to obtain AC resistance. Results in existing literature exactly match those of the methodology for calculating AC resistance using current density. The corresponding skin effect observed is as shown in FIGURE 4-7:

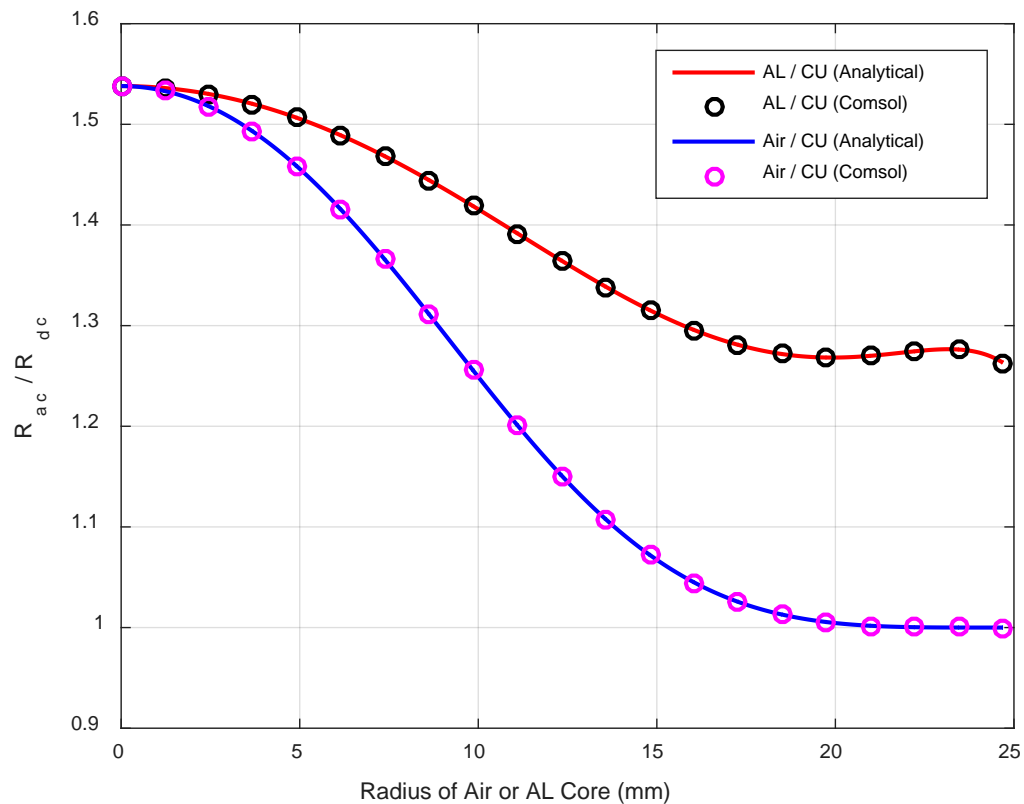


FIGURE 4-7: Skin effect in bi-media conductors

It can be observed here that the skin effect of Air / CU approaches one, as an infinitely thin tube would have a flat DC current density. Like the AC to DC resistance ratio, the AC to DC inductance ratio can also be calculated with results shown in FIGURE 4-8:

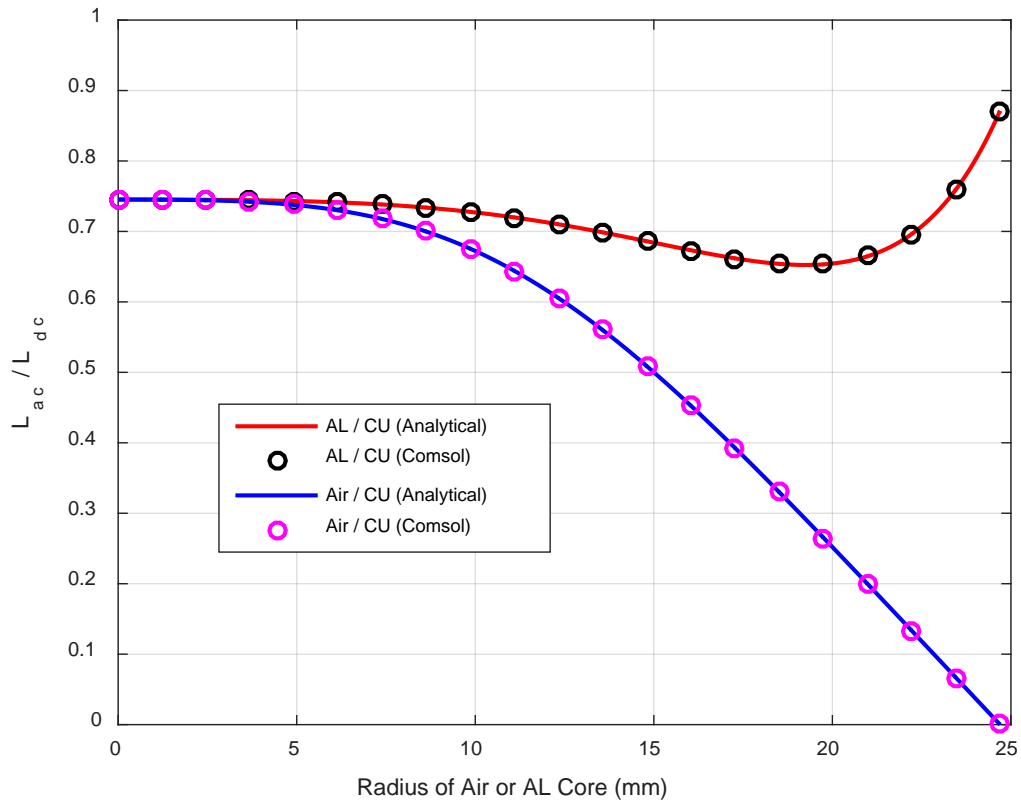


FIGURE 4-8: Inductance ratio in bi-media conductors

In reducing the AC/DC resistance ratio, it can also be observed that bi-media conductors can have smaller inductance, which is also an added benefit. The inductance is smaller because at a fixed frequency, as the conductor radius increases the magnetic field is present over an increasingly smaller volume of the conductor, thus the self-inductance decreases [6]. Alternatively, it has been shown that inductance always decreases as frequency increases in a solid round conductor. At a fixed frequency, if a solid round

conductor were transformed into a hollow conductor of the same cross-sectional area the inductance would also go down as the thickness of the tube becomes thinner [39].

The optimal point for the design of each conductor is different. The Air / CU conductor has an AC resistance minima at 9.2 mm, whereas the AL / CU conductor has its minima at 11.3 mm. The minima do not align exactly where the current density crosses zero. The optimal point to minimize AC resistance depends on both the increased DC resistance when removing or replacing some of the copper core and the volume under the curve used in calculating the skin effect. As such, the optimal point of an Air / CU bi-media conductor will always have a positive current density. If the current density were negative in an Air / CU conductor the DC resistance would still decrease while volume under the curve also decreased, which could only increase AC resistance. However, for the optimal design of an AL / CU conductor, it makes sense to have some of the aluminum with a negative current density since there is still more copper with a high enough current density to make up for the backwards-flowing negative current in the aluminum. Note that the backwards-flowing current on the inside of the conductor results from conduction current being less than the eddy current opposing it. The current density distributions of optimally designed bi-media conductors (i.e. AC resistance minimized at radii of 9.2 mm for the Air / CU conductor and 11.3 mm for the AL / CU conductor) are shown in FIGURE 4-9:

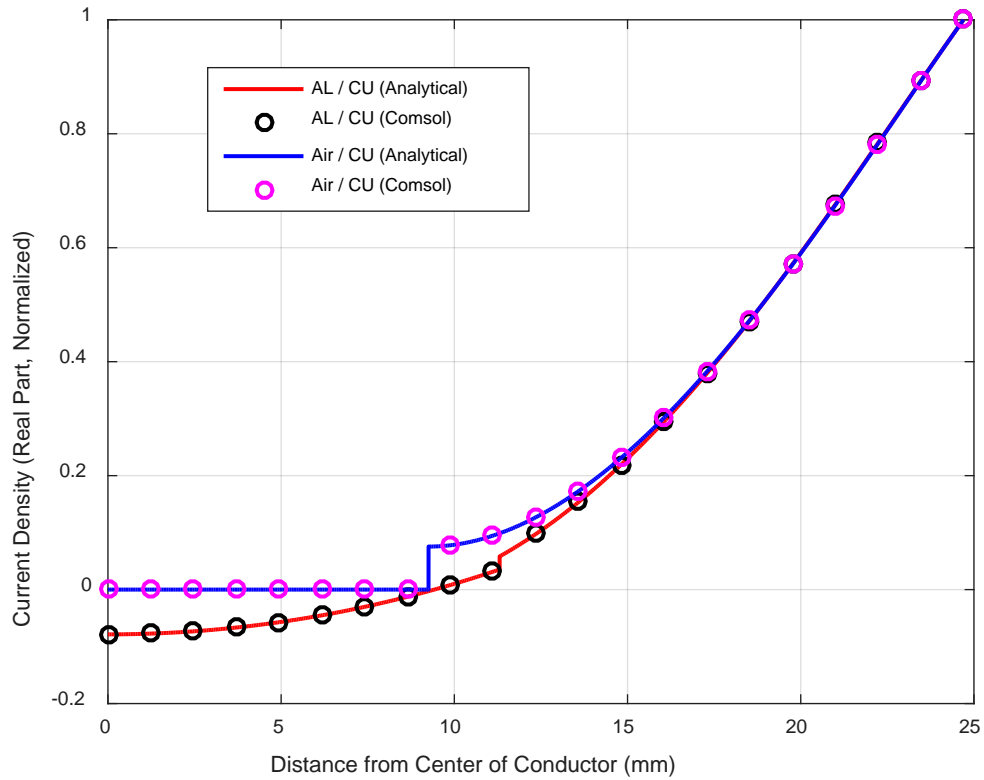


FIGURE 4-9: Current density in optimal bi-media conductors

By studying conductors of different radii, the application range at power frequencies becomes more evident. Conductors of fixed outer radii from 5 mm to 30 mm in 5 mm increments are examined. The metals used here are copper with an aluminum core. The DC resistances of these conductors are shown in FIGURE 4-10:

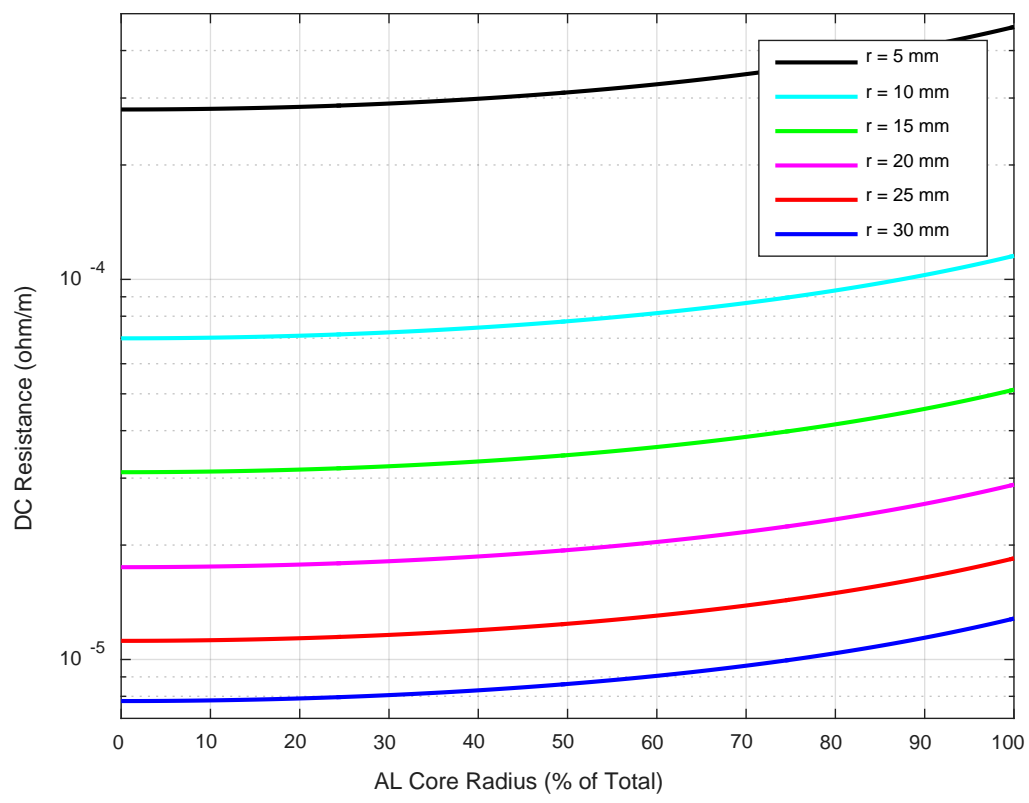


FIGURE 4-10: DC Resistance in various radii AL / CU conductors

The x-axes have been formatted such that the diameter of the aluminum core is shown as a percentage of the entire conductor diameter. The y-values is logarithmic, so the DC resistance of all sizes can be viewed on a single plot. Adding aluminum increases the DC resistance, as the copper and aluminum act as two resistors in parallel. Intuitively, it may seem reasonable to assume that adding aluminum would also increase AC resistance. However this is not always the case, as shown in FIGURE 4-11:

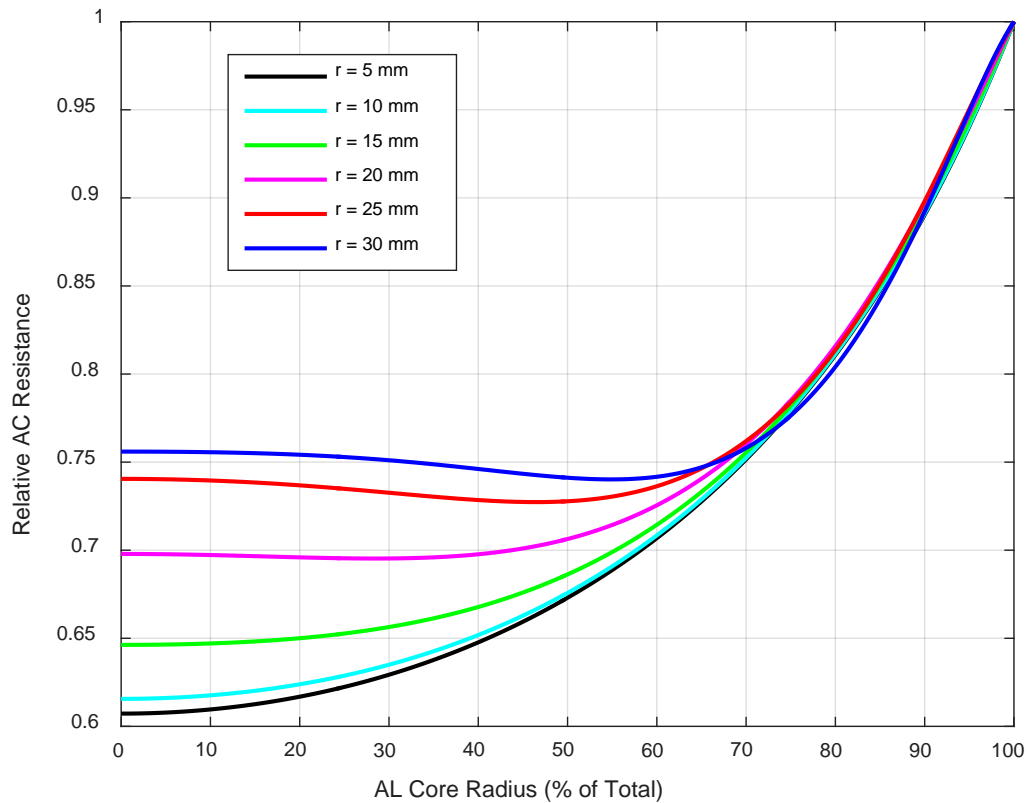


FIGURE 4-11: AC Resistance in various radii AL / CU conductors

The y-axis of the AC resistance curves have been scaled with their all-aluminum values to allow easy comparison of their nature in response to increasing the size of the aluminum core. This figure shows that the AC resistance of an all-copper conductor on the left side of the graph approaches the ratio of aluminum to copper conductivity as the total conductor outer diameter is decreased. This is because smaller conductors are less impacted by the skin effect, as their current density distribution approaches uniform DC current density. From here it can be observed that when the radius of the conductor exceeds 15 mm there is an inflection in the AC resistance where a minima presents itself and the optimal design is going to be a mix of both aluminum and copper. The corresponding skin effect is shown in FIGURE 4-12:

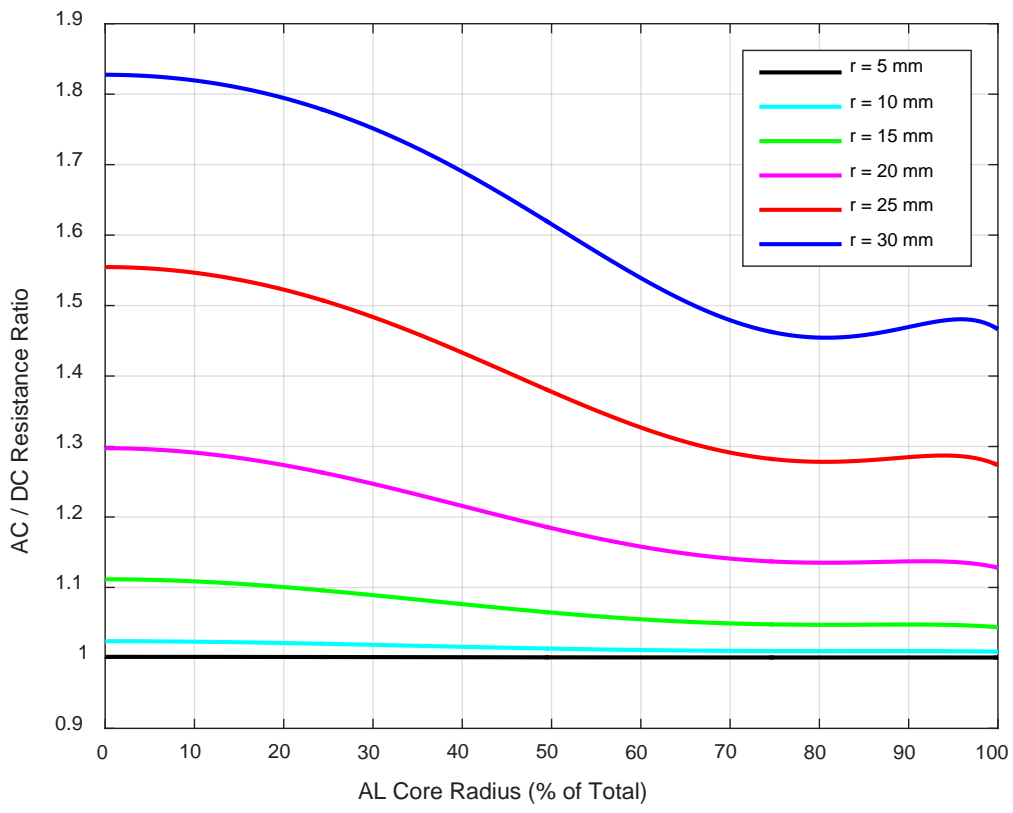


FIGURE 4-12: Skin effect in various radii AL / CU conductors

It is also of interest to see what would happen if the conductor core were copper with aluminum on the outside. In this case, the DC resistance plot would be as shown in FIGURE 4-13:

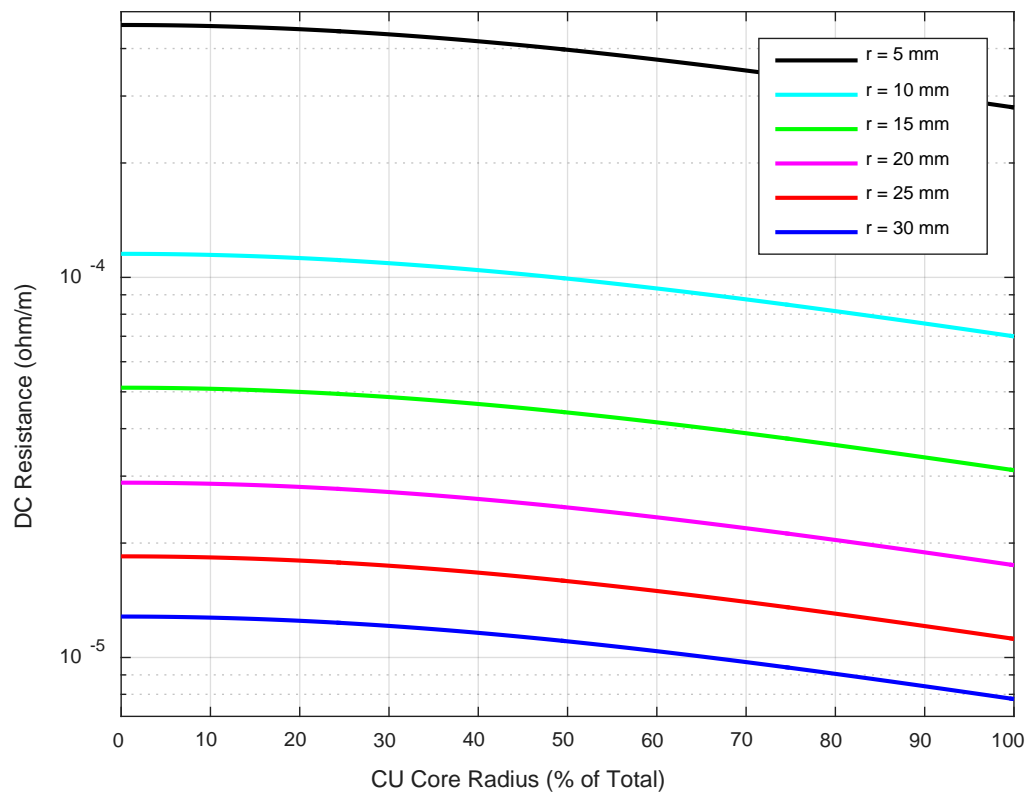


FIGURE 4-13: DC resistance in various radii CU / AL conductors

The DC resistance in this case decreases as copper is added in place of aluminum, as would be expected. The AC resistance has the opposite trend that was seen on the AL / CU conductor, as shown in FIGURE 4-14:

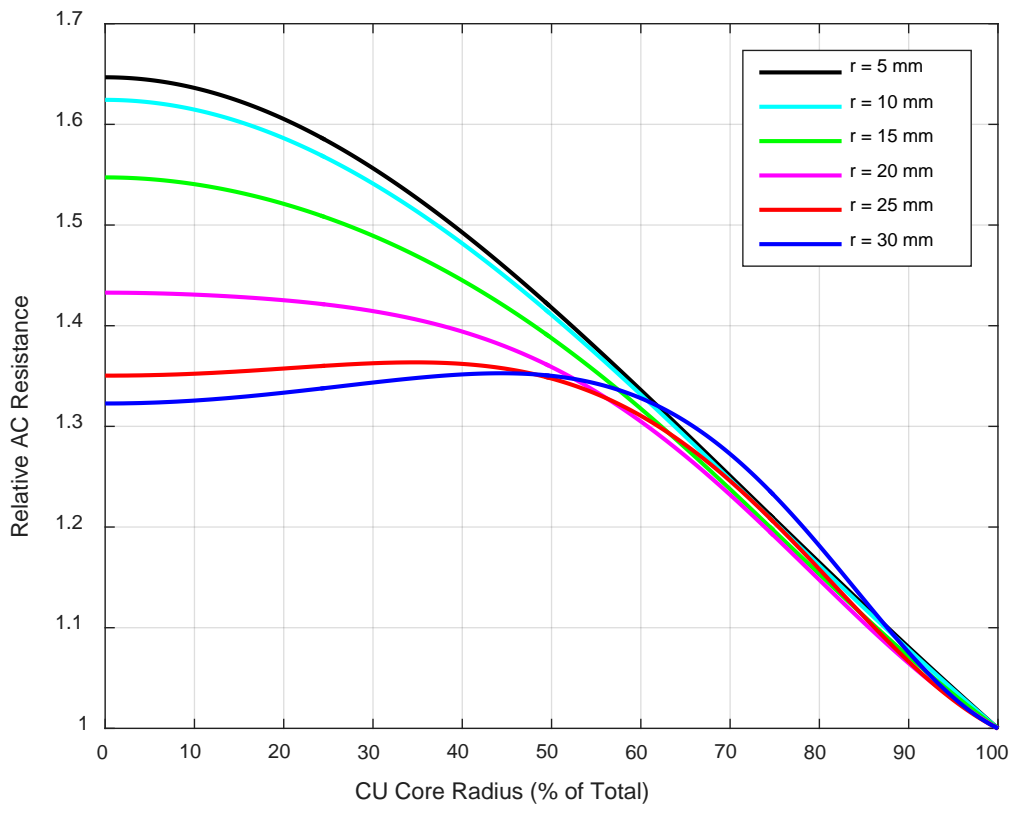


FIGURE 4-14: AC resistance in various radii CU / AL conductors

Here, we see that adding a copper core to an aluminum conductor with radii greater than 20 mm will actually result in higher AC resistance. For practical purposes it makes no sense to increase AC resistance, which is particularly true given the factor that copper is more expensive than aluminum. The corresponding skin effect for these conductors is shown in FIGURE 4-15:

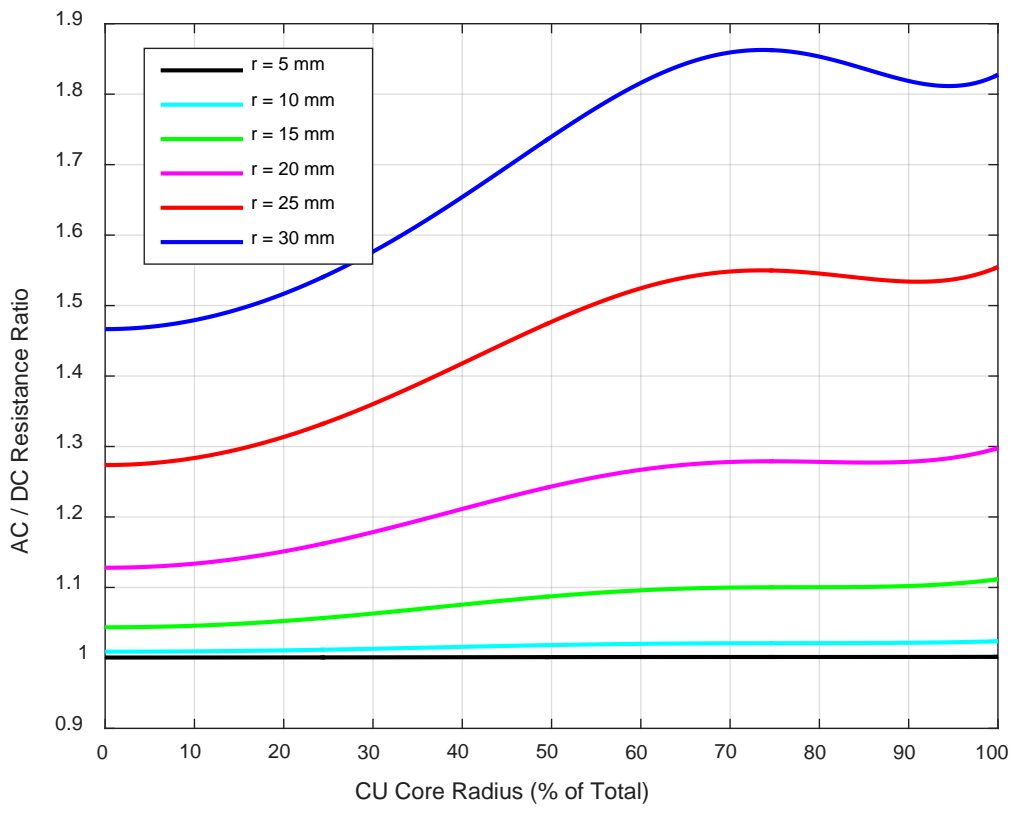


FIGURE 4-15: Skin effect in various radii CU / AL conductors

The plots for Air / CU compared to AL / CU are practically the same. The only differences are that the DC and AC resistances approach infinity as the conductor becomes air only and the AC/DC resistance ratios of all sizes approach one. The same inflection phenomena of the AC resistance happens for the same reason as in AL / CU conductors, however the optimal radius for the AC resistance minima shifts slightly radially inward.

CHAPTER 5: EXPERIMENTAL VALIDATION

5.1 Overview

This chapter details the laboratory measurements done on two samples. It begins with a discussion on the background of the theory behind the AC measurement technique used. Following this, there is a more specific discussion on the actual equipment used for the measurements. After the specific test measurement setup has been described, specifics about the cable samples being tested are discussed. Once the measurements are made on the samples the experimental results are presented. This chapter is concluded with commentary on these measurements and an analysis of how well the theoretical solution matches the laboratory measurements. Note that the analysis performed in this chapter are carried out at a temperature of 20°C, since this is closest to ambient temperature during testing and the temperature results are normally adjusted to in the conductor design standard [92]. The frequency used is variable, and the specific frequency used for each test is stated along with all results and plots.

5.2 AC Resistance Laboratory Testing

There are several techniques used today for making laboratory measurements of AC resistance. All methods can be divided into two basic methodologies: the thermal method and the electrical method [115]. Typically, in the thermal method an insulated cable is installed in a tube of known thermal properties. A large amount of AC current is then used to heat the conductor to a steady state temperature, such that no more increased joule

heating occurs. Using the measured temperature drop across the tube, the ohmic heating power losses of the conductor can be calculated, which is then used to calculate AC resistance [70]. Some minor drawbacks of this methodology are the high energy costs and long waiting times (typically > 10 hours). Additionally, this method has the more critical challenges of (i) large cross-sectional area conductors being difficult to bring to steady state temperature, and (ii) the fact that the test cannot be performed on a production length of cable wound on a drum – due to mutual heating between the windings of cable [45].

The electrical method is most commonly performed by injecting AC current into the conductor and calculating AC resistance using the conductor voltage drop and phase angle measurement between the voltage and current. A power analyzer can be used to make these measurements. In order to get an accurate measurement of AC resistance it is imperative that the measurement equipment has high accuracy in the sensing of phase angle and waveform amplitudes. It is recommended to use equipment with phase error uncertainty of less than $\pm 5 \times 10^{-5}$ and amplitude uncertainty of less than $\pm 1 \times 10^{-2}$ [46]. In order to ensure accurate phase angle displacement of the current measurement, a shunt should be used. Previous AC resistance measurements taken at a sampling rate of 125 kSa/s were able to show accurate results of a high voltage cable with a large power conductor at frequencies up to 100 Hz [44]. If the sampling rate is not high enough the phase shift of the voltage created by the self-inductance of all circuit components results in inaccurate measurements. For accurate phase angle resolution on power cables a sampling rate of at least 1 MSa/s is recommended when testing at power frequencies [64]. However, to ensure accurate readings at higher frequencies a sampling rate of 10 MSa/s is recommended [96]. The insulation between the two conductors (i.e. the conductor and

shield wires) forms a capacitor. At very high frequencies (MHz range), the leakage current can become significant resulting in erroneous AC resistance measurements. Since the AC resistance is calculated with the real power divided by the square of the current (RMS value), when the measured current increases the AC resistance decreases and therefore appears lower than it truly is. However, the leakage current is so small it has no effect on the frequencies tested here. Still, it is recommended that measurements be done on complete production lengths of cable to help minimize error due to parasitic effects [44].

The electrical method accuracy is further dependent on the absence of external magnetic fields and magnetic materials [64]. This test method is typically performed with the cable conductor and shield connected in series (i.e. the shield is used as a coaxial return conductor). The shield minimizes the voltage drop along the conductor due to inductance, as the coaxial configuration allows for the cancellation of the magnetic field outside of the cable shield to a large extent [116]. Hence, testing can be done with the cable wound on a reel without high losses from the proximity effect being introduced by nearby windings of the conductor. The setup of this test method taken from existing literature [64] is shown in FIGURE 5-1:

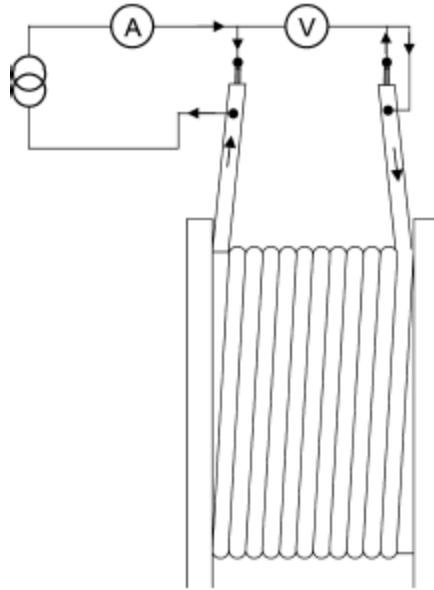


FIGURE 5-1: General AC resistance measurement test setup

Passing current through any conductor introduces some ohmic heating losses which change the conductor resistance. However, the amount of current injected with this test methodology is typically a small percentage of the rated current carrying capacity of the conductor, and thus any increase in conductor resistance is considered negligible. The ambient temperature is important for measurement purposes since the copper and aluminum DC resistance changes by approximately 0.4% per degree Celsius over the temperature range used for power cables [94]. Therefore, it is recommended that the cable be maintained at a reasonably constant temperature for at least 12 hours before measuring DC resistance [77]. When using the cable shield as a return path, the separation distance of the two conductors is negligible, assuming the conductor is perfectly concentric and centered around a perfectly concentric shielding layer. However, the reality of manufacturing is that a perfectly concentric cable is an impossibility. Therefore, the manufacturing tolerances must be closely monitored since the non-concentric set-up can

significantly increase current density on the nearer sides of the conductors and result in erroneous AC resistance measurements [45].

Some additional factors that influence the AC resistance measurement of the electrical test method include contact resistance of connectors, voltage measurement tap-offs, metallic shield design, and the influence of metallic objects. Poor electromechanical contact leads to uneven current density distribution inserted into the wires of the conductor. When clamping a connector onto a conductor the contact resistance can be reduced by using a large enough contact area, lower resistivity contacting media, and enough compressive force to ensure a sufficient contact depth [117]. The influence of contact resistance down the length of the conductor between strands past the connector can be mitigated by testing a long length of cable since it increases the chances of better contact spots between wires [118]. Effectively, a long cable increases the measured resistance and hence reduces the noise (contact resistance) to signal (conductor resistance) ratio. This has the effect of making the contact resistance relatively small compared to the resistance of the test object. Further, it is recommended that wide-area contact voltage tap-offs be used [45]. A concentric wire metallic shield, as opposed to a metallic corrugated sheath, must be used when measuring AC resistance of a cable conductor wound on a reel. This is because magnetic coupling occurs between the conductor and shield/sheath when the cable is wound on a drum that is much higher in the case of the sheath [46]. When a corrugated outer sheath is used it creates a non-uniform geometry in the cable, that affects the apparent AC/DC resistance ratio of the conductor and sheath that is more pronounced at higher frequencies [14] or when the cable is bent [46]. Experimental research measurements done long ago showed negligible impact from the proximity effect of metallic objects greater

than 20 cm away [31]. This has been recently corroborated with the recommendation that the cable be placed at least 50 cm above a metallic ground in order for it to have insignificant impact on AC resistance [45].

The testing performed in the following sections is done using the electrical method described above. It is advisable to perform AC resistance measurements over a range of frequencies since it allows for the accuracy of the results to be more easily verified against other measurements and theoretical calculations [46]. However, care must be taken when doing this since higher frequencies introduce additional error. Testing long lengths of cable is good for accuracy, but expensive for testing purposes. Cigré working group D1.54 is working on methodologies for accurate testing of shorter lengths, such as two meters [96] [45]. Testing short lengths introduces additional sources of error that can be generally ignored when the conductor is tested on a reel. For example, it has been shown that inhomogeneous current insertion on long lengths of cable does not influence AC resistance measurements but such effects have not yet been determined for short lengths of cable [45]. The following section describes setup of the testing performed on long lengths of cable.

5.2.1 Test Setup

The test setup requires a current source to generate the current circulated around the loop, and a measurement device to measure the current generated and the voltage drop across the conductor. The waveform of the current is created using a BK Precision model 4005DDS signal generator. This signal is then connected to a 2000 watt Gemini XGA-2000 power amplifier to increase the signal strength. The output of the power amplifier is connected to a custom-made 10 VAC 6000 amp L/C Magnetics high-current transformer. The transformer was designed to heat large low resistance conductors by injecting high

current at low voltage. The measurement of the voltage and current is made using a Tektronix PA1000 single-phase power analyzer. The power analyzer has 1 and 20 amp shunts for accurate current measurements, and a sampling rate of 1 MSa/s. The connection of the equipment is shown in FIGURE 5-2:

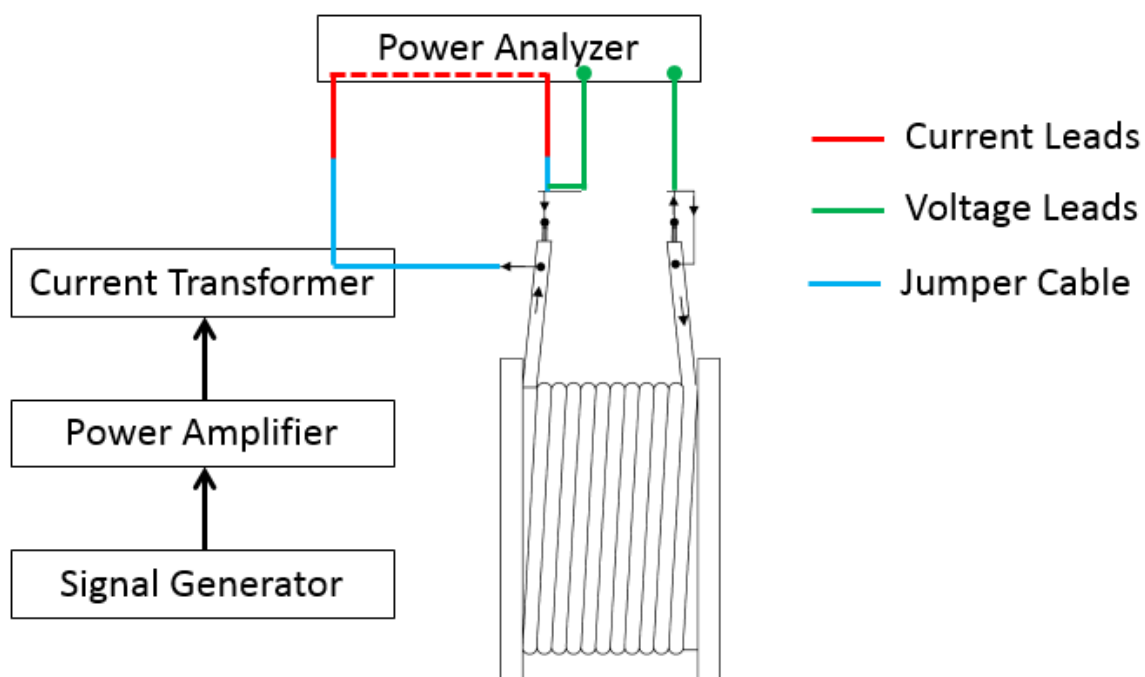


FIGURE 5-2: Detailed AC resistance measurement test setup

A photograph of the test setup is shown in FIGURE 5-3:

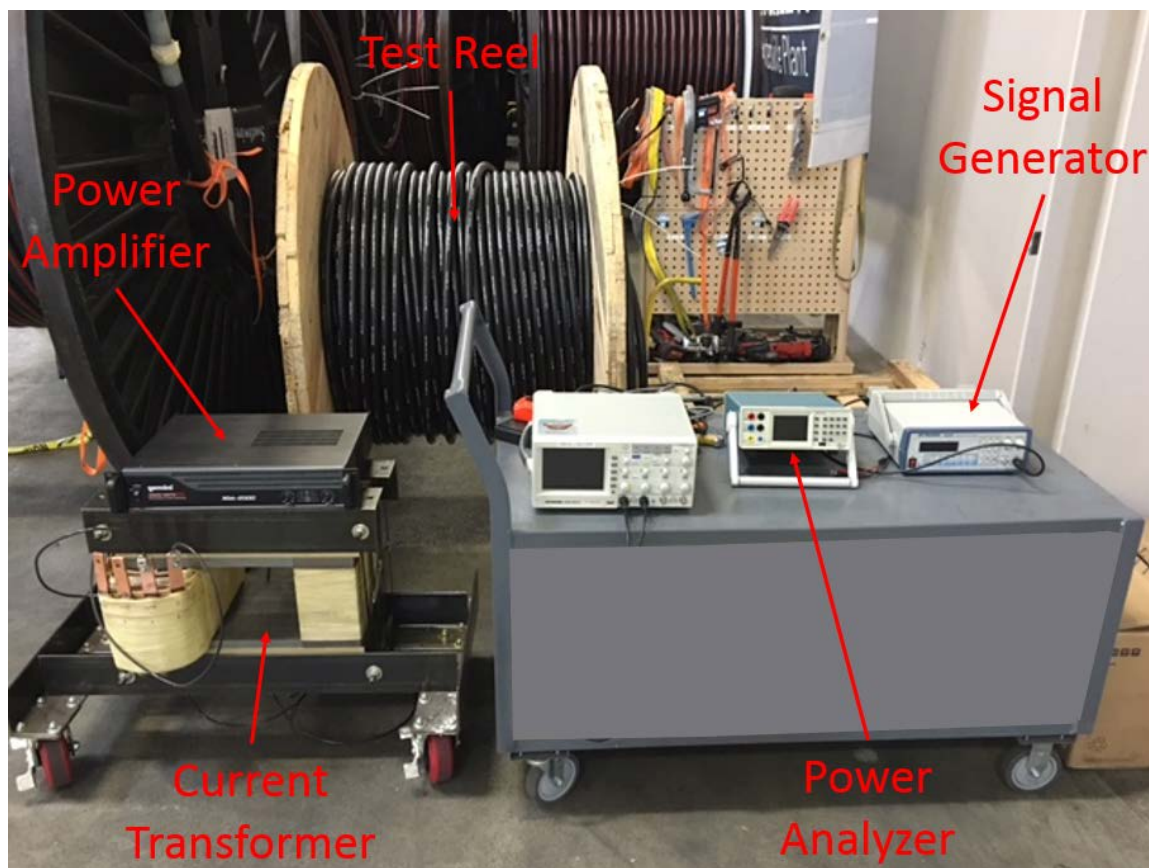


FIGURE 5-3: Picture of AC resistance measurement test setup

The corresponding circuit diagram for this setup is shown in FIGURE 5-4:

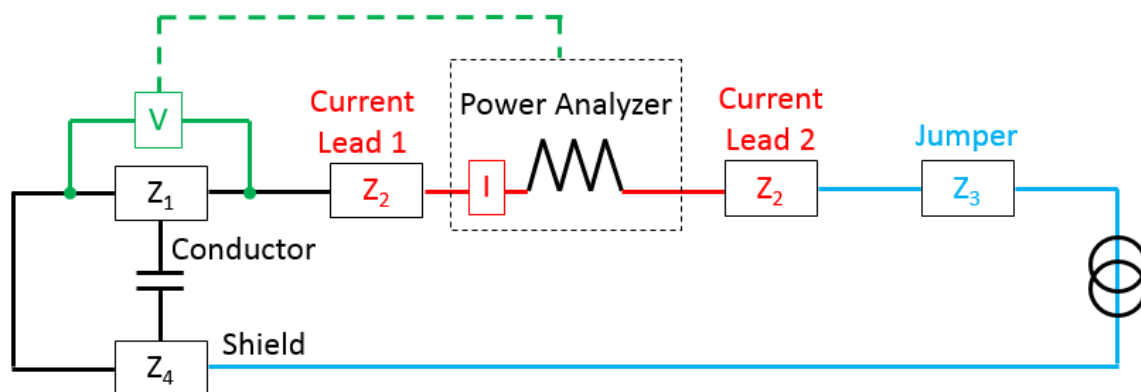


FIGURE 5-4: Circuit diagram of AC resistance measurement test setup

The current leads and internal resistance of the power analyzer can be assumed to have negligible impact on the measurement accuracy. Likewise, the shunt capacitance between the cable conductor and shield can also be assumed to have negligible impact over

the range of test frequencies (i.e. it acts as an open circuit). All connection points to the cable, shield and jumper have associated contact resistances. It is particularly important that good electrical contact be made on either side of the conductor to ensure uniform current insertion. Because this is a closed circuit and the shunt capacitance acts as open, the current can be measured at any point in the circuit.

The current transformer had been originally purchased under the assumption that the testing frequency would be 60 Hz. Therefore, the equipment had been specifically designed for this frequency. It is possible that distorted waveforms (i.e. not perfectly sinusoidal due to signal clipping since the ferromagnetic core is electromagnetically saturated) may be produced as a result. Also, operating the transformer at frequencies lower than 60 Hz lowers its inductive reactance, which increases current flowing through the primary winding. Care was taken when operating at lower frequencies to ensure the transformer was not damaged by burning the primary winding. Furthermore, the power analyzer was also purchased for intended measurements at power frequencies. Experience has shown that a sampling rate of 500 Sa/cycle is sufficient to accurately measure amplitudes and phase differences of the voltage and current waveforms. The maximum test frequency for this criteria is shown in FIGURE 5-5:

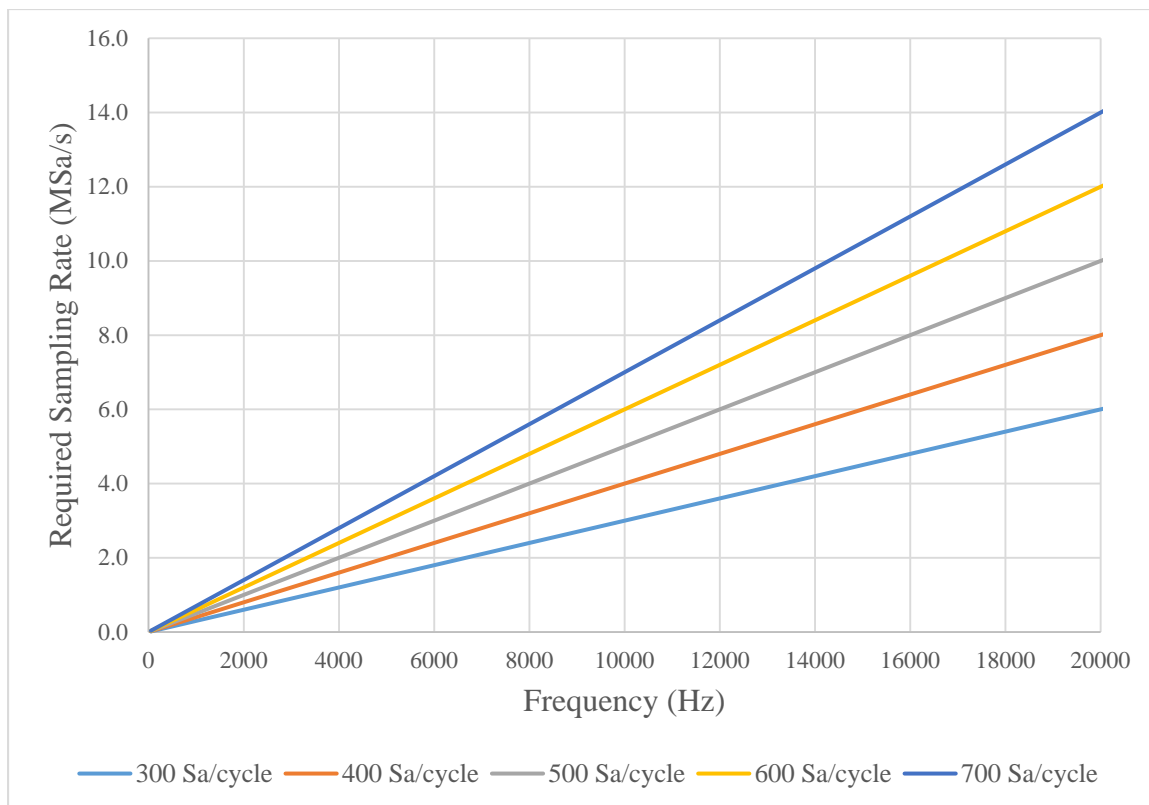


FIGURE 5-5: Sampling rate versus frequency

It can be observed that to accurately measure 20 kHz at a recommended sampling frequency of 500 Sa/cycle, the sampling rate of the equipment should be of 10 MSa/s or higher. Since the PA1000 samples at 1 MSa/s the following zoomed in view of FIGURE 5-5 shows the expected range of accuracy in FIGURE 5-6. This shows that for measurements at frequencies greater than 2 kHz the measurement accuracy for the power analyzer will start to degrade, as this is below 500 Sa/cycle.

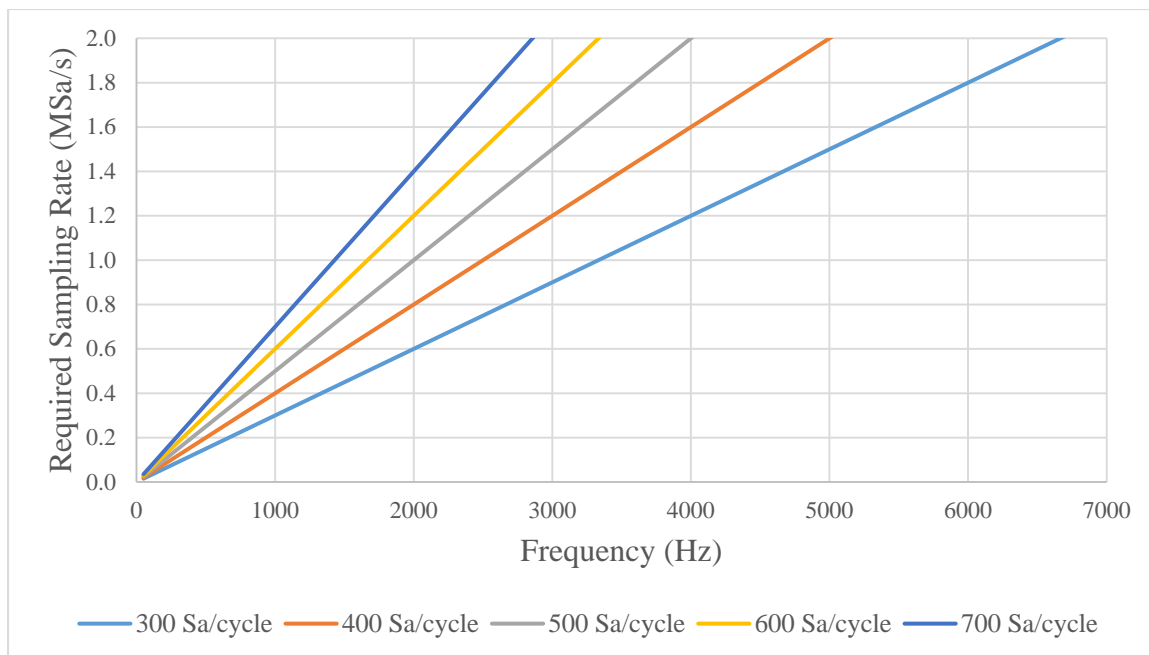


FIGURE 5-6: Sampling rate versus frequency (zoomed view)

5.2.2 Cable Samples

The conductors tested were in cable samples that had passed through complete manufacturing operations. The AC resistance of conductors changes throughout the manufacturing process, due to the variable diameter of the strands (i.e. quality control during conductor wire drawing), stretching and work-hardening (particularly during conductor compaction), helical twisting of wires resulting in a longer than linear length, and winding/unwinding on reels [119]. As stated previously, there are two cable samples that were tested. The first sample was constructed with a Copperweld® #1/0 AWG copper-clad aluminum conductor. The sample was donated by Copperweld® in Fayetteville, Tennessee in their interest to have a formulated and proven analytical solution developed for calculating AC resistance in their bimetallic conductors. Note that they are currently the largest producers and suppliers of bimetallics in the world by volume. The conductor is a solid design, and the copper and aluminum are metallurgically bonded using a process

designed by Copperweld® [4]. Unlike the work proposed in this dissertation, it was never the intention of Copperweld® to create a conductor that reduces AC resistance by using both the copper and aluminum as current carrying media. However, if this sample were tested over a high range of frequencies it could be used to prove the theory of a large bi-media conductor at power frequencies. Since larger conductors operating at a lower frequency have equivalent counterparts of smaller conductors operating at a higher frequency, testing could be done on either to effectively prove the same thing. This is ideal for matching the theory since the analytical solution is also for a solid design. However, there are two downsides: the cross-sectional area of the conductor and the amount of copper to aluminum used. Skin effect does not become more pronounced until conductors have a large enough cross-sectional area. As previously seen in FIGURE 4-12, a conductor of 5 mm radius (or an area of 79 mm²) is practically operating at a unity skin effect at power frequency. That is, there is a negligible increase in the AC resistance versus DC resistance. To account for this, a higher test frequency was used, as it has the same effect as a lower frequency on a larger conductor. The problem with increasing the frequency is that testing above 2 kHz degrades measurement accuracy since less than 500 Sa/cycle are being measured. The second downside is the relatively small amount of copper used in the design. The highest percentage of copper by volume (CBV) that can be manufactured is 15%. Therefore, this was the chosen CBV as it allowed for the highest window of visibility at the lowest possible test frequency. These downsides aren't generally an issue for copper-clad aluminum conductors, as their intended application is not the same. Copperweld® is normally using the copper cladding as a way to prevent corrosion and improve electrical contacts, while gaining the benefits of the lower cost and weight of aluminum. The

following certificate of compliance was created for the conductor as shown on TABLE 5-1. The important specifications here that are pertinent to testing are the diameter and copper volume. Using this data, TABLE 5-2 was produced to show information relevant to testing.

TABLE 5-1: CCA conductor certificate of compliance

CEV3260D-OA		.3260" CCA 15% HARD			Rewind (10)	
Track ID	Heat No	Diameter 0.3228 - 0.3292 in [8.199 - 8.362] [mm]	Breakload 1308 Min lbs [6 Min] [kN]	Elongation 1.5 Min PERCENT	Copper Volume 13 - 17 PERCENT	Tensile 16000 Min psi [110.3 Min] [N/mm2]
FG1030171	73599	0.3265 [8.293]	2771 [12]	5.00	16.4	33096 [228.2]

TABLE 5-2: CCA conductor data

Layer	Diameter	Radius	Volume	Area	DC Resistance
	mm	Mm	%	mm ²	ohm/m @ 20C
Aluminum	7.583	3.791	83.60%	45.16	6.259E-04
Copper	8.293	4.147	16.40%	8.86	1.946E-03
Total	8.293	4.147	100.00%	54.02	4.736E-04

In order to perform testing, this conductor was manufactured into a medium voltage power cable. This allows the cable to be used in a coaxial configuration, since the shield wires are used as a return conductor during testing. A picture of the manufactured cable is shown in FIGURE 5-7:



FIGURE 5-7: Picture of CCA test sample

Although it is difficult to see, there is a small 0.355 mm thick layer of copper cladding around the aluminum conductor. In order to see the desired effect of the bi-media conductor design is it necessary that a significant amount of the current density is concentrated in the copper layer. The frequency range for the test was 60 Hz to 20 kHz. A selection of the obtained current density plots over this range are shown in FIGURE 5-8:

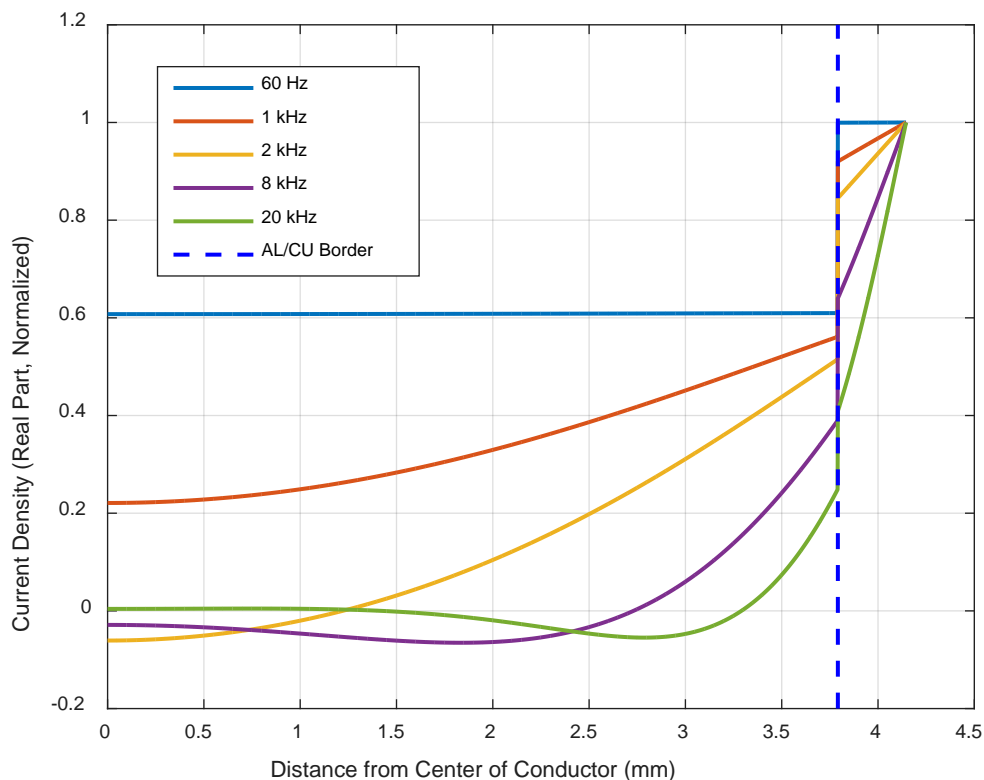


FIGURE 5-8: Calculated current density in CCA conductor

It can be observed that current density of a wire this small at 60 Hz is practically that of its operation during DC current. That is, the current density is basically 100% of its surface value throughout the copper layer, and then drops to 61% (i.e. conductivity of aluminum versus copper) in the aluminum layer. It is important to look at how the AC/DC resistance ratio of all copper and all aluminum conductors compare to the bi-media design being tested. Examining such values ensures that the measured AC/DC resistance ratio is correct to the theory, as opposed to being closer to an all copper or all aluminum conductor. Theoretical plots for the AC/DC resistance ratio in all copper and all aluminum conductors of the same diameter for comparison to the bi-media conductor are shown in FIGURE 5-9:

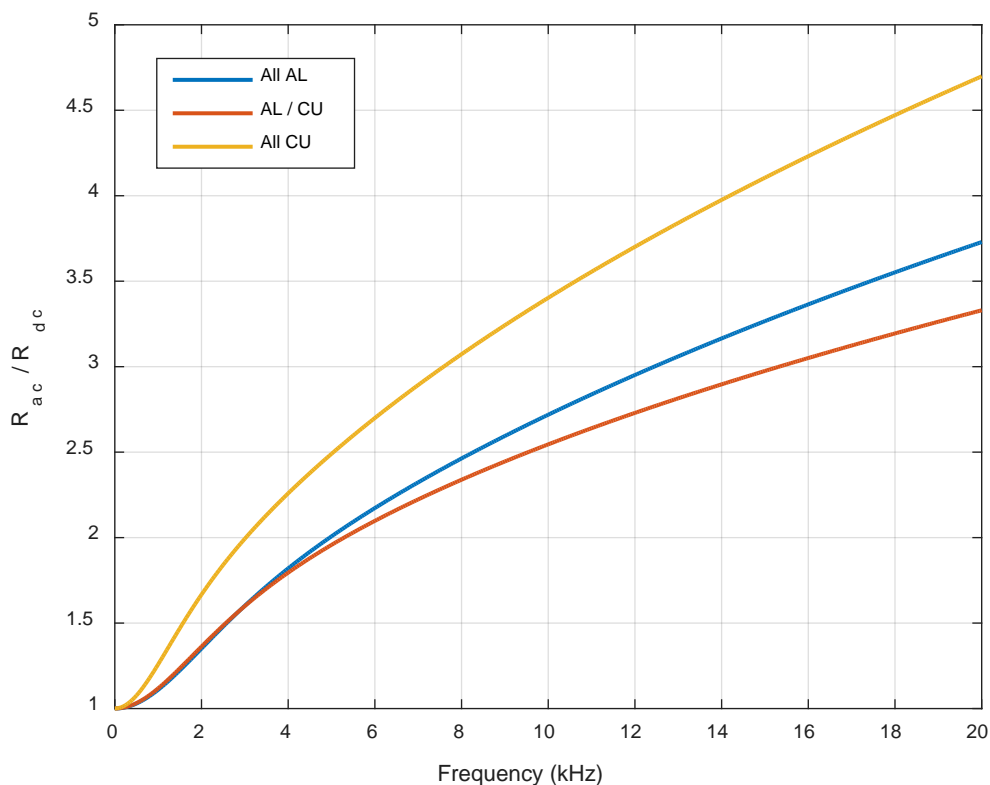


FIGURE 5-9: AC/DC resistance ratio in CCA conductor

At 4 kHz the power analyzer is only taking 250 Sa/cycle, which is half the desired value of at least 500 Sa/cycle. Therefore, it is not expected that correct data will be obtained for higher test frequencies. It can be observed on this plot that the skin effect has a different shape at first when compared to higher frequencies. This is because the Bessel function is exponentially decreasing, and also decreases faster at higher frequencies. Hence, the skin depth is also decreasing. At five skin depths nearly all the current flows within the outer cross-sectional area above this depth, and the inside can be removed with negligible impact on the AC resistance. This is why as frequency becomes sufficiently high, the skin effect becomes a linear function. The most complicated region of the skin effect in a single medium conductor is when the conductor radius is one (i.e. no longer uniform current density) to five skin depths. Within this region the entirety of the

conductor has a noticeable impact on skin effect. A table view of some of the data points for which the current density was plotted is shown on TABLE 5-3:

TABLE 5-3: Skin effect in CCA conductor

Frequency	R_{ac} / R_{dc}	Skin Depth, δ (CU)	# of Skin Depths
Hz		mm	$(r_2 - r_1) / \delta$
60	1.001	8.532	0.042
1000	1.118	2.090	0.170
2000	1.362	1.478	0.240
8000	2.339	0.739	0.481
20000	3.332	0.467	0.760

The highest skin effect in general on designs that would practically be made (i.e. 3000 mm² segmented copper with a $k_s = 0.8$) is nearly 1.9 at 20°C. The skin depth is shown on this table, alongside copper thickness ($r_2 - r_1 = 0.355$ mm) divided by the skin depth. This shows the number of skin depth the copper thickness is at the given frequency. At 8 kHz the current density is being nearly equally affected by both the copper and aluminum layers, and the thickness of the copper is approximately half of a skin depth. The most representative frequency range of the CCA conductor current density distribution to that of a large power conductor at 60 Hz (i.e. frequency range when current density distribution between copper and aluminum media is similar) occurs between 2 and 8 kHz on the copper-clad aluminum conductor. However, it is still of interest to test at higher frequencies to observe the effects of forcing the majority of the current into the thin outer copper layer. When the frequency is very low the copper layer has a negligible effect on AC resistance, and when very high the aluminum has a negligible effect on AC resistance. This can be demonstrated by plotting the change in the AC/DC resistance ratio for the bi-media design versus the all aluminum equivalent OD conductor (as it basically is under DC conditions), as shown in FIGURE 5-10:

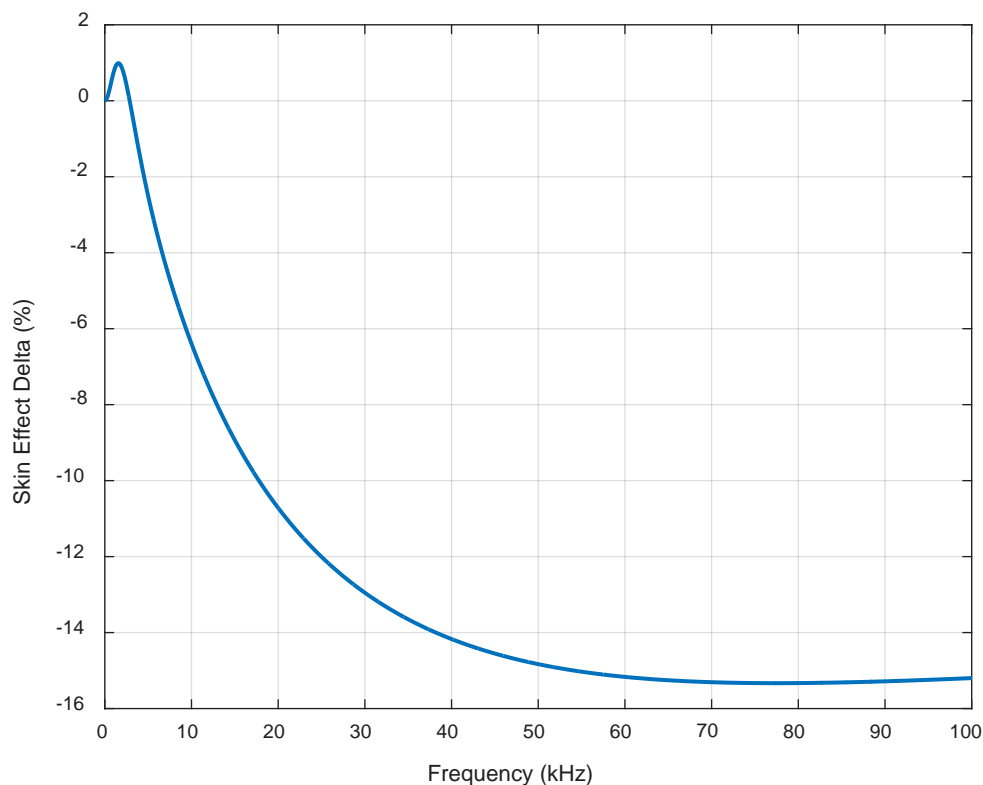


FIGURE 5-10: AC/DC resistance ratio in CCA vs all AL conductor

In this plot it can be observed that past a certain frequency the AC/DC resistance ratio between the all aluminum and bi-media conductors stops changing. This indicates that on frequencies above approximately 40 kHz nearly all the current is traveling in the copper cladding layer of the bi-media conductor. At 40 kHz the skin depth of copper is 0.3304 mm, which is consistent with the thickness of the copper cladding. Therefore, the frequency range of 10 to 20 kHz still provides useful information for comparison to the mathematical theory of the bi-media conductor. This high frequency range would not be of as much interest on a larger conductor, but is on this test sample due to the relatively small thickness of the copper compared to the aluminum. This behavior of the current density being primarily in the copper layer can also be seen by looking at the AC resistance.

FIGURE 5-11 shows the AC resistance of the copper-clad aluminum conductor over the range of frequencies being tested:

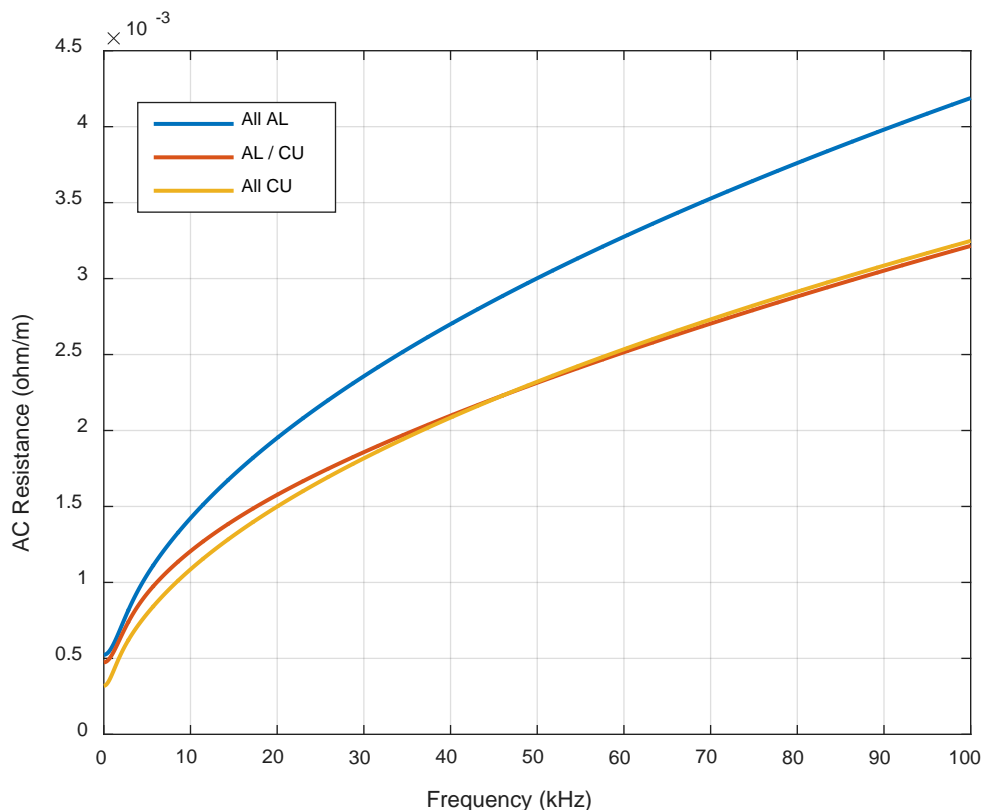


FIGURE 5-11: AC resistance in CCA conductor

FIGURE 5-11 shows that the AC resistance of the copper-clad aluminum conductor starts nearly equal to the all aluminum conductor and becomes nearly the same as the all copper conductor. This shows the current at low frequencies being concentrated in the aluminum layer and then shifting to the copper layer at high frequencies. From 50 to 100 kHz, the bi-media conductor has a lower AC resistance than the all copper conductor. This is because this is the range in which the negative current density in the copper can be improved with aluminum. If the plot was extended to cover higher frequencies, the AL /

CU and all copper designs would be practically the same, as practically all of the current would be traveling solely in the copper layer.

The second sample manufactured was done using a stranded conductor with a cross-sectional area of 2570 mm^2 . It was a non-standard cross-sectional area design, as the cable was made purely for the proof of concept in testing as reused conductor design tooling from a previously manufactured custom sized conductor. The advantage of this test sample versus the first test sample is that the conductor is an appropriately sized design to prove the derived mathematical theory at power frequency. Additionally, the equipment being used for measurement purposes was also chosen for testing at power frequency. The disadvantages of this design are that it is stranded instead of solid, its large size makes it more difficult to work with (e.g. the conductor weighed 18.37 kg/m), and the low resistance of the conductor makes contact resistances more substantial in the measurements. All conductors this large must be stranded, so the test sample is still ideal from a manufacturing point of view. However, the stranding of the conductor will add a slight amount of measurement error due to the reactance of the spirals. It is expected that the stranded bi-media conductor will perform the same way the stranded single medium conductors do. By this it is meant that the AC/DC resistance ratio of the stranded conductor will be the same as the AC/DC resistance ratio of a solid conductor having the same cross-sectional area. The following measurements were made on the manufactured test sample, shown in TABLE 5-4:

TABLE 5-4: 2570 mm² bi-media conductor dimensions

Layer	Stranded		Solid		Solid	Solid
	Diameter	Radius	Diameter	Radius		
	mm		mm		mm ²	ohm/m @ 20C
Aluminum	34.00	17.00	31.87	15.93	797.7	3.543E-02
Copper	59.90	29.95	57.20	28.60	1772.1	9.729E-03
Total	59.90	29.95	57.20	28.60	2569.7	7.633E-03

The conductor aluminum and copper layers were weighed on a production sample and the DC resistance was measured during production using a Schuetz Messtechnik MR 300 C-A digital micro ohm meter in a temperature and humidity environmentally controlled test chamber. The DC resistance measured was 2.0% higher than calculated based on weights. This is expected since stranding the conductor effectively increases its length and therefore causes a slight increase in resistance. A photograph of the DC resistance test proceeding conductor manufacturing (i.e. before manufacturing into a power cable) is shown in FIGURE 5-12:



FIGURE 5-12: Picture of post-stranding DC resistance measurement setup

In order to perform testing, this conductor was manufactured into a power cable. Unlike the first test sample that was a typical medium voltage power cable design, this test sample is a non-standard design. Because the testing current and voltage is very low a reduced amount of insulating materials were used. It is still important that the cable be concentric, as a non-concentric cable design results in a non-uniform current density distribution in the conductor. This is due to an uneven distance and therefore uneven proximity effect between the conductor and the shielding. A picture of the manufactured conductor is shown in FIGURE 5-13:

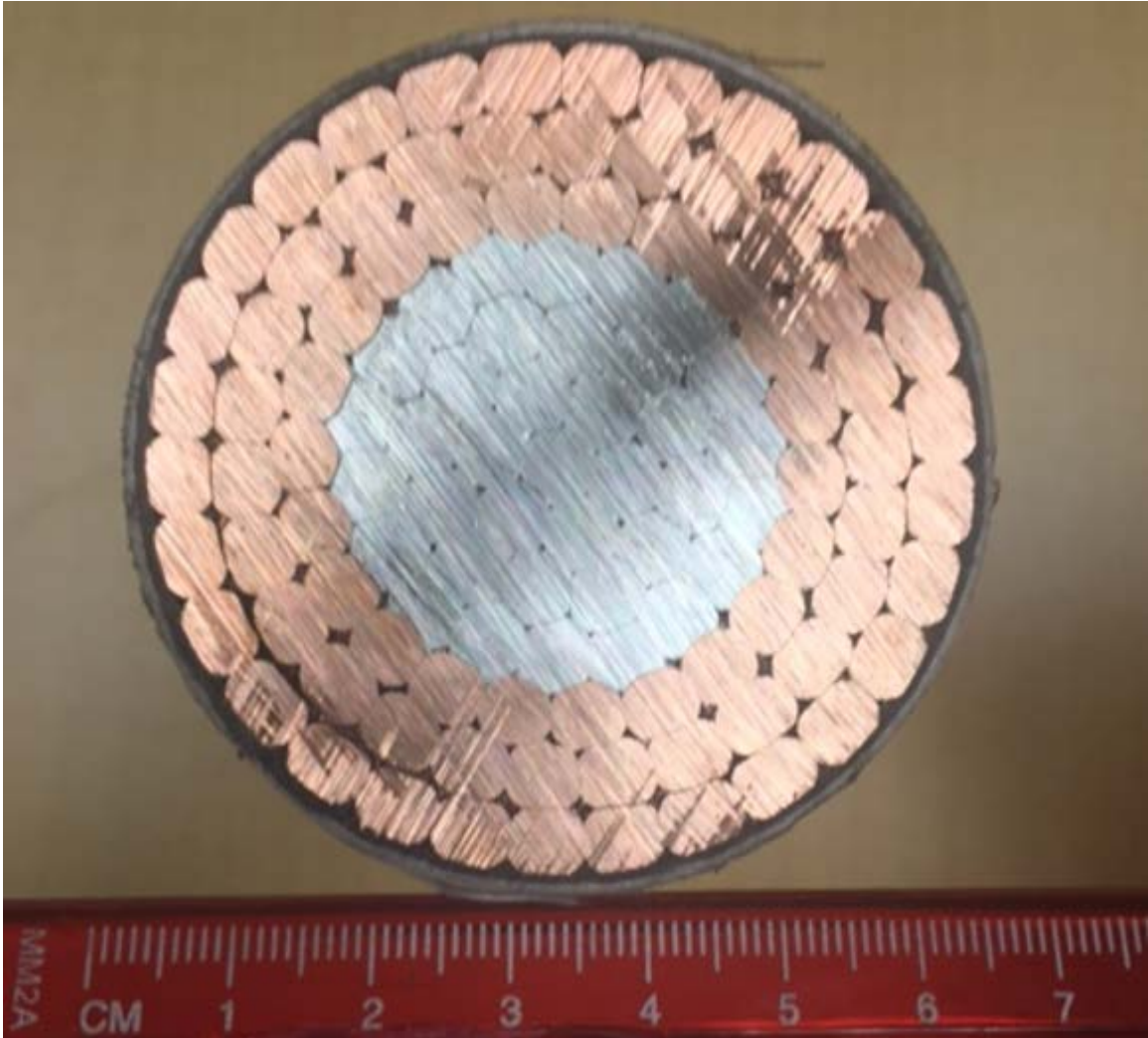


FIGURE 5-13: Picture of 2570 mm² bi-media conductor

The frequency range for the test will be 30 to 200 Hz. Some current density plots over this range are shown in FIGURE 5-14:

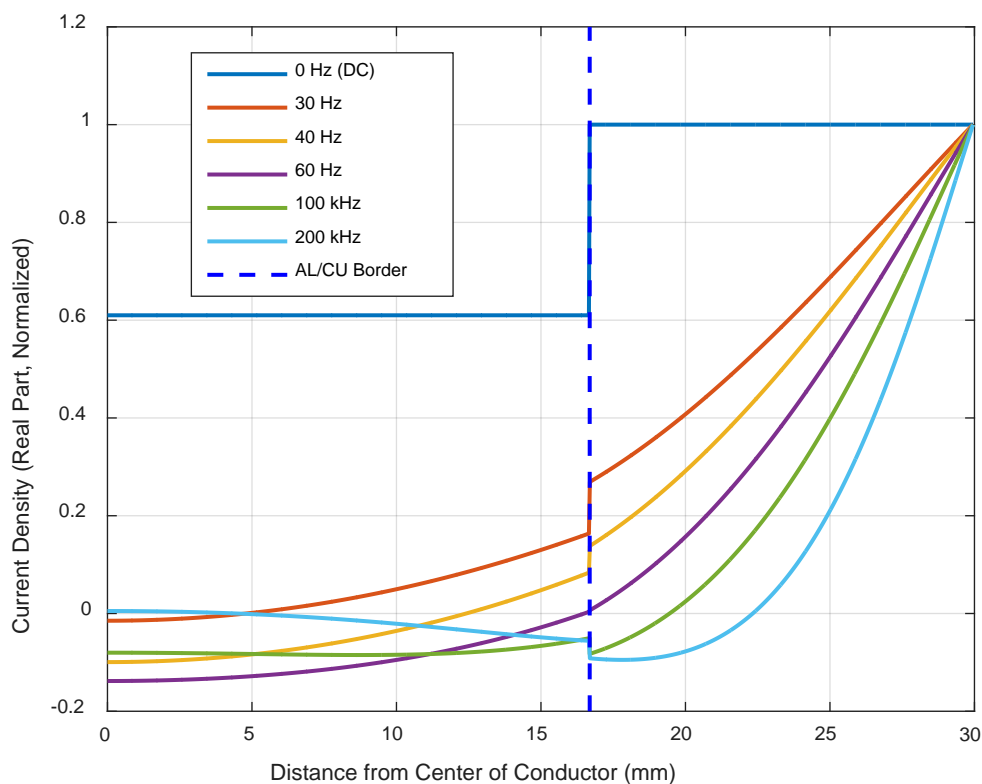


FIGURE 5-14: Calculated current density in 2570 mm² bi-media conductor

It can be observed that the current density distribution of such a large conductor has a significant change from uniform DC current density distribution even for frequencies as low as 30 Hz. It is again important to look at how the AC/DC resistance ratio of all copper and all aluminum conductors compare to the bi-media design being tested. Theoretical plots for the AC/DC resistance ratio in all copper and all aluminum conductors of the same cross-sectional area for comparison to the bi-media conductor are shown in FIGURE 5-15:

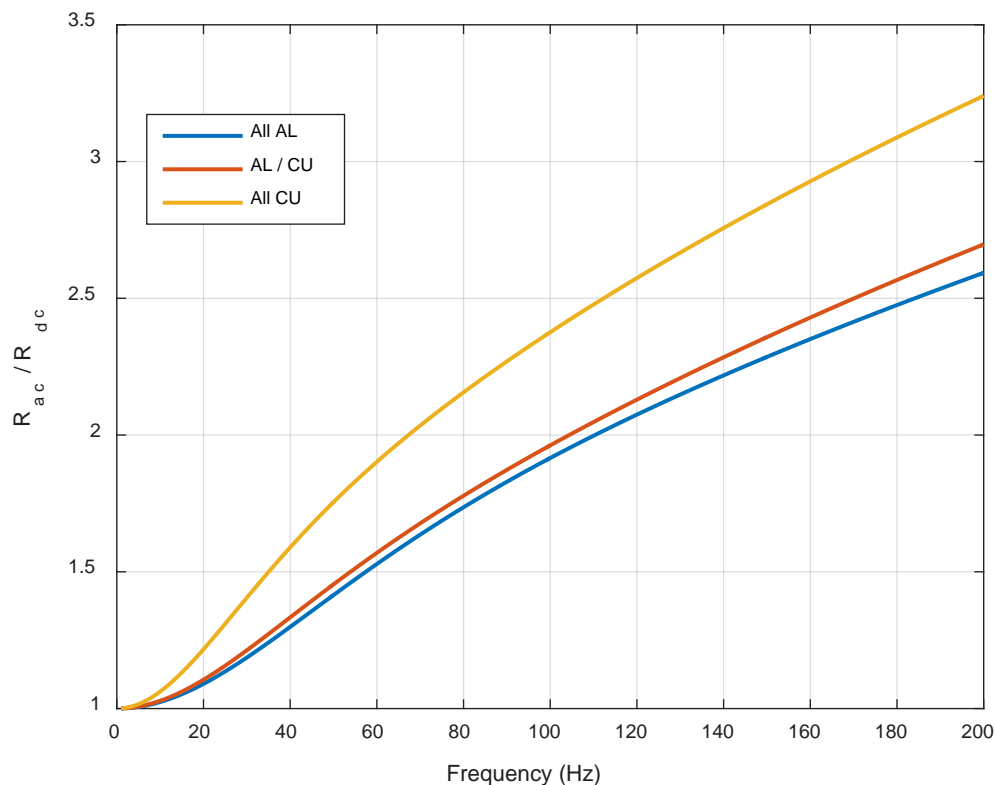


FIGURE 5-15: AC/DC resistance ratio in 2570 mm² bi-media conductor

This shows that the bi-media conductor AC/DC resistance ratio is nearly the same for the all aluminum and bi-media conductors. A table view of some of the data points for which the current density was plotted is shown on TABLE 5-5:

TABLE 5-5: Skin effect in 2570 mm² bi-media conductor

Frequency	R_{ac} / R_{dc}	Skin Depth, δ (CU)	# of Skin Depths
Hz		mm	$(r_2 - r_1) / \delta$
30	1.439	12.065	1.050
60	1.950	8.532	1.485
100	2.436	6.608	1.917
140	2.828	5.585	2.268
200	3.325	4.673	2.710

The equivalent solid copper thickness ($r_2 - r_1 = 12.67$ mm) over the skin depth is shown in TABLE 5-5, which indicates the number of skin depths the copper thickness is

at the given frequency. Unlike the first test sample, the thickness of the copper layer at all test frequencies is greater than half of its skin depth. Therefore, it should be easy to discern the effects of the current density being affected by both the copper and aluminum layers from it being affected by only the copper or aluminum layer at 30 Hz. Also, the highest test frequency of 200 Hz is not susceptible to measurement inaccuracies due to low sampling rates as the first test sample was. The change in AC/DC resistance ratio for the bi-media design versus the all aluminum equivalent OD conductor is shown in FIGURE 5-16:

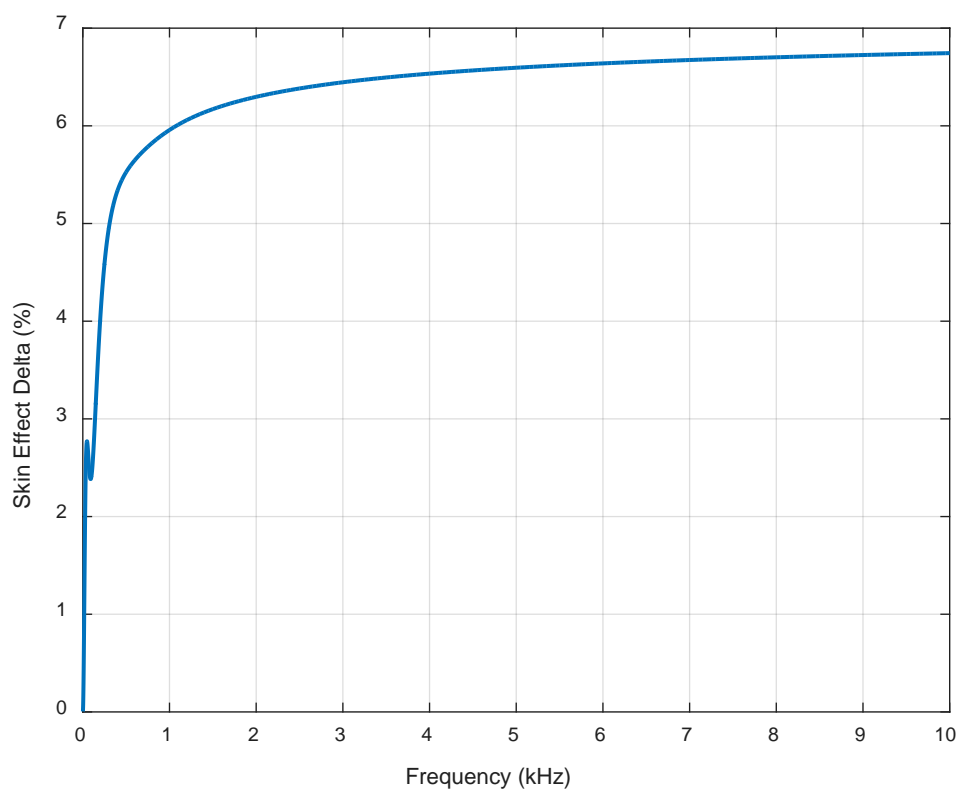


FIGURE 5-16: R_{ac} / R_{dc} in 2570 mm² bi-media vs all AL conductor

The inflection in the curve that occurs around 60 Hz represents the optimal conductor frequency where the AC resistance of the conductor has been reduced by

replacing some of the copper core with an aluminum core. In this plot it can be observed that past a certain frequency the skin effect ratio between the all aluminum and bi-media conductor stops changing. This indicates that on frequencies above approximately 2 kHz nearly all the current is traveling in the outer copper layer of the bi-media conductor. This behavior of the current density being primarily in the copper layer can also be seen by looking at the AC resistance. FIGURE 5-17 shows the AC resistance of the 2570 mm² bi-media conductor over the range of frequencies being tested:

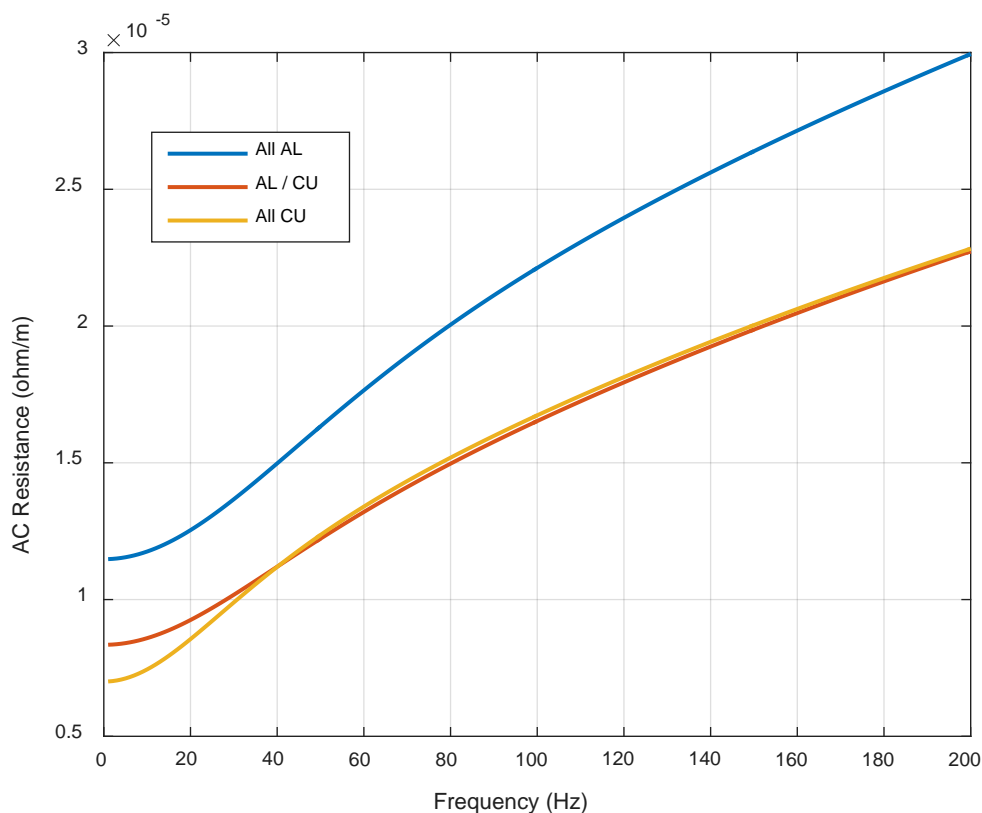


FIGURE 5-17: AC resistance in 2570 mm² bi-media conductor

FIGURE 5-17 shows that the AC resistance of the bi-media conductor starts between the all copper and all aluminum, since its DC resistance is between these two points. However, the AC resistance quickly becomes nearly equal to the all copper

conductor for frequencies at or above 30 Hz. This demonstrates that for frequencies above 30 Hz the bi-media conductor has basically the same AC resistance of an all copper conductor, despite having an inner core of aluminum. The frequency range above 40 Hz when the AC resistance of the AL / CU is less than the all copper conductor corresponds to the current density becoming negative in the core. Therefore, removing it or replacing it with a lower conductivity medium improves the AC resistance. If the plot showed up to higher frequencies the AL / CU and all copper designs would be practically the same, as basically all of the current would be traveling solely in the copper layer.

5.2.3 Experiment Results

The test was first performed on a 144 foot sample of copper-clad aluminum conductor cable. The small diameter of the cable made it possible to test the cable off of the reel. Only a small amount of mutual inductance between the coils was expected, since the magnetic field is mostly canceled outside of the cable due to the coaxial configuration. The cable was also on a wooden reel, which introduces less inductive effects as opposed to a steel reel. Still, to ensure as little mutual inductance between the test object and either itself or any other nearby objects, the cable was suspended in the air with two cranes in a high voltage laboratory. Photographs taken of the measurement setup are shown in FIGURE 5-18 and FIGURE 5-19:

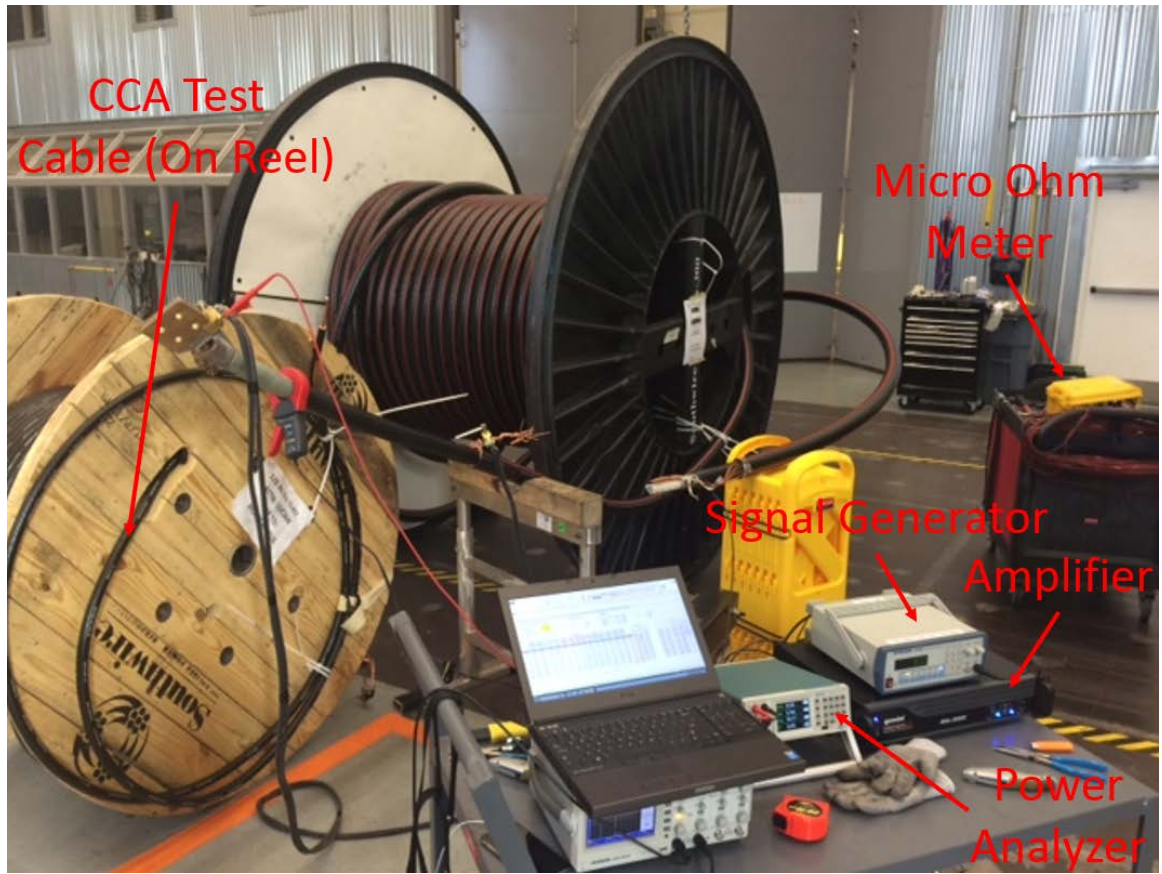


FIGURE 5-18: Equipment test setup of CCA conductor

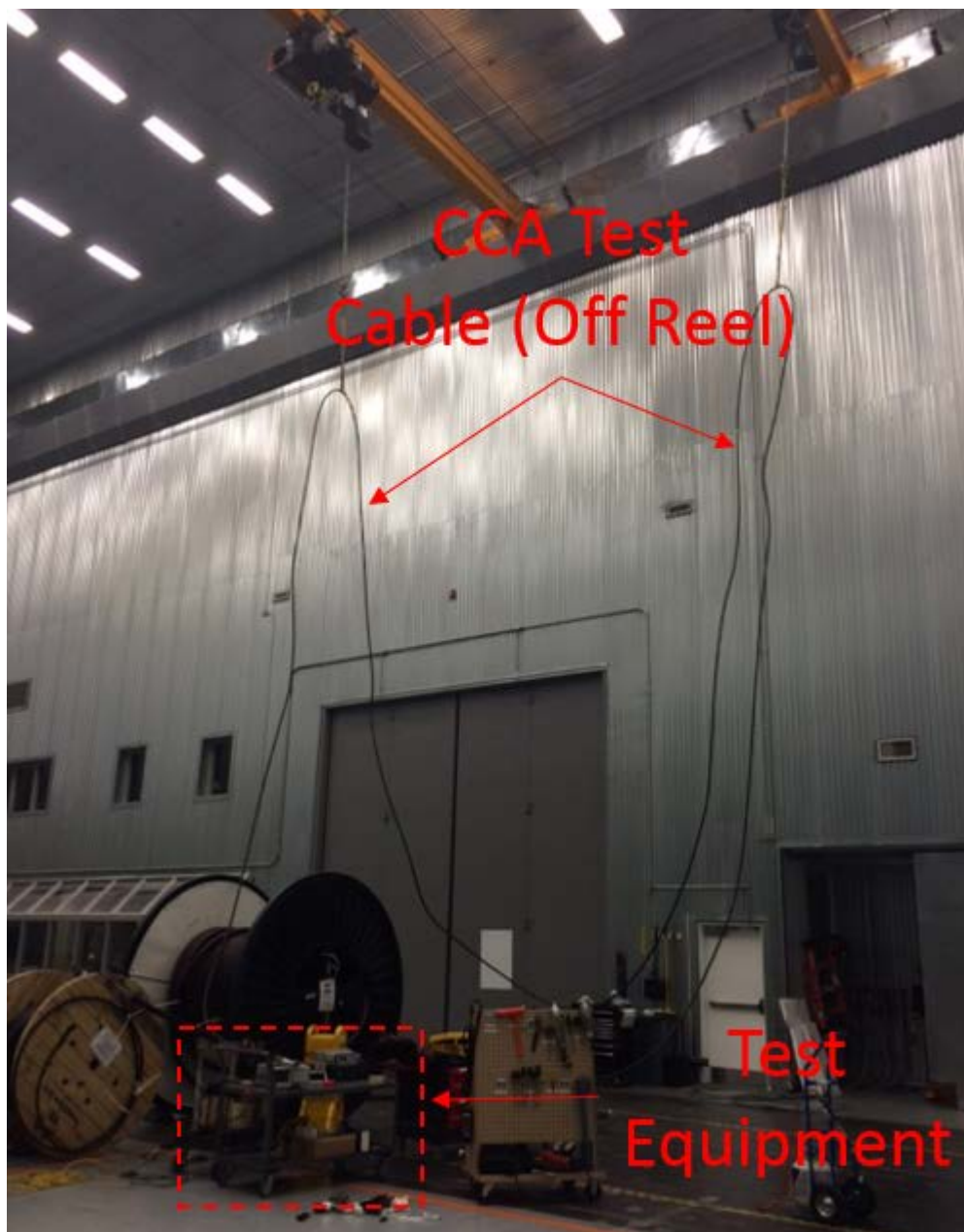


FIGURE 5-19: Cable test setup of CCA conductor

The DC resistance was measured as 2.106×10^{-2} ohm at 18.6°C using a Raytech Micro-Jr. 2 digital micro ohm meter. This value was then corrected to a unit length value at 20°C of 4.826×10^{-4} ohm/m. The power analyzer was used to measure real power and RMS current. Using these values the AC resistance was then calculated as follows:

$$P = \frac{1}{T} \int_0^T V_i \cdot I_i dt \quad (128)$$

$$I = \sqrt{\frac{1}{T} \int_0^T I_i^2 dt} \quad (129)$$

$$R_{ac} = \frac{P}{I^2} \quad (130)$$

The time step T for a sampling rate of 1 MSa/s is 1 μ s. The power analyzer display shows measurements that update two times every second (i.e. each display refresh is a result from 500 kSa). The logged values used to calculate AC resistance were saved every one second. Each time data values were logged (i.e. the real power and RMS current measurements made from the power analyzer) the values were the average of four measurement periods (i.e. two seconds, 2 MSa) using a measurement delay setting. This delay setting was chosen on the power analyzer to help obtain more consistent results, since the measurements sought after are not time dependent. Values were logged for fifteen seconds, and calculations of the AC/DC resistance ratios from each of the fifteen measurement sets consistently resulted in the same AC/DC resistance ratio. FIGURE 5-20 summarizes the results of the AC resistance ratios that were measured versus the theoretical results expected:

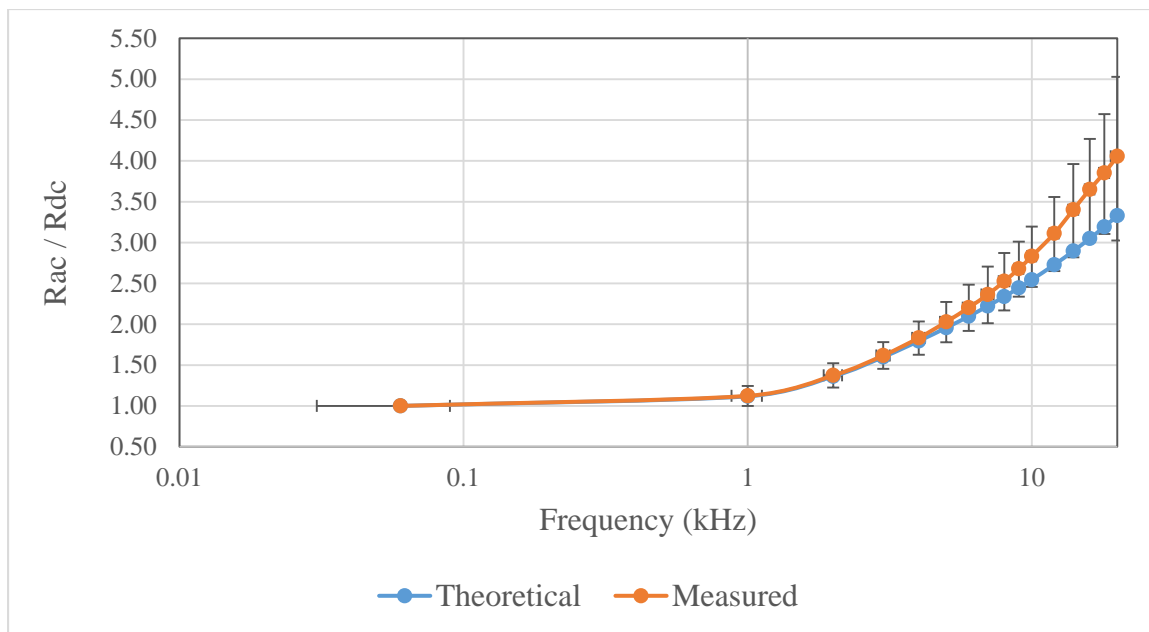


FIGURE 5-20: AC/DC resistance ratios measured on CCA conductor

The error bars shown are related to the measurement accuracy of the power analyzer. Due to a relatively low voltage applied (generally 0.3 to 0.9 V) to the test object, the voltage measurement accuracy range was wide. This wide range of voltage measurement accuracy further produced a wide range in the real power measurement accuracy since it is calculated using the voltage measurement. Since the AC/DC resistance ratios calculated for each set of measurements at the same frequency were consistent, it is believed that the measurement error due to the low voltage did not have a substantial effect on the accuracy of the measurements. However, the actual values expected are within the error bars of the measured values. It can be observed on the figure that the theoretical and measured values are very close up until approximately 4 kHz. The error between the actual and measured values is summarized in TABLE 5-6:

TABLE 5-6: Error in AC/DC resistance ratios measured on CCA conductor

Frequency (Hz)	Error (%)
60	0.0%
1000	0.5%
2000	0.9%
3000	1.2%
4000	2.2%
5000	3.7%
6000	5.1%
7000	6.4%
8000	8.0%
9000	9.6%
10000	11.3%
12000	14.1%
14000	17.5%
16000	19.7%
18000	20.6%
20000	21.8%

This data can also be viewed in terms of AC resistance as shown in FIGURE 5-21:

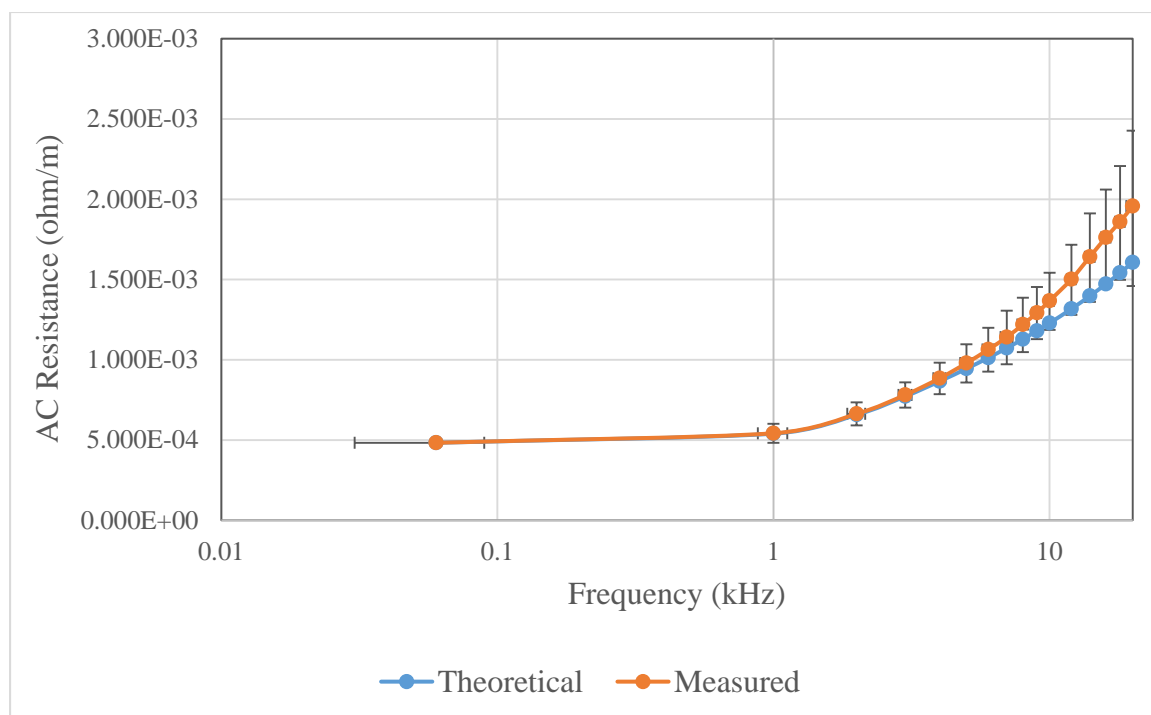


FIGURE 5-21: AC resistance measured on CCA conductor

As was expected due to the low number of samples per cycle for frequencies higher than 2 kHz, the accuracy of the results above 2 kHz are not reliable. The summary at the end of the chapter includes a more detailed analysis of other sources of error.

The test on the 2570 mm² conductor was performed on a 3452 foot sample of stranded copper around a stranded aluminum conductor core. The total cable diameter was approximately 110 mm. The large diameter and weight of the cable required it be tested on the steel reel. Also, due to the low resistance of the conductor the contact resistance of the connectors was removed from the DC resistance measurements. While this long cable length has the benefits of reducing error from contact resistance and non-homogeneous current insertion into the test object, it introduces a magnetic object in close proximity of the test object. Specifically, the reel with the cable on it effectively is acting as a large inductor. A photograph taken of the measurement setup is shown in FIGURE 5-22:



FIGURE 5-22: Equipment test setup of 2570 mm² conductor (steel reel)

The DC resistance (after removing contact resistance of the connectors) was measured as 7.983×10^{-3} ohm at 18.0°C using a Raytech Micro-Jr. 2 digital micro ohm meter. This value was then corrected to a unit length value at 20°C of 7.649×10^{-6} ohm/m. This value is 0.21% higher than originally measured on a test sample taken during manufacturing of the conductor. It is expected that conductor resistance increases through manufacturing. The contact resistance on the long length of 2570 mm² conductor comprised approximately 0.7% of the total resistance of the test object. FIGURE 5-23 summarizes the results of the AC resistance ratios that were measured versus the theoretical results expected:

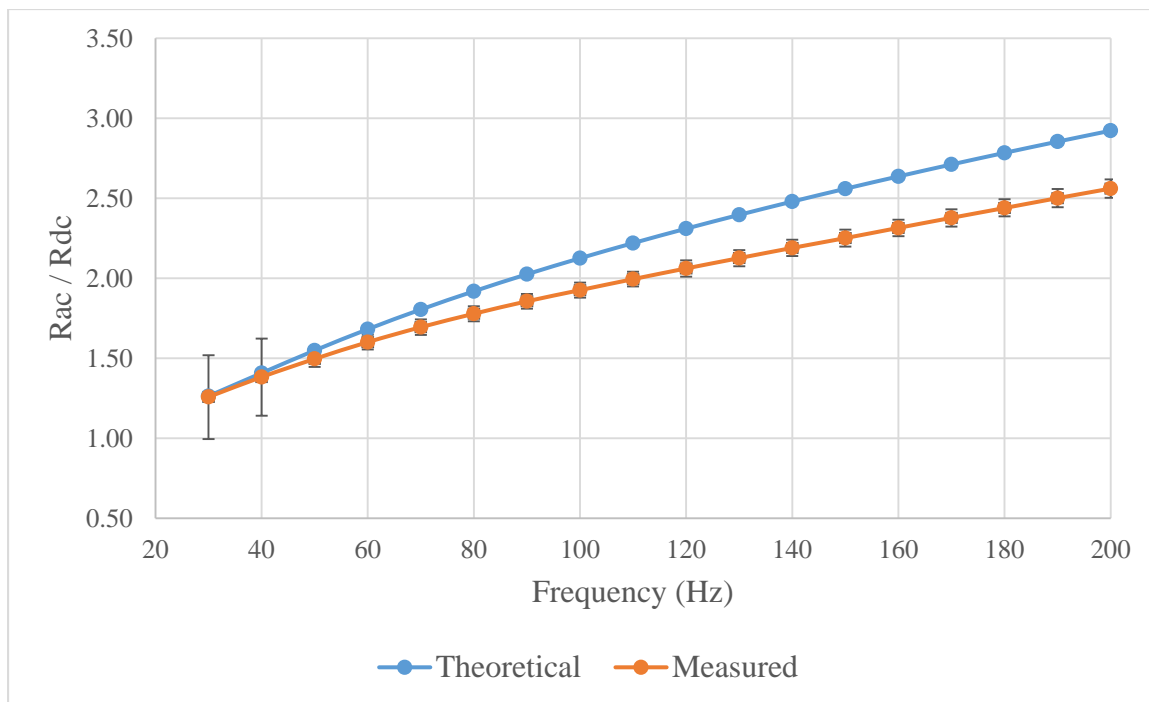


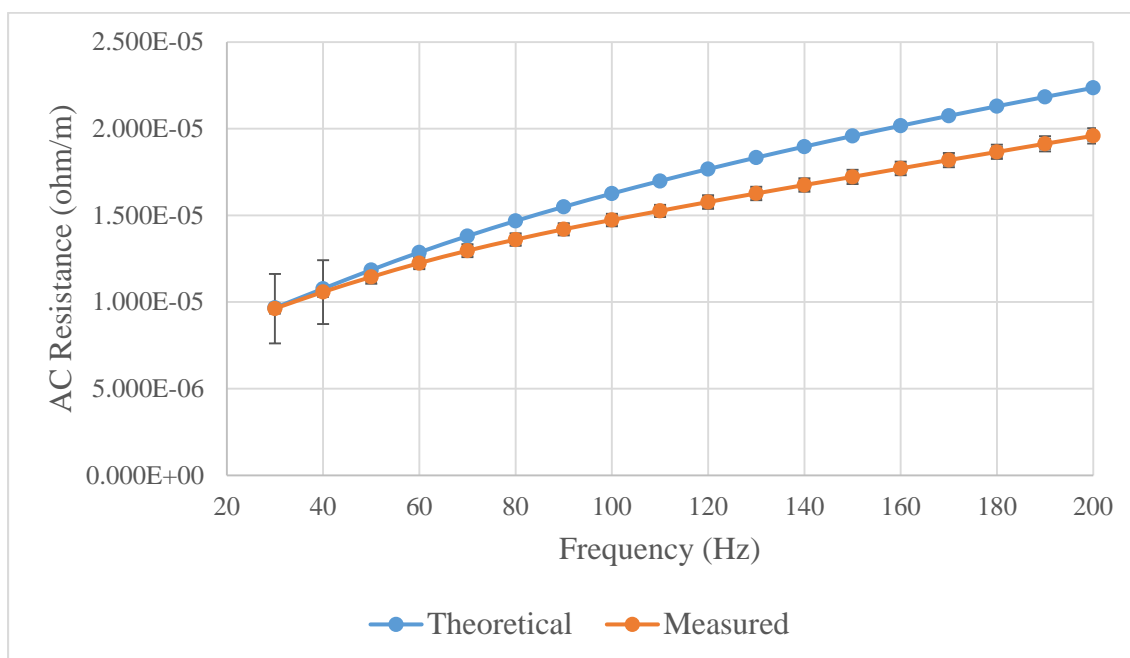
FIGURE 5-23: AC/DC resistance ratios of 2570 mm² conductor (steel reel)

The error bars are related to the measurement accuracy of the power analyzer. Due to a relatively low voltage applied (generally 0.3 to 0.9 V) to the test object the voltage measurement accuracy range was wide for frequencies outside the range of 45 – 850 Hz (i.e. 30 and 40 Hz here). This wide range of voltage measurement accuracy further produced a wide range in the real power measurement accuracy since it is calculated using the voltage measurement. It can be observed in FIGURE 5-23 that the theoretical and measured values continually diverge with increasing frequency. This is believed to be due to the inductive effect of the cable coiled on the steel reel. A wooden reel is not able to support this length of cable due to weight, but can be used for testing shorter lengths. The error between the actual and measured values is summarized in TABLE 5-7:

TABLE 5-7: Error in AC/DC resistance ratios of 2570 mm² conductor (steel reel)

Frequency (Hz)	Error (%)
30	-0.4%
40	-1.8%
50	-3.4%
60	-4.8%
70	-6.1%
80	-7.3%
90	-8.4%
100	-9.4%
110	-10.1%
120	-10.8%
130	-11.3%
140	-11.7%
150	-12.0%
160	-12.2%
170	-12.3%
180	-12.4%
190	-12.4%
200	-12.4%

This data can also be viewed in terms of AC resistance as shown in FIGURE 5-24:

FIGURE 5-24: AC resistance measured on 2570 mm² conductor (steel reel)

Due to the large difference between the theoretical and measured values shown on FIGURE 5-24 the cable was wound onto a wooden reel to reduce proximity effects of the steel reel. In order to further reduce proximity effects the cable was wound onto the reel with gaps between the windings. Testing on the 2570 mm^2 conductor was repeated for this cable on a 318 foot sample. A photograph taken of the measurement setup is shown in FIGURE 5-25:

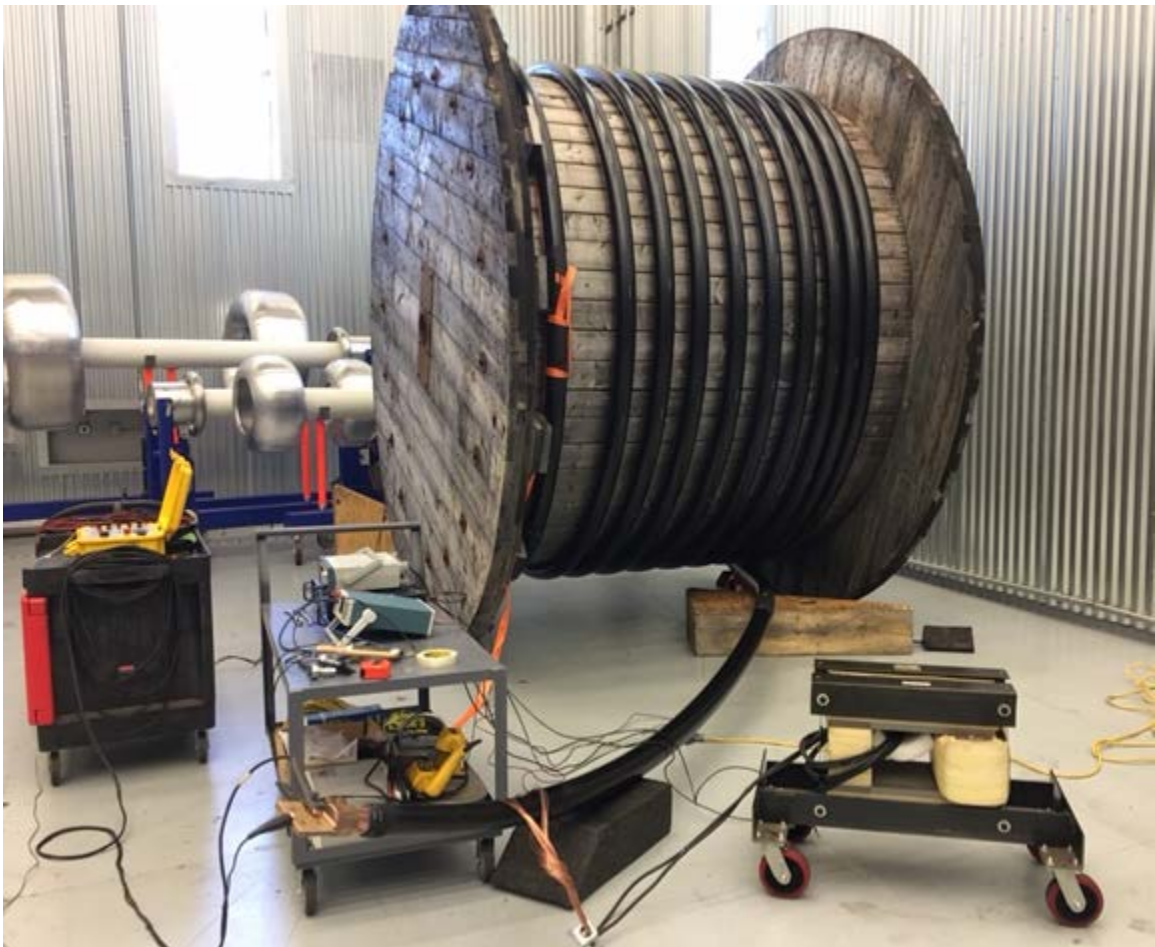


FIGURE 5-25: Equipment test setup of 2570 mm^2 conductor (wood reel)

The DC resistance (after removing contact resistance of the connectors) was measured as $7.334 \times 10^{-4} \text{ ohm}$ at 17.6°C using a Raytech Micro-Jr. 2 digital micro ohm meter. This value was then corrected to a unit length value at 20°C of $7.640 \times 10^{-6} \text{ ohm/m}$.

This value is 0.09% higher than originally measured on a test sample taken during manufacturing of the conductor, and within accuracy of the measuring equipment. Contact resistance of the connectors on this shorter length comprised approximately 7.2% of the total resistance measured in the test object. FIGURE 5-26 summarizes the results of the AC resistance ratios that were measured versus the theoretical results expected:

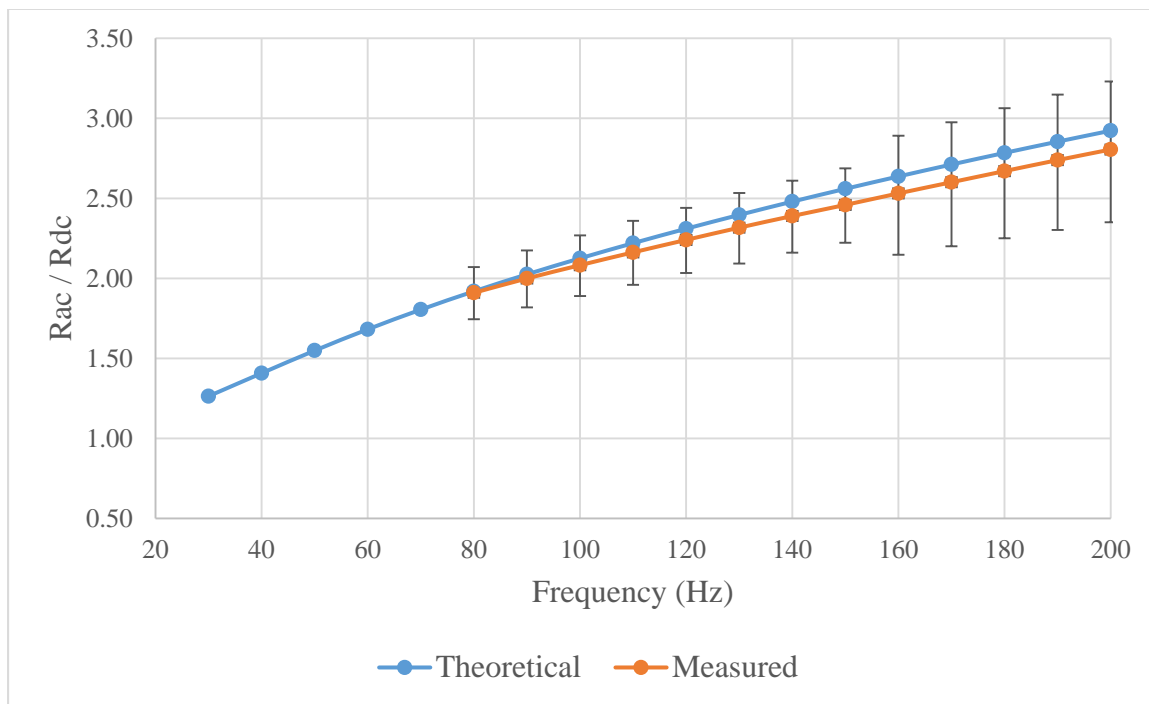


FIGURE 5-26: AC/DC resistance ratios of 2570 mm² conductor (wood reel)

The error bars are related to the measurement accuracy of the power analyzer. All voltages measured were within the highest accuracy range for frequency of the power analyzer (45 – 850 Hz). However, due to the reduced resistance of the test object resulting from a shorter length than measured on the steel reel the current applied (45 – 70 A) was higher than could be used on the 20 A shunt of the power analyzer. Therefore, a clamp-on ammeter with higher measurement error had to be used. This wide range of current measurement accuracy further produced a wide range in the real power measurement accuracy since it is calculated using the current measurement. Furthermore, higher current

injection was required to obtain a large enough voltage signal to measure with the power analyzer. For frequencies below 80 Hz this resulted in clipping of the waveform, and therefore limited measurements to frequencies starting at 80 Hz. It can be observed in FIGURE 5-26 that the theoretical and measured values diverge with increasing frequency. This is believed to be due to remaining inductive effects of metallic objects and spacing not able to be achieved between all windings as shown in FIGURE 5-25. Furthermore, higher frequencies also result in more pronounced manufacturing variance. That is, the exact geometry of the conductor has a larger effect on measurement results. The error between the actual and measured values is summarized in TABLE 5-8:

TABLE 5-8: Error in AC/DC resistance ratios of 2570 mm² conductor (wood reel)

Frequency (Hz)	Error (%)
80	-0.5%
90	-1.3%
100	-2.0%
110	-2.6%
120	-3.0%
130	-3.3%
140	-3.6%
150	-3.9%
160	-4.0%
170	-4.1%
180	-4.1%
190	-4.0%
200	-4.0%

This data can also be viewed in terms of AC resistance as shown in FIGURE 5-27:

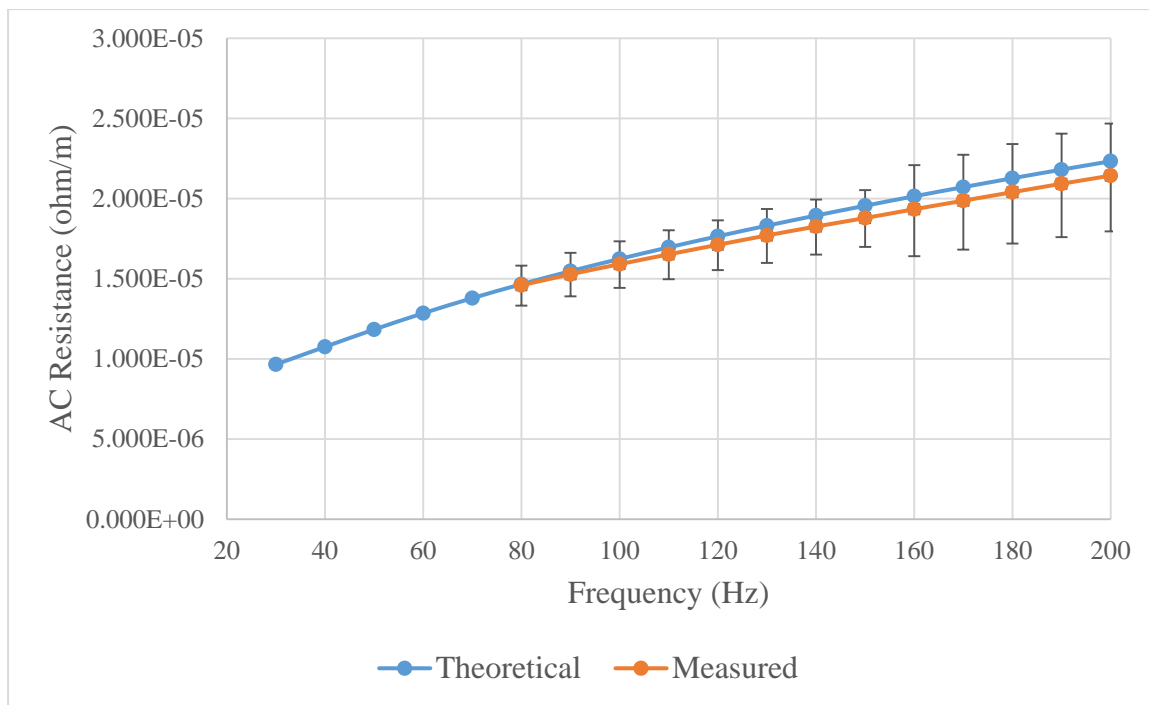


FIGURE 5-27: AC resistance measured on 2570 mm² conductor (wood reel)

At all frequencies tested there is a significant effect of the current density distribution in each layer. Considering the accuracy of the results versus an all aluminum or all copper conductor, the measured values show very good conformance with the theoretical values. It is apparent from the results the current density must be negative with a portion of the aluminum conductor, and thus improves AC resistance versus an all copper conductor of equal cross-sectional area. The summary in the following section concludes the chapter and includes a more detailed analysis of other sources of error.

5.2.4 Summary of Results and Observations

The AC resistance and AC/DC resistance ratios obtained for the two test samples showed good agreement with the theoretical results provided a sampling rate of 500 Sa/cycle or greater was used on the first test object. The second test object showed measured and theoretical results to be in the correct range for lower frequencies, but the inductive effects from the steel reel made it difficult to discern effects purely from the

conductor from those of mutual inductance. However, FIGURE 5-14 shows that at 30 Hz there is a significant contribution from both the copper and aluminum parts of the conductor. Therefore, the values obtained are still very close as compared to the conductor being all copper or all aluminum. Additionally, measurements made on the 2570 mm² bi-media conductor cable show close agreement with the theoretical results. Although the steel reel and low sampling rate (i.e. less than 500 Sa/cycle) are by far the largest contributors to the error in measurements, there are many other factors that are also sources of error. All the following factors, which cause increasing error with higher frequencies, contribute to the error in the measurements:

- the proximity effect between the conductor and shield (since the current is in opposite directions in the conductor and shield, the current density distribution in the conductor is further suppressed, resulting in a higher apparent AC/DC resistance ratio than caused by the conductor alone),
- the current transformer (since it was designed for 60 Hz, it is possible that distorted waveforms not perfectly sinusoidal were produced at other frequencies if the ferromagnetic core was saturated),
- penetration depth approaching design features (the theory is based on a solid round conductor; therefore, if the frequency is high enough that the skin depth is low enough to be comparable to the size of the conductor strands, the theory is not as accurate),
- manufacturing quality control of the copper cladding (very accurate thickness of the copper cladding and diameter of the conductor are essential when trying to

prove theory on such a small conductor, and therefore slight changes can result in large differences with respect to theoretical results),

- manufacturing quality control of the conductor roundness (a concentric conductor results in non-symmetric current density distribution not accounted for in theoretic calculations),
- manufacturing quality control of the cable roundness (not perfectly concentric cable results in non-symmetric current density distribution in the conductor since the distance between the conductor and shield is not consistent),
- the stranding of the conductor (the theory is based on a solid conductor, and therefore does not account for the reactance of the spirals),
- DC resistance affected by bends in the cable (bends compress the conductor on the inside effectively decreasing DC resistance and elongate it on the outside effectively increasing DC resistance, resulting in non-symmetric current density distribution),
- connection of the leads to the conductor (since current insertion into the conductor may not have been uniformly entering each strand, possibly due to high contact resistance)
- and cable geometry affected by bends in the cable (bends create compressive force inside the cable that puts the conductor more off center, which creates a non-symmetric current density distribution).

Now that the theoretical background and test results of bi-media designs have been presented, the next task is finding the correct application for them. The next chapter addresses how the bi-media designs are optimized, and what the ideal application range

(depending on operating conditions) is for these new conductors. The chapter also discusses how these new design can be used in the power industry.

CHAPTER 6: INDUSTRY APPLICATION

6.1 Overview

This chapter discusses how the new solutions of large bi-media power conductors can be implemented in the industry. Specifically, as found earlier, the important media that are presented are Air / CU and AL / CU. The Air / CU design is not something that hasn't been done in the past, but it has not been explored from the point of view of using the AC resistance minima in comparing it to existing designs. Copper-clad aluminum conductors, such as the AL / CU design, also currently exist in the industry, but not for large conductors and further has not had an analytical solution for calculation of skin effect.

When presenting these designs to the industry, it is important that there are standardized designs to simplify manufacturing and reduce cost to the consumer. However, standardized sizes do not tell the whole story of whether a bi-media conductor is more cost effective. In the case of AL / CU designs, the cross-sectional area is expected to be slightly higher than that of segmented copper, but the price may still be lower as some copper has been replaced with aluminum. Therefore, the bi-media conductors are compared with the typical design for large power conductors, namely segmented copper on the basis of material cost only (i.e. no manufacturing cost considered).

The next issue arising is if someone within the industry wants to create a non-standard design themselves. Implementation of the solutions described within this dissertation would require great knowledge of the subject and powerful PC tools such as

MATLAB to implement. To address this issue simplified polynomial equations are presented, in the same fashion that exist in industry standards currently. These allow for a simplified calculation of the cross-sectional area required for each medium in order to minimize AC resistance. Additionally, there are also simplified polynomial equations to calculate the AC/DC resistance ratio of any bi-media design of non-standard cross-sectional area.

Finally, concluding this chapter there is commentary on a full selection methodology, along with examples of how a practitioner of these calculations would go about choosing the lowest cost conductor design. There is also commentary contained throughout the chapter of important design considerations, and a summary detailing the lowest cost options. Note that the industry operates such conductors either at a temperature of 90°C or 105°C. Also, the power system frequency depending where in the world the system is located is either 50 or 60 Hz. Therefore, the data presented in this chapter covers all four of these permutations. Additionally, when figures and tables are presented these ranges are in the order of most to least applicable combination of temperature and frequency. Lower temperature and higher frequency are more conducive to the application window of bi-media conductors, and therefore the data is presented in order from most effective to least effective: 90°C/60Hz, 105°C/60Hz, 90°C/50Hz, and 105°C/50Hz. Recall that the minima of the AC resistance shifts depending on both frequency and temperature. Therefore, the presented designs are specific to a maximum conductor operating temperature and frequency.

One would naturally want to design the conductor around the maximum operating temperature since this is the point at which the skin effect is most critical to achieving the

desired capacity. This is why design of conductors is done at maximum operating temperature, such that one knows the maximum possible ampacity of the conductor.

It should be noted that the cost comparison done in this chapter should be viewed as the material cost to obtain wires required to strand the conductors presented. The wire drawing cost to make copper or aluminum from rod is relatively small, so costs presented could also be approximately viewed as the raw material costs. There is a price ratio that exists in the bi-media AL / CU designs when the price of copper to aluminum ratio dictates whether or not the design is cost effective. There are also additional costs not included here that would need to be addressed when utilizing such designs. When creating segmented conductors the individual segments must be twisted together in an additional operation after stranding, which can be quite costly. The cost of this is also a factor in determining when segmented conductors are used in place of stranded round conductors [75]. The diameter of AL / CU conductors are slightly larger than that of segmented conductors, and this will also affect the cost of additional materials required when manufacturing power cables. This is because the wall thickness of the polymer is usually a fixed thickness, thus starting with a larger diameter uses more material. Larger diameters may also affect maximum shipping lengths and size of installation accessories (e.g. joint bodies, clamps, conduits, etc.). The AL / CU conductors also have advantages versus all copper conductors besides cost. These relate to the decrease in weight. This property of the conductor can also affect manufacturing and shipping, since weight of the shipping reel can exceed equipment limitations. Further, when cables are installed underground they are commonly pulled into conduits for protection. Although the tensile strength of copper is greater than aluminum, this is overshadowed by the lighter weight of the conductor that

ultimately allows for lower pulling tensions. Thus, this leads to longer installation lengths and less cost. All these other factors affecting cost should be evaluated by industry practitioners when designing cables. Typically, the conductor material cost is by far the largest cost component of the cable and the most beneficial to reduce.

6.2 Standardized Sizes

Note that there are no standardized sizes for hollow conductors, since the point isn't to locate the AC resistance minima but is driven by the application (e.g. cooling liquid). However, designing a hollow conductor specifically for reducing the AC resistance also has advantages in that the empty center can be used for other purposes. For example, some possible applications include placing a fiber optic inside for distributed temperature sensing (DTS) or communications, or pumping a cooling liquid through to either lower conductor temperatures and reduce ohmic heating losses and allow for an increased ampacity rating.

The standardized sizes were created to match the nominal cross-sectional area conductors in current industry standards. As previously mention, the nominal and actual cross-sectional areas differ slightly. Therefore, the actual cross-sectional areas of the nominal conductors proposed were designed to match that of the actual cross-sectional areas of copper conductors calculated using their defined DC resistances. The optimal inner and outer radii were found such that they represent the minima of the AC resistance. Up until a certain point the addition of either an Air or AL core immediately begins to increase AC resistance. In this case it is shown that the optimal radii of the inner medium is zero, or the conductor is optimally all copper. For 90°C and 60 Hz, FIGURE 6-1 details the optimal inner versus outer medium radii:

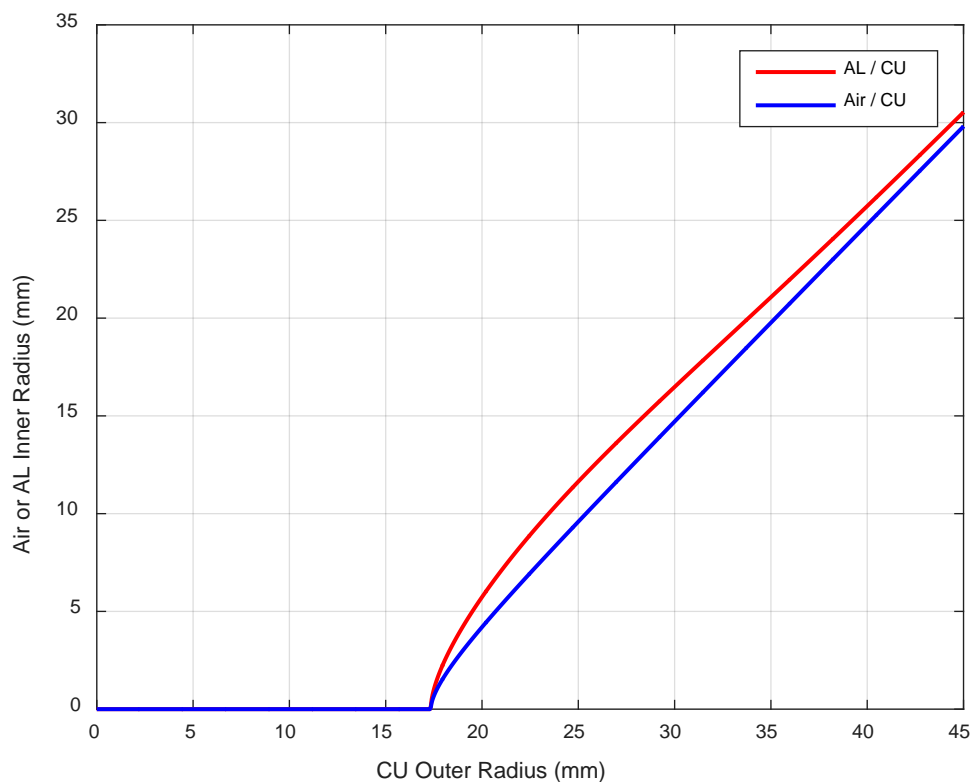


FIGURE 6-1: Optimal radii (90°C, 60 Hz)

This can also be viewed in terms of cross-sectional areas for each medium. This may be easier to conceptualize since conductors are generally discussed in terms of their cross-sectional areas as opposed to radii. FIGURE 6-2 shows the optimal conductor construction at 90°C and 60 Hz:

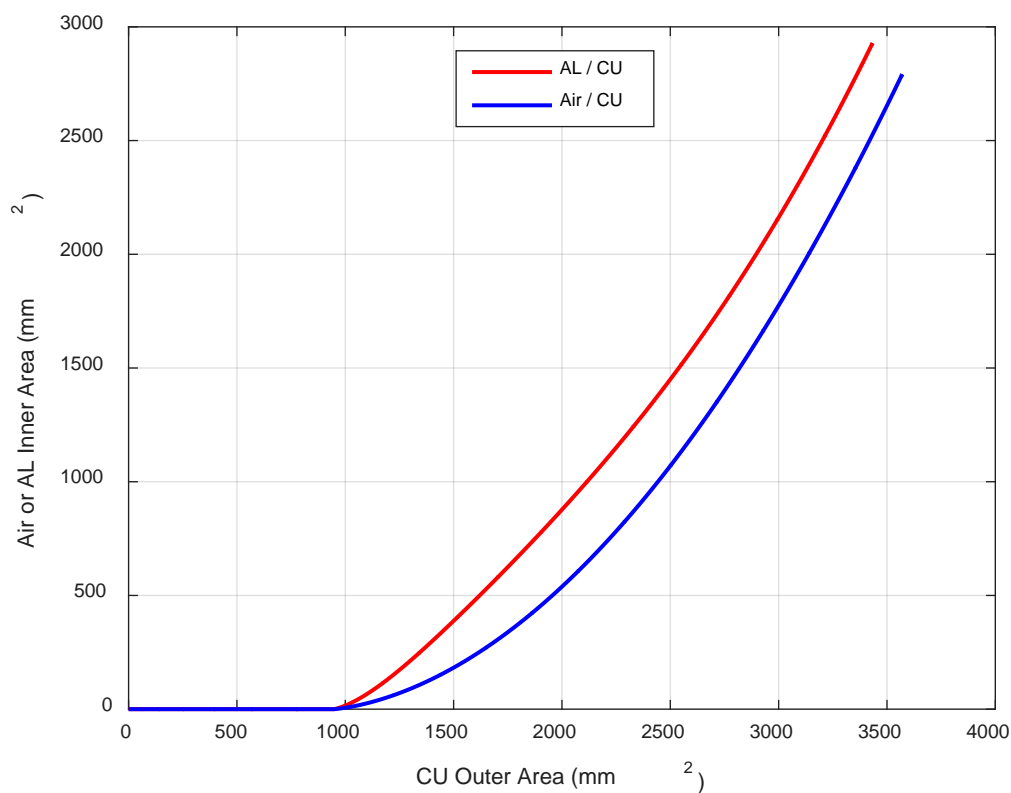


FIGURE 6-2: Optimal area (90°C, 60 Hz)

It can be observed that conductors of outer radii greater or equal than 17.3 mm (or areas greater than 943 mm²) have optimal bi-media designs. It is also of interest to see how the AC and DC resistances behave. Looking specifically at when the optimal designs become useable at 17.3 mm for Air / CU in FIGURE 6-3:

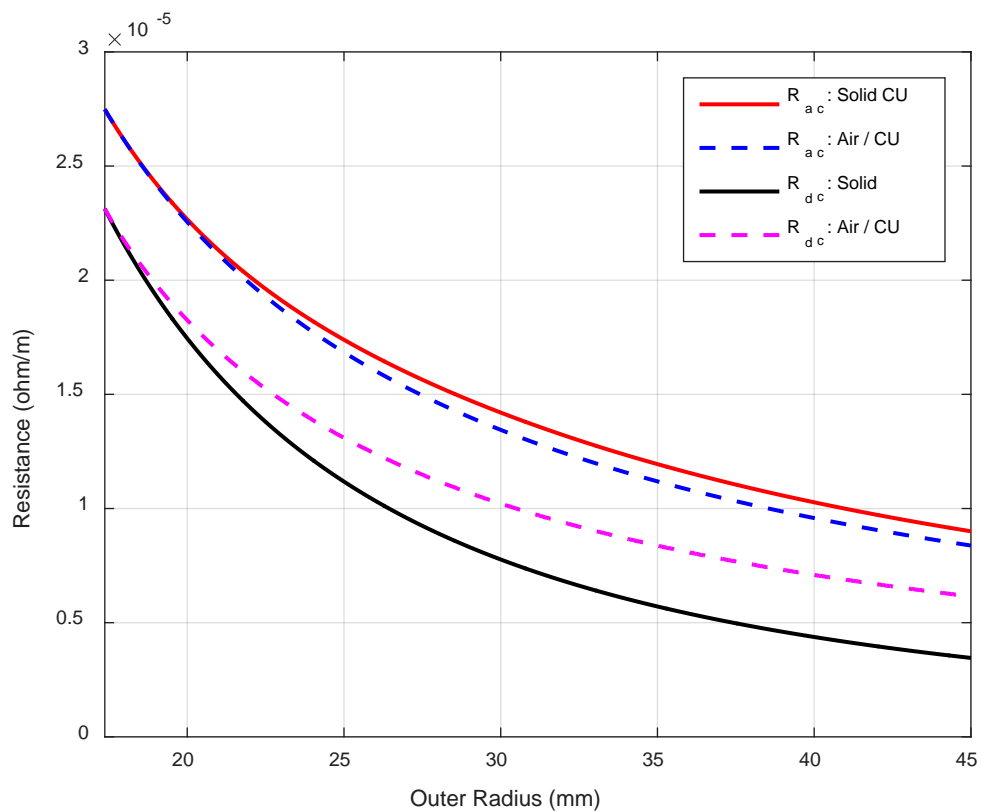


FIGURE 6-3: AC and DC resistance of optimal Air / CU conductors (90°C, 60 Hz)

FIGURE 6-3 shows that as the DC resistance is increasing with the removal of the core, the AC resistance is lowering. For an AL / CU conductor this plot is as shown in FIGURE 6-4:

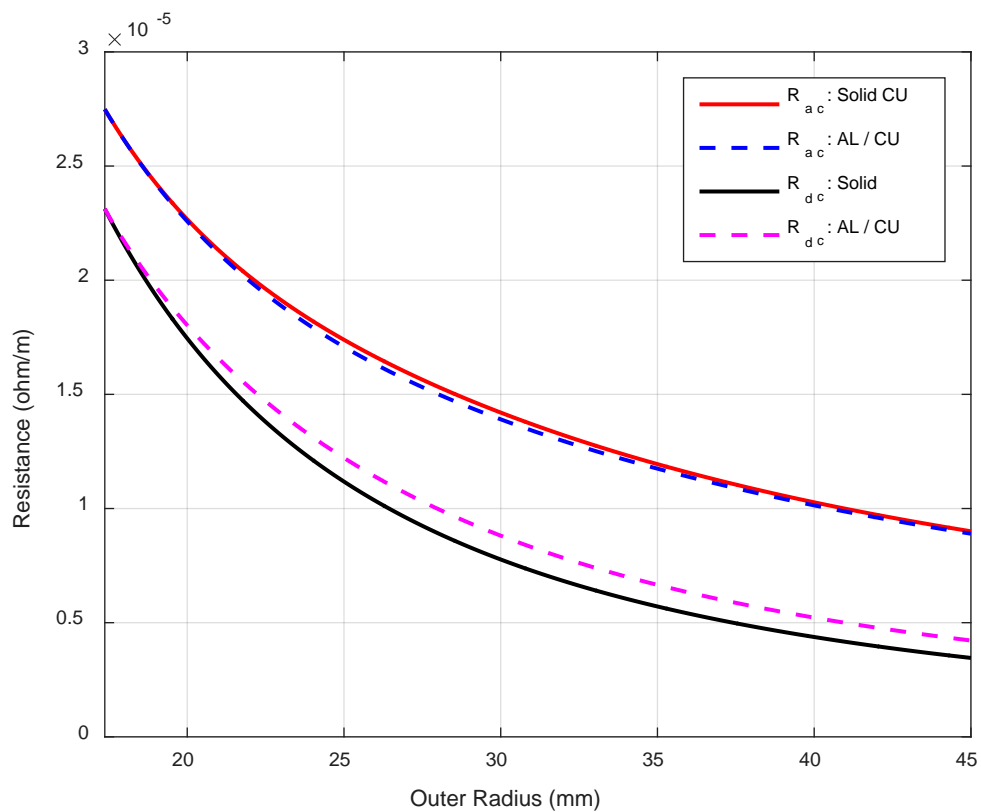


FIGURE 6-4: AC and DC resistance of optimal AL / CU conductors (90°C, 60 Hz)

The same effect occurs with AL / CU conductors, as does with Air / CU conductors.

For 105°C and 60 Hz, FIGURE 6-5 details the optimal inner versus outer medium radii:

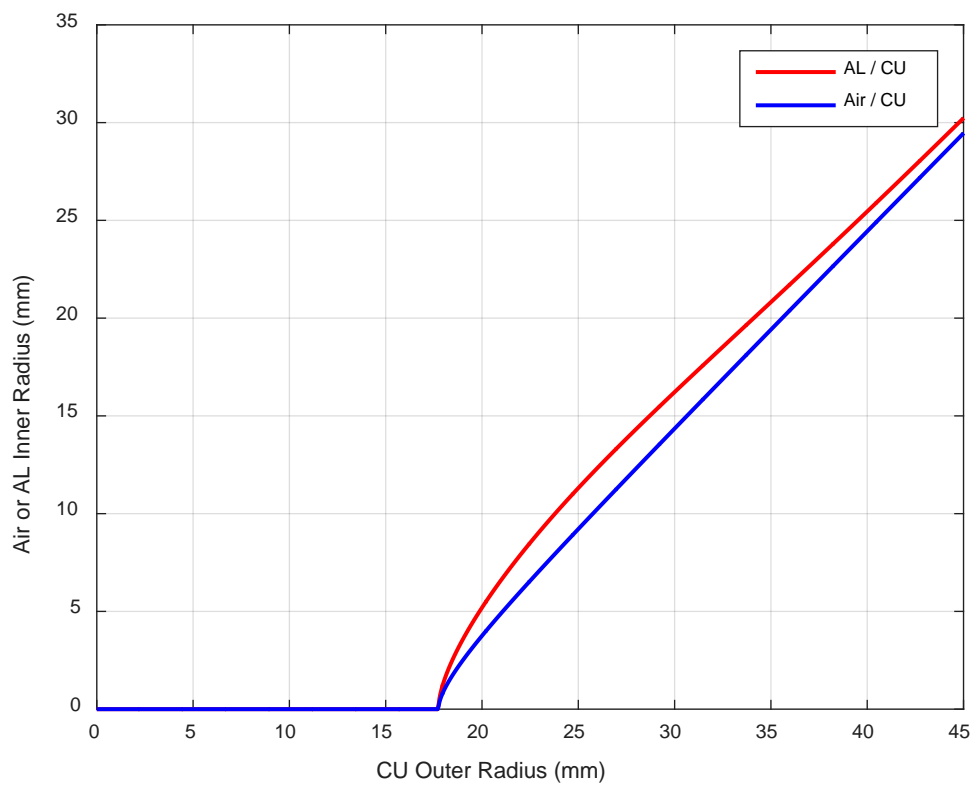


FIGURE 6-5: Optimal radii (105°C, 60 Hz)

FIGURE 6-6 shows the same data as FIGURE 6-5 in terms of cross-sectional areas for each medium:

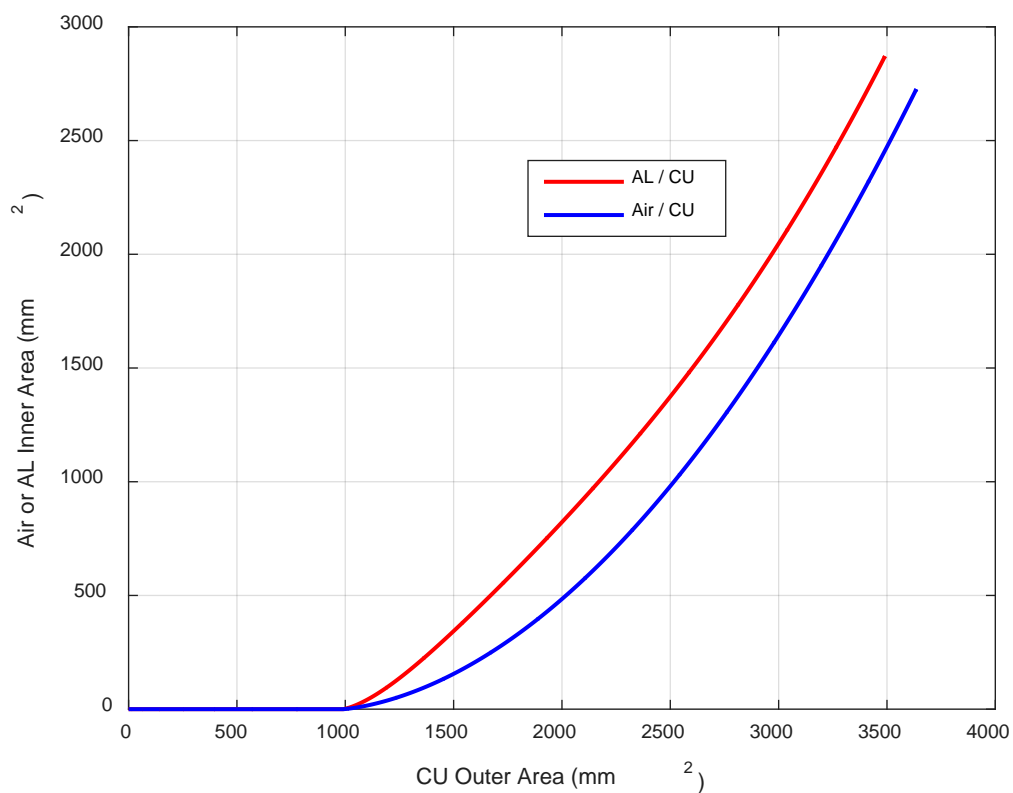


FIGURE 6-6: Optimal area (105°C, 60 Hz)

It can be observed that conductors of outer radii greater or equal than 17.7 mm (or areas greater than 988 mm²) have optimal bi-media designs. It is also of interest to see how the AC and DC resistances behave. Looking specifically at when the optimal designs become useable at 17.7 mm for Air / CU in FIGURE 6-7:

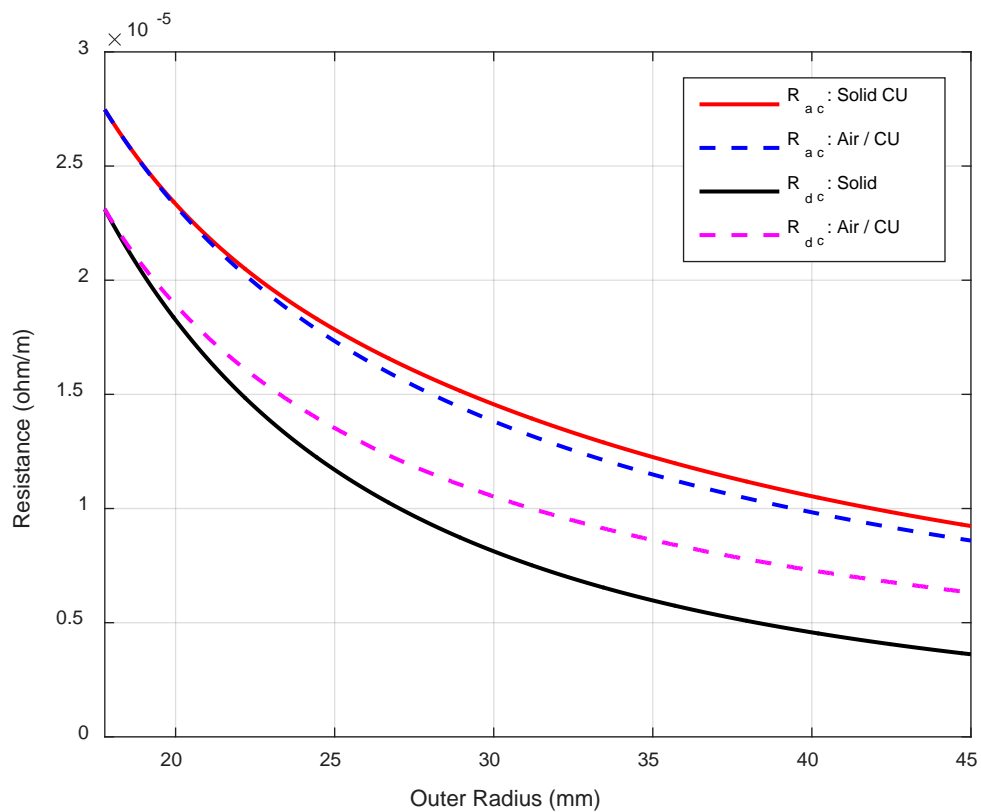


FIGURE 6-7: AC and DC resistance of optimal Air / CU conductors (105°C, 60 Hz)

FIGURE 6-7 shows that as the DC resistance is increasing with the removal of the core, the AC resistance is lowering. For an AL / CU conductor the resistance plot are as shown in FIGURE 6-8:

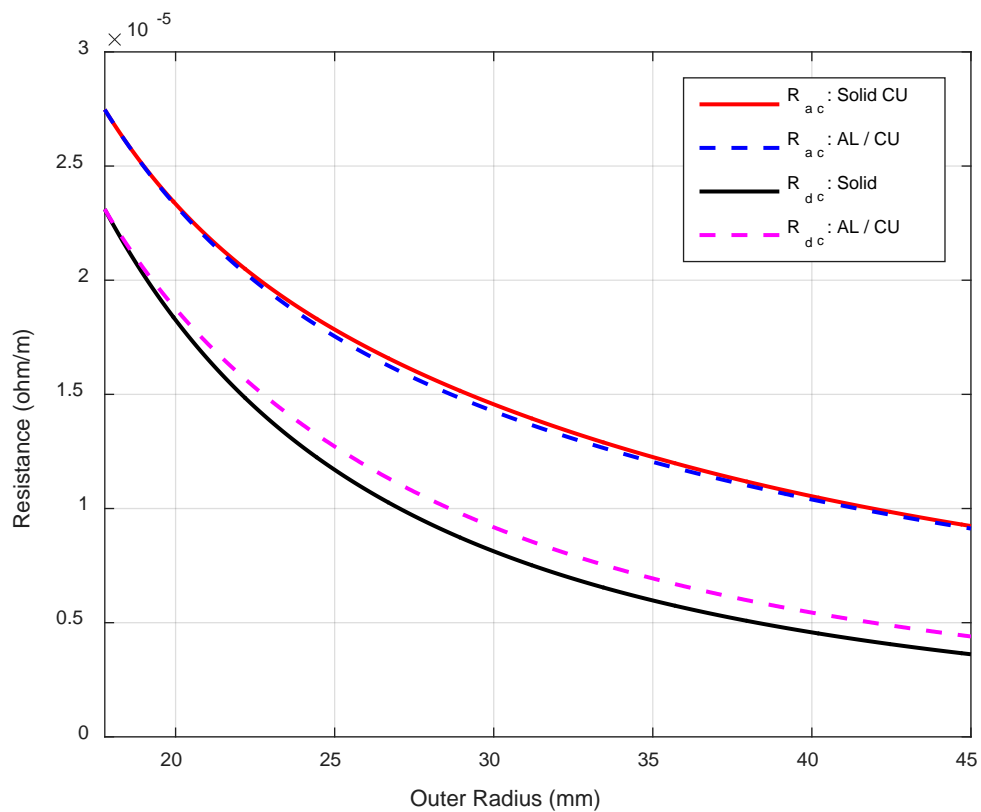


FIGURE 6-8: AC and DC resistance of optimal AL / CU conductors (105°C, 60 Hz)

For 90°C and 50 Hz, FIGURE 6-9 details the optimal inner versus outer medium radii:

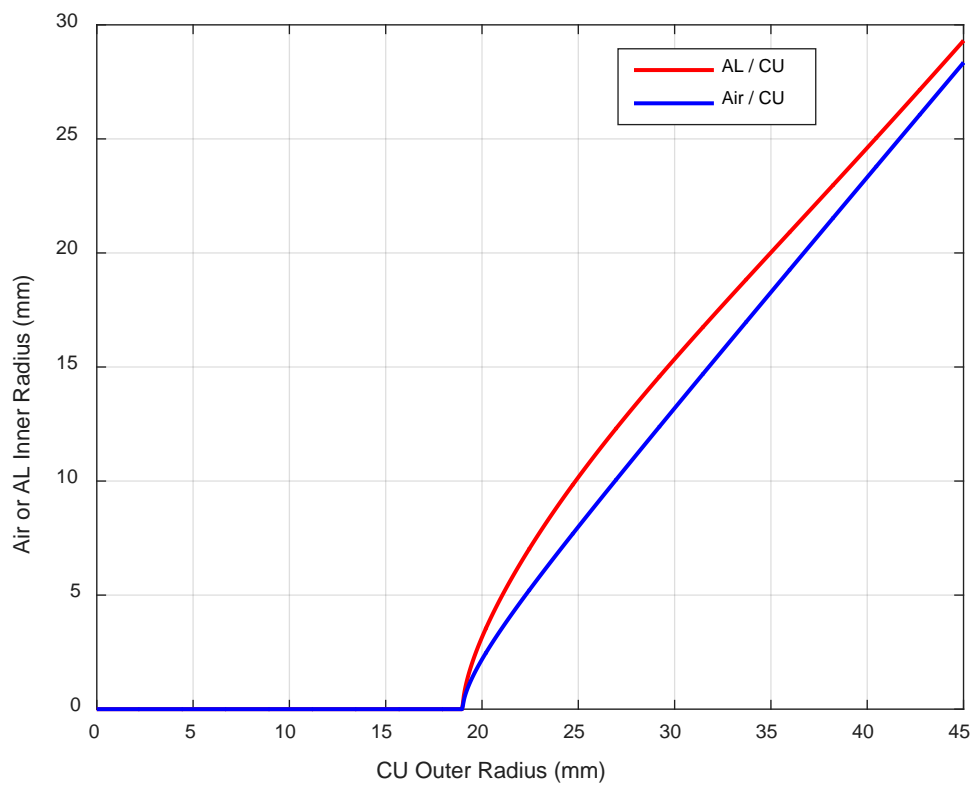


FIGURE 6-9: Optimal radii (90°C, 50 Hz)

FIGURE 6-10 shows the same information as FIGURE 6-9 in terms of cross-sectional areas for each medium:

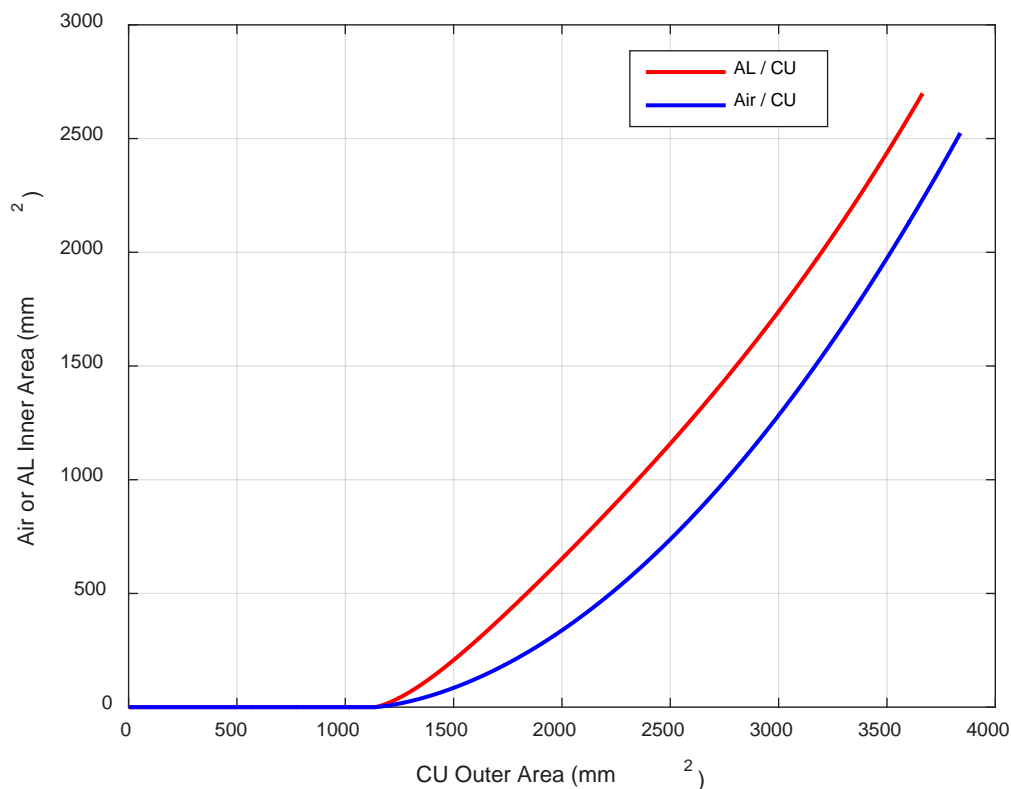


FIGURE 6-10: Optimal area (90°C, 50 Hz)

It can be observed that conductors of outer radii greater or equal than 19.0 mm (or areas greater than 1133 mm²) have optimal bi-media designs. The lower frequency has more of an effect than temperature does. Intuitively it makes sense this optimal design point is shifted right with frequency since the frequency is moving toward DC conditions where there would be no optimal point. In such cases the optimal design would always be all copper. It is also of interest to see how the AC and DC resistances behave. Looking specifically at when the optimal designs become useable at 19.0 mm for Air / CU in FIGURE 6-11:

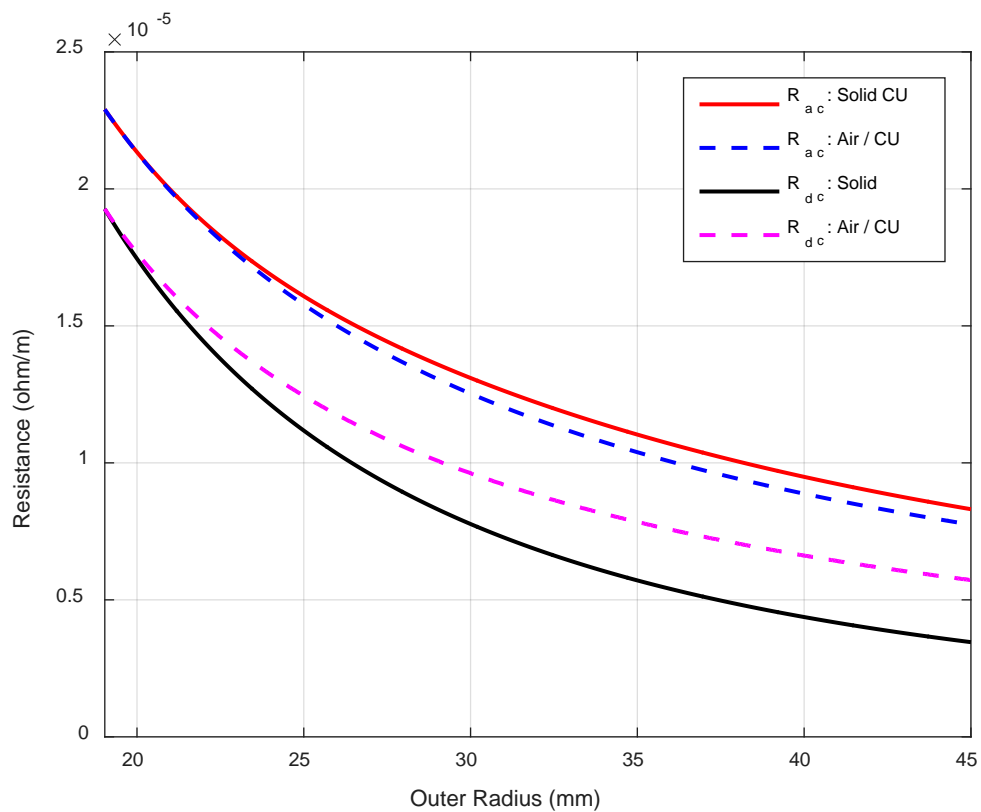


FIGURE 6-11: AC and DC resistance of optimal Air / CU conductors (90°C, 50 Hz)

For an AL / CU conductor the resistance plot are shown in FIGURE 6-12:

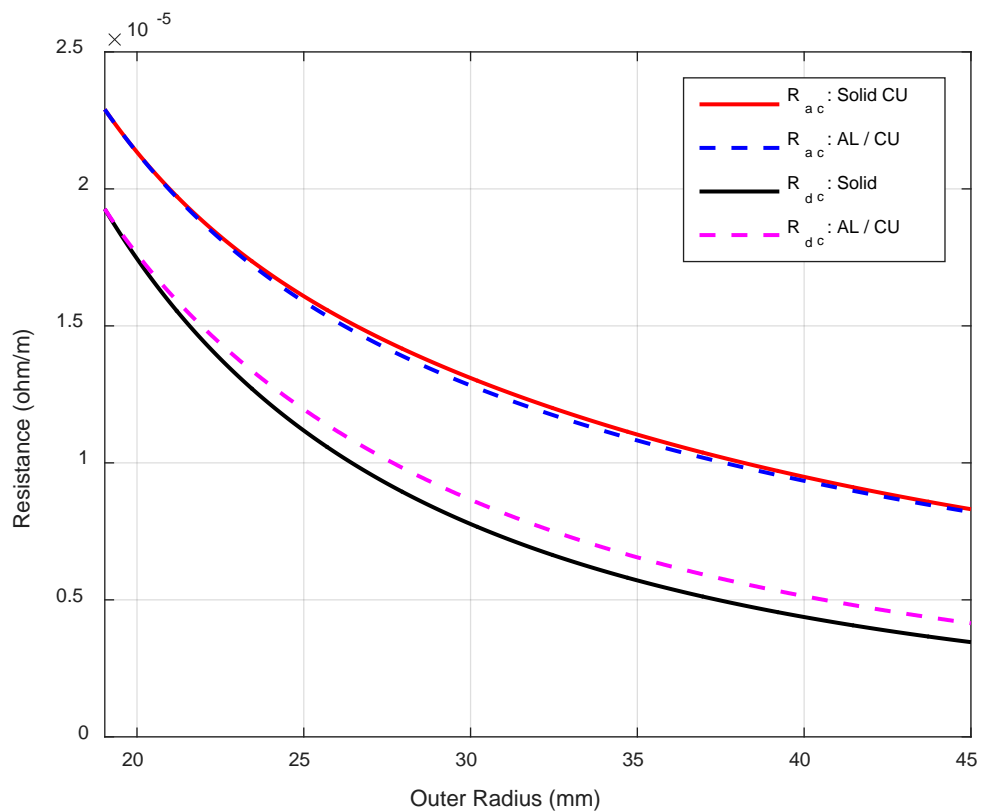


FIGURE 6-12: AC and DC resistance of optimal AL / CU conductors (90°C, 50 Hz)

For 105°C and 50 Hz, FIGURE 6-13 details the optimal inner versus outer medium radii:

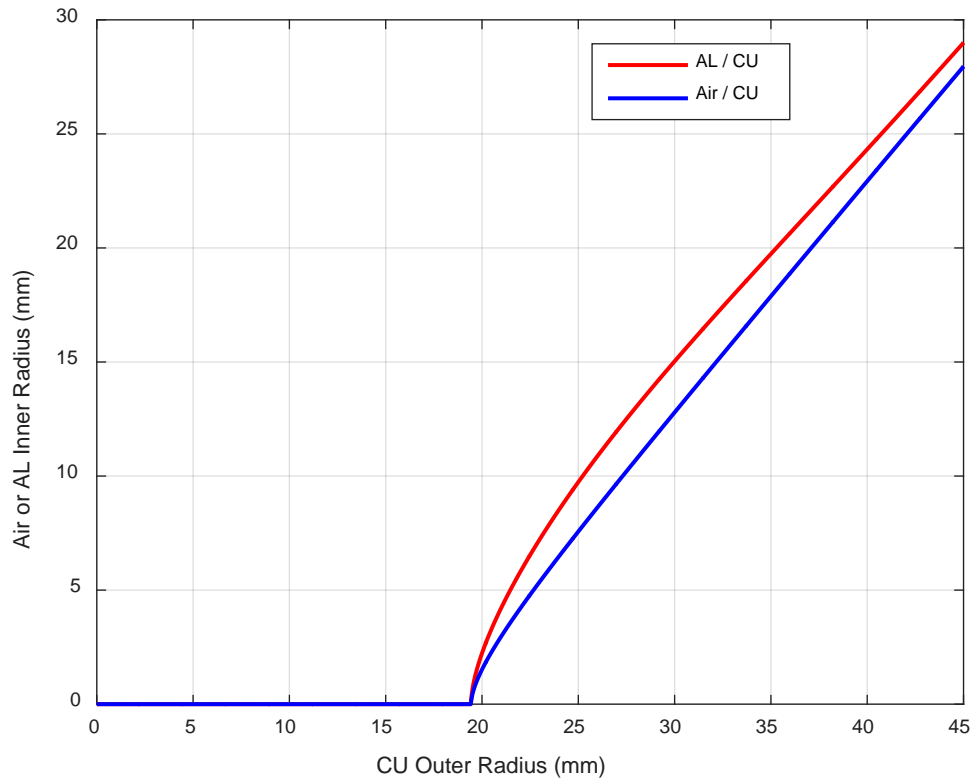


FIGURE 6-13: Optimal radii (105°C, 50 Hz)

FIGURE 6-14 shows the same information as FIGURE 6-13 in terms of cross-sectional areas for each medium:

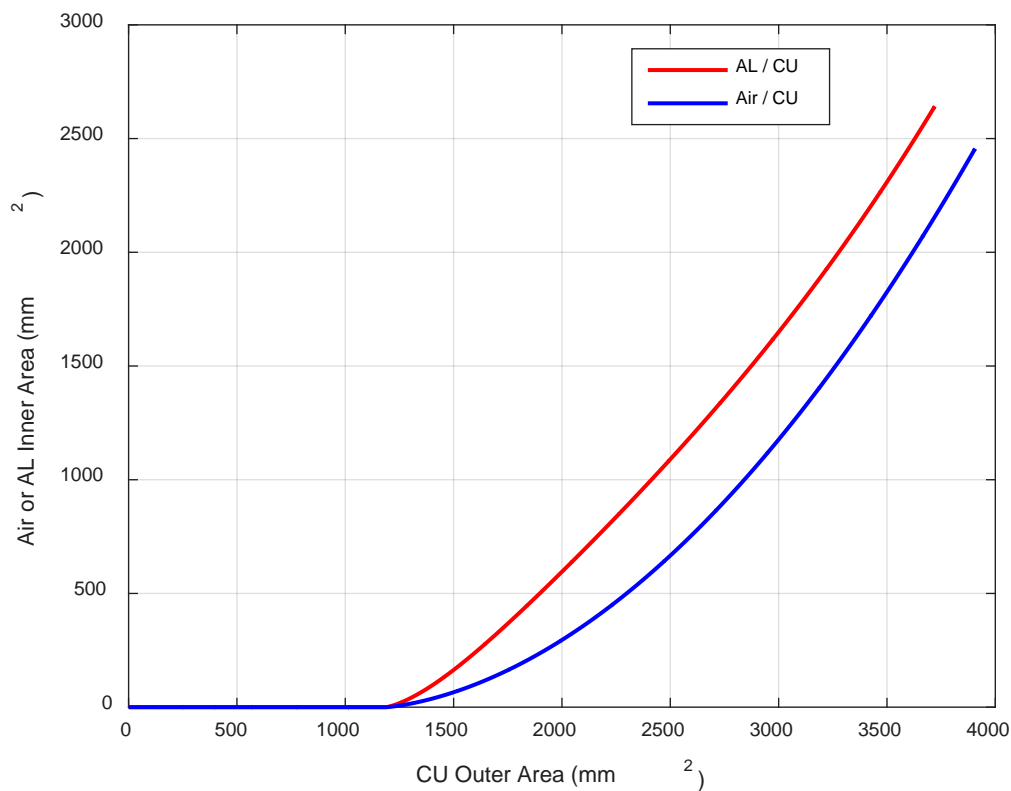


FIGURE 6-14: Optimal area (105°C, 50 Hz)

It can be observed that conductors of outer radii greater or equal than 19.4 mm (or areas greater than 1187 mm²) have optimal bi-media designs. It is also of interest to see how the AC and DC resistances behave. Looking specifically at when the optimal designs become useable at 19.4 mm for Air / CU in FIGURE 6-15:

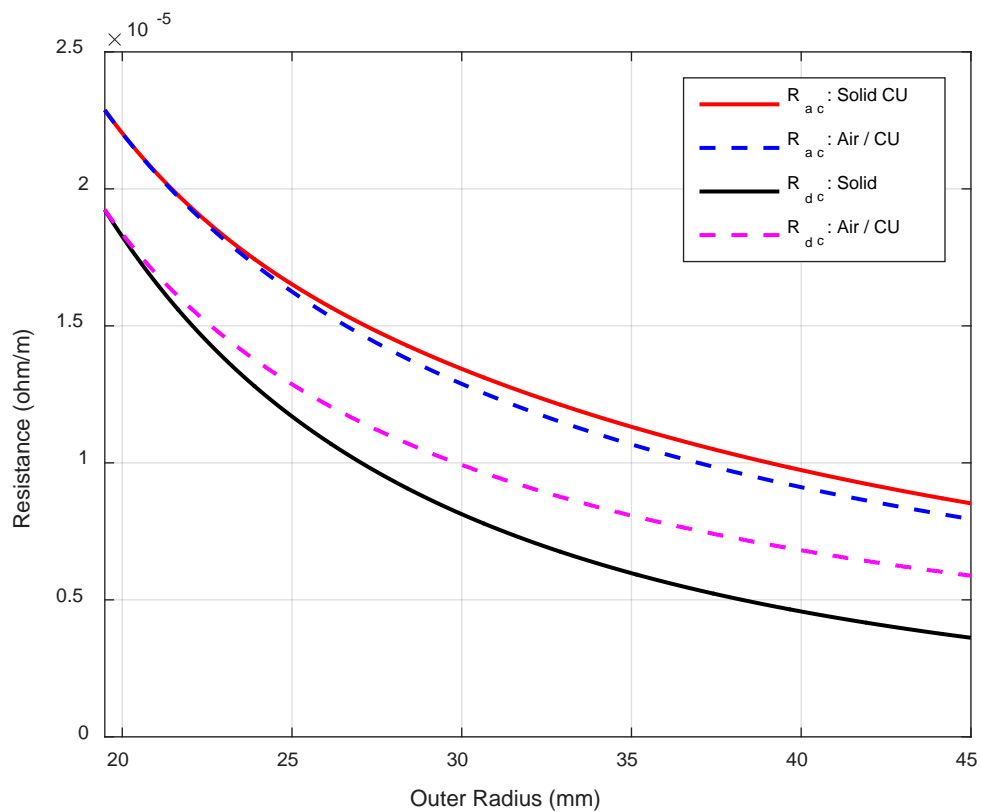


FIGURE 6-15: AC and DC resistance of optimal Air / CU conductors (105°C, 50 Hz)

For an AL / CU conductor the resistance plot is shown in FIGURE 6-16:

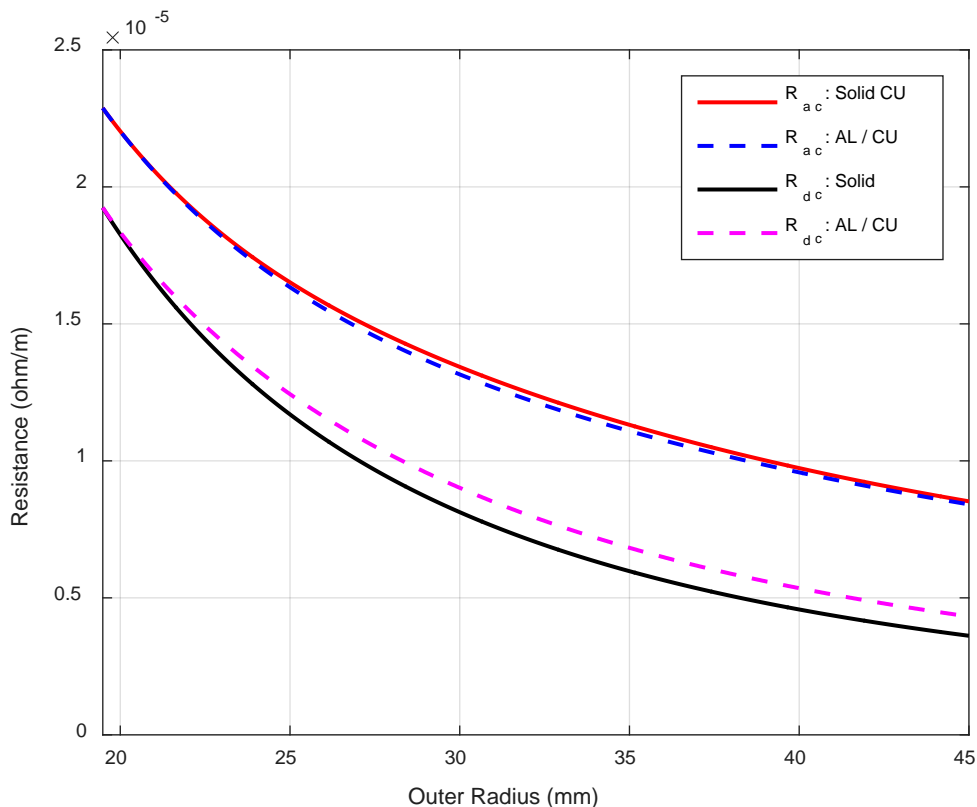


FIGURE 6-16: AC and DC resistance of optimal AL / CU conductors (105°C, 50 Hz)

Finally, using all the optimal radii, cross-sectional areas and DC resistances TABLE 6-1 through TABLE 6-4 summarizes the standardized designs for the various operating temperature and frequency combinations. Note that all tables go from 800 mm² to 3000 mm² conductors. However, a bi-media conductor is not always the optimal choice. When this occurs the row is highlighted red to signify the optimal design would be an all copper conductor as opposed to a bi-media Air / CU or AL / CU design:

TABLE 6-1: Standardized designs (90°C, 60 Hz)

ID	Area			Resistance			Solid Radius		
	Nominal	True		Total	True	AL or Air	Inner	Nominal	
		Total	AL or Air						CU
Air Core									
1	800	780.1	0.0	780.1	2.210E-02	Inf	2.210E-02	0.00	15.76
2	1000	982.9	3.3	979.6	1.760E-02	Inf	1.760E-02	1.02	17.69
3	1200	1178.4	36.7	1141.8	1.510E-02	Inf	1.510E-02	3.42	19.37
4	1400	1440.8	104.3	1336.5	1.290E-02	Inf	1.290E-02	5.76	21.42
5	1600	1722.2	196.4	1525.8	1.130E-02	Inf	1.130E-02	7.91	23.41
6	2000	2381.9	466.2	1915.7	9.000E-03	Inf	9.000E-03	12.18	27.54
7	2500	3337.7	943.2	2394.6	7.200E-03	Inf	7.200E-03	17.33	32.60
8	3000	4453.5	1580.0	2873.5	6.000E-03	Inf	6.000E-03	22.43	37.65
AL Core									
1	800	780.1	0.0	780.1	2.210E-02	Inf	2.210E-02	0.00	15.76
2	1000	979.6	6.5	973.1	1.765E-02	4.362E+00	1.772E-02	1.44	17.66
3	1200	1141.8	57.5	1084.3	1.540E-02	4.915E-01	1.590E-02	4.28	19.06
4	1400	1336.5	135.3	1201.2	1.343E-02	2.088E-01	1.435E-02	6.56	20.63
5	1600	1525.8	218.8	1306.9	1.197E-02	1.292E-01	1.319E-02	8.35	22.04
6	2000	1915.7	401.4	1514.3	9.801E-03	7.042E-02	1.139E-02	11.30	24.69
7	2500	2394.6	634.7	1759.9	8.030E-03	4.453E-02	9.797E-03	14.21	27.61
8	3000	2873.5	875.5	1998.0	6.809E-03	3.229E-02	8.629E-03	16.69	30.24

Bi-media not optimal

TABLE 6-2: Standardized designs (105°C, 60 Hz)

ID	Area			Resistance			Solid Radius		
	Nominal	True		Total	AL or Air	CU	Inner	Outer	
		AL or Air	CU						
	mm ²			ohm/km: DC @ 20C			mm		
Air Core									
1	800	780.1	0.0	780.1	2.210E-02	Inf	2.210E-02	0.00	15.76
2	1000	979.6	0.0	979.6	1.760E-02	Inf	1.760E-02	0.00	17.66
3	1200	1166.7	24.9	1141.8	1.510E-02	Inf	1.510E-02	2.82	19.27
4	1400	1421.0	84.5	1336.5	1.290E-02	Inf	1.290E-02	5.19	21.27
5	1600	1693.8	168.1	1525.8	1.130E-02	Inf	1.130E-02	7.31	23.22
6	2000	2332.7	417.0	1915.7	9.000E-03	Inf	9.000E-03	11.52	27.25
7	2500	3256.7	862.1	2394.6	7.200E-03	Inf	7.200E-03	16.57	32.20
8	3000	4333.6	1460.1	2873.5	6.000E-03	Inf	6.000E-03	21.56	37.14
AL Core									
1	800	780.1	0.0	780.1	2.210E-02	Inf	2.210E-02	0.00	15.76
2	1000	979.6	0.0	979.6	1.760E-02	Inf	1.760E-02	0.00	17.66
3	1200	1141.8	41.5	1100.3	1.532E-02	6.817E-01	1.567E-02	3.63	19.06
4	1400	1336.5	115.6	1220.9	1.335E-02	2.444E-01	1.412E-02	6.07	20.63
5	1600	1525.8	197.1	1328.6	1.190E-02	1.434E-01	1.298E-02	7.92	22.04
6	2000	1915.7	377.6	1538.1	9.750E-03	7.485E-02	1.121E-02	10.96	24.69
7	2500	2394.6	609.4	1785.2	7.993E-03	4.638E-02	9.658E-03	13.93	27.61
8	3000	2873.5	848.3	2025.2	6.781E-03	3.332E-02	8.513E-03	16.43	30.24

Bi-media not optimal

TABLE 6-3: Standardized designs (90°C, 50 Hz)

ID	Area			Resistance			Solid Radius		
	Nominal	True		Total	AL or Air	CU	Inner	Outer	
		AL or Air	CU						
	mm ²			ohm/km: DC @ 20C			mm		
Air Core									
1	800	780.1	0.0	780.1	2.210E-02	Inf	2.210E-02	0.00	15.76
2	1000	979.6	0.0	979.6	1.760E-02	Inf	1.760E-02	0.00	17.66
3	1200	1142.1	0.3	1141.8	1.510E-02	Inf	1.510E-02	0.33	19.07
4	1400	1371.6	35.1	1336.5	1.290E-02	Inf	1.290E-02	3.34	20.90
5	1600	1620.0	94.3	1525.8	1.130E-02	Inf	1.130E-02	5.48	22.71
6	2000	2200.5	284.8	1915.7	9.000E-03	Inf	9.000E-03	9.52	26.47
7	2500	3036.1	641.5	2394.6	7.200E-03	Inf	7.200E-03	14.29	31.09
8	3000	4005.3	1131.8	2873.5	6.000E-03	Inf	6.000E-03	18.98	35.71
AL Core									
1	800	780.1	0.0	780.1	2.210E-02	Inf	2.210E-02	0.00	15.76
2	1000	979.6	0.0	979.6	1.760E-02	Inf	1.760E-02	0.00	17.66
3	1200	1141.8	0.8	1141.0	1.510E-02	3.692E+01	1.511E-02	0.49	19.06
4	1400	1336.5	56.9	1279.6	1.312E-02	4.967E-01	1.347E-02	4.26	20.63
5	1600	1525.8	129.7	1396.0	1.169E-02	2.179E-01	1.235E-02	6.43	22.04
6	2000	1915.7	301.3	1614.4	9.588E-03	9.381E-02	1.068E-02	9.79	24.69
7	2500	2394.6	527.6	1866.9	7.877E-03	5.357E-02	9.235E-03	12.96	27.61
8	3000	2873.5	761.6	2111.9	6.692E-03	3.711E-02	8.164E-03	15.57	30.24

Bi-media not optimal

TABLE 6-4: Standardized designs (105°C, 50 Hz)

ID	Area			Resistance			Solid Radius		
	Nominal	True		Total	AL or Air	CU	Inner	Outer	
		AL or Air	CU						AL or Air
	mm ² ohm/km: DC @ 20C								
	Air Core								
1	800	780.1	0.0	780.1	2.210E-02	Inf	2.210E-02	0.00	15.76
2	1000	979.6	0.0	979.6	1.760E-02	Inf	1.760E-02	0.00	17.66
3	1200	1141.8	0.0	1141.8	1.510E-02	Inf	1.510E-02	0.00	19.06
4	1400	1359.0	22.4	1336.5	1.290E-02	Inf	1.290E-02	2.67	20.80
5	1600	1599.6	73.9	1525.8	1.130E-02	Inf	1.130E-02	4.85	22.57
6	2000	2162.4	246.7	1915.7	9.000E-03	Inf	9.000E-03	8.86	26.24
7	2500	2971.2	576.6	2394.6	7.200E-03	Inf	7.200E-03	13.55	30.75
8	3000	3908.0	1034.5	2873.5	6.000E-03	Inf	6.000E-03	18.15	35.27
	AL Core								
1	800	780.1	0.0	780.1	2.210E-02	Inf	2.210E-02	0.00	15.76
2	1000	979.6	0.0	979.6	1.760E-02	Inf	1.760E-02	0.00	17.66
3	1200	1141.8	0.0	1141.8	1.510E-02	Inf	1.510E-02	0.00	19.06
4	1400	1336.5	38.6	1297.9	1.305E-02	7.324E-01	1.328E-02	3.50	20.63
5	1600	1525.8	107.3	1418.5	1.162E-02	2.635E-01	1.215E-02	5.84	22.04
6	2000	1915.7	274.7	1641.0	9.533E-03	1.029E-01	1.051E-02	9.35	24.69
7	2500	2394.6	498.8	1895.8	7.837E-03	5.667E-02	9.094E-03	12.60	27.61
8	3000	2873.5	731.3	2142.2	6.661E-03	3.865E-02	8.048E-03	15.26	30.24

Bi-media not optimal

The outer diameter of stranded conductors varies between manufacturers because both the compaction that the conductor stranding equipment is able to achieve and the designs of the conductors (e.g. diameter, lay lengths and number of strands, hardness of copper and aluminum wire used for manufacturing, etc.) change. TABLE 6-5 shows the radii for compact stranded conductors from one manufacturer that are used as an estimate for the compaction ratio (i.e. ratio of compact stranded to solid conductor radius) on bi-media conductors:

TABLE 6-5: Compaction Ratio of Stranded Conductors

ID	Area		Outer Radius		Compaction Ratio		
	Nominal	True	Solid	Stranded	Outer		
	mm ²	mm ²	mm		Actual	Approx.	Error (%)
1	800	780.1	15.76	16.85	1.0693	1.0691	-0.01%
2	1000	979.6	17.66	18.95	1.0731	1.0759	0.26%
3	1200	1141.8	19.06	20.60	1.0806	1.0786	-0.18%
4	1400	1336.5	20.63	22.20	1.0763	1.0787	0.23%
5	1600	1525.8	22.04	23.70	1.0754	1.0763	0.08%
6	2000	1915.7	24.69	26.30	1.0651	1.0652	0.01%
7	2500	2394.6	27.61	28.80	1.0432	1.0456	0.24%
8	3000	2873.5	30.24	31.00	1.0250	1.0271	0.20%

The formula for the approximation of the compaction ratio was created using a polynomial regression, as shown in FIGURE 6-17:

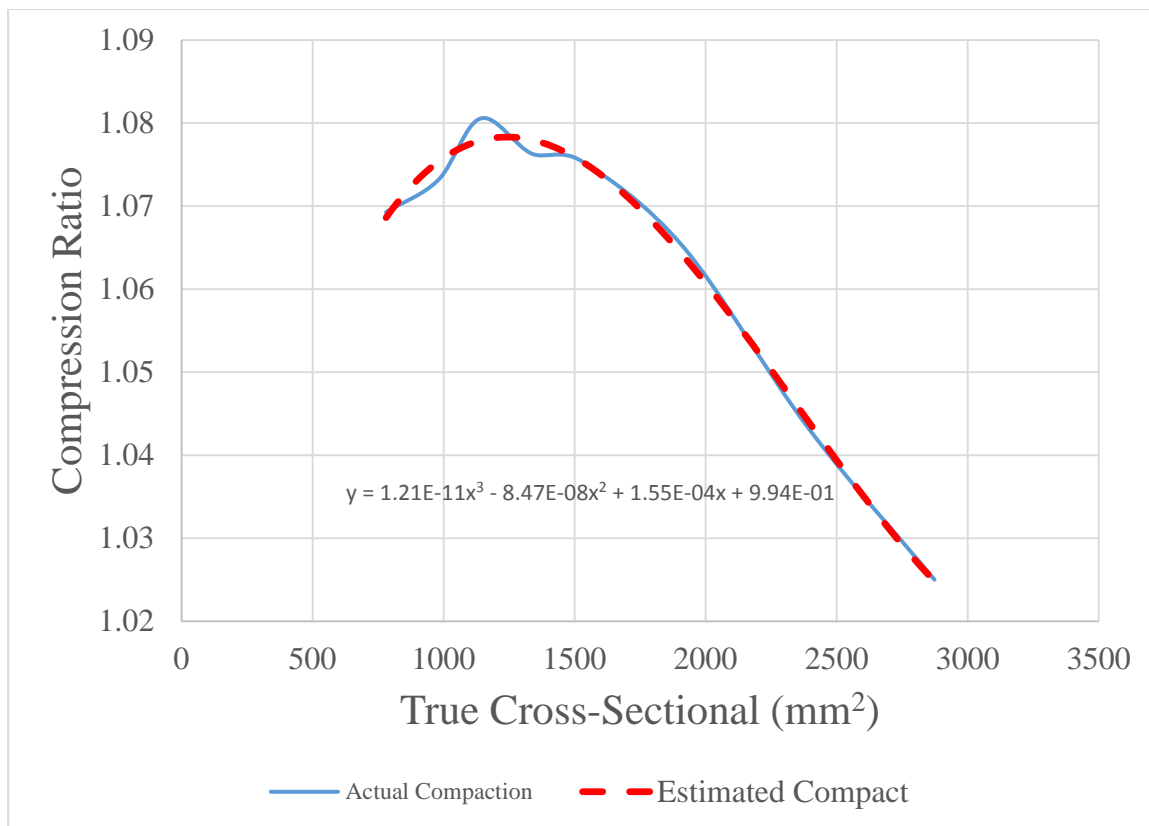


FIGURE 6-17: Compaction Ratio of Stranded Conductors

As shown on TABLE 6-5, the approximated formula shown on FIGURE 6-17 has a maximum error of 0.26% for nominal cross-sectional areas up to 3000 mm². Because the hardness of copper and aluminum are different, some further variation can be expected for the compaction ratios of bi-media designs. All stranded radii discussed herein are purely for illustrative purposes, and not meant to be theoretical values. TABLE 6-6 and TABLE 6-7 show the approximate stranded radii of the optimally designed bi-media conductors of standardized cross-sectional areas, along with their AC resistances at the given operating temperatures and frequencies listed:

TABLE 6-6: Stranded Radii and AC Resistance of Standardized Bi-Media (60 Hz)

ID	Nominal Area	Stranded Radius		R_{ac} @ 90°C	Stranded Radius		R_{ac} @ 105°C
		Inner	Outer		Inner	Outer	
	mm ²	mm		ohm/km	mm		ohm/km
Air Core							
1	800	0.00	16.19	3.193E-02	0.00	16.19	3.310E-02
2	1000	1.05	18.17	2.681E-02	0.00	18.14	2.778E-02
3	1200	3.51	19.89	2.358E-02	2.89	19.79	2.450E-02
4	1400	5.92	22.00	2.057E-02	5.33	21.84	2.140E-02
5	1600	8.12	24.05	1.831E-02	7.51	23.85	1.906E-02
6	2000	12.51	28.28	1.492E-02	11.83	27.99	1.555E-02
7	2500	17.63	33.17	1.215E-02	16.87	32.79	1.267E-02
8	3000	23.03	38.67	1.025E-02	22.14	38.15	1.070E-02
AL Core							
1	800	0.00	16.19	3.193E-02	0.00	16.19	3.310E-02
2	1000	1.48	18.14	2.690E-02	0.00	18.14	2.780E-02
3	1200	4.39	19.58	2.414E-02	3.73	19.58	2.491E-02
4	1400	6.74	21.18	2.171E-02	6.23	21.18	2.237E-02
5	1600	8.57	22.64	1.995E-02	8.14	22.64	2.053E-02
6	2000	11.61	25.36	1.737E-02	11.26	25.36	1.784E-02
7	2500	14.60	28.36	1.527E-02	14.31	28.36	1.567E-02
8	3000	17.15	31.06	1.380E-02	16.88	31.06	1.415E-02

TABLE 6-7: Stranded Radii and AC Resistance of Standardized Bi-Media (50 Hz)

ID	Nominal Area	Stranded Radius		R_{ac} @ 90°C	Stranded Radius		R_{ac} @ 105°C
		Inner	Outer		Inner	Outer	
	mm ²	mm		ohm/km	mm		ohm/km
Air Core							
1	800	0.00	16.19	3.087E-02	0.00	16.19	3.208E-02
2	1000	0.00	18.14	2.568E-02	0.00	18.14	2.661E-02
3	1200	0.34	19.58	2.288E-02	0.00	19.58	2.366E-02
4	1400	3.43	21.46	2.007E-02	2.75	21.36	2.085E-02
5	1600	5.63	23.32	1.791E-02	4.98	23.18	1.862E-02
6	2000	9.78	27.18	1.466E-02	9.10	26.95	1.526E-02
7	2500	14.61	31.79	1.198E-02	13.88	31.50	1.248E-02
8	3000	19.50	36.67	1.013E-02	18.64	36.23	1.056E-02
AL Core							
1	800	0.00	16.19	3.087E-02	0.00	16.19	3.208E-02
2	1000	0.00	18.14	2.568E-02	0.00	18.14	2.661E-02
3	1200	0.51	19.58	2.289E-02	0.00	19.58	2.366E-02
4	1400	4.37	21.18	2.047E-02	3.60	21.18	2.113E-02
5	1600	6.60	22.64	1.870E-02	6.00	22.64	1.927E-02
6	2000	10.06	25.36	1.616E-02	9.60	25.36	1.662E-02
7	2500	13.31	28.36	1.413E-02	12.94	28.36	1.451E-02
8	3000	15.99	31.06	1.272E-02	15.67	31.06	1.306E-02

6.3 Replacement of Segmented Conductors

The applicability of bi-media designs can be more easily demonstrated by comparing the cost of standardized cross-sectional areas of segmented conductors to those of bi-media having equal AC resistance. As was seen previously, segmented conductors have an empirically derived k_s factor used to adjust the value of a solid/stranded design (i.e. $k_s = 1.0$) to the lower resistance obtained using a segmented design. There are four k_s values that are to be examined: $k_s = 0.8$ for extruded insulation on conductors where the individual layers of strands have a bidirectional lay, $k_s = 0.62$ for extruded insulation on conductors where the individual layers of strands have a unidirectional lay (shown to decrease AC resistance in segmented conductors [120]), $k_s = 0.435$ for fluid/paper/PPL

insulation, and $k_s = 0.35$ for extruded insulation on conductors where the individual strands are enameled. It should also be noted that enameled wires have a different cost than bare copper wires. A challenge to address is how to make the information presented timeless as the price of copper and aluminum change. To do this the price ratio of copper to aluminum is used. Also, enameled wires add the complicating factor of their additional cost. To address this separate cost adders are presented for each percentage of price increase of the enameled wires over the bare copper wires alone. Currently, the price increase to enamel copper wires adds 30% to the wire price. However, to insulate all wires from each other not every strand needs to be enameled. Instead every other row either has every other strand enameled (insulates each strand from bordering strands in the same layer) or all strands enameled (insulates each strand from bordering strands in the same layer as well as strands in the layer above and below it). This ensures no two bare wires are touching while at the same time enameling as few strands as possible. The most cost effective choice for which layer has all strands enameled depends on how many stranded layers the conductor has, as shown on TABLE 6-8:

TABLE 6-8: Percent of enameled wires in segmented conductors

Layer Number	Strands per Layer	Segment Wires	Segment Enameled Wires		Total Enameled Wires	
			Number	%	Number	%
0	1	1	0	0.0%	0	0.0%
1	6	7	0	0.0%	0	0.0%
2	12	19	0	0.0%	0	0.0%
3	18	37	9	24.3%	45	22.1%
4	24	61	24	54.1%	165	50.9%
5	30	91	15	52.7%	240	50.6%
6	36	127	36	66.1%	420	64.2%
7	42	169	21	62.1%	525	60.8%

When enameled wires are used in segmented conductors, typically the center wire and first two layers are not enameled. The third layer then has all wires enameled and fourth layer has every other wire enameled. This pattern of every wire in the layer and every other wire in the layer continues throughout the design and ensures no bare wire past the second layer is touching another bare wire. After assembling these segments into a finished conductor, assuming the center core has 19 bare wire strands and the conductor has 5 segments, the average number of enameled strands in the total conductor is between 22.1% and 64.2%. Most commonly conductor segments have 60 to 90 wires, so the total conductor would require approximately 51% of the wires to be enameled. The cost increase for the enameling in all following tables and calculations is assumed to be the cost increase for enameling wire times the percent of enameled wires in the segmented conductor design. The range of percent increase that is covered is from 12% up to 44%. This range was chosen because, as shown, at 12% price increase the enameled wire conductors are always more cost effective, and at 44% or higher price increase the enameled is only more cost effective when the price of aluminum exceeds the price of copper. This is an unlikely situation, as the price of copper over aluminum is currently around three times the cost.

The only material cost of the Air / CU designs is that of the copper. This is also the case for non-enameled segmented copper conductors. Therefore, if less copper is required for the Air / CU conductor design it must be more cost effective (i.e. because it requires less copper) than the non-enameled segmented copper conductor. This can be observed in FIGURE 6-18, which shows the weight (i.e. material consumption) of a segmented copper

conductors (independent of k_s) compared to the weight that would be required for Air / CU conductors to have the same AC resistance:

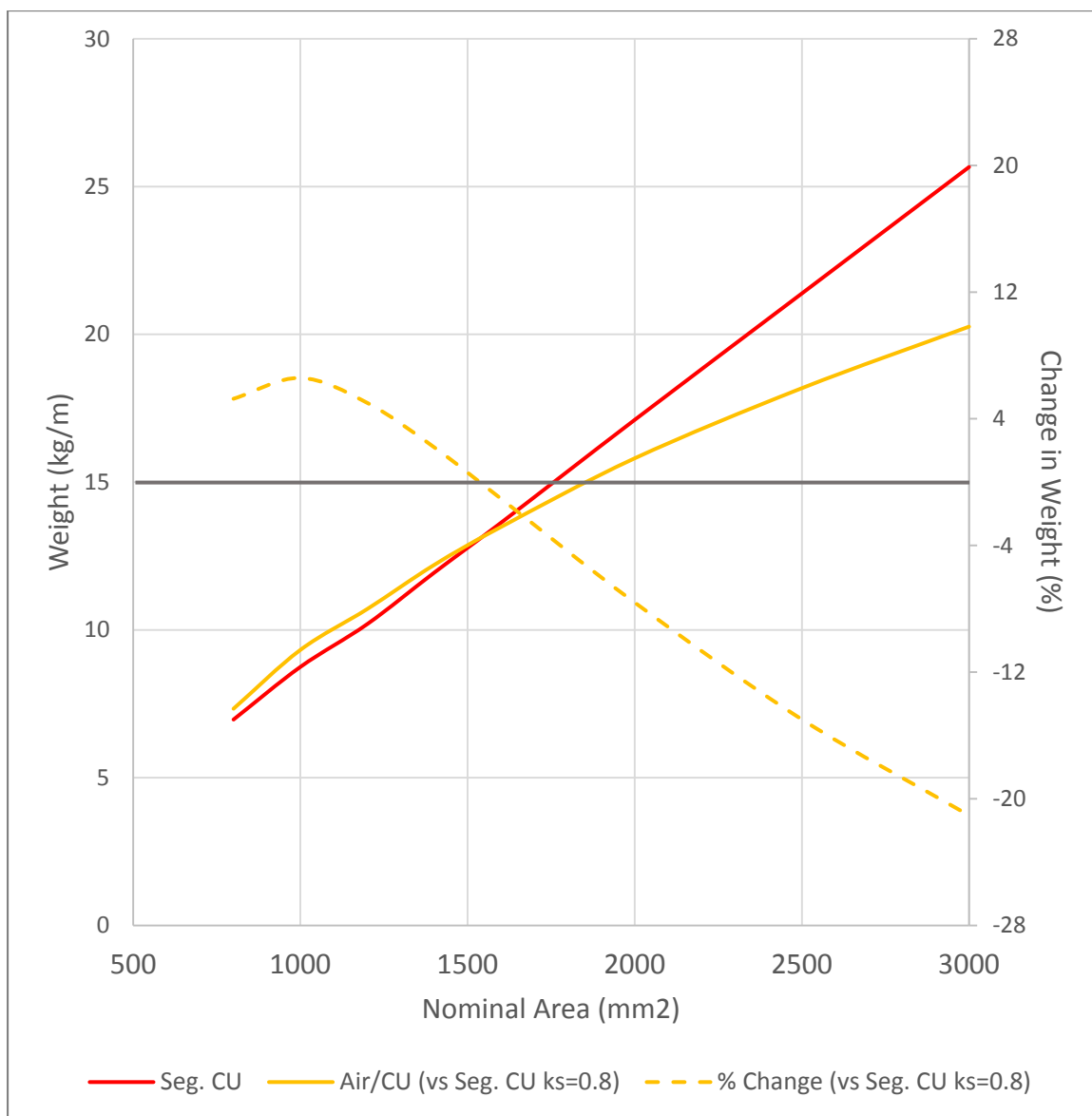


FIGURE 6-18: Weight of Air / CU ($k_s=0.8$) vs segmented CU

FIGURE 6-18 shows that the material consumption of the Air / CU conductor is initially greater than the segmented copper conductor, but becomes less just past 1500 mm². At this point the change in weight is zero, since the two conductor designs use the same amount of copper. Therefore, at this point the material cost for both conductor designs is

the same. The Air / CU conductor is never more cost effective than the segmented copper conductor until the material consumptions cross, since in the beginning “optimal” designs amount to comparing the copper cross-sectional area required to make a solid copper conductor with the same AC resistance as a segmented copper conductor. As such, the solid copper conductor always requires more cross-sectional area and is thus never cost effective. Adversely, at the point when the cross-sectional area becomes smaller for Air / CU than segmented copper the cost of the Air / CU conductor is always cost effective. The general shape of material consumption of all Air / CU designs of equal AC resistance compared to segmented copper conductors at 90°C and 60 Hz is shown in FIGURE 6-19:

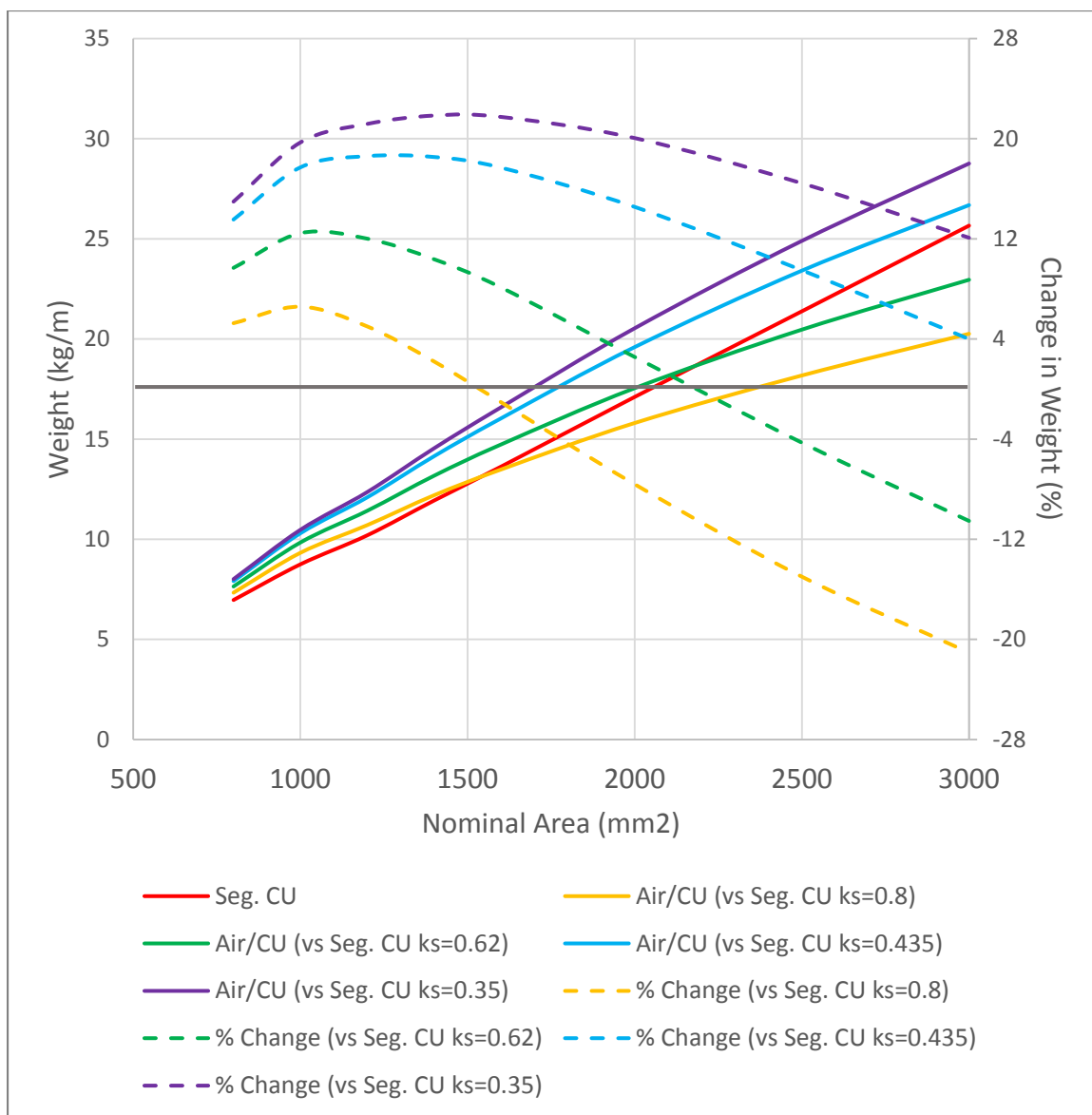


FIGURE 6-19: Weight of Air / CU vs segmented CU (enamel = 0%)

It can be seen that the weight of the segmented copper and Air / CU designs cross for $k_s = 0.8$ and $k_s = 0.62$, but not for $k_s = 0.435$ and $k_s = 0.35$. The crossing point, or alternatively where the change in weight is zero, indicates the point at which the Air / CU becomes more cost effective than segmented copper. Whereas a $k_s = 0.435$ never crosses and is therefore never cost effective, $k_s = 0.35$ changes depending on the enameling cost. Note here that the cost of enamel is assumed to be zero. Adding the enamel won't change

the weight, however it does change the cost effectiveness. The cost effective point shifts depending on the cost adder percentage of the enameled wire. To illustrate this data is plotted with an “effective” weight. As opposed to real weight, which is all that is needed to compare cost effectiveness in Air / CU conductors to bare copper segmented conductors, the “effective” weight has the weight adjusted to be representative of the cost to enamel the wires. As an example, the plot above is repeated with the enameling cost price increase changed to 30% (approximate cost today) as shown in FIGURE 6-20:

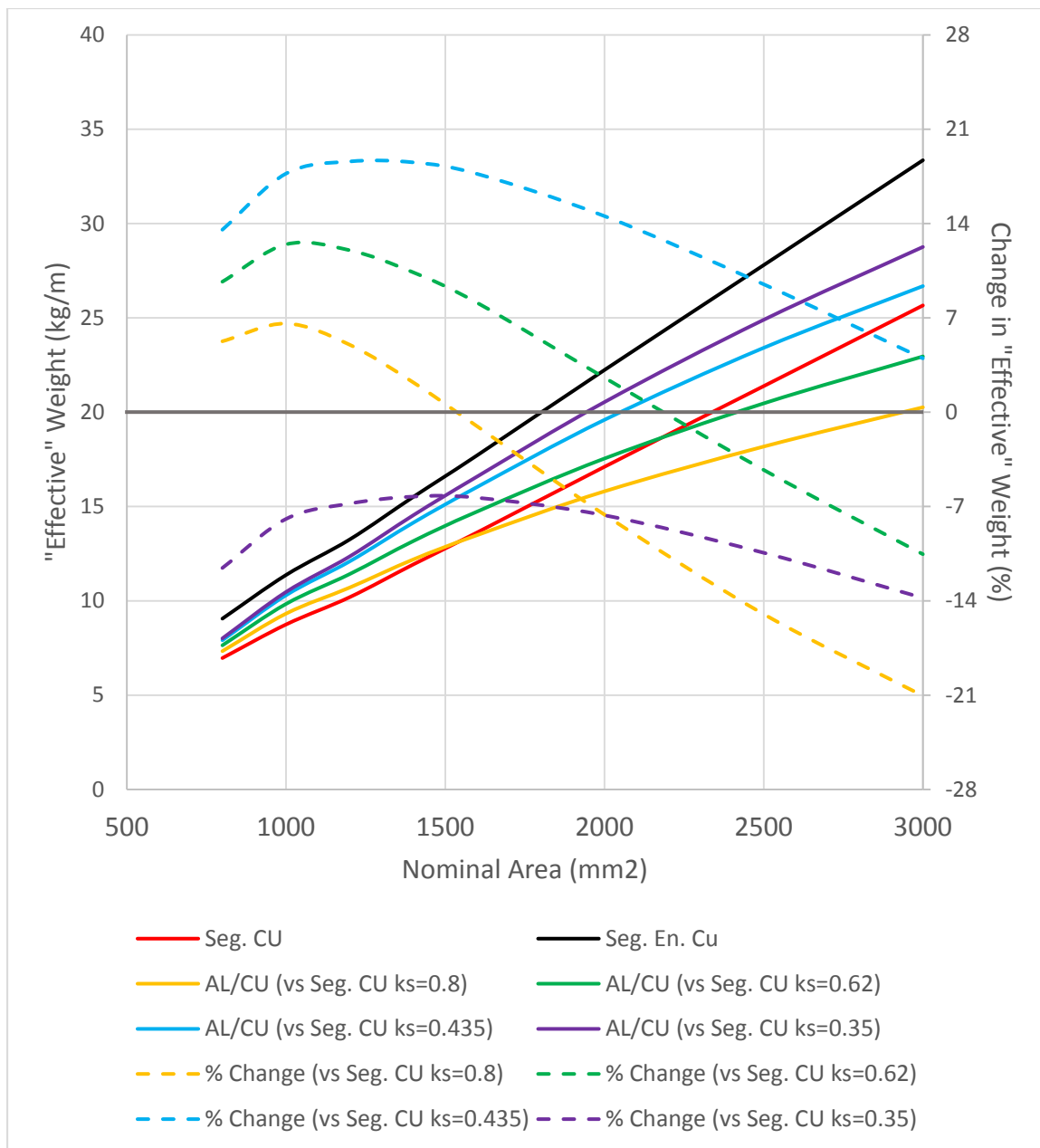


FIGURE 6-20: “Effective” weight of Air / CU vs segmented CU (enamel = 30%)

Now, the “effective” weight of the segmented enameled conductor has increased, causing a shift in when it becomes cost effective. This shows that not only does the enamel solution cross the Air / CU solution, but at today’s cost it does so and becomes cost effective even before any other segmented conductor type. Looking at some more specific examples helps further clarify what is happening. FIGURE 6-21 demonstrates what

happens in comparing the cross-sectional area of the copper used in Air / CU designs versus segmented copper designs ($k_s = 0.8$) at 90°C and 60 Hz:

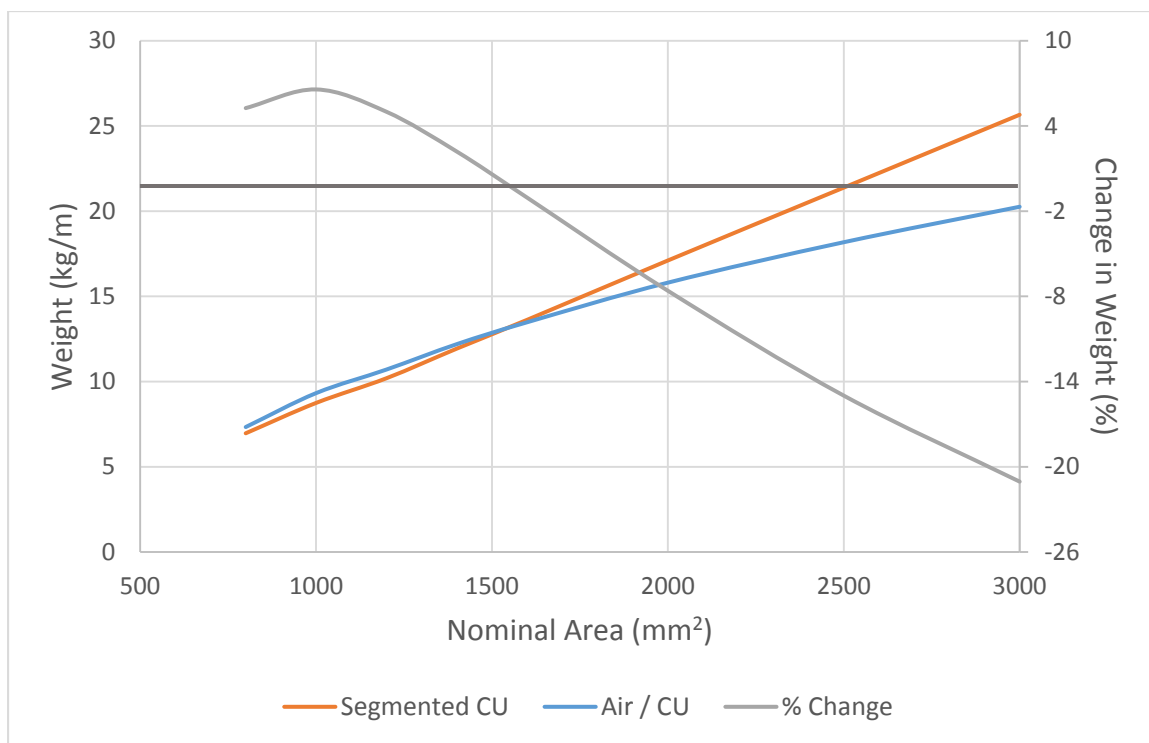


FIGURE 6-21: Weight of Air / CU vs segmented CU ($k_s=0.8$)

This shows that there is one crossing point, around 1600 mm² where the areas of the Air / CU and segmented copper are equal. This is also the point the change in areas between the two designs goes from positive (i.e. Air / CU uses more copper) to negative (i.e. Air / CU uses less copper), and the Air / CU design is more cost effective.

All of this becomes much more complicated when discussing enameled wires, due to the cost increase of the enamel. Most often, the enameled conductor design is either initially less expensive and stays less expensive (cost increase of enamel $\leq 12\%$), or initially more expensive and stays more expensive (cost increase of enamel $\geq 22\%$). However, between 12% and 22% there can be strange behavior where it goes back and forth between cost effective and not cost effective. First, FIGURE 6-22 shows an example

under the assumptions of 60 Hz and 90°C on an enameled conductor (i.e. $k_s = 0.35$) using a cost of enamel price increase of 20% as compared to an Air / CU conductor:

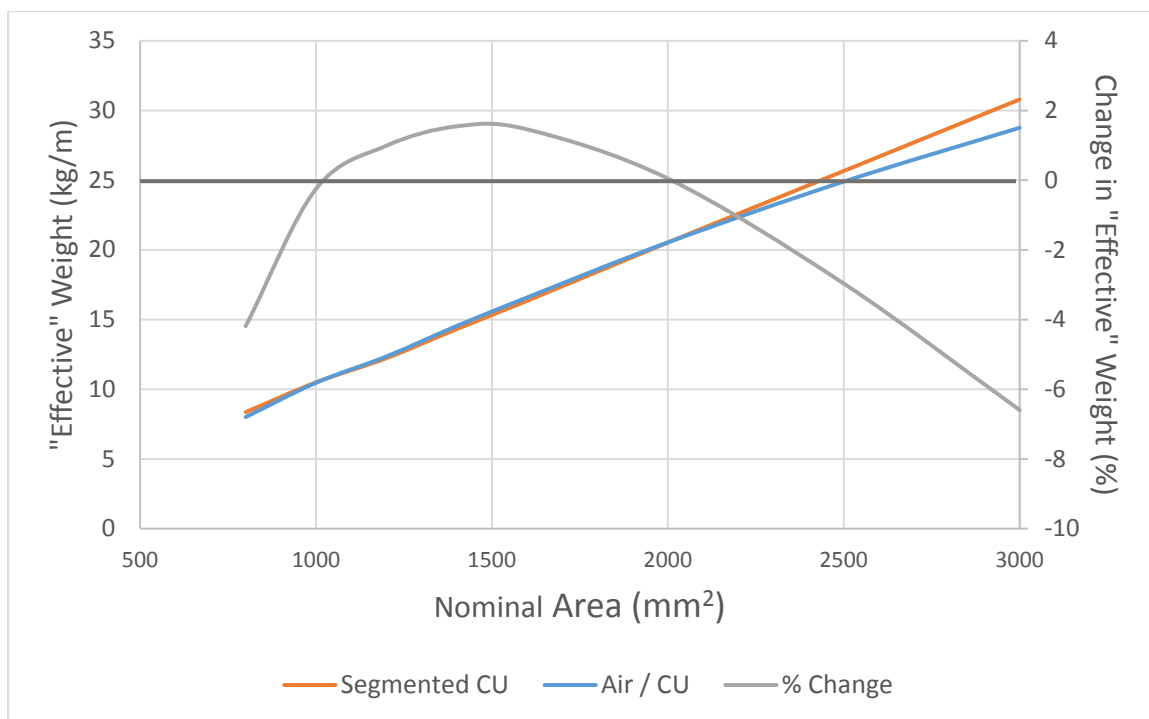


FIGURE 6-22: “Effective” weight of Air / CU vs enameled CU ($k_s=0.35$)

Because of the cost of the enameled wires, it is observed that initially the cost of a segmented copper conductor with enameled wires is more than a Air / CU conductor composed of all copper with equal AC resistance. This is never the case when not using enameled wires. However, in this case it starts off more expensive, then becomes less, and again becomes more. The three sections can be thought of as (1) the initial cost of enamel being more expensive, (2) the barely optimal design of the Air / CU being more expensive, and (3) the optimal design of the Air / CU being less expensive. The reason for the second region is that generally, as the conductor design area increases, so does the effectiveness of the Air / CU design. However, since the core starts from all copper there is initially little return of decreased AC resistance and replacement of a larger section of the core. This

occurs between about 1000 mm² to 2000 mm². In the final region a large section of the core is being replaced by air, and thus eventually the Air / CU conductor is more cost effective than the enameled copper conductor.

When discussing the cost effectiveness of AL / CU conductors this becomes even more complicated. They behave in a similar way as the Air / CU conductors, however now not only the “effective” weight of the enamel wires must be accounted for but also the “effective” weight of the aluminum. Due to the two media being used the cost effective point shifts depending on the price ratio of copper to aluminum. This has the interesting effect of introducing additional inflection points as shown in FIGURE 6-23 (assuming a copper to aluminum cost ratio of three times and 0% pricing increase for enameled wires):

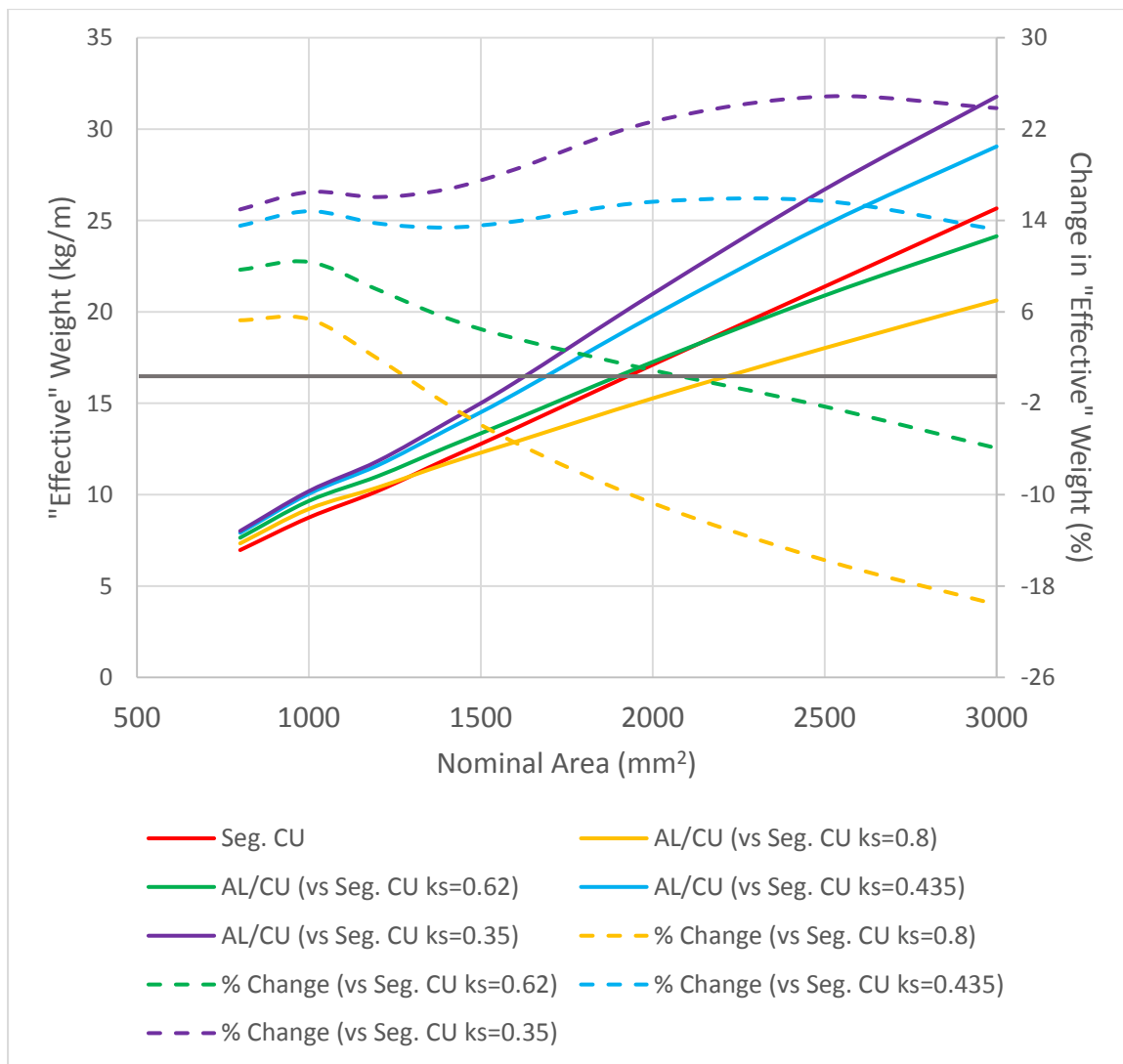


FIGURE 6-23: “Effective” weight of AL / CU vs segmented CU (enamel = 0%)

This shows that at three times multiple of the price of copper to aluminum (as is today) the segmented conductors with $k_s = 0.8$ and 0.62 have cost effective solutions for AL / CU conductors. These shift depending on the cost ratios, which are provided in the tables. Whereas with Air / CU there was only a maximum of the change in “effective” weight as the effectiveness of the hollow air core became more apparent, replacing the air core with aluminum has a different effect. As the copper core is replaced with aluminum at first the small area replaced is nearly negligible and the plot behaves almost as if it were

air. However, as the AL / CU becomes more effective the “effective” weight begins to increase with the growing aluminum core. Eventually, the increasingly large aluminum core becomes large enough that it makes up a large enough part of the total “effective” weight of the conductor and the change in “effective” weight versus a segmented conductor is only decreasing. The effect of increasing the enameled wire cost adder to 30% is shown in FIGURE 6-24:

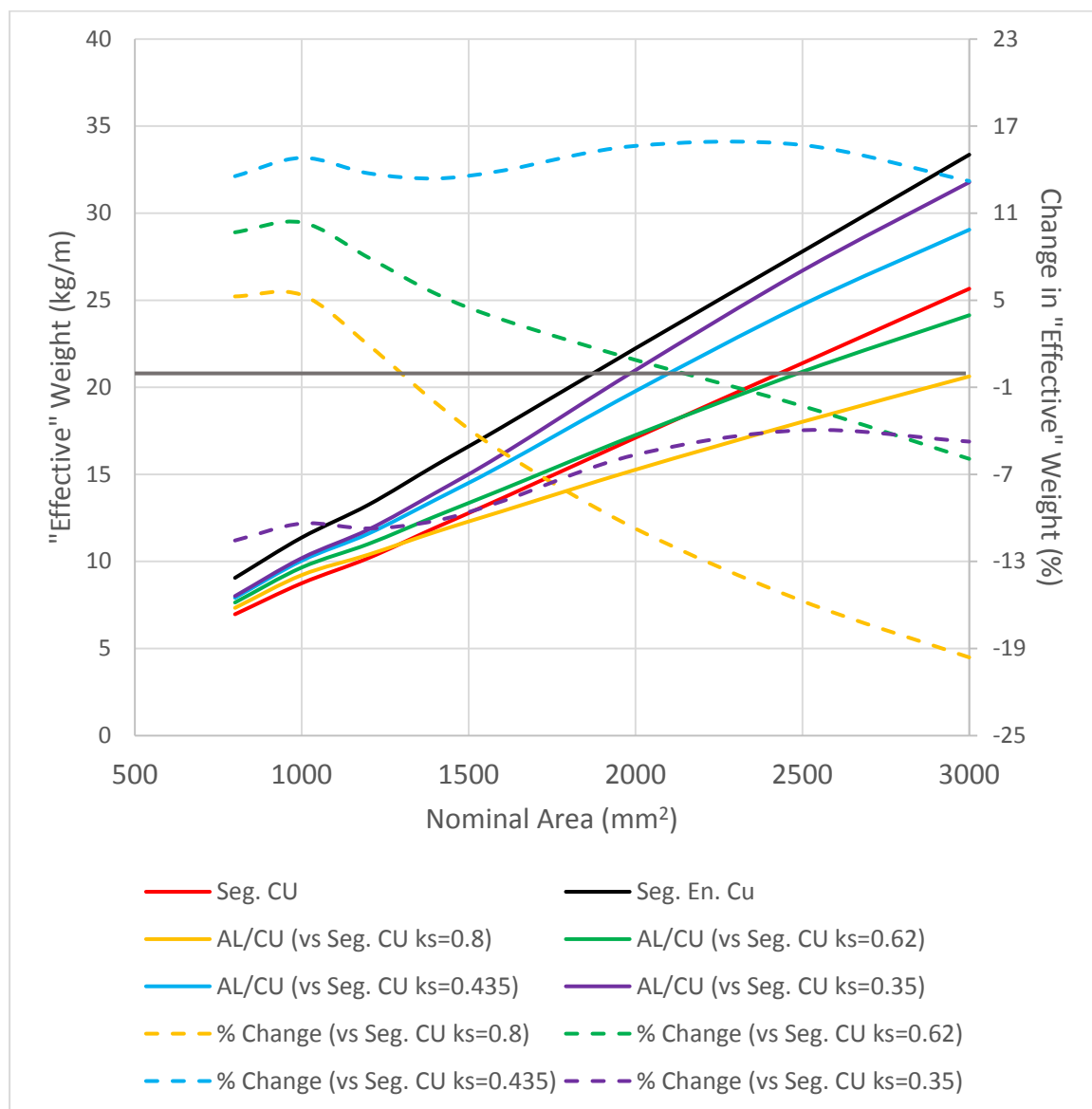


FIGURE 6-24: “Effective” weight of AL / CU vs segmented CU (enamel = 30%)

Here it can be seen that at a 30% enamel cost adder the enamel conductor always has a larger “effective” weight and therefore cost. To illustrate further with some unique scenarios a few more detailed examples are shown. In the first example, the price ratios chosen are 0.4 and 1. This means either the price of copper is 0.4 that of aluminum or equal. Note that an equal price also means the “effective” weight is the actual weight, as there is no adjustment of the aluminum weight to be reflective of the price ratio. Of course, this would be unexpected in reality, as the price of copper is roughly three times that of aluminum. However, for illustrative purposes it shows important things on FIGURE 6-25 (for 60 Hz, 90°C, and $k_s = 0.8$):

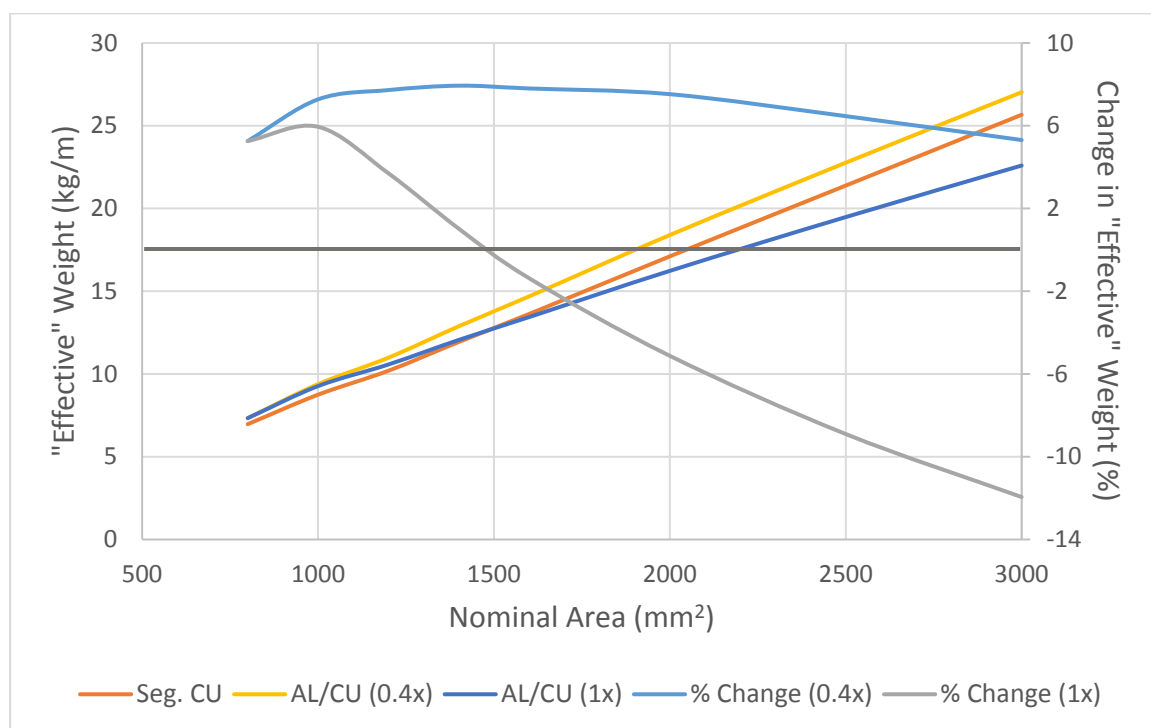


FIGURE 6-25: “Effective” weight of AL / CU vs segmented CU ($k_s=0.8$)

It is seen that the weight of AL / CU always starts higher than segmented copper. This is expected since more copper is required in a non-optimal conductor to have equal AC resistance to a segmented design. That is, this point is before a minima in AC resistance

exists and therefore the conductor is a single medium copper non-segmented conductor. At a price ratio of 0.4 the AL / CU design never becomes cost effective, and hence its “effective” weight is always above the segmented copper weight. The even price ratio crosses around 1500 mm².

The final analysis of the cost effective ratio behavior is for enameled conductors compared to AL / CU conductors, using an enameling cost increase of 16%. Like the 20% used for the Air / CU comparison, this range also produces unique results. This is particularly true for the cost ratios of copper to aluminum of five and twenty times. This is shown on FIGURE 6-26:

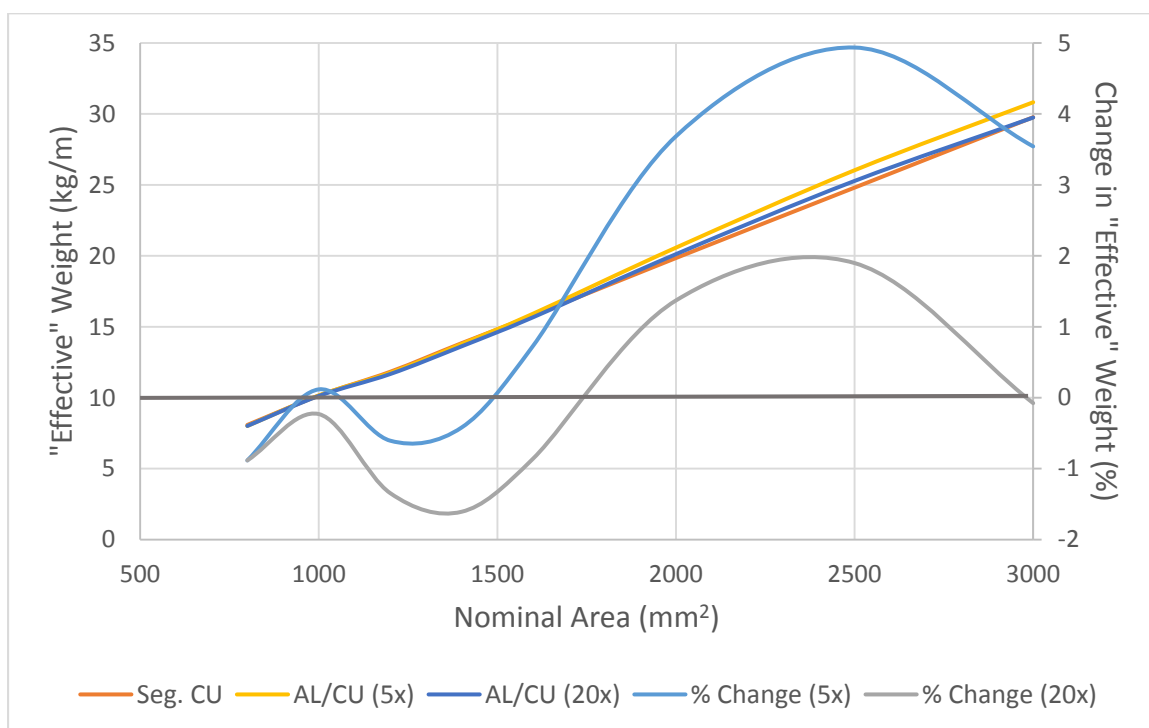


FIGURE 6-26: “Effective” weight of AL / CU vs enameled CU ($k_s=0.35$)

Here, the cost of the enameled conductor again is initially more expensive than that of a solid/stranded copper conductor with the same AC resistance. Although the cross-sectional area of the solid/stranded conductor is greater, it is irrelevant since it is

overshadowed by the cost of the enameled wires. Then, as previously described, a smaller amount of aluminum comes into play in the equation, but has negligible effect and the curve decreases like in Air / CU. However, once this amount of aluminum becomes more significant there is a second effect mirroring the first effect. Depending on the cost increase of enameled wire and the copper to aluminum price ratio, this double effect could cause the “effective” weights to cross multiple times.

Now the actual weights, broken up into copper and aluminum and not cost adjusted are compared. FIGURE 6-27 shows the cross-sectional area and metal consumption required for Air / CU conductors to have the same AC resistance as compared to segmented CU operating at 90°C and 60 Hz, using a k_s of 0.8:

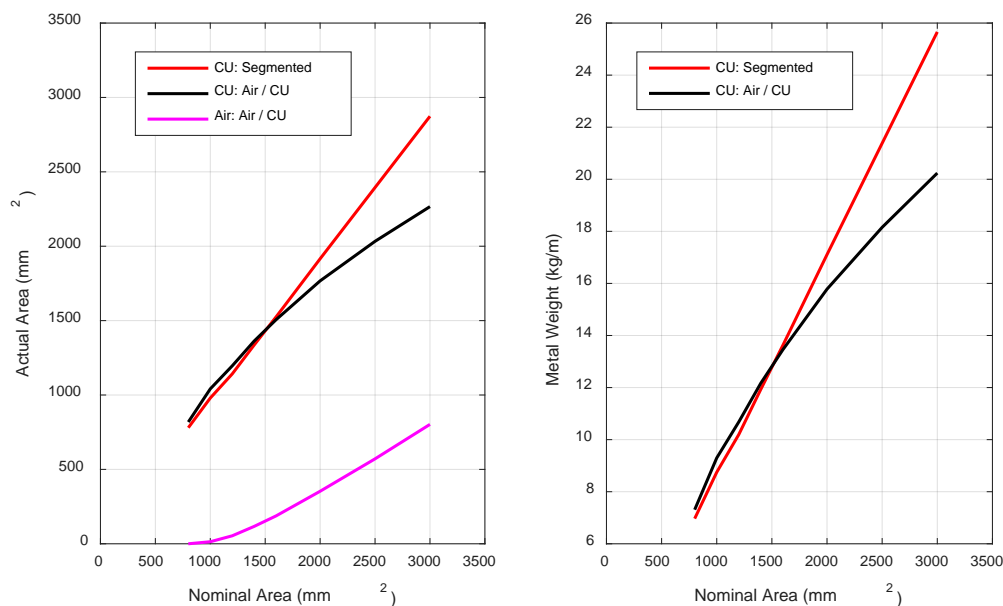


FIGURE 6-27: Areas and weights of Air / CU conductors ($k_s=0.8$, 90°C, 60 Hz)

The point at which the copper in the segmented and Air / CU conductors cross is also the point the Air / CU conductor becomes more cost effect, as less copper is being used and the air has no cost. FIGURE 6-28 shows this for 105°C and 60 Hz:

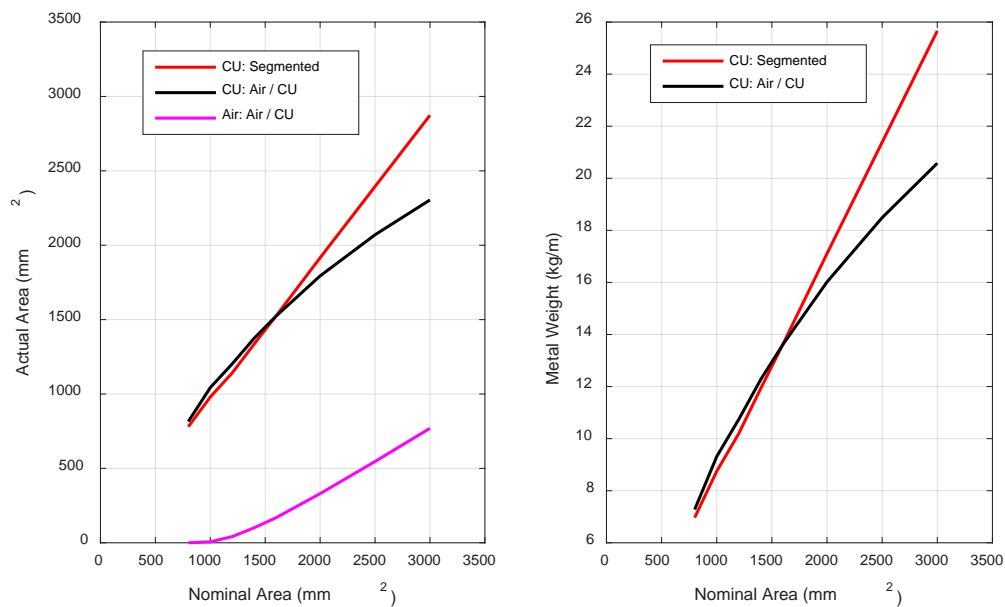


FIGURE 6-28: Areas and weights of Air / CU conductors ($k_s=0.8$, 105°C , 60 Hz)

FIGURE 6-29 shows this for 90°C and 50 Hz:

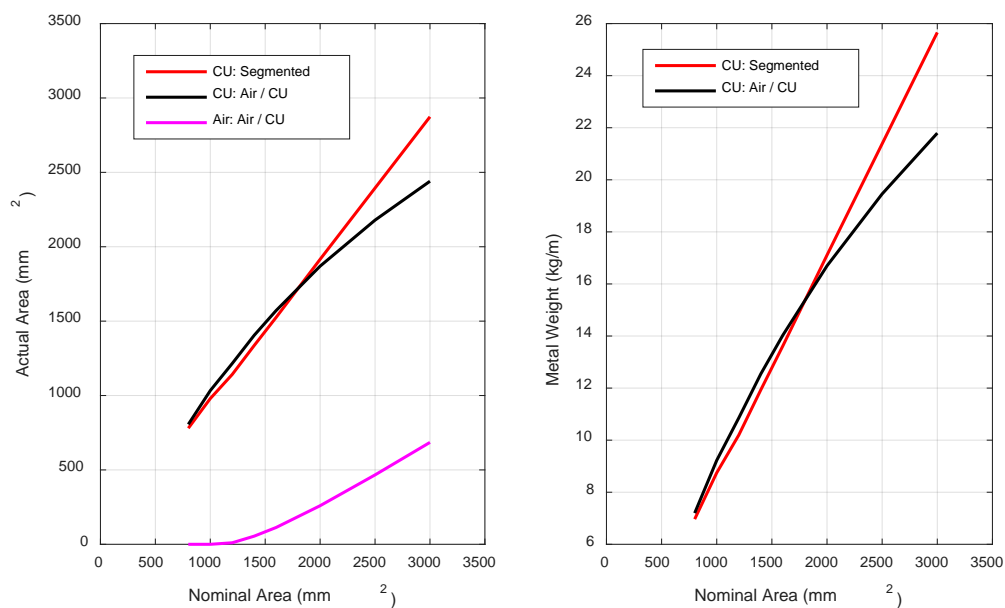


FIGURE 6-29: Areas and weights of Air / CU conductors ($k_s=0.8$, 90°C , 50 Hz)

FIGURE 6-30 shows this for 105°C and 50 Hz:

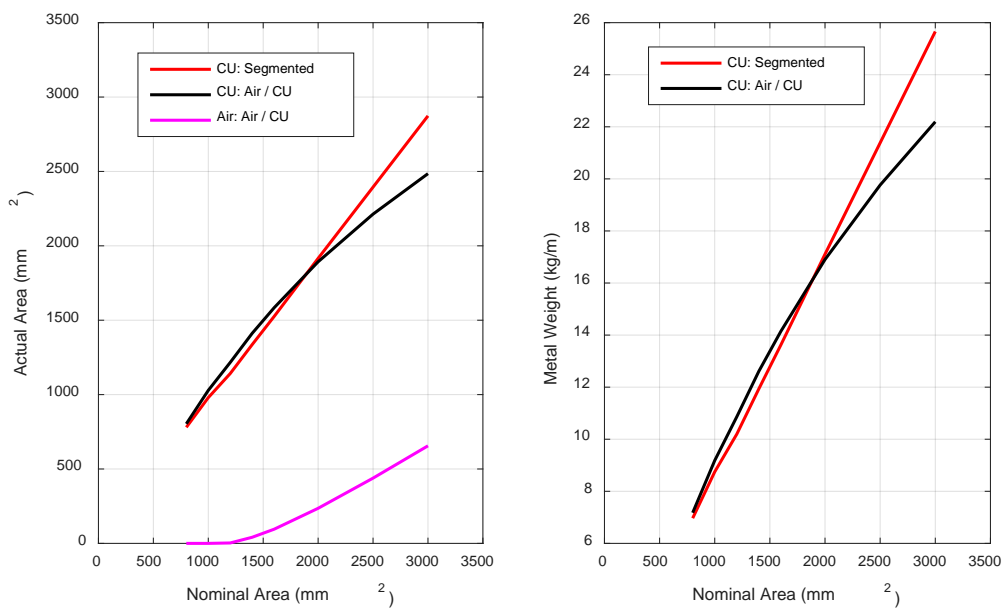


FIGURE 6-30: Areas and weights of Air / CU conductors ($k_s=0.8$, 105°C, 50 Hz)

FIGURE 6-31 shows this for 90°C and 60 Hz, using a k_s of 0.62:

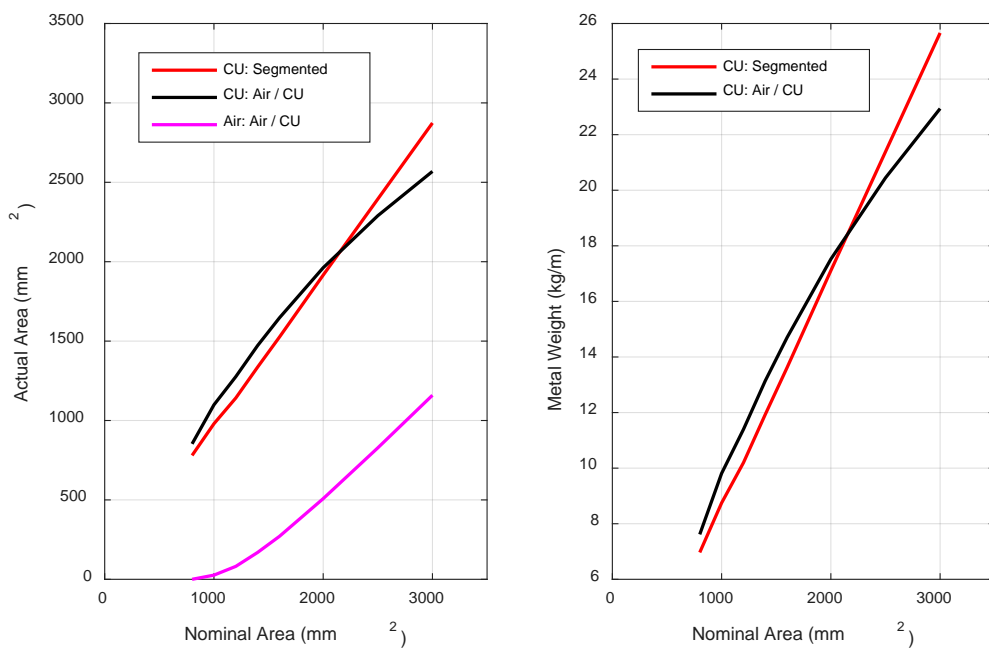


FIGURE 6-31: Areas and weights of Air / CU conductors ($k_s=0.62$, 90°C, 60 Hz)

FIGURE 6-32 shows this for 105°C and 60 Hz:

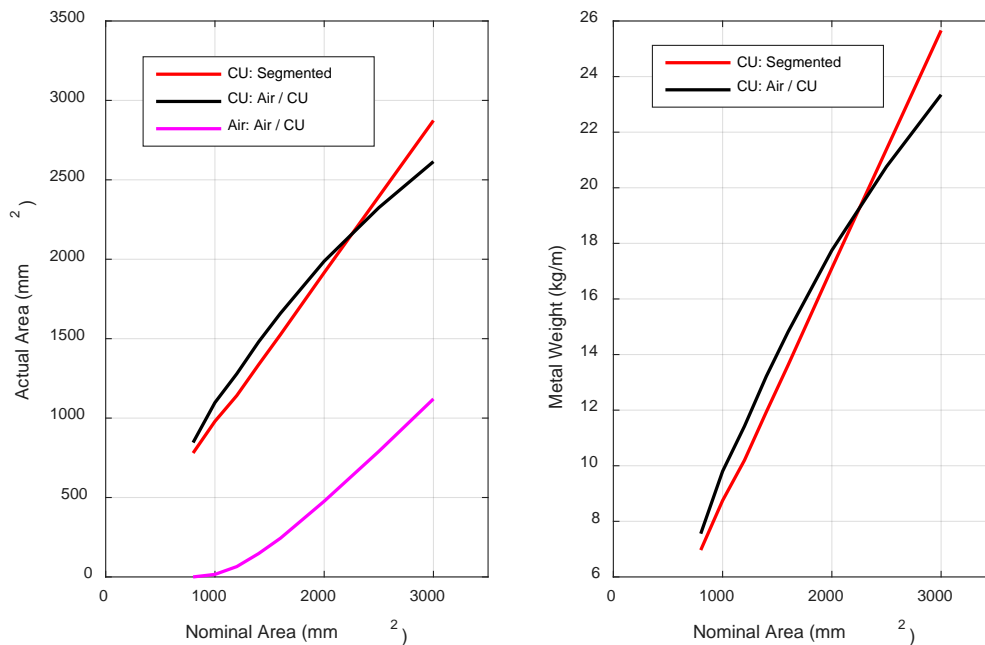


FIGURE 6-32: Areas and weights of Air / CU conductors ($k_s=0.62$, 105°C, 60 Hz)

FIGURE 6-33 shows this for 90°C and 50 Hz:

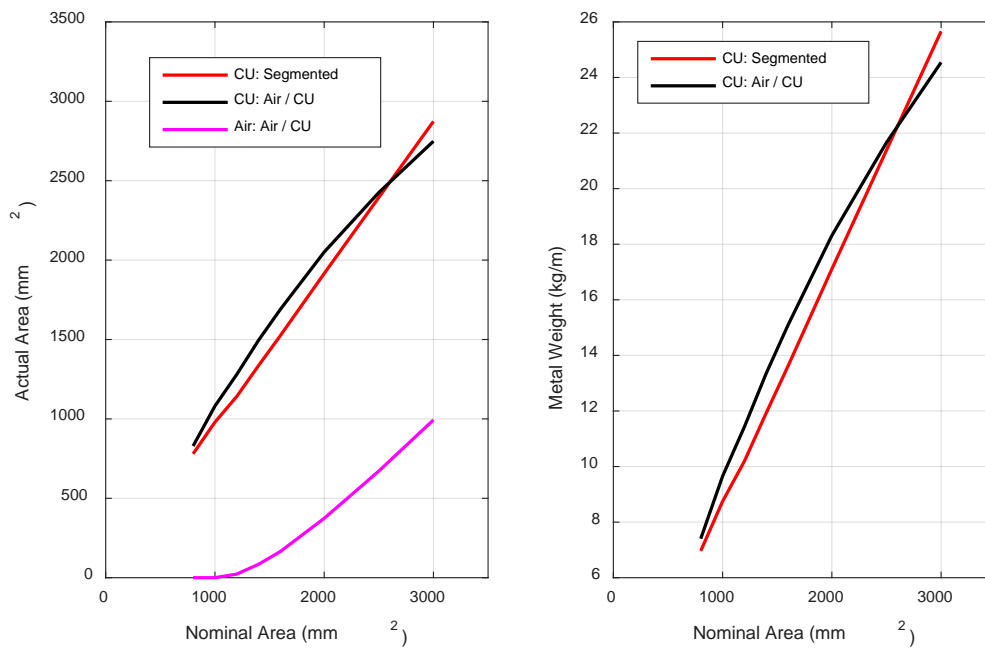


FIGURE 6-33: Areas and weights of Air / CU conductors ($k_s=0.62$, 90°C, 50 Hz)

FIGURE 6-34 shows this for 105°C and 50 Hz:

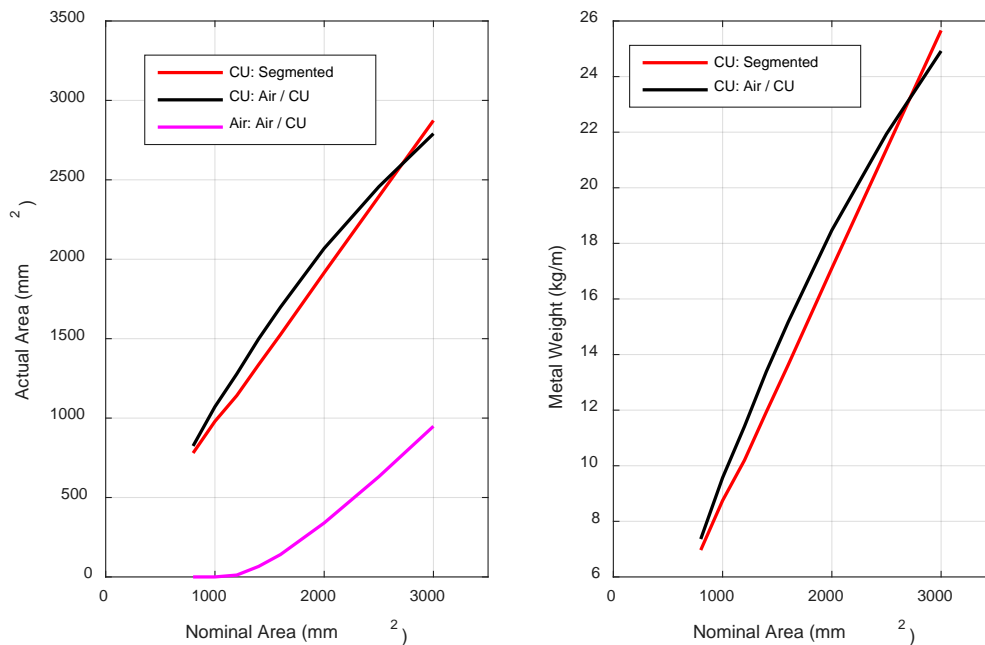


FIGURE 6-34: Areas and weights of Air / CU conductors ($k_s=0.62$, 105°C, 50 Hz)

FIGURE 6-35 shows this for 90°C and 60 Hz, using a k_s of 0.435:

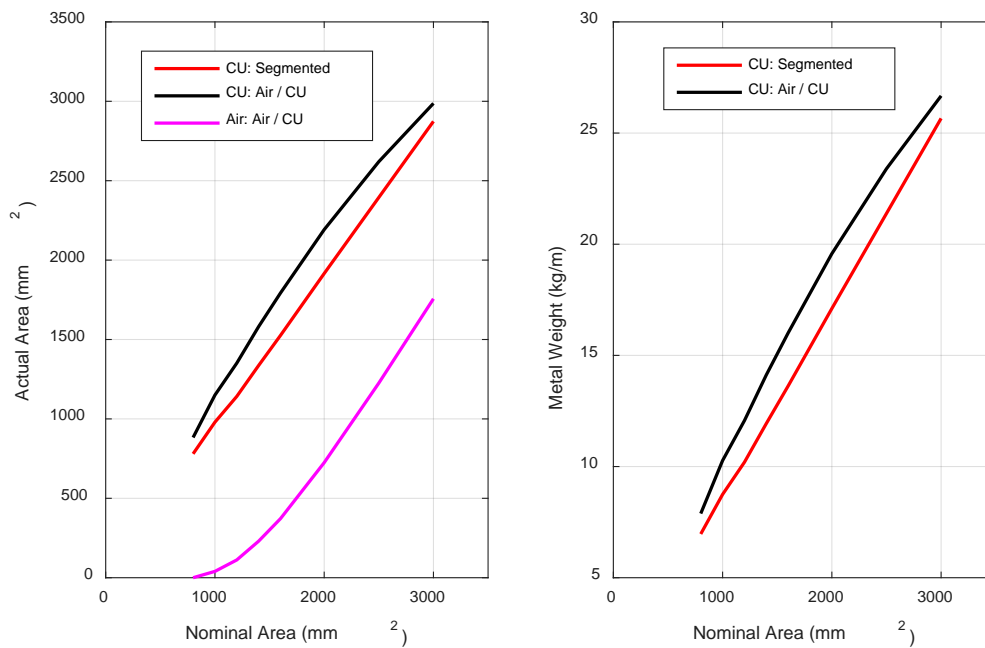


FIGURE 6-35: Areas and weights of Air / CU conductors ($k_s=0.435$, 90°C, 60 Hz)

It can be observed on these plots that there is no crossing of the segmented copper and Air / CU designs. Therefore, there is no optimal design that is more cost effect than the segmented designs. FIGURE 6-36 shows consumption for 105°C and 60 Hz:

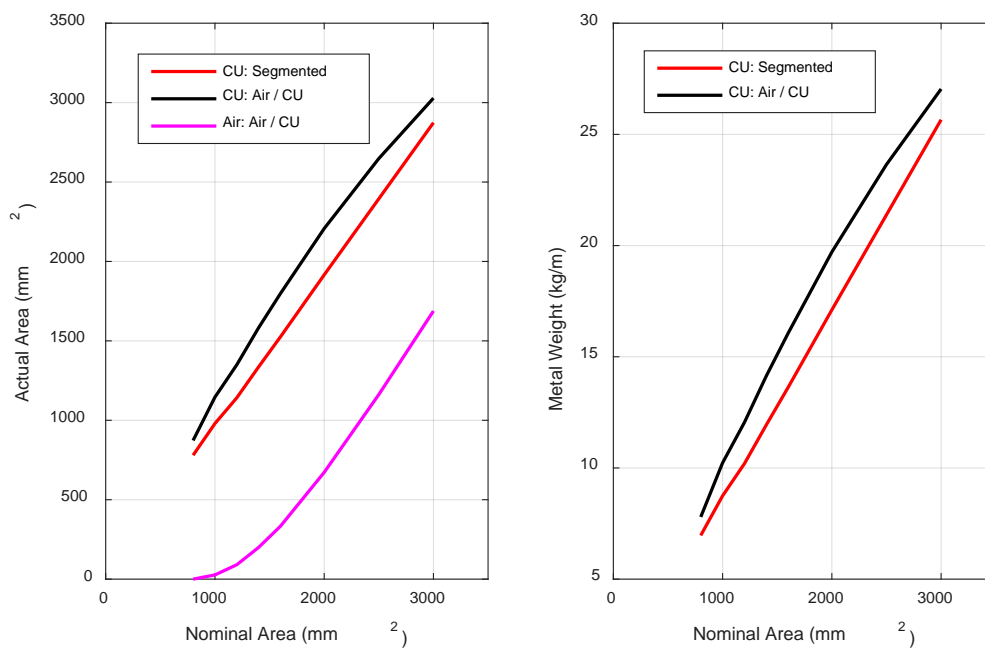


FIGURE 6-36: Areas and weights of Air / CU conductors ($k_s=0.435$, 105°C, 60 Hz)

FIGURE 6-37 shows this for 90°C and 50 Hz:

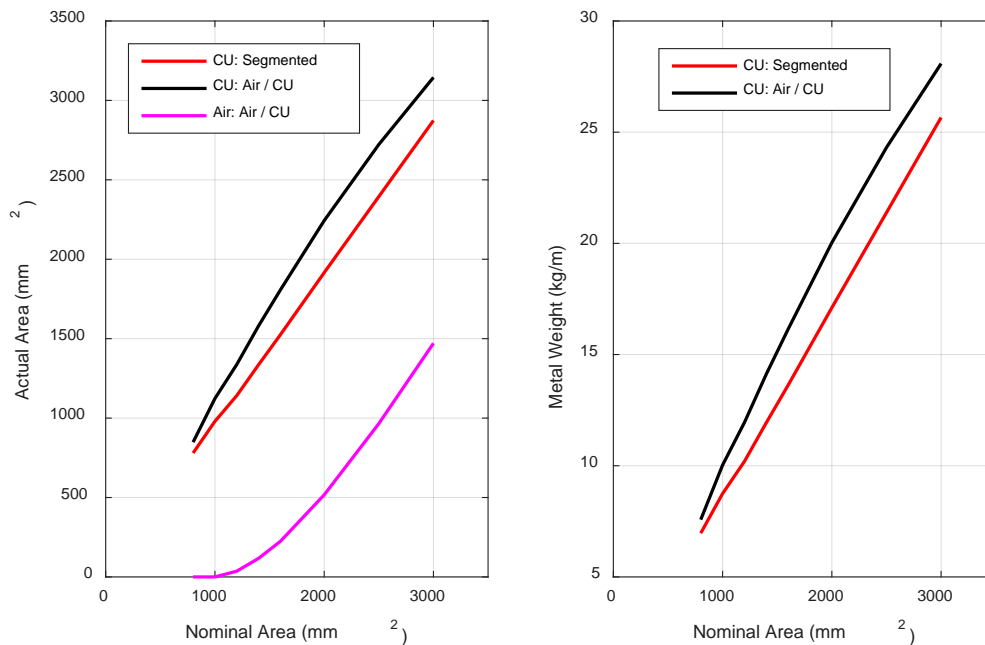


FIGURE 6-37: Areas and weights of Air / CU conductors ($k_s=0.435$, 90°C, 50 Hz)

FIGURE 6-38 shows this for 105°C and 50 Hz:

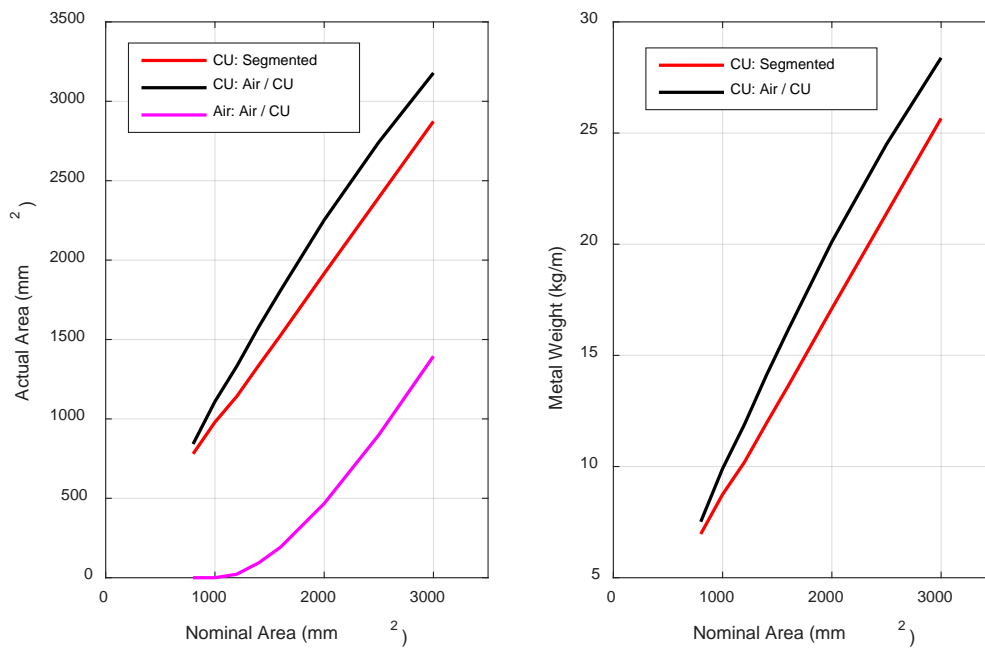


FIGURE 6-38: Areas and weights of Air / CU conductors ($k_s=0.435$, 105°C, 50 Hz)

FIGURE 6-39 shows this for 90°C and 60 Hz, using a k_s of 0.35:

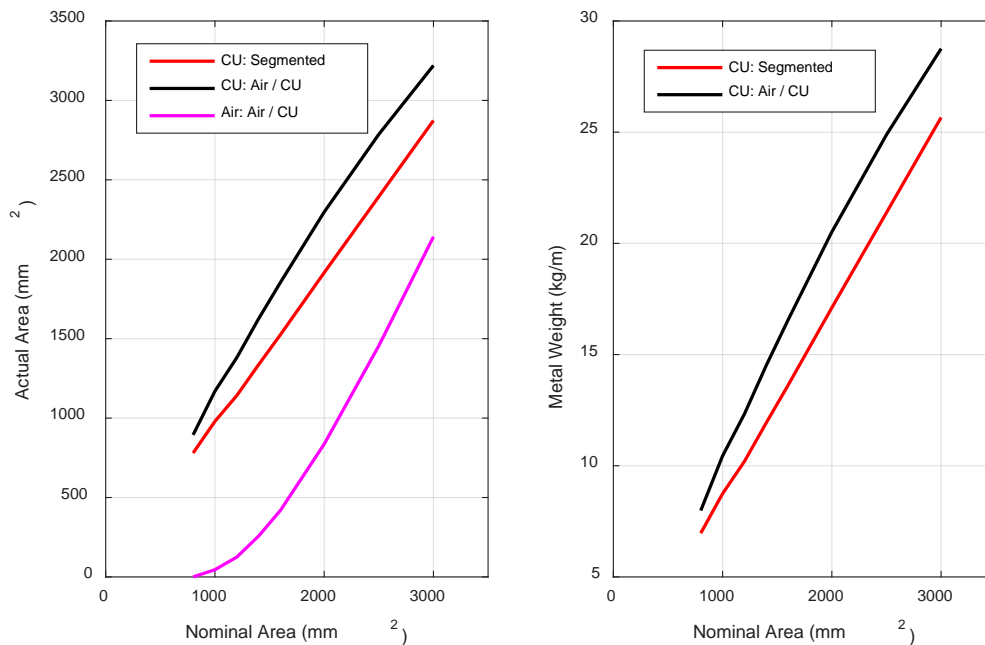


FIGURE 6-39: Areas and weights of Air / CU conductors ($k_s=0.35$, 90°C, 60 Hz)

Although the segmented copper and Air / CU do not cross this does not mean that the Air / CU is not more cost effective. Because of the cost of the enameled wires, the more cost effective solution depends on the percentage of price increase of the enameling. This is shown for 105°C and 60 Hz on FIGURE 6-40:

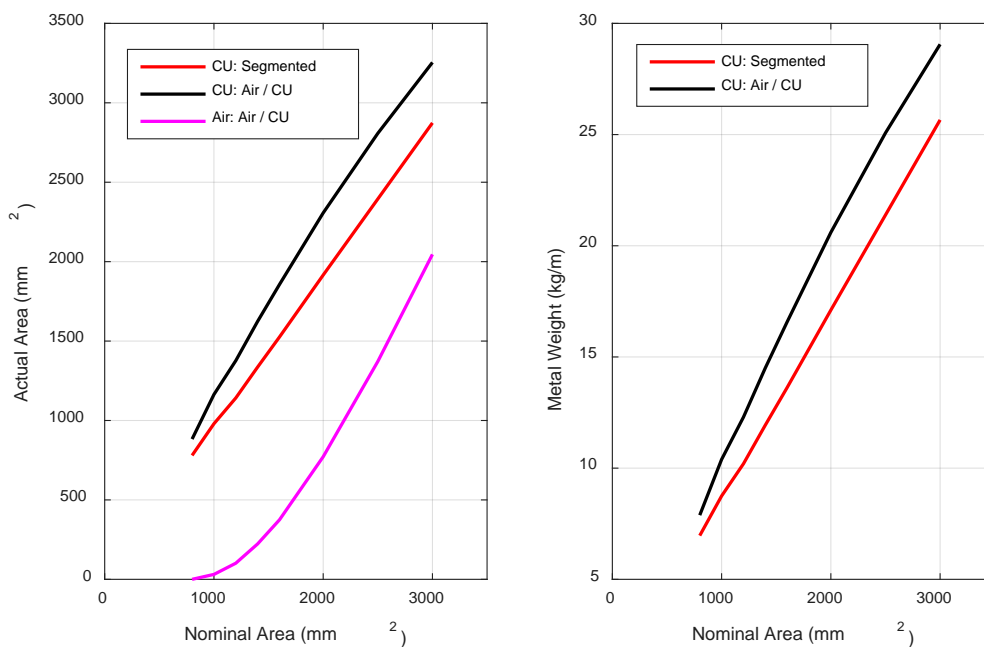


FIGURE 6-40: Areas and weights of Air / CU conductors ($k_s=0.35$, 105°C , 60 Hz)

FIGURE 6-41 shows this for 90°C and 50 Hz :

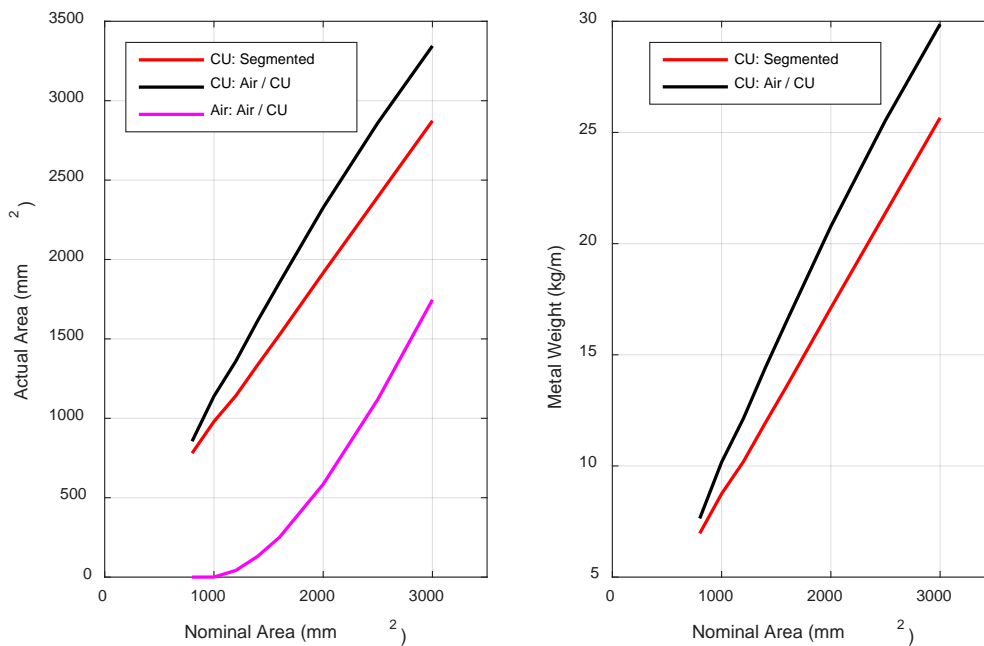


FIGURE 6-41: Areas and weights of Air / CU conductors ($k_s=0.35$, 90°C , 50 Hz)

FIGURE 6-42 shows this for 105°C and 50 Hz:

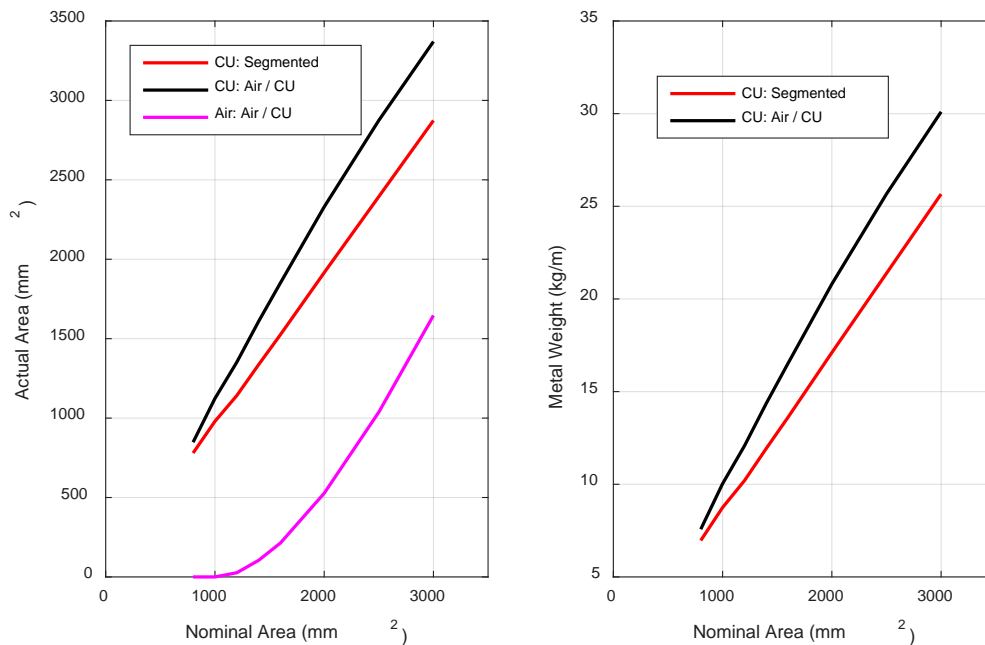


FIGURE 6-42: Areas and weights of Air / CU conductors ($k_s=0.35$, 105°C, 50 Hz)

FIGURE 6-43 shows the cross-sectional area and metal consumption required for AL / CU conductors to have the same AC resistance as compared to segmented CU operating at 90°C and 60 Hz, using a k_s of 0.8:

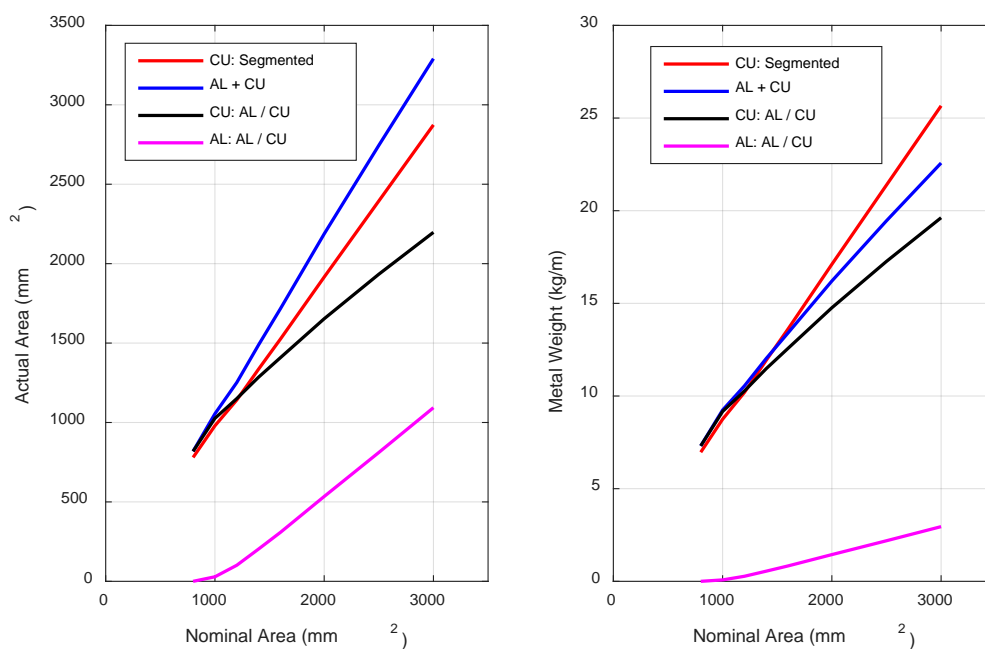


FIGURE 6-43: Areas and weights of AL / CU conductors ($k_s=0.8$, 90°C , 60 Hz)

The point at which the copper in the segmented and AL / CU conductors cross is also the point the AL / CU conductor becomes more cost effective depending on the cost ratio of copper to aluminum cost, as less copper is being used. This is shown on FIGURE 6-44 for 105°C and 60 Hz:

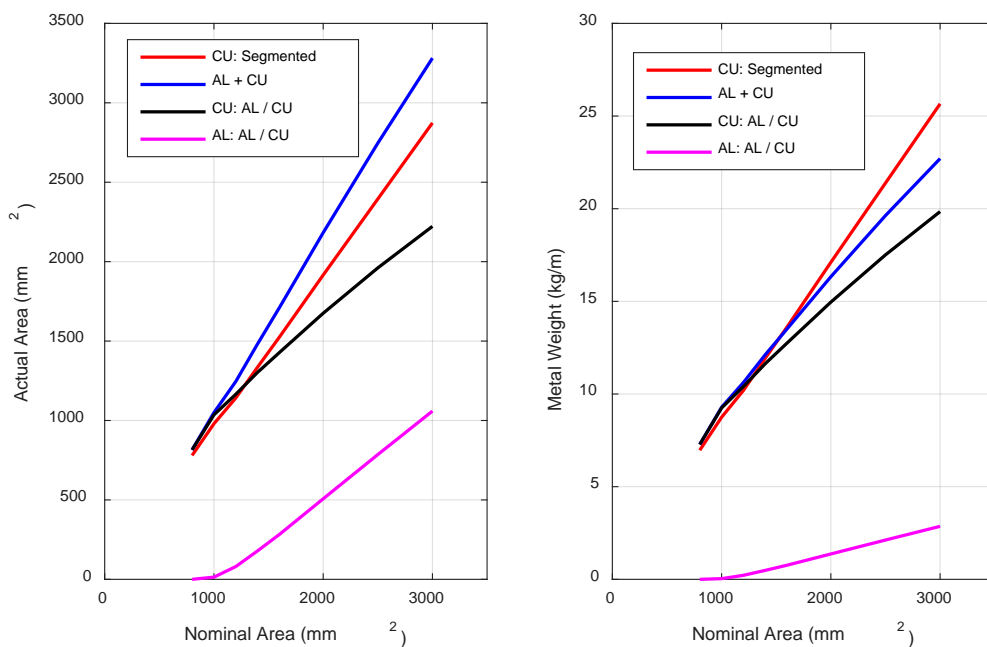


FIGURE 6-44: Areas and weights of AL / CU conductors ($k_s=0.8$, 105°C , 60 Hz)

FIGURE 6-45 shows this for 90°C and 50 Hz:

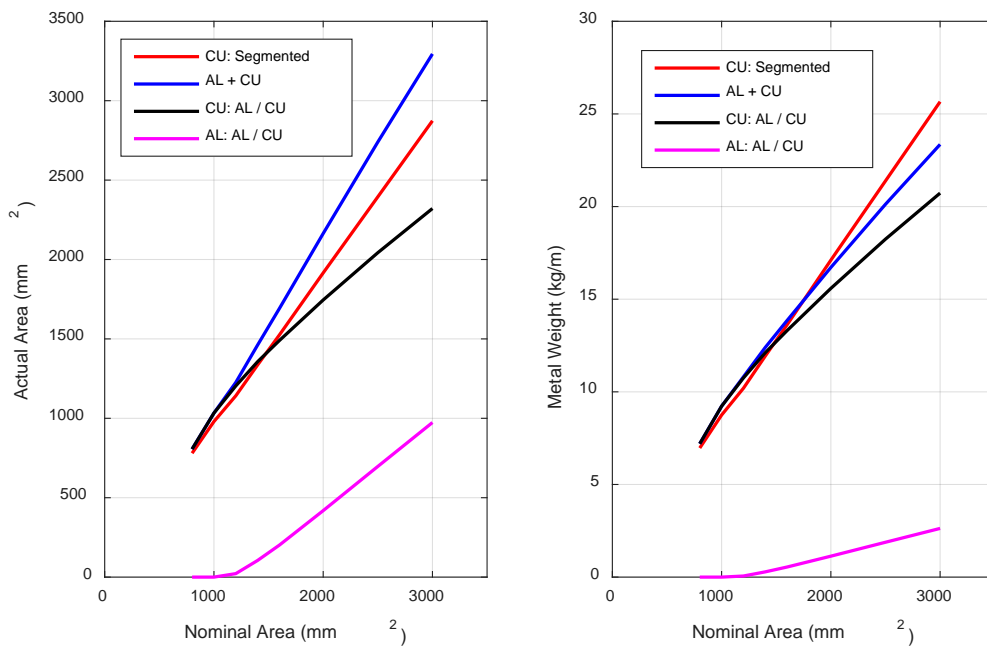


FIGURE 6-45: Areas and weights of AL / CU conductors ($k_s=0.8$, 90°C , 50 Hz)

FIGURE 6-46 shows this for 105°C and 50 Hz:

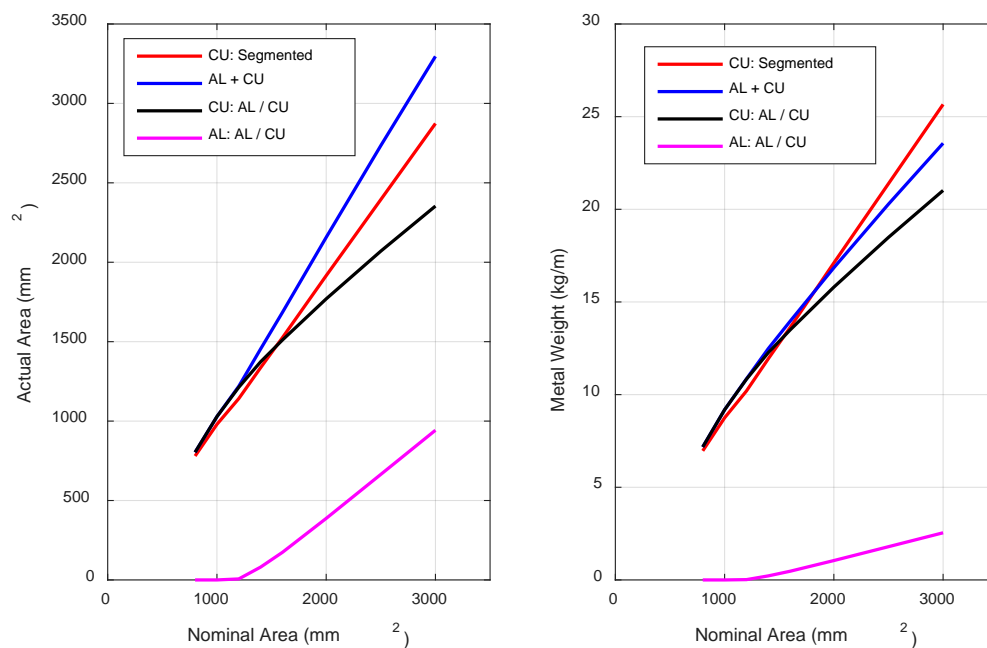


FIGURE 6-46: Areas and weights of AL / CU conductors ($k_s=0.8$, 105°C, 50 Hz)

FIGURE 6-47 shows this for 90°C and 60 Hz, using a k_s of 0.62:

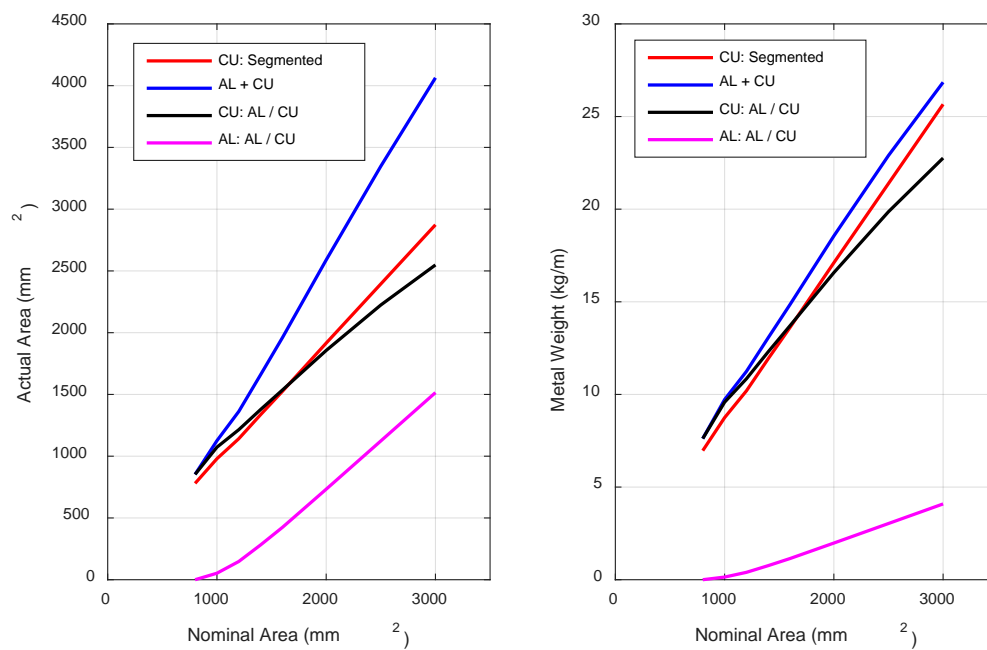


FIGURE 6-47: Areas and weights of AL / CU conductors ($k_s=0.62$, 90°C, 60 Hz)

FIGURE 6-48 shows this for 105°C and 60 Hz:

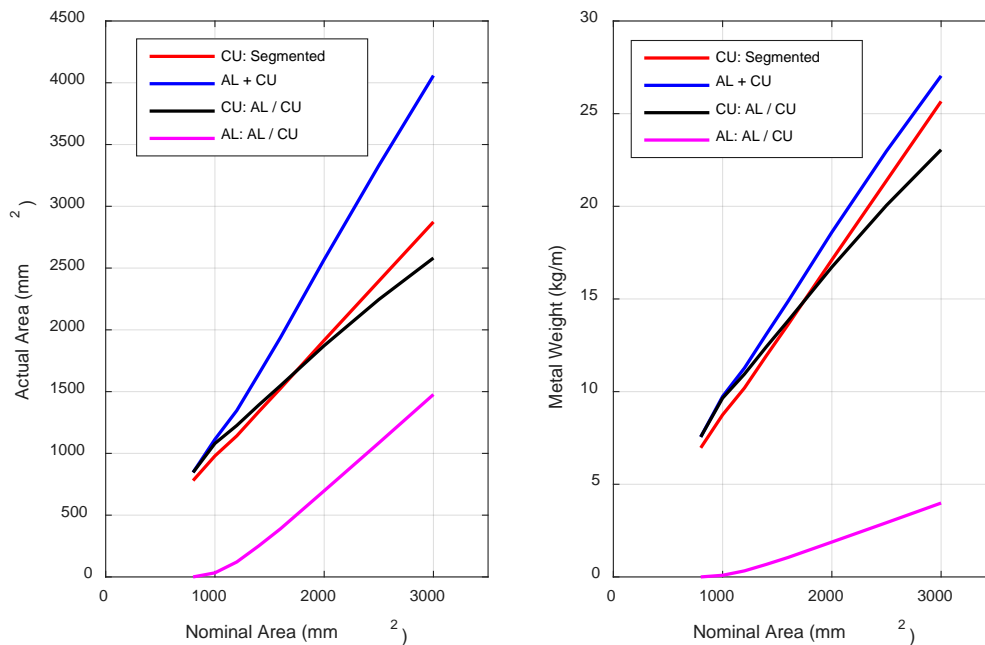


FIGURE 6-48: Areas and weights of AL / CU conductors ($k_s=0.62$, 105°C, 60 Hz)

FIGURE 6-49 shows this for 90°C and 50 Hz:

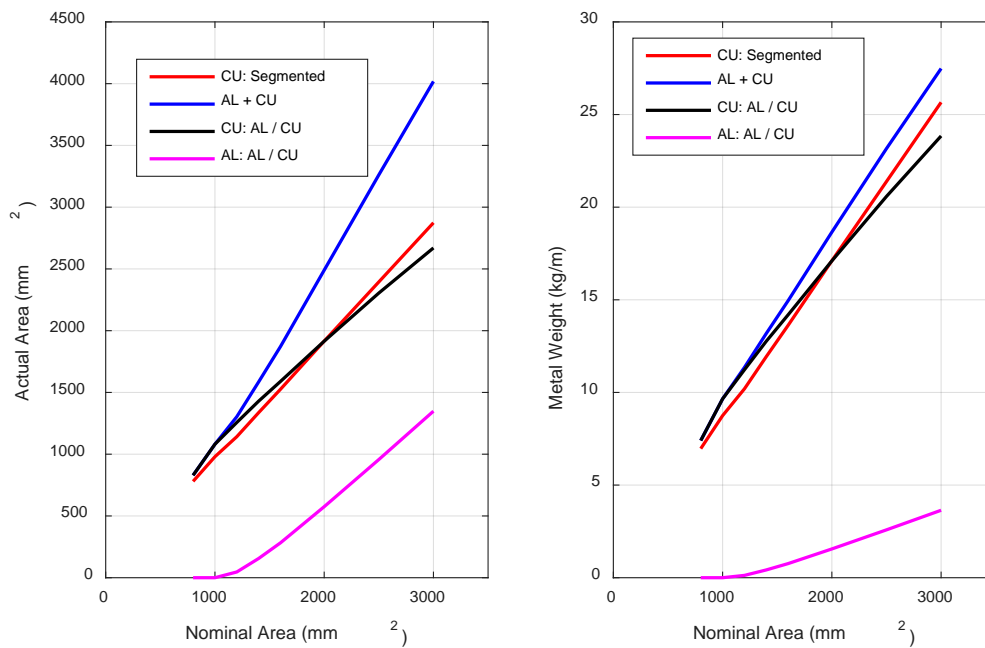


FIGURE 6-49: Areas and weights of AL / CU conductors ($k_s=0.62$, 90°C, 50 Hz)

FIGURE 6-50 shows this for 105°C and 50 Hz:

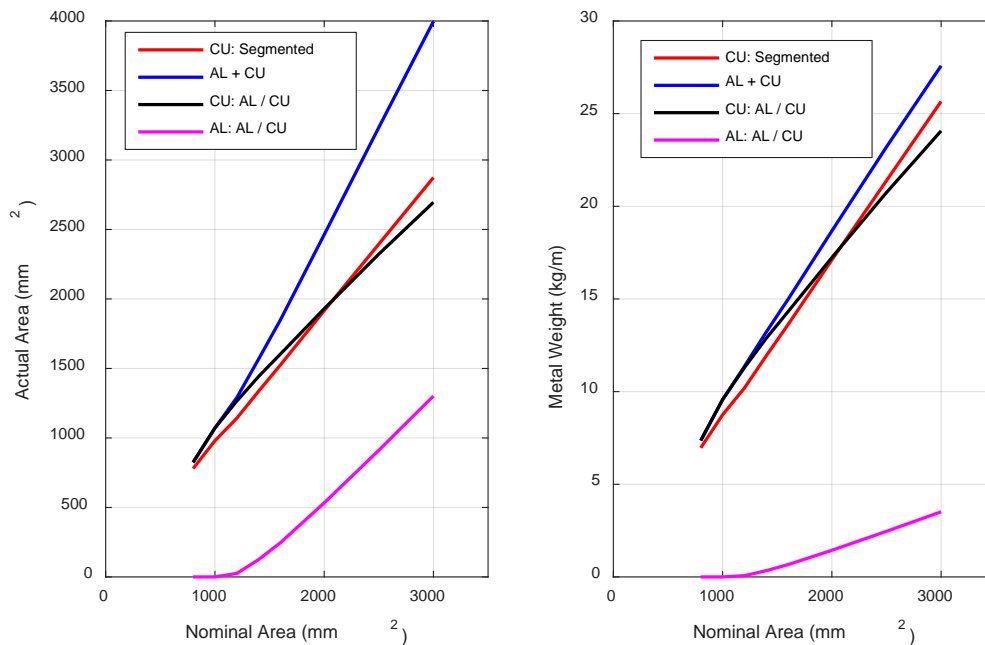


FIGURE 6-50: Areas and weights of AL / CU conductors ($k_s=0.62$, 105°C, 50 Hz)

FIGURE 6-51 shows this for 90°C and 60 Hz, using a k_s of 0.435:

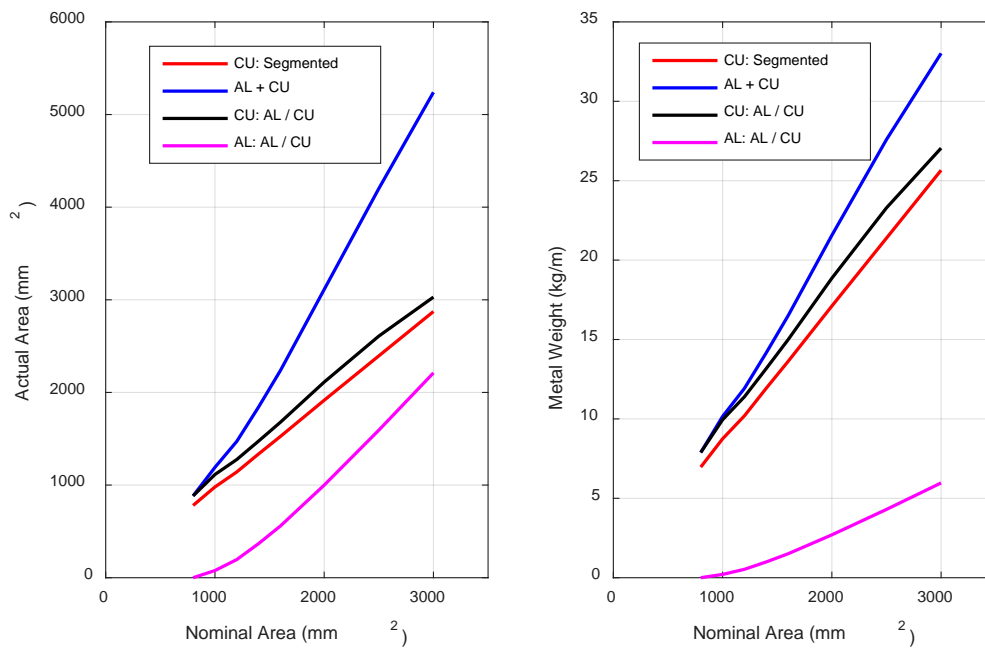


FIGURE 6-51: Areas and weights of AL / CU conductors ($k_s=0.435$, 90°C, 60 Hz)

It can be observed on these plots that there is no crossing of the segmented copper and AL / CU designs. Therefore, there is no optimal design that is more cost effect than the segmented designs. FIGURE 6-52 shows this for 105°C and 60 Hz:

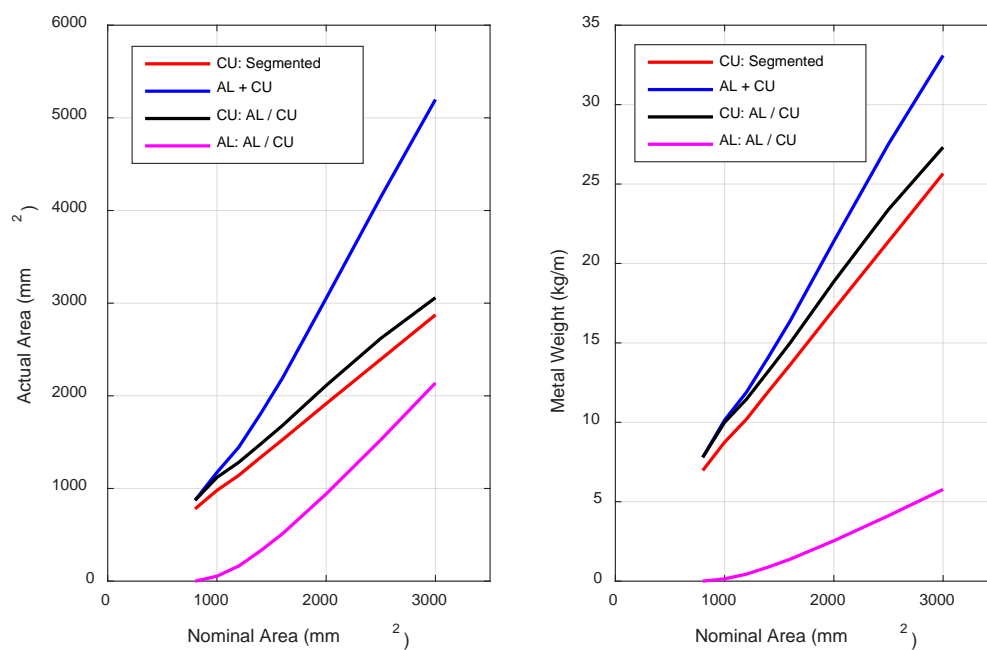


FIGURE 6-52: Areas and weights of AL / CU conductors ($k_s=0.435$, 105°C, 60 Hz)

FIGURE 6-53 shows this for 90°C and 50 Hz:

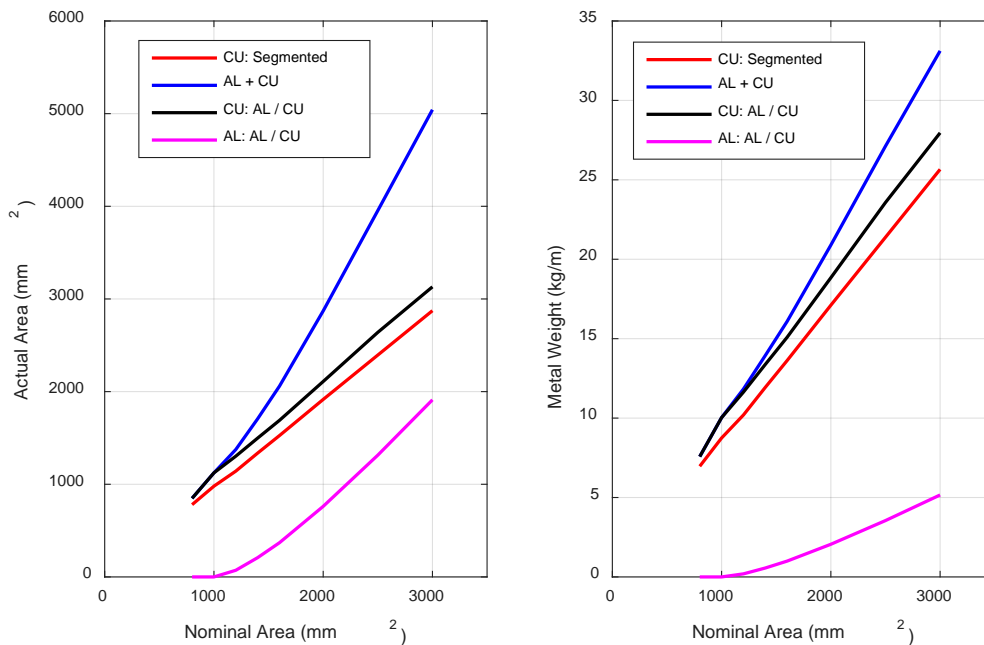


FIGURE 6-53: Areas and weights of AL / CU conductors ($k_s=0.435$, 90°C, 50 Hz)

FIGURE 6-54 shows this for 105°C and 50 Hz:

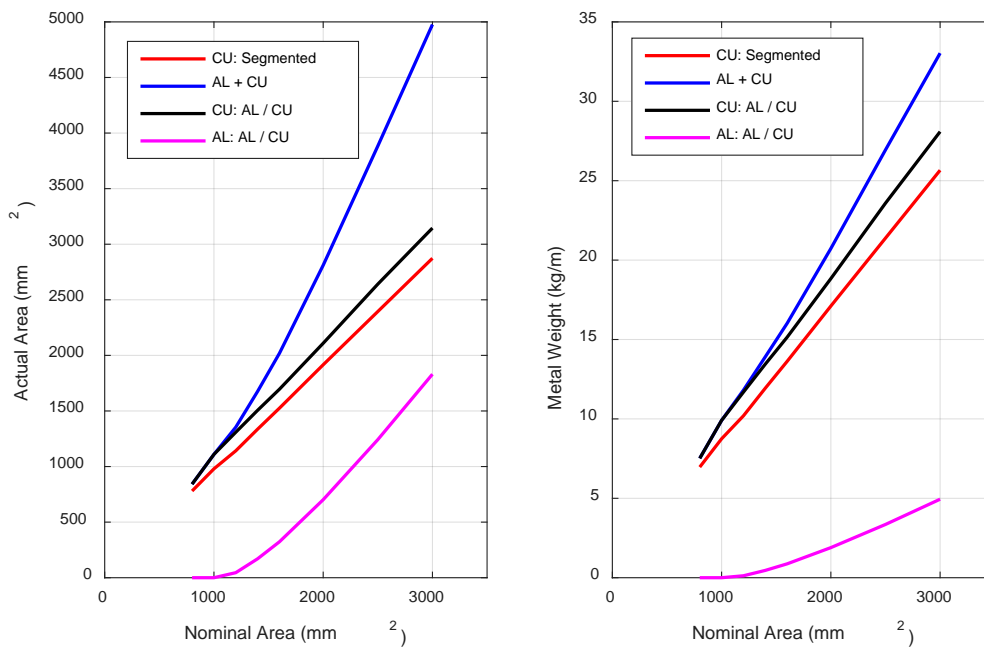


FIGURE 6-54: Areas and weights of AL / CU conductors ($k_s=0.435$, 105°C, 50 Hz)

FIGURE 6-55 shows this for 90°C and 60 Hz, using a k_s of 0.35:

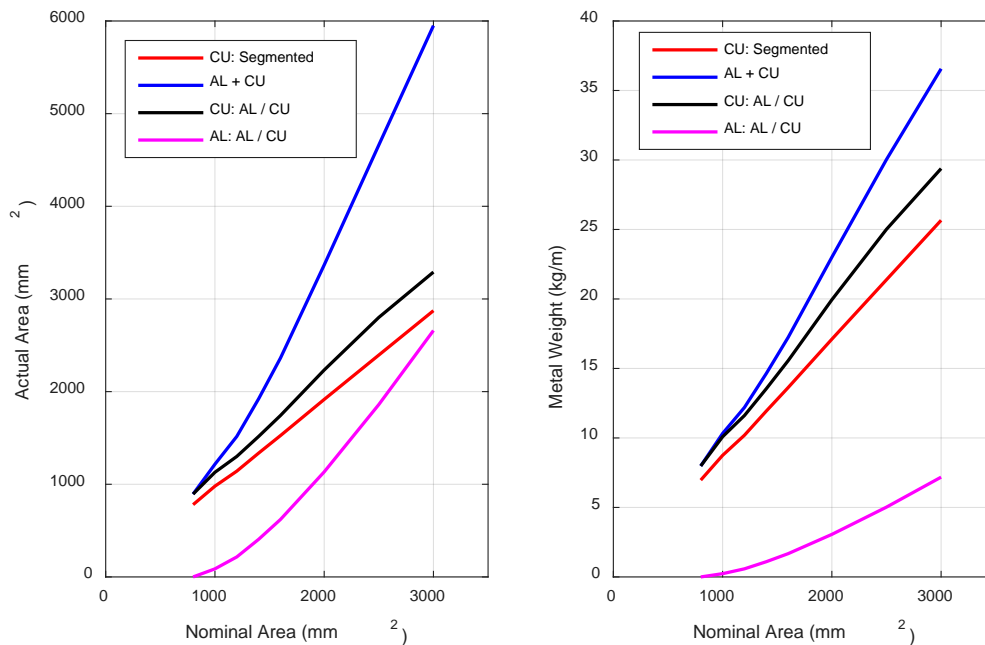


FIGURE 6-55: Areas and weights of AL / CU conductors ($k_s=0.35$, 90°C, 60 Hz)

Although the segmented copper and AL / CU do not cross this does not mean that the AL / CU is not more cost effective. Because of the cost of the enameled wires, the more cost effective solution depends on the percentage of price increase of the enameling.

FIGURE 6-56 shows this for 105°C and 60 Hz:

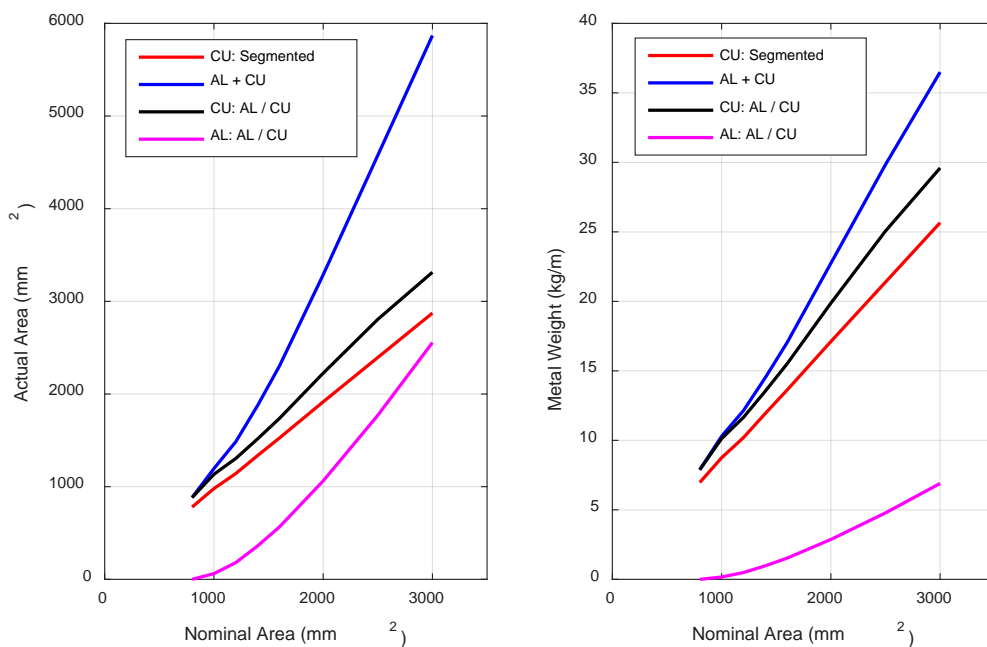


FIGURE 6-56: Areas and weights of AL / CU conductors ($k_s=0.35$, 105°C , 60 Hz)

FIGURE 6-57 shows this For 90°C and 50 Hz :

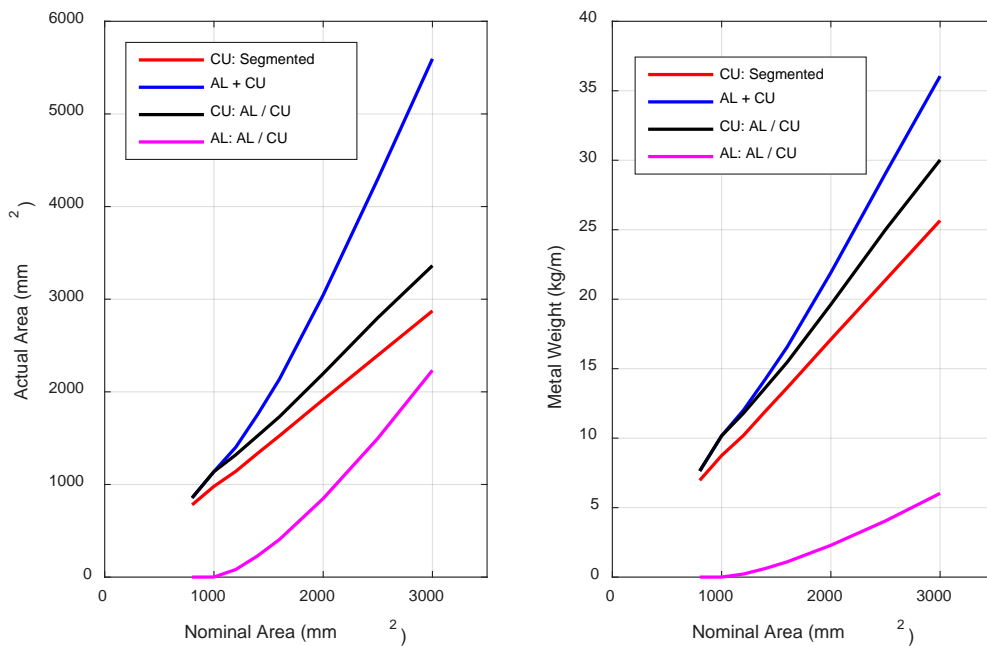


FIGURE 6-57: Areas and weights of AL / CU conductors ($k_s=0.35$, 90°C , 50 Hz)

FIGURE 6-58 shows this for 105°C and 50 Hz:

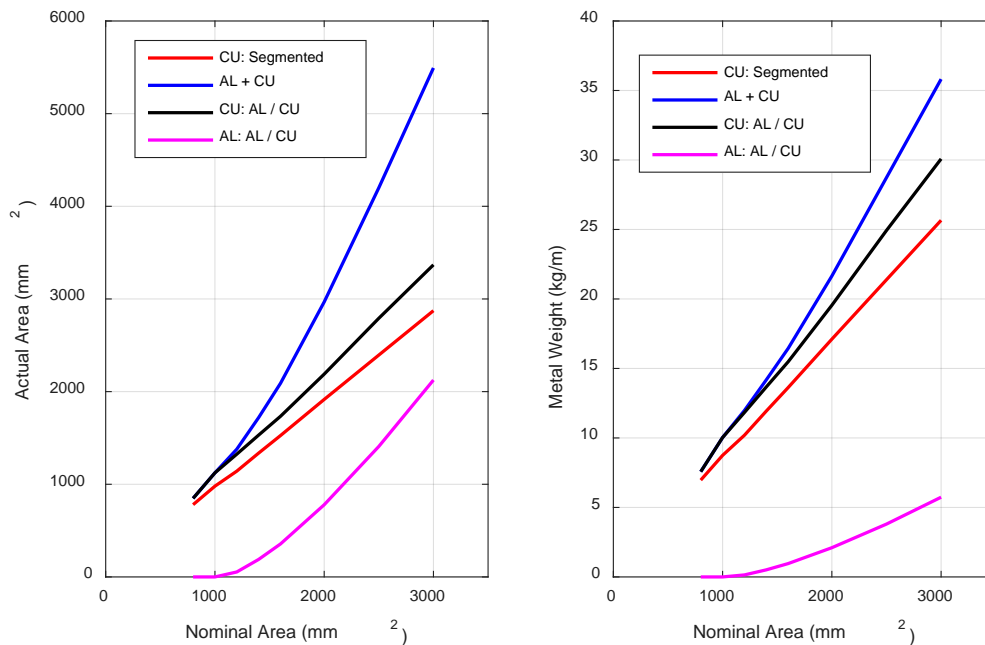


FIGURE 6-58: Areas and weights of AL / CU conductors ($k_s=0.35$, 105°C, 50 Hz)

Tables summarizing these results are presented next. Note that in addition to the red background used to indicate a solid/stranded conductor design is more optimal than a bi-media conductor, there are also yellow backgrounds used here. The yellow indicates that the design is never more cost effective than using a segmented copper conductor, as the bi-media design has more copper. Finally, there are also green backgrounds indicating the bi-media design is always cost effective. This is either the counterpart to the red or yellow coloring on Air / CU conductors when less copper is used, or in the Air / CU and AL / CU designs versus enameled wire conductors when less copper is used taking into consideration the cost increase of the enameling. For the AL / CU designs the cost ratio where the non-enameled segmented copper conductors and AL / CU conductors have the same cost can be found using the weights of the metals in the conductor. Electrical grade

aluminum has a density of 2.7 kg/m^3 , while the density of electrical grade copper is 8.93 kg/m^3 . Therefore, the weight of the aluminum and copper in a conductor is:

$$W_{AlCu_Al} = 2.7 \cdot A_{AL} \cdot 0.001 \quad (131)$$

$$W_{AlCu_Cu} = 8.93 \cdot A_{CU} \cdot 0.001 \quad (132)$$

Using these, the copper to aluminum cost ratio that produces the same cost for a segmented copper conductor of equal AC resistance to an AL / CU conductor is:

$$\frac{\$Cu}{\$Al} = \frac{W_{AlCu_Al}}{W_{S_Cu} - W_{AlCu_Cu}} \quad (133)$$

Note that on some “AL / CU” designs no aluminum is used (i.e. no optimal design or no AC resistance minimum exists). This happens at both 50 and 60 Hz on nominal area 800 mm^2 conductors, and at 50 Hz on nominal area 1000 mm^2 conductors. In these cases the AL / CU conductor is never the most cost effective solution. Furthermore, if the calculated cost ratio is negative then the AL / CU is also never the most cost effective solution. The final possibility is that the cost ratio comes out to a real number. In this case the meaning is that if the cost ratio of copper to aluminum is less than that number the AL / CU is never cost effective, but if more than that number it is always cost effective. If the cost ratio of copper to aluminum is exactly the same as the ratio the cost of the AL / CU and segmented conductor are exactly the same. Note that this equation can also be used in the case of enameled copper wires. In this case the cost of the enameled wires is incorporated as so:

$$\frac{\$Cu}{\$Al} = \frac{W_{AlCu_Al}}{W_{S_Cu} \cdot \left(1 + \frac{ECI\%}{100}\right) - W_{AlCu_Cu}} \quad (134)$$

Finally, the weights can also be used to directly calculate the cost delta in Air / CU conductors. The cost delta for the Air / Cu compared to the non-enameled segmented copper is:

$$CD = 100 x \frac{W_{AirCu_Cu} - W_{S_Cu}}{W_{S_Cu}} \quad (135)$$

This is the percentage difference in price of the Air / CU conductor compared to a segmented copper conductor. If compared to enameled copper, an added term for the cost of the enameling is used and the cost delta is:

$$CD = 100 x \frac{W_{AirCu_Cu} - W_{S_Cu} \cdot \left(1 + \frac{ECI\%}{100}\right)}{W_{S_Cu} \cdot \left(1 + \frac{ECI\%}{100}\right)} \quad (136)$$

For the AL / CU designs the formula is almost the same, except the cost ratio of copper to aluminum must be used as well. This is incorporated into the cost delta equation for non-enameled conductors as so:

$$CD = 100 x \frac{W_{AlCu_Cu} + \frac{W_{AlCu_Al}}{\$/Cu/\$/Al} - W_{S_Cu}}{W_{S_Cu}} \quad (137)$$

In the case where the segmented copper wires are enameled this becomes:

$$CD = 100 x \frac{W_{AlCu_Cu} + \frac{W_{AlCu_Al}}{\$/Cu/\$/Al} - W_{S_Cu} \cdot \left(1 + \frac{ECI\%}{100}\right)}{W_{S_Cu} \cdot \left(1 + \frac{ECI\%}{100}\right)} \quad (138)$$

The resulting tables for Air / CU and AL / CU conductors having an equal AC resistance as the segmented non-enameled and enameled copper conductors are shown on TABLE 6-9 through TABLE 6-36:

TABLE 6-9: Conductor data of equal R_{ac} conductors ($k_s=0.8$, 90°C , 60 Hz)

ID	Area			Resistance			Solid Radius		Cost Ratio	
	Nominal	True		Total	True		Inner	Outer		
		AL or Air	CU		AL or Air	CU			mm	
		mm ²		ohm/km: DC @ 20C		mm		\$CU/\$AL		
Air Core										
1	800	821.2	0.0	821.2	2.100E-02	Inf	2.100E-02	0.00	16.17	Never
2	1000	1057.7	13.8	1044.0	1.652E-02	Inf	1.652E-02	2.09	18.35	Never
3	1200	1252.6	53.6	1198.9	1.438E-02	Inf	1.438E-02	4.13	19.97	Never
4	1400	1482.9	117.0	1365.9	1.262E-02	Inf	1.262E-02	6.10	21.73	Never
5	1600	1697.6	187.8	1509.8	1.142E-02	Inf	1.142E-02	7.73	23.25	Always
6	2000	2123.0	353.1	1770.0	9.741E-03	Inf	9.741E-03	10.60	26.00	Always
7	2500	2606.5	570.9	2035.7	8.470E-03	Inf	8.470E-03	13.48	28.80	Always
8	3000	3071.3	802.6	2268.8	7.599E-03	Inf	7.599E-03	15.98	31.27	Always
AL Core										
1	800	821.2	0.0	821.2	2.100E-02	Inf	2.100E-02	0.00	16.17	Never
2	1000	1057.9	28.6	1029.2	1.647E-02	9.869E-01	1.675E-02	3.02	18.35	Never
3	1200	1254.7	101.3	1153.4	1.419E-02	2.791E-01	1.495E-02	5.68	19.99	Never
4	1400	1492.3	203.7	1288.6	1.220E-02	1.388E-01	1.338E-02	8.05	21.80	1.29
5	1600	1720.1	308.6	1411.5	1.078E-02	9.159E-02	1.222E-02	9.91	23.40	0.82
6	2000	2190.2	534.2	1656.0	8.699E-03	5.291E-02	1.041E-02	13.04	26.40	0.62
7	2500	2747.4	811.3	1936.1	7.092E-03	3.484E-02	8.905E-03	16.07	29.57	0.53
8	3000	3292.9	1093.3	2199.6	6.015E-03	2.585E-02	7.838E-03	18.66	32.38	0.49

Bi-media not optimal Lowest cost: segmented Lowest cost: bi-media

TABLE 6-10: Conductor data of equal R_{ac} conductors ($k_s=0.8$, 105°C , 60 Hz)

ID	Area			Resistance			Solid Radius		Cost Ratio	
	Nominal	True		Total	True		Inner	Outer		
		AL or Air	CU		AL or Air	CU				
	mm ²			ohm/km: DC @ 20C			mm		\$CU/\$AL	
Air Core										
1	800	817.7	0.0	817.7	2.108E-02	Inf	2.108E-02	0.00	16.13	Never
2	1000	1052.2	6.4	1045.8	1.649E-02	Inf	1.649E-02	1.42	18.30	Never
3	1200	1247.2	41.5	1205.7	1.430E-02	Inf	1.430E-02	3.64	19.93	Never
4	1400	1479.0	100.9	1378.1	1.251E-02	Inf	1.251E-02	5.67	21.70	Never
5	1600	1696.5	169.1	1527.4	1.129E-02	Inf	1.129E-02	7.34	23.24	Never
6	2000	2126.9	330.3	1796.6	9.596E-03	Inf	9.596E-03	10.25	26.02	Always
7	2500	2619.4	546.5	2072.9	8.317E-03	Inf	8.317E-03	13.19	28.88	Always
8	3000	3076.3	769.4	2306.9	7.474E-03	Inf	7.474E-03	15.65	31.29	Always
AL Core										
1	800	817.7	0.0	817.7	2.108E-02	Inf	2.108E-02	0.00	16.13	Never
2	1000	1052.2	13.8	1038.5	1.647E-02	2.055E+00	1.660E-02	2.09	18.30	Never
3	1200	1248.5	80.4	1168.1	1.417E-02	3.514E-01	1.476E-02	5.06	19.94	Never
4	1400	1485.8	179.4	1306.4	1.218E-02	1.575E-01	1.320E-02	7.56	21.75	1.80
5	1600	1714.4	283.0	1431.4	1.075E-02	9.986E-02	1.205E-02	9.49	23.36	0.91
6	2000	2185.2	507.1	1678.1	8.675E-03	5.573E-02	1.027E-02	12.71	26.37	0.65
7	2500	2748.7	785.4	1963.3	7.059E-03	3.599E-02	8.782E-03	15.81	29.58	0.55
8	3000	3283.7	1059.2	2224.6	6.006E-03	2.669E-02	7.750E-03	18.36	32.33	0.49

Bi-media not optimal Lowest cost: segmented Lowest cost: bi-media

TABLE 6-11: Conductor data of equal R_{ac} conductors ($k_s=0.8$, 90°C , 50 Hz)

ID	Area			Resistance			Solid Radius		Cost Ratio	
	Nominal	True		True			Inner	Outer		
		Total	AL or Air	CU	Total	AL or Air			CU	mm
Air Core										
1	800	808.8	0.0	808.8	2.132E-02	Inf	2.132E-02	0.00	16.05	Never
2	1000	1035.9	0.0	1035.9	1.664E-02	Inf	1.664E-02	0.00	18.16	Never
3	1200	1228.7	10.3	1218.4	1.415E-02	Inf	1.415E-02	1.81	19.78	Never
4	1400	1462.9	54.9	1408.0	1.225E-02	Inf	1.225E-02	4.18	21.58	Never
5	1600	1687.9	113.3	1574.6	1.095E-02	Inf	1.095E-02	6.00	23.18	Never
6	2000	2131.9	259.4	1872.5	9.208E-03	Inf	9.208E-03	9.09	26.05	Always
7	2500	2648.1	466.5	2181.6	7.903E-03	Inf	7.903E-03	12.19	29.03	Always
8	3000	3127.9	685.1	2442.9	7.058E-03	Inf	7.058E-03	14.77	31.55	Always
AL Core										
1	800	808.8	0.0	808.8	2.132E-02	Inf	2.132E-02	0.00	16.05	Never
2	1000	1035.9	0.0	1035.9	1.664E-02	Inf	1.664E-02	0.00	18.16	Never
3	1200	1228.8	22.0	1206.9	1.413E-02	1.287E+00	1.429E-02	2.64	19.78	Never
4	1400	1464.8	105.1	1359.6	1.211E-02	2.689E-01	1.268E-02	5.78	21.59	Never
5	1600	1695.5	202.0	1493.4	1.067E-02	1.399E-01	1.155E-02	8.02	23.23	1.89
6	2000	2166.6	418.7	1748.0	8.606E-03	6.751E-02	9.863E-03	11.54	26.26	0.75
7	2500	2742.4	697.0	2045.4	6.979E-03	4.055E-02	8.429E-03	14.90	29.55	0.60
8	3000	3296.9	973.5	2323.4	5.910E-03	2.903E-02	7.421E-03	17.60	32.40	0.54

Bi-media not optimal

Lowest cost: segmented

Lowest cost: bi-media

TABLE 6-12: Conductor data of equal R_{ac} conductors ($k_s=0.8$, 105°C , 50 Hz)

ID	Area			Resistance			Solid Radius		Cost Ratio	
	Nominal	True		True			Inner	Outer		
		Total	AL or Air	CU	Total	AL or Air			CU	mm
Air Core										
1	800	806.4	0.0	806.4	2.138E-02	Inf	2.138E-02	0.00	16.02	Never
2	1000	1031.2	0.0	1031.2	1.672E-02	Inf	1.672E-02	0.00	18.12	Never
3	1200	1222.2	2.8	1219.4	1.414E-02	Inf	1.414E-02	0.95	19.72	Never
4	1400	1456.3	41.2	1415.2	1.218E-02	Inf	1.218E-02	3.62	21.53	Never
5	1600	1682.5	95.4	1587.2	1.086E-02	Inf	1.086E-02	5.51	23.14	Never
6	2000	2131.5	235.8	1895.7	9.095E-03	Inf	9.095E-03	8.66	26.05	Always
7	2500	2654.4	438.6	2215.8	7.781E-03	Inf	7.781E-03	11.82	29.07	Always
8	3000	3143.3	655.7	2487.6	6.931E-03	Inf	6.931E-03	14.45	31.63	Always
AL Core										
1	800	806.4	0.0	806.4	2.138E-02	Inf	2.138E-02	0.00	16.02	Never
2	1000	1031.2	0.0	1031.2	1.672E-02	Inf	1.672E-02	0.00	18.12	Never
3	1200	1222.2	6.3	1215.9	1.414E-02	4.458E+00	1.418E-02	1.42	19.72	Never
4	1400	1457.4	81.0	1376.4	1.209E-02	3.491E-01	1.253E-02	5.08	21.54	Never
5	1600	1687.8	174.0	1513.8	1.064E-02	1.624E-01	1.139E-02	7.44	23.18	4.38
6	2000	2159.7	387.4	1772.3	8.584E-03	7.296E-02	9.728E-03	11.11	26.22	0.82
7	2500	2737.1	664.5	2072.7	6.958E-03	4.254E-02	8.318E-03	14.54	29.52	0.62
8	3000	3298.5	942.5	2356.1	5.882E-03	2.999E-02	7.318E-03	17.32	32.40	0.55

Bi-media not optimal Lowest cost: segmented Lowest cost: bi-media

TABLE 6-13: Conductor data of equal R_{ac} conductors ($k_s=0.62$, 90°C , 60 Hz)

ID	Area			Resistance			Solid Radius		Cost Ratio	
	Nominal	True		True			Inner	Outer		
		Total	AL or Air	CU	Total	AL or Air			CU	
	mm ²									\$CU/\$AL
Air Core										
1	800	855.7	0.0	855.7	2.015E-02	Inf	2.015E-02	0.00	16.50	Never
2	1000	1127.9	26.3	1101.6	1.565E-02	Inf	1.565E-02	2.89	18.95	Never
3	1200	1360.4	81.5	1279.0	1.348E-02	Inf	1.348E-02	5.09	20.81	Never
4	1400	1644.5	169.4	1475.1	1.169E-02	Inf	1.169E-02	7.34	22.88	Never
5	1600	1920.4	270.7	1649.7	1.045E-02	Inf	1.045E-02	9.28	24.72	Never
6	2000	2472.7	508.0	1964.8	8.775E-03	Inf	8.775E-03	12.72	28.06	Never
7	2500	3119.9	827.8	2292.1	7.522E-03	Inf	7.522E-03	16.23	31.51	Always
8	3000	3729.8	1159.1	2570.8	6.707E-03	Inf	6.707E-03	19.21	34.46	Always
AL Core										
1	800	855.7	0.0	855.7	2.015E-02	Inf	2.015E-02	0.00	16.50	Never
2	1000	1128.4	52.7	1075.8	1.556E-02	5.368E-01	1.603E-02	4.09	18.95	Never
3	1200	1365.2	147.6	1217.6	1.319E-02	1.915E-01	1.416E-02	6.86	20.85	Never
4	1400	1663.1	282.0	1381.2	1.110E-02	1.002E-01	1.248E-02	9.47	23.01	Never
5	1600	1963.4	424.3	1539.1	9.590E-03	6.662E-02	1.120E-02	11.62	25.00	Never
6	2000	2591.6	732.8	1858.8	7.477E-03	3.857E-02	9.276E-03	15.27	28.72	3.89
7	2500	3350.0	1123.5	2226.5	5.921E-03	2.516E-02	7.744E-03	18.91	32.66	2.02
8	3000	4065.3	1514.9	2550.4	4.962E-03	1.866E-02	6.760E-03	21.96	35.97	1.42

Bi-media not optimal Lowest cost: segmented Lowest cost: bi-media

TABLE 6-14: Conductor data of equal R_{ac} conductors ($k_s=0.62$, 105°C , 60 Hz)

ID	Area			Resistance			Solid Radius		Cost Ratio	
	Nominal	True		True			Inner	Outer		
		Total	AL or Air	CU	Total	AL or Air			CU	
	mm ²									
Air Core										
1	800	848.9	0.0	848.9	2.031E-02	Inf	2.031E-02	0.00	16.44	Never
2	1000	1116.4	16.0	1100.4	1.567E-02	Inf	1.567E-02	2.26	18.85	Never
3	1200	1347.0	65.1	1281.9	1.345E-02	Inf	1.345E-02	4.55	20.71	Never
4	1400	1630.2	147.2	1483.0	1.163E-02	Inf	1.163E-02	6.84	22.78	Never
5	1600	1906.6	244.0	1662.7	1.037E-02	Inf	1.037E-02	8.81	24.64	Never
6	2000	2467.0	476.6	1990.4	8.662E-03	Inf	8.662E-03	12.32	28.02	Never
7	2500	3117.7	790.4	2327.2	7.409E-03	Inf	7.409E-03	15.86	31.50	Always
8	3000	3737.3	1120.6	2616.6	6.589E-03	Inf	6.589E-03	18.89	34.49	Always
AL Core										
1	800	848.9	0.0	848.9	2.031E-02	Inf	2.031E-02	0.00	16.44	Never
2	1000	1116.6	33.1	1083.5	1.562E-02	8.538E-01	1.591E-02	3.25	18.85	Never
3	1200	1350.0	121.2	1228.8	1.324E-02	2.332E-01	1.403E-02	6.21	20.73	Never
4	1400	1644.0	250.6	1393.4	1.115E-02	1.128E-01	1.237E-02	8.93	22.88	Never
5	1600	1941.2	389.8	1551.4	9.636E-03	7.252E-02	1.111E-02	11.14	24.86	Never
6	2000	2572.2	697.2	1875.0	7.495E-03	4.054E-02	9.195E-03	14.90	28.61	5.18
7	2500	3332.4	1084.6	2247.8	5.926E-03	2.606E-02	7.670E-03	18.58	32.57	2.23
8	3000	4060.1	1476.8	2583.2	4.949E-03	1.914E-02	6.674E-03	21.68	35.95	1.54

Bi-media not optimal Lowest cost: segmented Lowest cost: bi-media

TABLE 6-15: Conductor data of equal R_{ac} conductors ($k_s=0.62$, 90°C , 50 Hz)

ID	Area			Resistance			Solid Radius		Cost Ratio	
	Nominal	True		True			Inner	Outer		
		Total	AL or Air	CU	Total	AL or Air			CU	
	mm ²			ohm/km: DC @ 20C			mm		\$CU/\$AL	
Air Core										
1	800	831.9	0.0	831.9	2.073E-02	Inf	2.073E-02	0.00	16.27	Never
2	1000	1083.9	0.0	1083.9	1.591E-02	Inf	1.591E-02	0.00	18.57	Never
3	1200	1306.0	22.7	1283.3	1.344E-02	Inf	1.344E-02	2.69	20.39	Never
4	1400	1583.9	84.7	1499.2	1.150E-02	Inf	1.150E-02	5.19	22.45	Never
5	1600	1859.3	165.4	1693.9	1.018E-02	Inf	1.018E-02	7.26	24.33	Never
6	2000	2427.3	373.9	2053.5	8.396E-03	Inf	8.396E-03	10.91	27.80	Never
7	2500	3099.4	671.5	2427.9	7.101E-03	Inf	7.101E-03	14.62	31.41	Never
8	3000	3744.0	993.4	2750.6	6.268E-03	Inf	6.268E-03	17.78	34.52	Always
AL Core										
1	800	831.9	0.0	831.9	2.073E-02	Inf	2.073E-02	0.00	16.27	Never
2	1000	1083.9	0.0	1083.9	1.591E-02	Inf	1.591E-02	0.00	18.57	Never
3	1200	1306.4	46.5	1259.9	1.338E-02	6.080E-01	1.368E-02	3.85	20.39	Never
4	1400	1588.2	155.8	1432.4	1.129E-02	1.814E-01	1.204E-02	7.04	22.48	Never
5	1600	1874.6	282.5	1592.2	9.771E-03	1.001E-01	1.083E-02	9.48	24.43	Never
6	2000	2492.8	575.1	1917.7	7.600E-03	4.915E-02	8.991E-03	13.53	28.17	Never
7	2500	3263.7	956.7	2306.9	5.965E-03	2.954E-02	7.474E-03	17.45	32.23	3.30
8	3000	4020.1	1348.2	2671.9	4.934E-03	2.096E-02	6.453E-03	20.72	35.77	2.02

Bi-media not optimal Lowest cost: segmented Lowest cost: bi-media

TABLE 6-16: Conductor data of equal R_{ac} conductors ($k_s=0.62$, 105°C , 50 Hz)

ID	Area			Resistance			Solid Radius		Cost Ratio	
	True		CU	True		CU	Inner	Outer		
	Total	AL or Air		Total	AL or Air					
	mm ²			ohm/km: DC @ 20C			mm		\$CU/\$AL	
Air Core										
1	800	827.3	0.0	827.3	2.084E-02	Inf	2.084E-02	0.00	16.23	Never
2	1000	1074.6	0.0	1074.6	1.605E-02	Inf	1.605E-02	0.00	18.49	Never
3	1200	1292.9	11.8	1281.0	1.346E-02	Inf	1.346E-02	1.94	20.29	Never
4	1400	1568.1	66.2	1501.8	1.148E-02	Inf	1.148E-02	4.59	22.34	Never
5	1600	1842.3	141.0	1701.3	1.013E-02	Inf	1.013E-02	6.70	24.22	Never
6	2000	2411.3	340.0	2071.3	8.324E-03	Inf	8.324E-03	10.40	27.71	Never
7	2500	3090.0	631.0	2459.0	7.011E-03	Inf	7.011E-03	14.17	31.36	Never
8	3000	3741.3	948.5	2792.7	6.174E-03	Inf	6.174E-03	17.38	34.51	Always
AL Core										
1	800	827.3	0.0	827.3	2.084E-02	Inf	2.084E-02	0.00	16.23	Never
2	1000	1074.6	0.0	1074.6	1.605E-02	Inf	1.605E-02	0.00	18.49	Never
3	1200	1293.0	25.1	1267.9	1.344E-02	1.126E+00	1.360E-02	2.83	20.29	Never
4	1400	1570.7	125.2	1445.5	1.133E-02	2.257E-01	1.193E-02	6.31	22.36	Never
5	1600	1853.2	246.5	1606.7	9.812E-03	1.147E-01	1.073E-02	8.86	24.29	Never
6	2000	2465.1	532.6	1932.5	7.638E-03	5.307E-02	8.922E-03	13.02	28.01	Never
7	2500	3236.7	911.4	2325.2	5.984E-03	3.101E-02	7.415E-03	17.03	32.10	3.97
8	3000	3998.9	1301.5	2697.4	4.938E-03	2.172E-02	6.392E-03	20.35	35.68	2.23

Bi-media not optimal Lowest cost: segmented Lowest cost: bi-media

TABLE 6-17: Conductor data of equal R_{ac} conductors ($k_s=0.435$, 90°C , 60 Hz)

ID	Area			Resistance			Solid Radius		Cost Ratio	
	Nominal	True		True			Inner	Outer		
		Total	AL or Air	CU	Total	AL or Air			CU	mm
Air Core										
1	800	885.8	0.0	885.8	1.946E-02	Inf	1.946E-02	0.00	16.79	Never
2	1000	1193.0	39.9	1153.1	1.495E-02	Inf	1.495E-02	3.56	19.49	Never
3	1200	1466.3	112.0	1354.3	1.273E-02	Inf	1.273E-02	5.97	21.60	Never
4	1400	1814.5	230.2	1584.3	1.088E-02	Inf	1.088E-02	8.56	24.03	Never
5	1600	2167.8	372.0	1795.7	9.601E-03	Inf	9.601E-03	10.88	26.27	Never
6	2000	2919.2	724.7	2194.5	7.856E-03	Inf	7.856E-03	15.19	30.48	Never
7	2500	3847.6	1225.7	2621.9	6.576E-03	Inf	6.576E-03	19.75	35.00	Never
8	3000	4744.7	1756.5	2988.3	5.770E-03	Inf	5.770E-03	23.65	38.86	Never
AL Core										
1	800	885.8	0.0	885.8	1.946E-02	Inf	1.946E-02	0.00	16.79	Never
2	1000	1194.2	77.3	1116.9	1.481E-02	3.658E-01	1.544E-02	4.96	19.50	Never
3	1200	1474.9	195.9	1279.0	1.233E-02	1.443E-01	1.348E-02	7.90	21.67	Never
4	1400	1846.9	368.5	1478.3	1.012E-02	7.669E-02	1.166E-02	10.83	24.25	Never
5	1600	2240.9	559.0	1681.9	8.523E-03	5.056E-02	1.025E-02	13.34	26.71	Never
6	2000	3114.0	999.5	2114.5	6.329E-03	2.828E-02	8.154E-03	17.84	31.48	Never
7	2500	4202.7	1592.8	2609.9	4.814E-03	1.774E-02	6.606E-03	22.52	36.58	Never
8	3000	5241.1	2210.8	3030.2	3.937E-03	1.278E-02	5.690E-03	26.53	40.85	Never

Bi-media not optimal Lowest cost: segmented Lowest cost: bi-media

TABLE 6-18: Conductor data of equal R_{ac} conductors ($k_s=0.435$, 105°C , 60 Hz)

ID	Area			Resistance			Solid Radius		Cost Ratio	
	Nominal	True		True			Inner	Outer		
		Total	AL or Air	CU	Total	AL or Air			CU	mm
	Air Core									
1	800	875.8	0.0	875.8	1.969E-02	Inf	1.969E-02	0.00	16.70	Never
2	1000	1175.2	26.6	1148.6	1.501E-02	Inf	1.501E-02	2.91	19.34	Never
3	1200	1443.2	90.7	1352.5	1.275E-02	Inf	1.275E-02	5.37	21.43	Never
4	1400	1785.9	200.0	1586.0	1.087E-02	Inf	1.087E-02	7.98	23.84	Never
5	1600	2135.0	333.6	1801.4	9.571E-03	Inf	9.571E-03	10.31	26.07	Never
6	2000	2882.1	672.4	2209.7	7.802E-03	Inf	7.802E-03	14.63	30.29	Never
7	2500	3812.2	1162.2	2650.0	6.506E-03	Inf	6.506E-03	19.23	34.84	Never
8	3000	4717.6	1688.0	3029.5	5.691E-03	Inf	5.691E-03	23.18	38.75	Never
	AL Core									
1	800	875.8	0.0	875.8	1.969E-02	Inf	1.969E-02	0.00	16.70	Never
2	1000	1175.7	53.3	1122.4	1.493E-02	5.303E-01	1.536E-02	4.12	19.35	Never
3	1200	1448.8	163.2	1285.5	1.245E-02	1.732E-01	1.341E-02	7.21	21.47	Never
4	1400	1810.1	327.7	1482.4	1.025E-02	8.624E-02	1.163E-02	10.21	24.00	Never
5	1600	2194.2	511.5	1682.7	8.643E-03	5.526E-02	1.025E-02	12.76	26.43	Never
6	2000	3055.7	941.2	2114.5	6.413E-03	3.003E-02	8.154E-03	17.31	31.19	Never
7	2500	4147.7	1525.7	2622.0	4.853E-03	1.853E-02	6.575E-03	22.04	36.34	Never
8	3000	5199.1	2138.9	3060.2	3.950E-03	1.321E-02	5.634E-03	26.09	40.68	Never

Bi-media not optimal Lowest cost: segmented Lowest cost: bi-media

TABLE 6-19: Conductor data of equal R_{ac} conductors ($k_s=0.435$, 90°C , 50 Hz)

ID	Area			Resistance			Solid Radius		Cost Ratio	
	Nominal	True		True			Inner	Outer		
		Total	AL or Air	CU	Total	AL or Air			CU	mm
	Air Core									
1	800	851.2	0.0	851.2	2.026E-02	Inf	2.026E-02	0.00	16.46	Never
2	1000	1126.3	0.0	1126.3	1.531E-02	Inf	1.531E-02	0.00	18.93	Never
3	1200	1377.1	36.3	1340.8	1.286E-02	Inf	1.286E-02	3.40	20.94	Never
4	1400	1701.4	117.2	1584.3	1.088E-02	Inf	1.088E-02	6.11	23.27	Never
5	1600	2035.4	224.8	1810.7	9.522E-03	Inf	9.522E-03	8.46	25.45	Never
6	2000	2762.7	516.7	2246.0	7.676E-03	Inf	7.676E-03	12.82	29.66	Never
7	2500	3689.5	965.1	2724.4	6.328E-03	Inf	6.328E-03	17.53	34.27	Never
8	3000	4617.2	1470.9	3146.4	5.480E-03	Inf	5.480E-03	21.64	38.34	Never
	AL Core									
1	800	851.2	0.0	851.2	2.026E-02	Inf	2.026E-02	0.00	16.46	Never
2	1000	1126.3	0.0	1126.3	1.531E-02	Inf	1.531E-02	0.00	18.93	Never
3	1200	1377.9	71.8	1306.1	1.277E-02	3.934E-01	1.320E-02	4.78	20.94	Never
4	1400	1709.5	208.2	1501.3	1.059E-02	1.358E-01	1.148E-02	8.14	23.33	Never
5	1600	2062.3	369.4	1692.8	8.988E-03	7.650E-02	1.019E-02	10.84	25.62	Never
6	2000	2873.5	761.6	2111.9	6.692E-03	3.711E-02	8.164E-03	15.57	30.24	Never
7	2500	3956.0	1314.3	2641.7	5.007E-03	2.151E-02	6.527E-03	20.45	35.49	Never
8	3000	5043.4	1911.4	3131.9	4.012E-03	1.479E-02	5.505E-03	24.67	40.07	Never

Bi-media not optimal
Lowest cost: segmented
Lowest cost: bi-media

TABLE 6-20: Conductor data of equal R_{ac} conductors ($k_s=0.435$, 105°C , 50 Hz)

ID	Area			Resistance			Solid Radius		Cost Ratio	
	Nominal	True		True		Inner	Outer			
		Total	AL or Air	CU	Total			AL or Air	CU	
	mm ²			ohm/km; DC @ 20C			mm		\$CU/\$AL	
Air Core										
1	800	844.6	0.0	844.6	2.041E-02	Inf	2.041E-02	0.00	16.40	Never
2	1000	1112.4	0.0	1112.4	1.550E-02	Inf	1.550E-02	0.00	18.82	Never
3	1200	1356.9	22.1	1334.8	1.292E-02	Inf	1.292E-02	2.65	20.78	Never
4	1400	1674.7	93.3	1581.5	1.090E-02	Inf	1.090E-02	5.45	23.09	Never
5	1600	2003.1	192.0	1811.2	9.519E-03	Inf	9.519E-03	7.82	25.25	Never
6	2000	2721.9	467.2	2254.7	7.647E-03	Inf	7.647E-03	12.19	29.44	Never
7	2500	3644.7	899.5	2745.2	6.281E-03	Inf	6.281E-03	16.92	34.06	Never
8	3000	4574.7	1394.6	3180.0	5.422E-03	Inf	5.422E-03	21.07	38.16	Never
AL Core										
1	800	844.6	0.0	844.6	2.041E-02	Inf	2.041E-02	0.00	16.40	Never
2	1000	1112.4	0.0	1112.4	1.550E-02	Inf	1.550E-02	0.00	18.82	Never
3	1200	1357.2	45.4	1311.8	1.287E-02	6.227E-01	1.314E-02	3.80	20.79	Never
4	1400	1679.7	170.6	1509.2	1.069E-02	1.657E-01	1.142E-02	7.37	23.12	Never
5	1600	2022.5	323.5	1699.0	9.092E-03	8.736E-02	1.015E-02	10.15	25.37	Never
6	2000	2813.6	701.9	2111.8	6.788E-03	4.027E-02	8.164E-03	14.95	29.93	Never
7	2500	3885.4	1242.3	2643.1	5.070E-03	2.275E-02	6.523E-03	19.89	35.17	Never
8	3000	4977.3	1830.8	3146.5	4.044E-03	1.544E-02	5.479E-03	24.14	39.80	Never

Bi-media not optimal
Lowest cost: segmented
Lowest cost: bi-media

TABLE 6-21: Conductor data of equal R_{ac} conductors ($k_s=0.35$, 90°C , 60 Hz)

ID	Area			Resistance			Solid Radius		
	Nominal	True		True			Inner	Outer	
		Total	AL or Air	CU	Total	AL or Air			CU
mm ² ohm/km; DC @ 20C									
Air Core									
1	800	897.0	0.0	897.0	1.922E-02	Inf	1.922E-02	0.00	16.90
2	1000	1218.1	45.5	1172.6	1.470E-02	Inf	1.470E-02	3.81	19.69
3	1200	1508.6	125.0	1383.7	1.246E-02	Inf	1.246E-02	6.31	21.91
4	1400	1886.0	257.4	1628.6	1.059E-02	Inf	1.059E-02	9.05	24.50
5	1600	2277.1	419.5	1857.6	9.281E-03	Inf	9.281E-03	11.56	26.92
6	2000	3136.2	836.4	2299.9	7.497E-03	Inf	7.497E-03	16.32	31.60
7	2500	4243.6	1455.3	2788.3	6.183E-03	Inf	6.183E-03	21.52	36.75
8	3000	5362.7	2141.8	3220.8	5.353E-03	Inf	5.353E-03	26.11	41.32
AL Core									
1	800	897.0	0.0	897.0	1.922E-02	Inf	1.922E-02	0.00	16.90
2	1000	1219.6	87.2	1132.4	1.454E-02	3.241E-01	1.523E-02	5.27	19.70
3	1200	1519.3	215.9	1303.4	1.201E-02	1.309E-01	1.323E-02	8.29	21.99
4	1400	1925.3	406.0	1519.3	9.757E-03	6.961E-02	1.135E-02	11.37	24.76
5	1600	2365.7	620.4	1745.3	8.118E-03	4.556E-02	9.879E-03	14.05	27.44
6	2000	3369.2	1133.7	2235.5	5.890E-03	2.493E-02	7.713E-03	19.00	32.75
7	2500	4662.8	1860.5	2802.3	4.379E-03	1.519E-02	6.153E-03	24.34	38.53
8	3000	5949.9	2659.3	3290.5	3.510E-03	1.063E-02	5.240E-03	29.10	43.52

Bi-media not optimal Lowest cost: segmented Lowest cost: bi-media

TABLE 6-22: Conductor data of equal R_{ac} conductors ($k_s=0.35$, 105°C , 60 Hz)

ID	Area			Resistance			Solid Radius		
	Nominal	True		True			Inner	Outer	
		Total	AL or Air	CU	Total	AL or Air			CU
		mm ²		ohm/km: DC @ 20C			mm		
Air Core									
1	800	885.7	0.0	885.7	1.947E-02	Inf	1.947E-02	0.00	16.79
2	1000	1197.6	31.0	1166.6	1.478E-02	Inf	1.478E-02	3.14	19.53
3	1200	1481.2	101.5	1379.7	1.250E-02	Inf	1.250E-02	5.68	21.71
4	1400	1850.4	223.1	1627.2	1.060E-02	Inf	1.060E-02	8.43	24.27
5	1600	2234.1	374.8	1859.3	9.273E-03	Inf	9.273E-03	10.92	26.67
6	2000	3081.2	771.9	2309.3	7.466E-03	Inf	7.466E-03	15.68	31.32
7	2500	4181.4	1371.7	2809.6	6.136E-03	Inf	6.136E-03	20.90	36.48
8	3000	5300.9	2045.9	3255.1	5.297E-03	Inf	5.297E-03	25.52	41.08
AL Core									
1	800	885.7	0.0	885.7	1.947E-02	Inf	1.947E-02	0.00	16.79
2	1000	1198.3	61.5	1136.8	1.468E-02	4.596E-01	1.517E-02	4.42	19.53
3	1200	1488.1	180.5	1307.7	1.216E-02	1.566E-01	1.319E-02	7.58	21.76
4	1400	1879.9	360.6	1519.2	9.913E-03	7.837E-02	1.135E-02	10.71	24.46
5	1600	2305.9	566.0	1740.0	8.268E-03	4.994E-02	9.909E-03	13.42	27.09
6	2000	3289.5	1062.2	2227.4	5.996E-03	2.661E-02	7.741E-03	18.39	32.36
7	2500	4578.2	1770.7	2807.5	4.435E-03	1.596E-02	6.141E-03	23.74	38.17
8	3000	5870.0	2555.1	3314.8	3.538E-03	1.106E-02	5.201E-03	28.52	43.23

Bi-media not optimal Lowest cost: segmented Lowest cost: bi-media

TABLE 6-23: Conductor data of equal R_{ac} conductors ($k_s=0.35$, 90°C , 50 Hz)

ID	Area			Resistance			Solid Radius		
	Nominal	True		Total	AL or Air	CU	Inner		Outer
		AL or Air	CU				AL or Air	CU	
Air Core									
1	800	858.1	0.0	858.1	2.009E-02	Inf	2.009E-02	0.00	16.53
2	1000	1142.1	0.4	1141.8	1.510E-02	Inf	1.510E-02	0.33	19.07
3	1200	1404.3	41.9	1362.4	1.266E-02	Inf	1.266E-02	3.65	21.14
4	1400	1748.1	130.9	1617.2	1.066E-02	Inf	1.066E-02	6.46	23.59
5	1600	2108.2	250.8	1857.5	9.282E-03	Inf	9.282E-03	8.93	25.91
6	2000	2913.8	584.8	2328.9	7.403E-03	Inf	7.403E-03	13.64	30.46
7	2500	3981.9	1119.3	2862.6	6.023E-03	Inf	6.023E-03	18.88	35.60
8	3000	5092.4	1746.3	3346.1	5.153E-03	Inf	5.153E-03	23.58	40.26
AL Core									
1	800	858.1	0.0	858.1	2.009E-02	Inf	2.009E-02	0.00	16.53
2	1000	1142.1	0.8	1141.3	1.510E-02	3.457E+01	1.511E-02	0.51	19.07
3	1200	1405.4	82.1	1323.3	1.255E-02	3.442E-01	1.303E-02	5.11	21.15
4	1400	1758.1	229.8	1528.3	1.033E-02	1.230E-01	1.128E-02	8.55	23.66
5	1600	2140.9	406.5	1734.5	8.697E-03	6.953E-02	9.940E-03	11.38	26.11
6	2000	3047.8	848.3	2199.5	6.346E-03	3.332E-02	7.839E-03	16.43	31.15
7	2500	4299.7	1498.1	2801.7	4.640E-03	1.887E-02	6.154E-03	21.84	37.00
8	3000	5595.4	2232.6	3362.8	3.649E-03	1.266E-02	5.127E-03	26.66	42.20

Bi-media not optimal
Lowest cost: segmented
Lowest cost: bi-media

TABLE 6-24: Conductor data of equal R_{ac} conductors ($k_s=0.35$, 105°C , 50 Hz)

ID	Area			Resistance			Solid Radius		
	Nominal	True		Total	True		Inner	Outer	
		AL or Air	CU		AL or Air	CU			
	mm ²		ohm/km: DC @ 20C		mm				
Air Core									
1	800	850.8	0.0	850.8	2.027E-02	Inf	2.027E-02	0.00	16.46
2	1000	1126.4	0.0	1126.4	1.531E-02	Inf	1.531E-02	0.00	18.94
3	1200	1381.2	26.5	1354.8	1.273E-02	Inf	1.273E-02	2.90	20.97
4	1400	1716.7	104.6	1612.0	1.070E-02	Inf	1.070E-02	5.77	23.38
5	1600	2068.7	214.0	1854.7	9.296E-03	Inf	9.296E-03	8.25	25.66
6	2000	2859.1	526.7	2332.4	7.392E-03	Inf	7.392E-03	12.95	30.17
7	2500	3913.7	1037.6	2876.1	5.995E-03	Inf	5.995E-03	18.17	35.30
8	3000	5017.7	1646.1	3371.6	5.114E-03	Inf	5.114E-03	22.89	39.97
AL Core									
1	800	850.8	0.0	850.8	2.027E-02	Inf	2.027E-02	0.00	16.46
2	1000	1126.4	0.0	1126.4	1.531E-02	Inf	1.531E-02	0.00	18.94
3	1200	1381.7	53.7	1328.0	1.267E-02	5.264E-01	1.298E-02	4.13	20.97
4	1400	1722.9	189.1	1533.8	1.045E-02	1.495E-01	1.124E-02	7.76	23.42
5	1600	2092.4	355.9	1736.4	8.826E-03	7.941E-02	9.929E-03	10.64	25.81
6	2000	2970.3	779.0	2191.3	6.466E-03	3.629E-02	7.868E-03	15.75	30.75
7	2500	4201.8	1408.4	2793.4	4.720E-03	2.007E-02	6.172E-03	21.17	36.57
8	3000	5493.9	2124.8	3369.1	3.696E-03	1.330E-02	5.117E-03	26.01	41.82

Bi-media not optimal
Lowest cost: segmented
Lowest cost: bi-media

TABLE 6-25: Cost effectiveness ($k_s=0.35$, 90°C , 60 Hz): enamel = 12–22%

ID	Cost Increase for Enamel											
	Area (Nominal)	12%	13%	14%	15%	16%	17%	18%	19%	20%	21%	22%
Air Core												
1	800	Never	Never	Never	Always							
2	1000	Never	Never	Never	Never	Never	Never	Never	Never	Never	Never	Always
3	1200	Never	Never	Never	Never	Never	Never	Never	Never	Never	Never	Always
4	1400	Never	Never	Never	Never	Never	Never	Never	Never	Never	Never	Always
5	1600	Never	Never	Never	Never	Never	Never	Never	Never	Never	Never	Always
6	2000	Never	Never	Never	Never	Never	Never	Never	Never	Never	Never	Always
7	2500	Never	Never	Never	Never	Never	Always	Always	Always	Always	Always	Always
8	3000	Never	Always									
AL Core												
1	800	Never	Never	Never	Always							
2	1000	Never	Never	Never	Never	6.70	1.92	1.12	0.79	0.61	0.50	0.42
3	1200	Never	Never	Never	6.75	3.10	2.01	1.49	1.18	0.98	0.83	0.73
4	1400	Never	Never	28.48	6.95	3.95	2.76	2.12	1.73	1.45	1.25	1.10
5	1600	Never	Never	Never	20.02	7.62	4.70	3.40	2.66	2.19	1.86	1.61
6	2000	Never	Never	Never	Never	Never	58.40	13.70	7.76	5.41	4.16	3.37
7	2500	Never	Never	Never	Never	Never	Never	24.11	11.90	7.90	5.91	4.72
8	3000	Never	Never	Never	57.33	18.80	11.25	8.02	6.23	5.10	4.31	3.74

Lowest cost: segmented █ █ Lowest cost: solid/stranded or bi-media

TABLE 6-26: Cost effectiveness ($k_s=0.35$, 90°C , 60 Hz): enamel = 23–33%

ID	Area (Nominal)	Cost Increase for Enamel										
		23%	24%	25%	26%	27%	28%	29%	30%	31%	32%	33%
Air Core												
1	800	Always	Always	Always	Always	Always	Always	Always	Always	Always	Always	Always
2	1000	Always	Always	Always	Always	Always	Always	Always	Always	Always	Always	Always
3	1200	Always	Always	Always	Always	Always	Always	Always	Always	Always	Always	Always
4	1400	Always	Always	Always	Always	Always	Always	Always	Always	Always	Always	Always
5	1600	Always	Always	Always	Always	Always	Always	Always	Always	Always	Always	Always
6	2000	Always	Always	Always	Always	Always	Always	Always	Always	Always	Always	Always
7	2500	Always	Always	Always	Always	Always	Always	Always	Always	Always	Always	Always
8	3000	Always	Always	Always	Always	Always	Always	Always	Always	Always	Always	Always
AL Core												
1	800	Always	Always	Always	Always	Always	Always	Always	Always	Always	Always	Always
2	1000	0.36	0.32	0.29	0.26	0.24	0.22	0.20	0.19	0.17	0.16	0.15
3	1200	0.65	0.58	0.53	0.48	0.44	0.41	0.39	0.36	0.34	0.32	0.30
4	1400	0.99	0.89	0.81	0.75	0.69	0.64	0.60	0.56	0.53	0.50	0.48
5	1600	1.43	1.28	1.16	1.06	0.97	0.90	0.84	0.79	0.74	0.70	0.66
6	2000	2.84	2.45	2.15	1.92	1.74	1.58	1.45	1.34	1.25	1.17	1.10
7	2500	3.93	3.37	2.95	2.62	2.36	2.14	1.96	1.81	1.68	1.57	1.47
8	3000	3.30	2.95	2.67	2.44	2.24	2.07	1.93	1.81	1.70	1.60	1.51

Lowest cost: segmented

Lowest cost: solid/stranded or bi-media

TABLE 6-27: Cost effectiveness ($k_s=0.35$, 90°C , 60 Hz): enamel = 34–44%

ID	Area (Nominal)	Cost Increase for Enamel												
		34%	35%	36%	37%	38%	39%	40%	41%	42%	43%	44%		
Air Core														
1	800	Always	Always	Always	Always	Always	Always	Always	Always	Always	Always	Always	Always	Always
2	1000	Always	Always	Always	Always	Always	Always	Always	Always	Always	Always	Always	Always	Always
3	1200	Always	Always	Always	Always	Always	Always	Always	Always	Always	Always	Always	Always	Always
4	1400	Always	Always	Always	Always	Always	Always	Always	Always	Always	Always	Always	Always	Always
5	1600	Always	Always	Always	Always	Always	Always	Always	Always	Always	Always	Always	Always	Always
6	2000	Always	Always	Always	Always	Always	Always	Always	Always	Always	Always	Always	Always	Always
7	2500	Always	Always	Always	Always	Always	Always	Always	Always	Always	Always	Always	Always	Always
8	3000	Always	Always	Always	Always	Always	Always	Always	Always	Always	Always	Always	Always	Always
AL Core														
1	800	Always	Always	Always	Always	Always	Always	Always	Always	Always	Always	Always	Always	Always
2	1000	0.15	0.14	0.13	0.13	0.12	0.12	0.11	0.11	0.11	0.10	0.10	0.10	0.09
3	1200	0.29	0.27	0.26	0.25	0.24	0.23	0.22	0.21	0.21	0.21	0.20	0.20	0.19
4	1400	0.45	0.43	0.41	0.39	0.38	0.36	0.35	0.34	0.34	0.32	0.31	0.31	0.30
5	1600	0.63	0.60	0.57	0.54	0.52	0.50	0.48	0.46	0.46	0.45	0.43	0.43	0.42
6	2000	1.03	0.98	0.93	0.88	0.84	0.80	0.77	0.74	0.74	0.71	0.68	0.68	0.66
7	2500	1.38	1.31	1.24	1.18	1.12	1.07	1.02	0.98	0.98	0.94	0.90	0.90	0.87
8	3000	1.44	1.37	1.30	1.24	1.19	1.14	1.10	1.06	1.06	1.02	0.98	0.98	0.95

Lowest cost: segmented

Lowest cost: solid/stranded or bi-media

TABLE 6-28: Cost effectiveness ($k_s=0.35$, 105°C , 60 Hz): enamel = 12–22%

ID	Area (Nominal) mm ²	Cost Increase for Enamel										
		12%	13%	14%	15%	16%	17%	18%	19%	20%	21%	22%
Air Core												
1	800	Never	Never	Always								
2	1000	Never	Never	Never	Never	Never	Never	Never	Never	Never	Never	Never
3	1200	Never	Never	Never	Never	Never	Never	Never	Never	Never	Never	Never
4	1400	Never	Never	Never	Never	Never	Never	Never	Never	Never	Never	Never
5	1600	Never	Never	Never	Never	Never	Never	Never	Never	Never	Never	Never
6	2000	Never	Never	Never	Never	Never	Never	Never	Never	Never	Never	Never
7	2500	Never	Never	Never	Never	Never	Never	Never	Never	Never	Never	Never
8	3000	Never	Never	Always								
AL Core												
1	800	Never	Never	Always								
2	1000	Never	Never	Never	Never	Never	Never	Never	Never	Never	Never	Never
3	1200	Never	Never	Never	10.16	3.25	1.93	1.38	0.97	0.64	0.48	0.32
4	1400	Never	Never	24.73	6.13	3.50	2.45	1.88	1.53	1.29	1.11	0.98
5	1600	Never	Never	Never	11.66	5.72	3.79	2.83	2.26	1.88	1.61	1.41
6	2000	Never	Never	Never	Never	Never	22.99	9.70	6.14	4.50	3.54	2.93
7	2500	Never	Never	Never	Never	Never	Never	29.53	12.72	8.11	5.95	4.70
8	3000	Never	Never	Never	Never	41.85	16.37	10.17	7.38	5.79	4.76	4.05

Lowest cost: segmented █ Lowest cost: solid/stranded or bi-media █

TABLE 6-29: Cost effectiveness ($k_s=0.35$, 105°C , 60 Hz): enamel = 23–33%

ID	Area (Nominal)	Cost Increase for Enamel										
		23%	24%	25%	26%	27%	28%	29%	30%	31%	32%	33%
Air Core												
1	800	Always	Always	Always	Always	Always	Always	Always	Always	Always	Always	Always
2	1000	Always	Always	Always	Always	Always	Always	Always	Always	Always	Always	Always
3	1200	Always	Always	Always	Always	Always	Always	Always	Always	Always	Always	Always
4	1400	Always	Always	Always	Always	Always	Always	Always	Always	Always	Always	Always
5	1600	Always	Always	Always	Always	Always	Always	Always	Always	Always	Always	Always
6	2000	Always	Always	Always	Always	Always	Always	Always	Always	Always	Always	Always
7	2500	Always	Always	Always	Always	Always	Always	Always	Always	Always	Always	Always
8	3000	Always	Always	Always	Always	Always	Always	Always	Always	Always	Always	Always
AL Core												
1	800	Always	Always	Always	Always	Always	Always	Always	Always	Always	Always	Always
2	1000	0.27	0.24	0.21	0.19	0.17	0.16	0.15	0.14	0.13	0.12	0.11
3	1200	0.56	0.50	0.46	0.42	0.38	0.35	0.33	0.31	0.29	0.27	0.26
4	1400	0.87	0.79	0.72	0.66	0.61	0.57	0.53	0.50	0.47	0.45	0.42
5	1600	1.25	1.13	1.02	0.94	0.87	0.80	0.75	0.70	0.66	0.62	0.59
6	2000	2.49	2.17	1.92	1.72	1.56	1.43	1.32	1.22	1.14	1.07	1.00
7	2500	3.88	3.31	2.88	2.55	2.29	2.08	1.90	1.75	1.63	1.52	1.42
8	3000	3.52	3.11	2.79	2.53	2.31	2.13	1.97	1.84	1.72	1.62	1.52

Lowest cost: segmented

Lowest cost: solid/stranded or bi-media

TABLE 6-30: Cost effectiveness ($k_s=0.35$, 105°C , 60 Hz): enamel = 34–44%

ID	Area (Nominal)	Cost Increase for Enamel												
		34%	35%	36%	37%	38%	39%	40%	41%	42%	43%	44%		
Air Core														
1	800	Always	Always	Always	Always	Always	Always	Always	Always	Always	Always	Always	Always	Always
2	1000	Always	Always	Always	Always	Always	Always	Always	Always	Always	Always	Always	Always	Always
3	1200	Always	Always	Always	Always	Always	Always	Always	Always	Always	Always	Always	Always	Always
4	1400	Always	Always	Always	Always	Always	Always	Always	Always	Always	Always	Always	Always	Always
5	1600	Always	Always	Always	Always	Always	Always	Always	Always	Always	Always	Always	Always	Always
6	2000	Always	Always	Always	Always	Always	Always	Always	Always	Always	Always	Always	Always	Always
7	2500	Always	Always	Always	Always	Always	Always	Always	Always	Always	Always	Always	Always	Always
8	3000	Always	Always	Always	Always	Always	Always	Always	Always	Always	Always	Always	Always	Always
AL Core														
1	800	Always	Always	Always	Always	Always	Always	Always	Always	Always	Always	Always	Always	Always
2	1000	0.11	0.10	0.10	0.09	0.09	0.09	0.08	0.08	0.08	0.08	0.07	0.07	0.07
3	1200	0.25	0.23	0.22	0.21	0.20	0.20	0.20	0.19	0.19	0.18	0.17	0.17	0.16
4	1400	0.40	0.38	0.37	0.35	0.34	0.34	0.32	0.31	0.31	0.30	0.29	0.28	0.27
5	1600	0.56	0.54	0.51	0.49	0.47	0.47	0.45	0.43	0.43	0.42	0.40	0.39	0.37
6	2000	0.95	0.90	0.85	0.81	0.77	0.77	0.74	0.71	0.71	0.68	0.65	0.63	0.60
7	2500	1.33	1.26	1.19	1.13	1.08	1.08	1.03	0.98	0.98	0.94	0.90	0.87	0.84
8	3000	1.44	1.37	1.30	1.24	1.19	1.14	1.14	1.09	1.09	1.05	1.01	0.97	0.94

Lowest cost: segmented

Lowest cost: solid/stranded or bi-media

TABLE 6-31: Cost effectiveness ($k_s=0.35$, 90°C , 50 Hz): enamel = 12–22%

ID	Area (Nominal)	Cost Increase for Enamel											
		12%	13%	14%	15%	16%	17%	18%	19%	20%	21%	22%	
Air Core													
1	800	Always	Always	Always	Always	Always	Always	Always	Always	Always	Always	Always	Always
2	1000	Never	Never	Never	Never	Never	Never	Never	Never	Never	Never	Never	Never
3	1200	Never	Never	Never	Never	Never	Never	Never	Never	Never	Never	Never	Never
4	1400	Never	Never	Never	Never	Never	Never	Never	Never	Never	Never	Never	Never
5	1600	Never	Never	Never	Never	Never	Never	Never	Never	Never	Never	Never	Never
6	2000	Never	Never	Never	Never	Never	Never	Never	Never	Never	Never	Never	Never
7	2500	Never	Never	Never	Never	Never	Never	Never	Never	Never	Never	Never	Never
8	3000	Never	Never	Never	Never	Never	Never	Never	Never	Never	Never	Never	Never
AL Core													
1	800	Always	Always	Always	Always	Always	Always	Always	Always	Always	Always	Always	Always
2	1000	Never	Never	Never	Never	Never	Never	Never	Never	Never	Never	Never	Never
3	1200	Never	Never	Never	Never	20.90	1.97	1.03	0.70	0.53	0.43	0.36	0.68
4	1400	Never	Never	Never	8.01	3.15	1.96	1.42	1.12	0.92	0.78	0.68	0.97
5	1600	Never	Never	25.02	6.09	3.47	2.42	1.86	1.51	1.27	1.10	0.97	1.86
6	2000	Never	Never	Never	72.14	11.29	6.13	4.20	3.20	2.58	2.16	1.86	3.78
7	2500	Never	Never	Never	Never	Never	Never	18.93	9.46	6.31	4.73	3.78	4.72
8	3000	Never	Never	Never	Never	Never	Never	24.17	11.91	7.90	5.91	4.72	4.72

Lowest cost: segmented Lowest cost: solid/stranded or bi-media

TABLE 6-33: Cost effectiveness ($k_s=0.35$, 90°C , 50 Hz): enamel = 34–44%

ID	Area (Nominal)	Cost Increase for Enamel												
		34%	35%	36%	37%	38%	39%	40%	41%	42%	43%	44%		
Air Core														
1	800	Always	Always	Always	Always	Always	Always	Always	Always	Always	Always	Always	Always	Always
2	1000	Always	Always	Always	Always	Always	Always	Always	Always	Always	Always	Always	Always	Always
3	1200	Always	Always	Always	Always	Always	Always	Always	Always	Always	Always	Always	Always	Always
4	1400	Always	Always	Always	Always	Always	Always	Always	Always	Always	Always	Always	Always	Always
5	1600	Always	Always	Always	Always	Always	Always	Always	Always	Always	Always	Always	Always	Always
6	2000	Always	Always	Always	Always	Always	Always	Always	Always	Always	Always	Always	Always	Always
7	2500	Always	Always	Always	Always	Always	Always	Always	Always	Always	Always	Always	Always	Always
8	3000	Always	Always	Always	Always	Always	Always	Always	Always	Always	Always	Always	Always	Always
AL Core														
1	800	Always	Always	Always	Always	Always	Always	Always	Always	Always	Always	Always	Always	Always
2	1000	0.00	0.00	0.00	0.00	0.00	0.00	0.00	0.00	0.00	0.00	0.00	0.00	0.00
3	1200	0.12	0.11	0.11	0.10	0.10	0.09	0.09	0.09	0.09	0.09	0.08	0.08	0.08
4	1400	0.26	0.25	0.24	0.23	0.22	0.22	0.21	0.20	0.20	0.20	0.19	0.18	0.18
5	1600	0.40	0.38	0.36	0.35	0.33	0.32	0.32	0.31	0.29	0.29	0.28	0.27	0.27
6	2000	0.70	0.66	0.63	0.60	0.58	0.55	0.55	0.53	0.51	0.49	0.49	0.47	0.46
7	2500	1.11	1.05	1.00	0.95	0.90	0.86	0.86	0.82	0.79	0.79	0.76	0.73	0.70
8	3000	1.38	1.31	1.24	1.18	1.12	1.07	1.07	1.02	0.98	0.98	0.94	0.90	0.87

Lowest cost: segmented

Lowest cost: solid/stranded or bi-media

TABLE 6-34: Cost effectiveness ($k_s=0.35$, 105°C , 50 Hz): enamel = 12–22%

ID	Area (Nominal)	Cost Increase for Enamel											
		12%	13%	14%	15%	16%	17%	18%	19%	20%	21%	22%	
Air Core													
1	800	Always	Always	Always	Always	Always	Always	Always	Always	Always	Always	Always	Always
2	1000	Never	Never	Never	Always								
3	1200	Never	Never	Never	Never	Never	Never	Never	Never	Never	Never	Never	Never
4	1400	Never	Never	Never	Never	Never	Never	Never	Never	Never	Never	Never	Never
5	1600	Never	Never	Never	Never	Never	Never	Never	Never	Never	Never	Never	Never
6	2000	Never	Never	Never	Never	Never	Never	Never	Never	Never	Never	Never	Never
7	2500	Never	Never	Never	Never	Never	Never	Never	Never	Never	Never	Never	Never
8	3000	Never	Never	Never	Never	Never	Never	Never	Never	Never	Never	Never	Never
AL Core													
1	800	Always	Always	Always	Always	Always	Always	Always	Always	Always	Always	Always	Always
2	1000	Never	Never	Never	Always								
3	1200	Never	Never	Never	Never	Never	Never	Never	Never	Never	Never	Never	Never
4	1400	Never	Never	Never	18.01	3.46	1.91	1.32	1.01	0.82	0.69	0.59	0.59
5	1600	Never	Never	Never	35.73	5.89	2.21	1.68	1.36	1.14	0.98	0.86	0.86
6	2000	Never	Never	Never	Never	20.04	4.70	3.40	2.66	2.19	1.86	1.61	1.61
7	2500	Never	Never	Never	Never	Never	51.42	13.21	7.58	5.31	4.09	3.33	3.33
8	3000	Never	Never	Never	Never	Never	Never	29.70	12.76	8.12	5.96	4.70	4.70

Lowest cost: segmented

Lowest cost: solid/stranded or bi-media

TABLE 6-35: Cost effectiveness ($k_s=0.35$, 105°C , 50 Hz): enamel = 23–33%

ID	Area (Nominal)	Cost Increase for Enamel										
		23%	24%	25%	26%	27%	28%	29%	30%	31%	32%	33%
Air Core												
1	800	Always	Always	Always	Always	Always	Always	Always	Always	Always	Always	Always
2	1000	Always	Always	Always	Always	Always	Always	Always	Always	Always	Always	Always
3	1200	Always	Always	Always	Always	Always	Always	Always	Always	Always	Always	Always
4	1400	Always	Always	Always	Always	Always	Always	Always	Always	Always	Always	Always
5	1600	Always	Always	Always	Always	Always	Always	Always	Always	Always	Always	Always
6	2000	Always	Always	Always	Always	Always	Always	Always	Always	Always	Always	Always
7	2500	Always	Always	Always	Always	Always	Always	Always	Always	Always	Always	Always
8	3000	Always	Always	Always	Always	Always	Always	Always	Always	Always	Always	Always
AL Core												
1	800	Always	Always	Always	Always	Always	Always	Always	Always	Always	Always	Always
2	1000	Always	Always	Always	Always	Always	Always	Always	Always	Always	Always	Always
3	1200	0.21	0.18	0.16	0.15	0.13	0.12	0.11	0.10	0.10	0.09	0.09
4	1400	0.52	0.46	0.42	0.38	0.35	0.32	0.30	0.28	0.26	0.25	0.23
5	1600	0.77	0.69	0.63	0.58	0.53	0.50	0.46	0.44	0.41	0.39	0.37
6	2000	1.43	1.28	1.16	1.06	0.97	0.90	0.84	0.79	0.74	0.70	0.66
7	2500	2.80	2.42	2.13	1.90	1.72	1.57	1.44	1.33	1.24	1.16	1.09
8	3000	3.89	3.31	2.88	2.55	2.29	2.08	1.90	1.75	1.63	1.52	1.42

Lowest cost: segmented

Lowest cost: solid/stranded or bi-media

The tables showing the cost effectiveness of bi-media conductors as compared to segmented conductors using enameled wires show that a bi-media conductor would never be the most cost effective solution if the price increase to enamel wires is 12% or less. For Air / CU conductors the solution is always more cost effective if the price to enamel wires is 22% or greater. Between 12% and 22% for Air / CU designs it depends on the price to enamel wires, and can go either way. Similarly, the AL / CU conductors are never cost effective if the cost to enamel wires is 13% or less. If the cost increase for the enamel is 18% or higher than the cost effectiveness depends on the price ratio of copper to aluminum. Between 13% and 18% the cost effectiveness can vary between cross-sectional areas of the individual conductors.

It is important to keep in mind that the outer radius of the bi-media design is increasing as the values of k_s are decreasing (i.e. increasingly large cross-sectional areas of bi-media conductors are required to have the same AC resistance as the segmented copper conductors, whose AC resistance decreases with lower k_s values), since the outer diameter affects additional aspects in the cost associated with a conductor. The cost analysis in this dissertation is limited to material costs of the conductor (i.e. copper wire, aluminum wire, and enameling of copper wire), but the diameter of the conductor also affects the amount of materials used on cable layers above the conductor, and the final diameter of the cable affects shipping and installation costs. Since the formula for estimating the compaction ratio of stranded conductors shown on FIGURE 6-17 only went up to maximum nominal cross-sectional area of 3000 mm², for sizes larger than 3000 mm² it is assumed that the compaction is held at 1.0271. Using this approximate formula for stranded conductor radii in conjunction with the assumption of a fixed compaction ratio for conductor cross-

sectional areas greater than 3000mm², TABLE 6-37 through TABLE 6-40 were created to demonstrate the effect stranding the bi-media conductor has on the diameter. This is then for comparison to the segmented copper conductor diameter of equal AC resistance it is intended to replace. In TABLE 6-37 to TABLE 6-40 the cells are color coded red if the bi-media design is not cost effective compared to the segmented conductor design of equal AC resistance. If the bi-media design is cost effective, then the cell is color coded either yellow or green. Yellow indicates the radius of bi-media design is larger than the radius of the segmented conductor design of equal AC resistance. In the case the cell is color coded green it means the bi-media design is both more cost effective than the segmented conductor design and has a smaller outer radius. When a k_s of 0.35 is used the cost to enamel the copper strands of the conductor determines whether or not the design is cost effective. Therefore, TABLE 6-40 only has cells that are color coded yellow or green. TABLE 6-37 through TABLE 6-40 show the approximate stranded diameters calculated for the bi-media conductors compared to segmented copper conductors of equal AC resistance:

TABLE 6-37: Stranded Radii of Bi-Media Conductors ($k_s=0.8$)

ID	Nominal Area mm ²	Segmented Outer Radius mm	Bi-Media Radius							
			90°C, 60 Hz		105°C, 60 Hz		90°C, 50 Hz		105°C, 50 Hz	
			Inner	Outer	Inner	Outer	Inner	Outer	Inner	Outer
		mm		mm		mm		mm		
Air Core										
1	800	18.0	0.00	16.61	0.00	16.57	0.00	16.48	0.00	16.46
2	1000	19.4	2.15	18.85	1.46	18.80	0.00	18.65	0.00	18.61
3	1200	21.4	4.24	20.51	3.73	20.46	1.86	20.31	0.98	20.26
4	1400	23.2	6.27	22.31	5.82	22.28	4.29	22.16	3.72	22.11
5	1600	24.9	7.94	23.88	7.53	23.87	6.17	23.81	5.66	23.77
6	2000	27.2	10.89	26.70	10.53	26.73	9.33	26.76	8.90	26.75
7	2500	31.0	13.85	29.58	13.55	29.66	12.52	29.82	12.14	29.86
8	3000	33.9	16.33	31.94	15.99	31.97	15.07	32.20	14.74	32.27
AL Core										
1	800	18.0	0.00	16.61	0.00	16.57	0.00	16.48	0.00	16.46
2	1000	19.4	3.10	18.85	2.15	18.80	0.00	18.65	0.00	18.61
3	1200	21.4	5.83	20.53	5.20	20.48	2.72	20.31	1.46	20.26
4	1400	23.2	8.27	22.39	7.76	22.34	5.94	22.18	5.21	22.12
5	1600	24.9	10.18	24.03	9.75	23.99	8.24	23.86	7.64	23.81
6	2000	27.2	13.39	27.12	13.05	27.09	11.86	26.97	11.41	26.93
7	2500	31.0	16.51	30.37	16.24	30.38	15.30	30.35	14.94	30.32
8	3000	33.9	18.99	32.96	18.69	32.92	17.92	32.98	17.63	32.99

Smaller Radius Larger Radius Not Cost Effective

TABLE 6-38: Stranded Radii of Bi-Media Conductors ($k_s=0.62$)

ID	Nominal Area mm ²	Segmented Outer Radius mm	Bi-Media Radius							
			90°C, 60 Hz		105°C, 60 Hz		90°C, 50 Hz		105°C, 50 Hz	
			Inner	Outer	Inner	Outer	Inner	Outer	Inner	Outer
		mm		mm		mm		mm		
Air Core										
1	800	18.0	0.00	16.95	0.00	16.88	0.00	16.71	0.00	16.67
2	1000	19.4	2.97	19.46	2.32	19.36	0.00	19.08	0.00	19.00
3	1200	21.4	5.23	21.37	4.68	21.27	2.76	20.94	1.99	20.84
4	1400	23.2	7.54	23.50	7.03	23.40	5.33	23.06	4.72	22.95
5	1600	24.9	9.53	25.39	9.05	25.30	7.45	24.99	6.88	24.87
6	2000	27.2	13.06	28.82	12.65	28.78	11.20	28.55	10.68	28.46
7	2500	31.0	16.57	32.16	16.19	32.15	14.93	32.07	14.47	32.03
8	3000	33.9	19.62	35.20	19.30	35.25	18.17	35.28	17.76	35.27
AL Core										
1	800	18.0	0.00	16.95	0.00	16.88	0.00	16.71	0.00	16.67
2	1000	19.4	4.21	19.47	3.33	19.36	0.00	19.08	0.00	19.00
3	1200	21.4	7.04	21.41	6.38	21.29	3.95	20.94	2.90	20.84
4	1400	23.2	9.73	23.63	9.17	23.50	7.23	23.09	6.48	22.97
5	1600	24.9	11.94	25.68	11.44	25.53	9.74	25.09	9.10	24.95
6	2000	27.2	15.69	29.50	15.30	29.39	13.90	28.93	13.37	28.77
7	2500	31.0	19.24	33.23	18.91	33.15	17.77	32.82	17.35	32.70
8	3000	33.9	22.55	36.95	22.27	36.92	21.28	36.74	20.91	36.64

Smaller Radius Larger Radius Not Cost Effective

TABLE 6-39: Stranded Radii of Bi-Media Conductors ($k_s=0.435$)

ID	Nominal Area mm ²	Segmented Outer Radius mm	Bi-Media Radius							
			90°C, 60 Hz		105°C, 60 Hz		90°C, 50 Hz		105°C, 50 Hz	
			Inner	Outer	Inner	Outer	Inner	Outer	Inner	Outer
		mm		mm		mm		mm		
Air Core										
1	800	18.0	0.00	17.25	0.00	17.15	0.00	16.91	0.00	16.84
2	1000	19.4	3.66	20.02	2.99	19.87	0.00	19.45	0.00	19.33
3	1200	21.4	6.13	22.19	5.52	22.01	3.49	21.50	2.73	21.35
4	1400	23.2	8.79	24.68	8.19	24.49	6.27	23.90	5.60	23.71
5	1600	24.9	11.18	26.98	10.58	26.78	8.69	26.14	8.03	25.94
6	2000	27.2	15.58	31.27	15.02	31.10	13.17	30.46	12.52	30.23
7	2500	31.0	20.26	35.90	19.70	35.68	17.89	34.98	17.25	34.73
8	3000	33.9	24.29	39.92	23.81	39.80	22.22	39.38	21.64	39.19
AL Core										
1	800	18.0	0.00	17.25	0.00	17.15	0.00	16.91	0.00	16.84
2	1000	19.4	5.09	20.03	4.23	19.87	0.00	19.45	0.00	19.33
3	1200	21.4	8.11	22.26	7.40	22.06	4.91	21.51	3.90	21.35
4	1400	23.2	11.12	24.90	10.49	24.65	8.36	23.96	7.57	23.75
5	1600	24.9	13.70	27.43	13.11	27.14	11.14	26.32	10.42	26.06
6	2000	27.2	18.21	32.14	17.69	31.87	15.99	31.06	15.35	30.74
7	2500	31.0	23.13	37.57	22.63	37.32	21.01	36.45	20.42	36.12
8	3000	33.9	27.25	41.95	26.80	41.78	25.33	41.15	24.79	40.88

Smaller Radius Larger Radius Not Cost Effective

TABLE 6-40: Stranded Radii of Bi-Media Conductors ($k_s=0.35$)

ID	Nominal Area mm ²	Segmented Outer Radius mm	Bi-Media Radius											
			90°C, 60 Hz			105°C, 60 Hz			90°C, 50 Hz			105°C, 50 Hz		
			Inner	Outer	mm	Inner	Outer	mm	Inner	Outer	mm	Inner	Outer	mm
Air Core														
1	800	18.0	0.00	17.35	0.00	17.25	0.00	16.97	0.00	16.97	0.00	16.90	0.00	16.90
2	1000	19.4	3.91	20.22	3.23	20.05	0.34	19.58	0.00	19.58	0.00	19.45	0.00	19.45
3	1200	21.4	6.48	22.51	5.84	22.30	3.75	21.71	2.98	21.71	2.98	21.54	2.98	21.54
4	1400	23.2	9.30	25.17	8.66	24.93	6.63	24.23	5.93	24.23	5.93	24.01	5.93	24.01
5	1600	24.9	11.87	27.65	11.22	27.39	9.18	26.61	8.48	26.61	8.48	26.36	8.48	26.36
6	2000	27.2	16.65	32.24	16.01	31.99	14.00	31.24	13.30	31.24	13.30	30.99	13.30	30.99
7	2500	31.0	22.11	37.75	21.46	37.47	19.39	36.57	18.67	36.57	18.67	36.25	18.67	36.25
8	3000	33.9	26.82	42.44	26.21	42.19	24.22	41.35	23.51	41.35	23.51	41.05	23.51	41.05
AL Core														
1	800	18.0	0.00	17.35	0.00	17.25	0.00	16.97	0.00	16.97	0.00	16.90	0.00	16.90
2	1000	19.4	5.41	20.24	4.54	20.06	0.52	19.58	0.00	19.58	0.00	19.45	0.00	19.45
3	1200	21.4	8.51	22.59	7.78	22.35	5.25	21.72	4.25	21.72	4.25	21.54	4.25	21.54
4	1400	23.2	11.68	25.43	11.00	25.12	8.78	24.30	7.97	24.30	7.97	24.05	7.97	24.05
5	1600	24.9	14.43	28.18	13.79	27.83	11.68	26.81	10.93	26.81	10.93	26.51	10.93	26.51
6	2000	27.2	19.33	33.32	18.72	32.94	16.80	31.84	16.13	31.84	16.13	31.49	16.13	31.49
7	2500	31.0	24.99	39.57	24.38	39.21	22.43	38.00	21.75	38.00	21.75	37.56	21.75	37.56
8	3000	33.9	29.88	44.70	29.29	44.40	27.38	43.35	26.71	43.35	26.71	42.95	26.71	42.95

Smaller Radius Larger Radius Not Cost Effective

At a fixed k_s value, the diameter change for the four combinations of temperature and frequency is a similar value. With this, TABLE 6-41 was created to summarize the average change in outer radius of the conductor when going from a segmented copper conductor to a bi-media design of the same AC resistance:

TABLE 6-41: Average Change in Radius for Stranded Segmented vs Bi-Media

ID	Nominal Area	Change in Outer Radius			
		$k_s = 0.8$	$k_s = 0.62$	$k_s = 0.435$	$k_s = 0.35$
	mm ²	mm	mm	mm	%
Air Core					
1	800	-8.2%	-6.6%	-5.4%	-4.9%
2	1000	-3.5%	-0.9%	1.4%	2.2%
3	1200	-4.7%	-1.4%	1.7%	2.9%
4	1400	-4.2%	0.1%	4.3%	6.0%
5	1600	-4.3%	1.0%	6.3%	8.4%
6	2000	-1.7%	5.3%	13.1%	16.2%
7	2500	-4.1%	3.6%	13.9%	19.4%
8	3000	-5.3%	4.0%	16.7%	23.2%
AL Core					
1	800	-8.2%	-6.6%	-5.4%	-4.9%
2	1000	-3.5%	-0.9%	1.4%	2.2%
3	1200	-4.7%	-1.3%	1.8%	3.0%
4	1400	-4.1%	0.4%	4.8%	6.6%
5	1600	-3.9%	1.7%	7.4%	9.8%
6	2000	-0.6%	7.2%	15.6%	19.1%
7	2500	-2.1%	6.4%	18.9%	24.5%
8	3000	-2.8%	8.6%	22.2%	29.3%

This data can also be presented graphically, as shown in FIGURE 6-61:

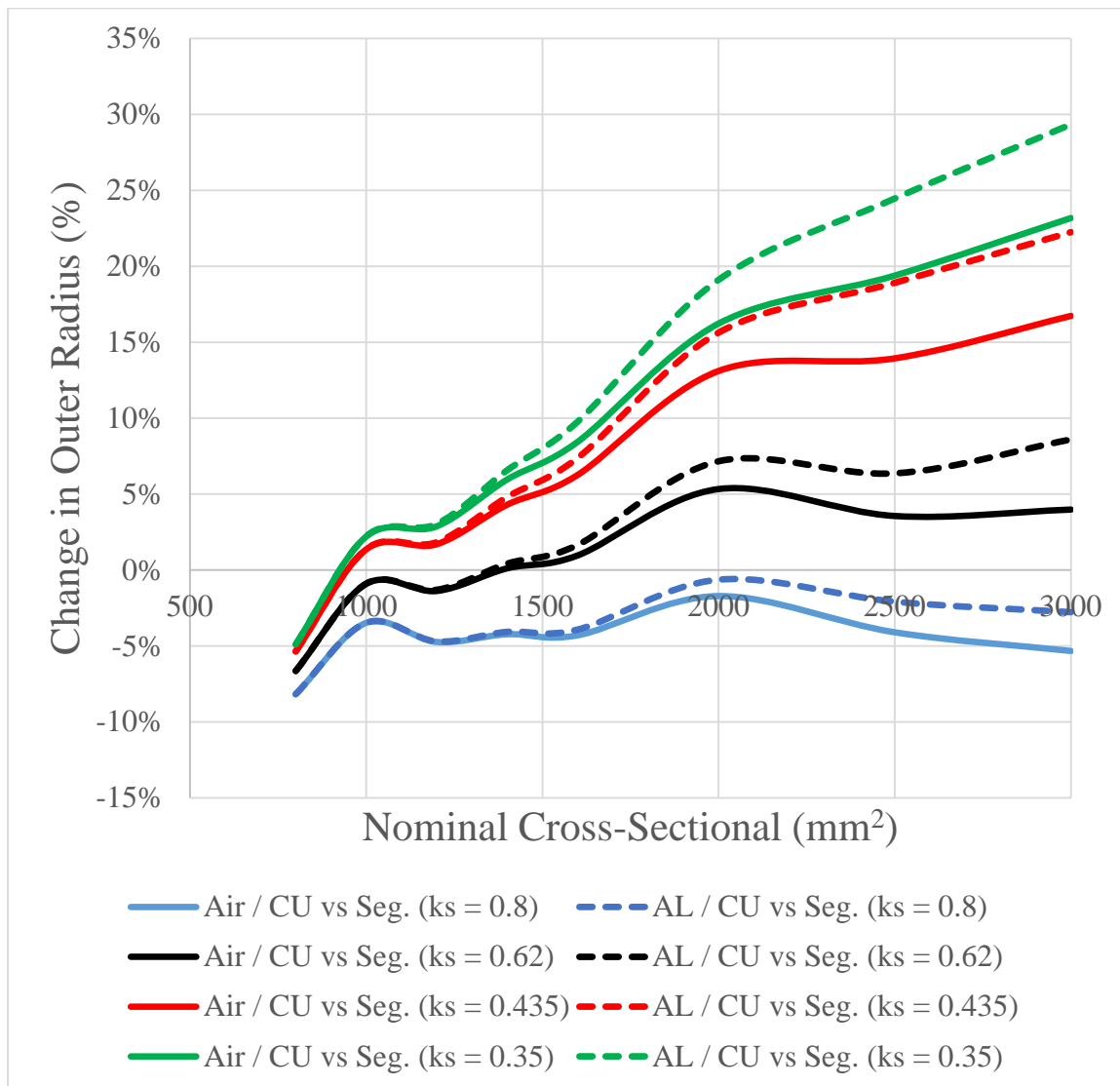


FIGURE 6-59: Average Change in Radius for Stranded Segmented vs Bi-Media

FIGURE 6-61 shows that for a k_s of 0.8 any designs that is cost effective will have the additional benefit of having a smaller radius, and therefore additional material, transportation, and installation cost savings as well.

6.4 Simplified Equations

At this point it has been identified bi-media conductors are in certain cases more cost effective solutions than segmented copper conductors. However, implementing the complicated Bessel functions for everyday calculations when sizing conductors requires

approximations. This is done using polynomial equations to approximate the analytical solution over the frequency and temperature ranges applicable to power conductors. For conductors larger than 1000 mm^2 (when solid/stranded conductors switch to segmented conductors), hollow core conductors are not immediately more cost effective than segmented conductors. This is because initially the AC resistance of an (approximately) solid/stranded conductor is being compared to a segmented conductor that immediately benefits from its design and achieves a reduction in AC resistance. However, on large enough conductors the hollow core conductor can be the most cost effective design if optimized to its lowest AC resistance. Although the solution for calculating AC resistance of hollow core conductors exists, this application range has been overlooked. For the AL / CU conductors the application range has not been explored. In general, AL / CU have an earlier point at which they become cost effective as compared to Air / CU. It should be noted however, that both have more cost effective ranges depending on the segmented empirical factor k_s , in addition to operating temperature and frequency. Further, it should be noted this factor is not as accurate to the true solution of skin effect in solid/stranded conductors when used for segmented conductors. In the case of segmented conductors, there are many additional variables impacting the skin effect. Some of the more significant characteristics are addressed by using different k_s values, such as stranding lay direction, type of insulation on cables, and if the wires are enameled. However, these still do not address other known design factors influencing the skin effect, such as number of segments and separating tape composition or even lack thereof in the construction. Given the fact that a cost effective solution exists, a simpler way of formulating the optimal radii or area that minimizes AC resistance needs to be found.

It should be kept in mind that for the designs of Air / CU and AL / CU there are different optimal designs for 50 and 60 Hz, as well as 90°C and 105°C. This means there are eight total simplified equations that are required for all combinations of media, frequencies, and temperatures. Furthermore, there currently exists an analytical solution for Air / CU skin effect, as well as a good approximation technique. However, an equation for skin effect in AL / CU conductors does not exist. Therefore, this equation is formulated as a simplified polynomial as well. In doing so, it is found the ranges of the Bessel function input argument that are ideal to minimize AC resistance differ from the existing ones used in the industry. In the case of the approximation of skin effect in AL / CU conductors equations were used that mimicked those of the existing equations and input argument ranges as much as possible. Specifically, the one equation that could be reused is the one using the lowest range of the Bessel function input argument. This is because the lowest range does not change for bi-media conductors as they do not become an optimal choice by possessing an AC resistance lower than an all copper conductor until the conductor has reached a certain cross-sectional area. However, whereas this range normally applies to input arguments up to 2.8 the new equations switch at 2.5. The input argument is a function of frequency, temperature, and DC resistance. It is also important that the equation be valid starting from a temperature of 20°C. This is important because this is generally close to ambient temperature, and therefore the temperature at which testing is performed and/or the results are adjusted to. The maximum possible temperature of 140°C used in short term emergency conditions on certain cable designs is also verified, although it is the lowest temperature that is associated with the first optimal cross-sectional area. The 140°C is only applicable to medium voltage cables. In high voltage, where such large conductor designs

would more expectedly be encountered, ratings are rarely above 105°C. The Bessel function input argument calculated for existing simplified equations is dependent upon the cross-sectional area of the conductor (i.e. DC resistance). Therefore, a small enough Bessel function input argument ending range of the first equation for calculating the increase in AC resistance must be chosen such that it corresponds to a cross-sectional area lower than when bi-media conductors become optimal. This occurs at an input argument of 2.5, which is the reason the existing equation for calculating the increase in AC resistance for conductors with an input argument up to 2.8 can only be used up until an input argument of 2.5. TABLE 6-42 demonstrates the first optimal bi-media cross-sectional areas for various temperature and frequencies, and hence the reason the application range of the first equation for calculating the increased AC resistance has been changed:

TABLE 6-42: Input argument cross-sectional area vs temperature

Frequency	Temperature	Area
Hz	°C	mm ²
Input Argument = 2.5		
50	20	858
	90	673
	105	643
	140	583
60	20	715
	90	561
	105	536
	140	486
Input Argument = 2.8		
50	20	1076
	90	844
	105	806
	140	731
60	20	896
	90	703
	105	672
	140	609

Alternatively, this information can be view graphically as shown in FIGURE 6-60:

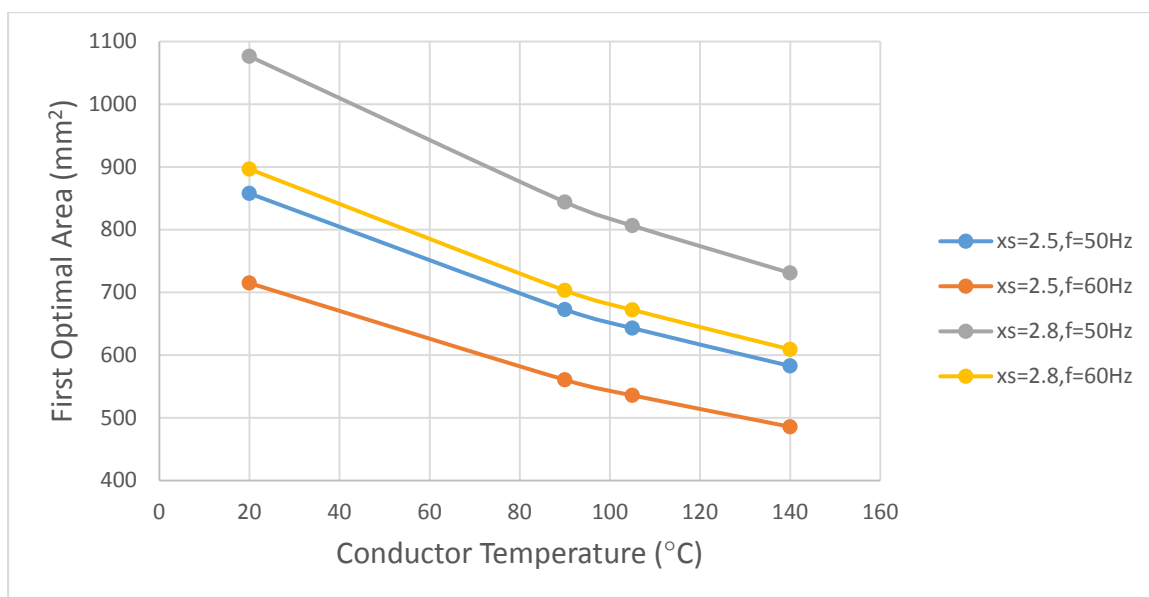


FIGURE 6-60: Input argument cross-sectional area vs temperature

The input argument was chosen at 2.5 because this corresponds to an 858 mm² copper conductor at 50 Hz and 20°C, which is the just before AL / CU conductor started to become an optimal design. Recall that the Bessel function input argument is calculated as follows:

$$x_s = \sqrt{\frac{\omega\mu}{\pi R_{dc}}} k_s \quad (139)$$

The recommended ranges and equations, derived using a polynomial regression, are as follow:

For $x_s \leq 2.5$ (same as existing equation used to $x_s \leq 2.8$):

$$y_s = \frac{x_s^4}{192 + 0.8x_s^4} \quad (140)$$

For $2.5 < x_s < 2.7$:

$$y_s = 1.6172x_s^3 - 12.8131x_s^2 + 34.02x_s - 30.0615 \quad (141)$$

For $x_s \geq 2.7$:

$$y_s = -0.01516x_s^3 + 0.20012x_s^2 - 0.57637x_s + 0.61188 \quad (142)$$

The error of these equations was checked over the entire ranges of frequencies from 50-60 Hz, temperatures of 20-140°C, and cross-sectional areas up to 4000 mm². The error was found in all cases be at a maximum of 0.23% from the true solution calculated using the analytical equations. The skin effect shown for 50 and 60 Hz and 90°C and 105°C in AL / CU conductors, compared to solid copper and segmented copper with a $k_s = 0.8$ for reference are shown in FIGURE 6-61 through FIGURE 6-64:

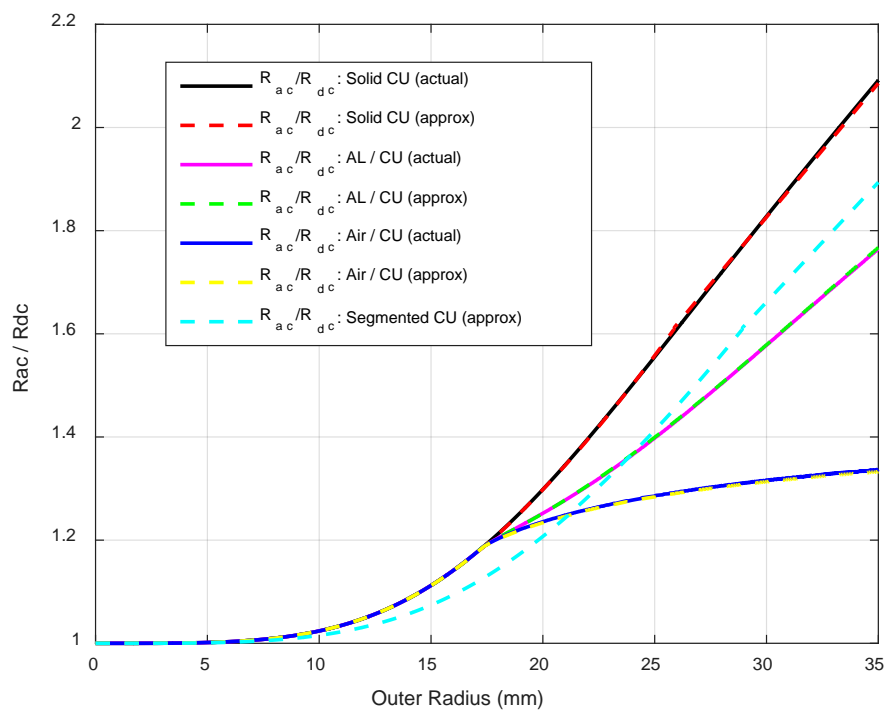


FIGURE 6-61: Skin effect in bi-media conductors (90°C, 60 Hz)

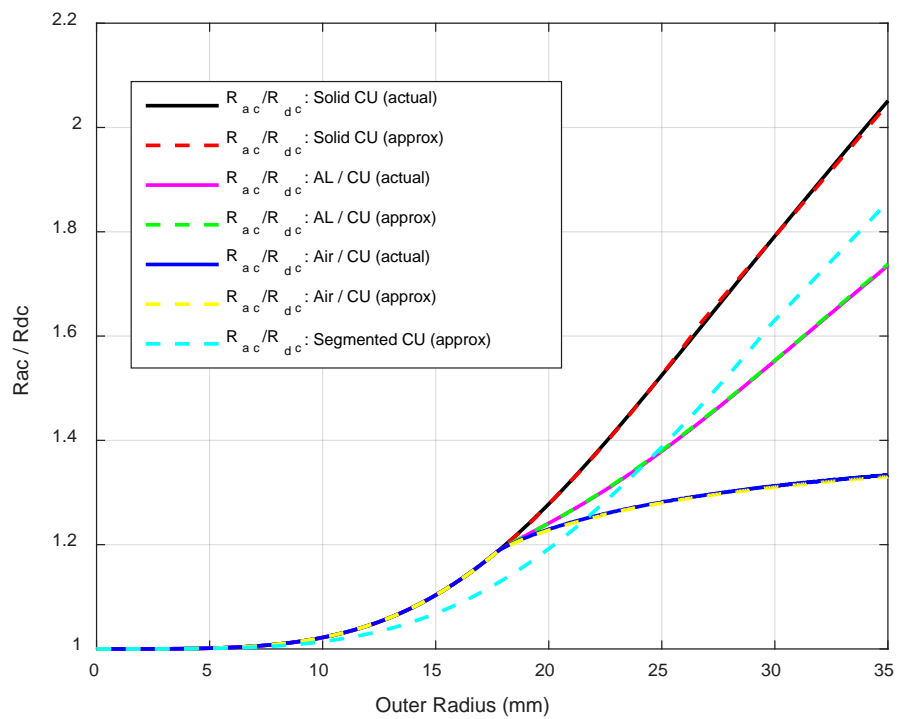


FIGURE 6-62: Skin effect in bi-media conductors (105°C, 60 Hz)

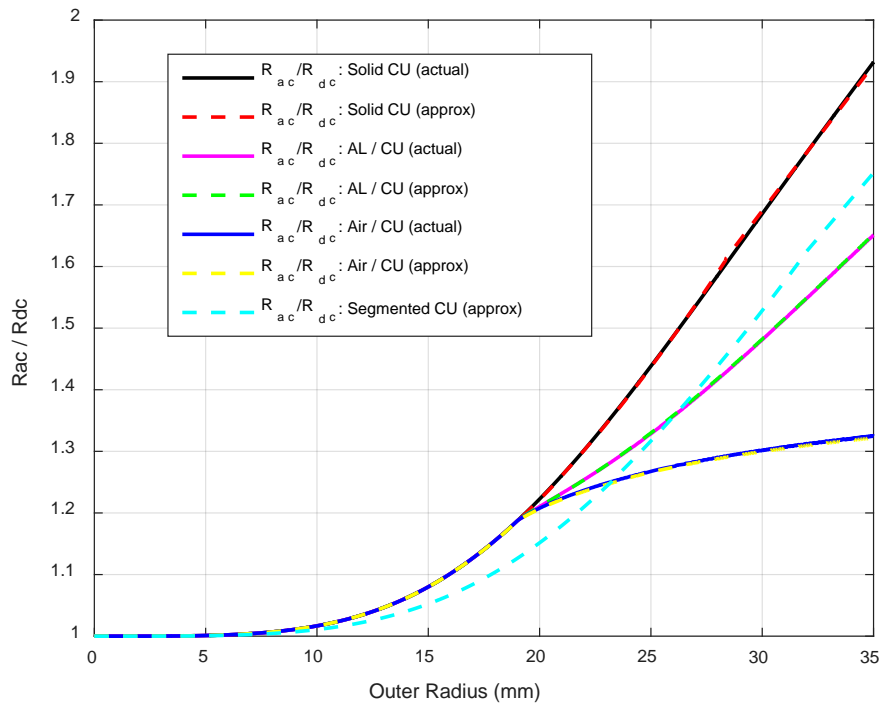


FIGURE 6-63: Skin effect in bi-media conductors (90°C, 50 Hz)

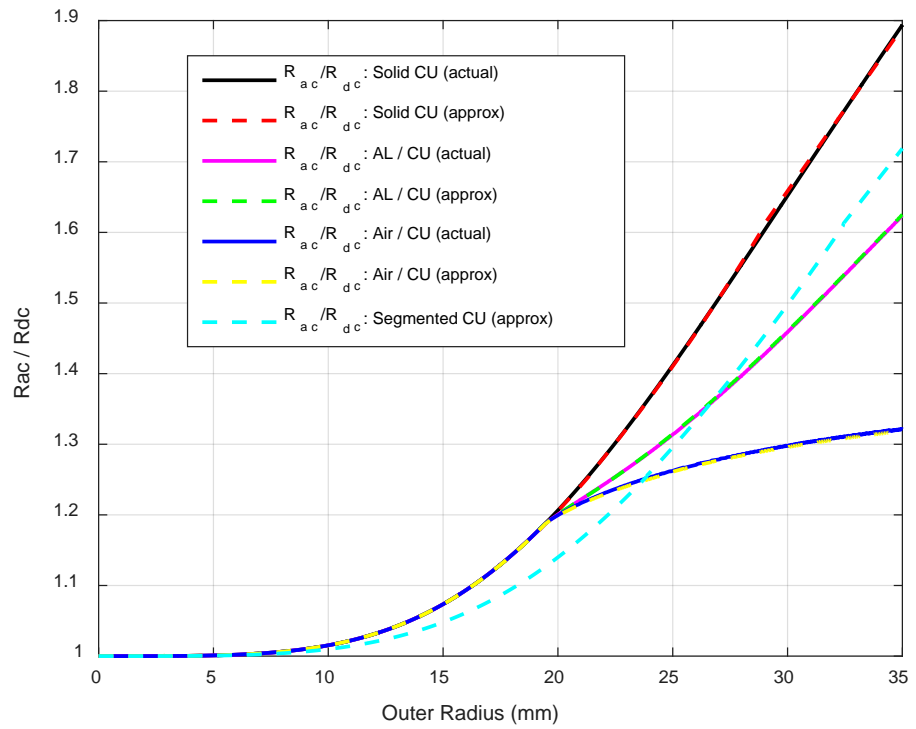


FIGURE 6-64: Skin effect in bi-media conductors (105°C, 50 Hz)

It should be kept in mind that the skin effect is more representative of return on the cost of the media used, as opposed to maximum capacity (i.e. lowest AC resistance). At an equally sized conductor, the DC resistance of a bi-media design is higher than a segmented copper design. Therefore, the cost effectiveness results from comparison of the metals used.

The next sets of simplified polynomial equations, again found using polynomial regression, define the cross-sectional area of the optimal conductor designs for Air / CU and AL / CU. Meaning, for an Air / CU conductor, using the required copper cross-sectional area as input the result is the cross-sectional area of the air core. Using these two areas all the pertinent characteristics of the conductor can be calculated. Namely, this includes inner/outer radii, DC resistance at any operating temperature, the skin effect coefficient, skin effect input argument, skin effect factor, and ultimately AC resistance at any operating temperature. There are four separate equations, based on different operating temperature and frequency. These are:

For 60 Hz and 90°C:

$$\begin{aligned}
 A_{Air} = & 1.25437919020408E - 18 * A_{CU}^6 - 1.84755691815890E - 14 * A_{CU}^5 + \\
 & 1.11503121142173E - 10 * A_{CU}^4 - 3.53299622659472E - 07 * A_{CU}^3 + \\
 & 9.69334930152081E - 04 * A_{CU}^2 - 1.08128498143403E + 00 * A_{CU} + \\
 & 3.77137798800870E + 02
 \end{aligned}
 \tag{143}$$

For 60 Hz and 105°C:

$$\begin{aligned}
 A_{Air} = & 1.19408108397020E - 18 * A_{CU}^6 - 1.79955215496484E - 14 * A_{CU}^5 + \\
 & 1.11208936700212E - 10 * A_{CU}^4 - 3.61123507833422E - 07 * A_{CU}^3 +
 \end{aligned}
 \tag{144}$$

$$9.84156415836556E - 04 * A_{CU}^2 - 1.12578693992406E + 00 * A_{CU} + \\ 4.08342631132636 + 02$$

For 50 Hz and 90°C:

$$A_{Air} = 1.07171713483463E - 18 * A_{CU}^6 - 1.73277688405018E - 14 * A_{CU}^5 + \\ 1.15091119088856E - 10 * A_{CU}^4 - 4.02462545808335E - 07 * A_{CU}^3 + \\ 1.07360354422799E - 03 * A_{CU}^2 - 1.31310441145641E + 00 * A_{CU} + \\ 5.33897142246036E + 02 \quad (145)$$

For 50 Hz and 105°C:

$$A_{Air} = 1.07063579005418E - 18 * A_{CU}^6 - 1.76945120426135E - 14 * A_{CU}^5 + \\ 1.20191876945413E - 10 * A_{CU}^4 - 4.30018744773316E - 07 * A_{CU}^3 + \\ 1.13414127335248E - 03 * A_{CU}^2 - 1.41003447701232E + 00 * A_{CU} + \\ 5.93785727623285E + 02 \quad (146)$$

Sixth-order polynomial equations are used, each with fifteen point precision in scientific notation. The error on these equations is initially higher and quickly drops to negligible on larger cross-sectional areas. The error can potentially be larger on designs where the bi-media conductors just become optimal, and thus the cross-sectional area is extremely small. It would be unlikely to design a conductor like this anyhow, since segmented copper conductors are more effective than bi-media conductors when first switching from a single medium to two media. This is due to the fact the dual benefit of the lower AC resistance and cost savings in replacing copper with aluminum have not yet crossed an effective point. The error associated with these equations as compared to results obtained with the analytical solution is shown on FIGURE 6-65:

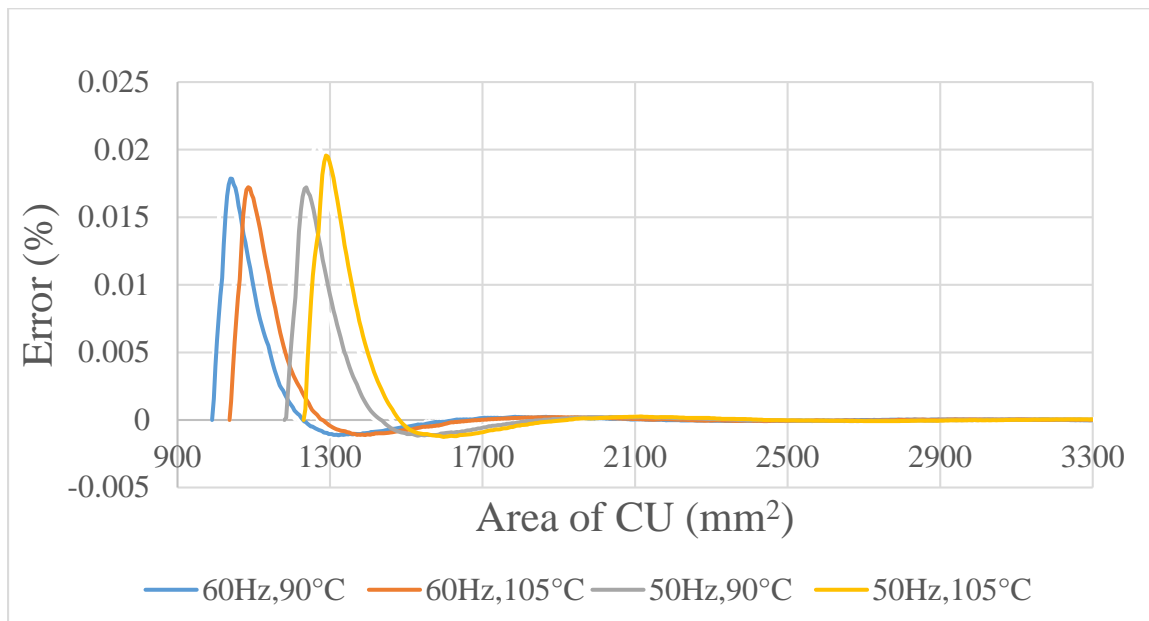


FIGURE 6-65: Error in Air / CU area estimation

As such, the recommended minimum value of each equation is also the starting point of the error plots, summarized on TABLE 6-43:

TABLE 6-43: Minimum recommended area for AL / CU polynomial equations

Frequency	Temperature	Area
Hz	°C	mm ²
60	90	995
	105	1030
50	90	1150
	105	1185

Like the Air / CU polynomial equations, the AL / CU polynomial equations were found using polynomial regression. Unlike the Air / CU equations where the input is the cross-sectional area of the copper, the AL / CU equations are setup such that the input is the total area of the conductor. This is generally what is wanted, only for Air / CU the total metallic area is that of the copper alone. So, for an AL / CU conductor, using the required total cross-sectional area as the input the result is the cross-sectional area of the aluminum core. Using these two areas, again all the pertinent characteristics of the conductor can be

calculated. In this case they include inner/outer radii, DC resistance at any operating temperature, skin effect input argument, skin effect factor, and ultimately AC resistance at any operating temperature. Note in this case the skin effect coefficient k_s is always one. The four separate equations, also based on different operating temperatures and frequencies are:

For 60 Hz and 90°C:

$$\begin{aligned}
 A_{AL} = & 2.27233034121657E - 19 * A_T^6 - 5.40220523439884E - 15 * A_T^5 + \\
 & 5.12826808869369E - 11 * A_T^4 - 2.46885753144709E - 07 * A_T^3 + \\
 & 6.51728141057046E - 04 * A_T^2 - 4.11885885752697E - 01 * A_T - \\
 & 2.95777588460297E + 01
 \end{aligned} \tag{147}$$

For 60 Hz and 105°C:

$$\begin{aligned}
 A_{AL} = & 2.31465023269955E - 19 * A_T^6 - 5.55869109798586E - 15 * A_T^5 + \\
 & 5.34582879602743E - 11 * A_T^4 - 2.61563735270292E - 07 * A_T^3 + \\
 & 7.01474911245554E - 04 * A_T^2 - 4.96583753625960E - 01 * A_T + \\
 & 4.08626114751126E + 00
 \end{aligned} \tag{148}$$

For 50 Hz and 90°C:

$$\begin{aligned}
 A_{AL} = & 2.44675579400316E - 19 * A_T^6 - 6.04590109451908E - 15 * A_T^5 + \\
 & 6.03170190079064E - 11 * A_T^4 - 3.09115255315304E - 07 * A_T^3 + \\
 & 8.69893069510596E - 04 * A_T^2 - 7.97855108191292E - 01 * A_T + \\
 & 1.40901102410344E + 02
 \end{aligned} \tag{149}$$

For 50 Hz and 105°C:

$$\begin{aligned}
 A_{AL} = & 2.52383039735396E - 19 * A_T^6 - 6.28922567091373E - 15 * A_T^5 + \\
 & 6.34365358862712E - 11 * A_T^4 - 3.29729679547230E - 07 * A_T^3 + \\
 & 9.42277611614648E - 04 * A_T^2 - 9.28339573389156E - 01 * A_T + \\
 & 2.07521460458207E + 02
 \end{aligned}
 \tag{150}$$

The error on these equations behaves exactly as those in the Air / CU designs, and for the same reason. The error associated with these equations as compared to results obtained with the analytical solution are shown on FIGURE 6-66:

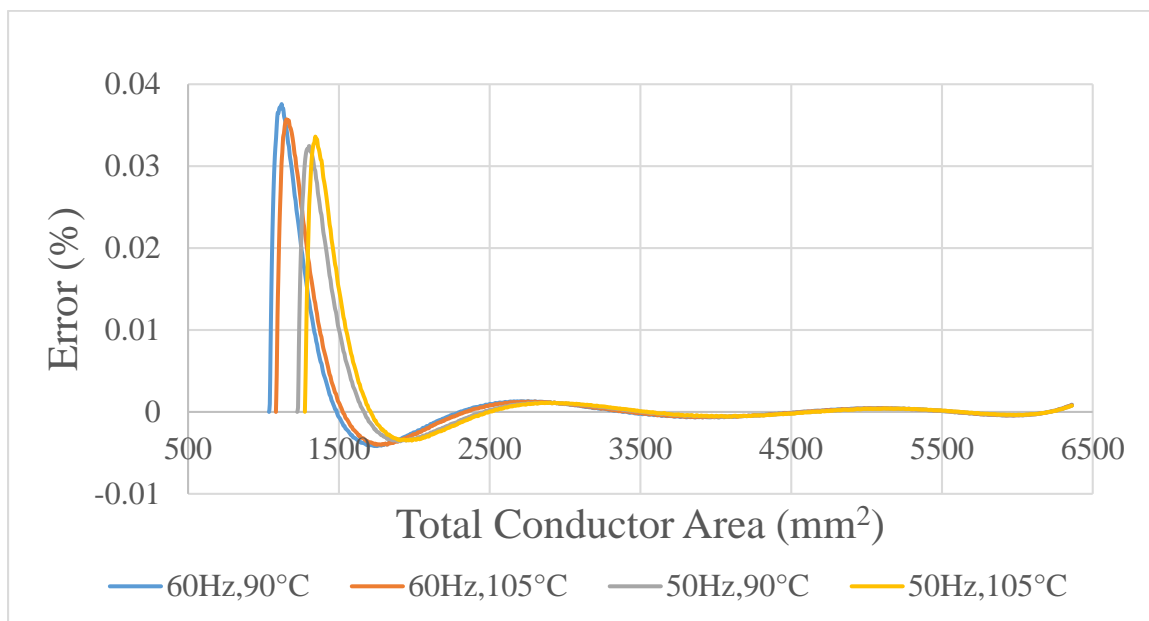


FIGURE 6-66: Error in AL / CU area estimation

As such, the recommended minimum value of each equation is also the starting point of the error plots, summarized on TABLE 6-44:

TABLE 6-44: Minimum recommended area for Air / CU polynomial equations

Frequency	Temperature	Area
Hz	°C	mm ²
60	90	1040
	105	1085
50	90	1225
	105	1275

6.5 Selection Methodology

The selection of the most cost effective design is the most important factor in the design of the conductor in the industry. As was seen on the tables, this depends on the price ratio of copper to aluminum. Copper is generally in the vicinity of three times the cost of aluminum. Therefore, a case study on the most cost effective design has been done using two, three, and four times multipliers. The cost difference (delta) in materials for the bi-media design is compared to that of only copper, as used in segmented conductors. Because the Air / CU conductors have only copper, the multiplier of aluminum to copper is irrelevant. On some of the smaller nominal cross-sectional area designs it can be observed that the AL / CU design has the same cost delta for two to four times. The reason for this is that the design is not optimal, and therefore there is no aluminum in it. Hence, as for the Air / CU conductors the cost delta is independent of the aluminum to copper multiplier. The following tables have cells color coded red when the cost delta is greater than zero, or alternatively segmented is the most cost effective design. This is the exact opposite when the cells are color coded green. In some cells color coded green “Mixed” is seen to indicate the most cost effective design is that of a bi-media conductor, but could be Air / CU or AL / CU depending on the cost ratio of copper to aluminum. Note that all these summarized points refer specifically to a two, three, or four times aluminum to copper multiplier in cost. TABLE 6-45 through TABLE 6-60 summarizes the results of the most

cost effect design for each operating temperature, frequency, and k_s value of the segmented conductor and bi-media designs of the same AC resistance:

TABLE 6-45: Cost deltas of bi-media designs (60 Hz, 90°C, $k_s=0.8$)

Nominal Area mm ²	Cost Delta (%)				Most Cost Effective Design
	Air / CU	AL / CU			
		\$Cu/\$Al = 2X	\$Cu/\$Al = 3X	\$Cu/\$Al = 4X	
800	5.1%	5.1%	5.1%	5.1%	Segmented
1000	6.4%	5.4%	5.2%	5.2%	Segmented
1200	4.9%	2.2%	1.8%	1.6%	Segmented
1400	2.1%	-1.4%	-2.2%	-2.5%	AL / CU
1600	-1.1%	-4.5%	-5.5%	-6.0%	AL / CU
2000	-7.7%	-9.4%	-10.8%	-11.5%	AL / CU
2500	-15.0%	-14.1%	-15.8%	-16.6%	Mixed
3000	-21.1%	-17.7%	-19.7%	-20.6%	Air / CU

TABLE 6-46: Cost deltas of bi-media designs (60 Hz, 105°C, $k_s=0.8$)

Nominal Area mm ²	Cost Delta (%)				Most Cost Effective Design
	Air / CU	AL / CU			
		\$Cu/\$Al = 2X	\$Cu/\$Al = 3X	\$Cu/\$Al = 4X	
800	4.7%	4.7%	4.7%	4.7%	Segmented
1000	6.6%	6.1%	6.0%	6.0%	Segmented
1200	5.5%	3.2%	2.9%	2.7%	Segmented
1400	3.0%	-0.3%	-1.0%	-1.3%	AL / CU
1600	0.0%	-3.5%	-4.4%	-4.9%	AL / CU
2000	-6.3%	-8.5%	-9.8%	-10.5%	AL / CU
2500	-13.5%	-13.1%	-14.8%	-15.6%	Mixed
3000	-19.8%	-17.0%	-18.9%	-19.8%	Mixed

TABLE 6-47: Cost deltas of bi-media designs (50 Hz, 90°C, $k_s=0.8$)

Nominal Area mm ²	Cost Delta (%)				Most Cost Effective Design
	Air / CU	AL / CU			
		\$Cu/\$Al = 2X	\$Cu/\$Al = 3X	\$Cu/\$Al = 4X	
800	3.5%	3.5%	3.5%	3.5%	Segmented
1000	5.6%	5.6%	5.6%	5.6%	Segmented
1200	6.6%	5.9%	5.8%	5.7%	Segmented
1400	5.2%	2.8%	2.4%	2.2%	Segmented
1600	3.1%	-0.2%	-0.9%	-1.2%	AL / CU
2000	-2.3%	-5.5%	-6.6%	-7.2%	AL / CU
2500	-8.9%	-10.2%	-11.7%	-12.4%	AL / CU
3000	-15.0%	-14.1%	-15.8%	-16.6%	Mixed

TABLE 6-48: Cost deltas of bi-media designs (50 Hz, 105°C, $k_s=0.8$)

Nominal Area mm ²	Cost Delta (%)				Most Cost Effective Design
	Air / CU	AL / CU			
		\$Cu/\$Al = 2X	\$Cu/\$Al = 3X	\$Cu/\$Al = 4X	
800	3.2%	3.2%	3.2%	3.2%	Segmented
1000	5.1%	5.1%	5.1%	5.1%	Segmented
1200	6.7%	6.5%	6.4%	6.4%	Segmented
1400	5.8%	3.8%	3.5%	3.3%	Segmented
1600	3.9%	0.8%	0.3%	0.0%	AL / CU
2000	-1.1%	-4.5%	-5.5%	-6.0%	AL / CU
2500	-7.5%	-9.3%	-10.7%	-11.4%	AL / CU
3000	-13.5%	-13.1%	-14.7%	-15.6%	Mixed

TABLE 6-49: Cost deltas of bi-media designs (60 Hz, 90°C, $k_s=0.62$)

Nominal Area mm ²	Cost Delta (%)				Most Cost Effective Design
	Air / CU	AL / CU			
		\$Cu/\$Al = 2X	\$Cu/\$Al = 3X	\$Cu/\$Al = 4X	
800	9.5%	9.5%	9.5%	9.5%	Segmented
1000	12.3%	10.5%	10.2%	10.1%	Segmented
1200	11.9%	8.5%	7.8%	7.5%	Segmented
1400	10.3%	6.4%	5.4%	4.8%	Segmented
1600	8.0%	5.0%	3.6%	2.9%	Segmented
2000	2.5%	2.7%	0.8%	-0.1%	Mixed
2500	-4.3%	0.0%	-2.3%	-3.5%	Air / CU
3000	-10.6%	-3.3%	-6.0%	-7.3%	Air / CU

TABLE 6-50: Cost deltas of bi-media designs (60 Hz, 105°C, $k_s=0.62$)

Nominal Area mm ²	Cost Delta (%)				Most Cost Effective Design
	Air / CU	AL / CU			
		\$Cu/\$Al = 2X	\$Cu/\$Al = 3X	\$Cu/\$Al = 4X	
800	8.7%	8.7%	8.7%	8.7%	Segmented
1000	12.2%	11.0%	10.8%	10.7%	Segmented
1200	12.2%	9.1%	8.6%	8.3%	Segmented
1400	10.9%	7.0%	6.0%	5.6%	Segmented
1600	8.9%	5.5%	4.2%	3.5%	Segmented
2000	3.8%	3.3%	1.5%	0.6%	Segmented
2500	-2.9%	0.7%	-1.6%	-2.8%	Air / CU
3000	-9.0%	-2.4%	-5.0%	-6.2%	Air / CU

TABLE 6-51: Cost deltas of bi-media designs (50 Hz, 90°C, $k_s=0.62$)

Nominal Area mm ²	Cost Delta (%)				Most Cost Effective Design
	Air / CU	AL / CU			
		\$Cu/\$Al = 2X	\$Cu/\$Al = 3X	\$Cu/\$Al = 4X	
800	6.5%	6.5%	6.5%	6.5%	Segmented
1000	10.5%	10.5%	10.5%	10.5%	Segmented
1200	12.3%	10.8%	10.6%	10.5%	Segmented
1400	12.1%	8.8%	8.3%	8.0%	Segmented
1600	10.9%	7.1%	6.1%	5.7%	Segmented
2000	7.1%	4.6%	3.1%	2.3%	Segmented
2500	1.3%	2.3%	0.3%	-0.7%	Mixed
3000	-4.3%	0.0%	-2.3%	-3.5%	Air / CU

TABLE 6-52: Cost deltas of bi-media designs (50 Hz, 105°C, $k_s=0.62$)

Nominal Area mm ²	Cost Delta (%)				Most Cost Effective Design
	Air / CU	AL / CU			
		\$Cu/\$Al = 2X	\$Cu/\$Al = 3X	\$Cu/\$Al = 4X	
800	5.9%	5.9%	5.9%	5.9%	Segmented
1000	9.6%	9.6%	9.6%	9.6%	Segmented
1200	12.1%	11.3%	11.1%	11.1%	Segmented
1400	12.3%	9.5%	9.0%	8.8%	Segmented
1600	11.4%	7.7%	6.8%	6.4%	Segmented
2000	8.1%	5.0%	3.6%	2.9%	Segmented
2500	2.6%	2.8%	0.9%	-0.1%	Mixed
3000	-2.8%	0.7%	-1.6%	-2.7%	Air / CU

As is next shown on TABLE 6-53 to TABLE 6-56, a k_s of 0.435 has no cost effective solution versus segmented copper. However, it is still interesting to see the increased cost over segmented copper of such designs. For example, construction of a segmented copper conductor may not be possible depending on available equipment or weight limitations. Additionally, segmented copper has the additional cost of twisting the segments together, which is a costly operation. Such cost deltas are beneficial here in evaluating the possibility of constructing a conductor design more costly in terms of raw materials, but potentially less costly in terms of total construction.

TABLE 6-53: Cost deltas of bi-media designs (60 Hz, 90°C, $k_s=0.435$)

Nominal Area mm ²	Cost Delta (%)				Most Cost Effective Design
	Air / CU	AL / CU			
		\$Cu/\$Al = 2X	\$Cu/\$Al = 3X	\$Cu/\$Al = 4X	
800	13.4%	13.4%	13.4%	13.4%	Segmented
1000	17.6%	15.1%	14.7%	14.5%	Segmented
1200	18.5%	14.5%	13.6%	13.2%	Segmented
1400	18.4%	14.7%	13.3%	12.6%	Segmented
1600	17.6%	15.7%	13.8%	12.9%	Segmented
2000	14.5%	18.2%	15.6%	14.3%	Segmented
2500	9.5%	19.0%	15.7%	14.0%	Segmented
3000	4.0%	17.1%	13.2%	11.3%	Segmented

TABLE 6-54: Cost deltas of bi-media designs (60 Hz, 105°C, $k_s=0.435$)

Nominal Area mm ²	Cost Delta (%)				Most Cost Effective Design
	Air / CU	AL / CU			
		\$Cu/\$Al = 2X	\$Cu/\$Al = 3X	\$Cu/\$Al = 4X	
800	12.1%	12.1%	12.1%	12.1%	Segmented
1000	17.1%	15.3%	15.0%	14.9%	Segmented
1200	18.3%	14.6%	13.9%	13.6%	Segmented
1400	18.6%	14.5%	13.3%	12.7%	Segmented
1600	18.0%	15.3%	13.6%	12.7%	Segmented
2000	15.3%	17.7%	15.3%	14.0%	Segmented
2500	10.6%	19.1%	15.9%	14.3%	Segmented
3000	5.4%	17.7%	14.0%	12.1%	Segmented

TABLE 6-55: Cost deltas of bi-media designs (50 Hz, 90°C, $k_s=0.435$)

Nominal Area mm ²	Cost Delta (%)				Most Cost Effective Design
	Air / CU	AL / CU			
		\$Cu/\$Al = 2X	\$Cu/\$Al = 3X	\$Cu/\$Al = 4X	
800	8.9%	8.9%	8.9%	8.9%	Segmented
1000	14.8%	14.8%	14.8%	14.8%	Segmented
1200	17.3%	15.2%	14.9%	14.7%	Segmented
1400	18.4%	14.6%	13.8%	13.4%	Segmented
1600	18.6%	14.5%	13.3%	12.7%	Segmented
2000	17.2%	16.2%	14.2%	13.2%	Segmented
2500	13.7%	18.6%	15.8%	14.4%	Segmented
3000	9.5%	19.0%	15.7%	14.0%	Segmented

TABLE 6-56: Cost deltas of bi-media designs (50 Hz, 105°C, $k_s=0.435$)

Nominal Area mm ²	Cost Delta (%)				Most Cost Effective Design
	Air / CU	AL / CU			
		\$Cu/\$Al = 2X	\$Cu/\$Al = 3X	\$Cu/\$Al = 4X	
800	8.1%	8.1%	8.1%	8.1%	Segmented
1000	13.4%	13.4%	13.4%	13.4%	Segmented
1200	16.8%	15.4%	15.2%	15.1%	Segmented
1400	18.2%	14.7%	14.1%	13.8%	Segmented
1600	18.6%	14.5%	13.4%	12.9%	Segmented
2000	17.6%	15.7%	13.9%	12.9%	Segmented
2500	14.6%	18.2%	15.6%	14.3%	Segmented
3000	10.6%	19.1%	15.9%	14.3%	Segmented

TABLE 6-57 to TABLE 6-60 represents enameled copper wires, as a k_s of 0.35 is used. For this a price increase of 15% was assumed over the cost of bare copper wire, which is what it currently is since the cost increase of enameled wire is 30% and 50% of strands are enameled).

TABLE 6-57: Cost deltas of bi-media designs (60 Hz, 90°C, $k_s=0.35$)

Nominal Area mm ²	Cost Delta (%)				Most Cost Effective Design
	Air / CU	AL / CU			
		\$Cu/\$Al = 2X	\$Cu/\$Al = 3X	\$Cu/\$Al = 4X	
800	0.0%	0.0%	0.0%	0.0%	Mixed
1000	4.1%	1.7%	1.3%	1.1%	Segmented
1200	5.4%	1.7%	0.9%	0.5%	Segmented
1400	6.0%	2.8%	1.5%	0.8%	Segmented
1600	5.9%	4.8%	3.0%	2.1%	Segmented
2000	4.4%	9.3%	6.7%	5.4%	Segmented
2500	1.3%	12.0%	8.6%	6.9%	Segmented
3000	-2.5%	11.7%	7.7%	5.7%	Air / CU

TABLE 6-58: Cost deltas of bi-media designs (60 Hz, 105°C, $k_s=0.35$)

Nominal Area mm ²	Cost Delta (%)				Most Cost Effective Design
	Air / CU	AL / CU			
		\$Cu/\$Al = 2X	\$Cu/\$Al = 3X	\$Cu/\$Al = 4X	
800	-1.3%	-1.3%	-1.3%	-1.3%	Mixed
1000	3.6%	1.7%	1.5%	1.3%	Segmented
1200	5.1%	1.7%	1.0%	0.6%	Segmented
1400	5.9%	2.4%	1.2%	0.6%	Segmented
1600	6.0%	4.0%	2.4%	1.6%	Segmented
2000	4.8%	8.4%	6.0%	4.7%	Segmented
2500	2.0%	11.7%	8.4%	6.8%	Segmented
3000	-1.5%	12.0%	8.1%	6.2%	Air / CU

TABLE 6-59: Cost deltas of bi-media designs (50 Hz, 90°C, $k_s=0.35$)

Nominal Area mm ²	Cost Delta (%)				Most Cost Effective Design
	Air / CU	AL / CU			
		\$Cu/\$Al = 2X	\$Cu/\$Al = 3X	\$Cu/\$Al = 4X	
800	-4.4%	-4.4%	-4.4%	-4.4%	Mixed
1000	1.4%	1.3%	1.3%	1.3%	Segmented
1200	3.8%	1.7%	1.4%	1.3%	Segmented
1400	5.2%	1.7%	0.9%	0.6%	Segmented
1600	5.9%	2.4%	1.2%	0.6%	Segmented
2000	5.7%	5.7%	3.7%	2.7%	Segmented
2500	4.0%	10.0%	7.2%	5.9%	Segmented
3000	1.3%	12.0%	8.6%	6.9%	Segmented

TABLE 6-60: Cost deltas of bi-media designs (50 Hz, 105°C, $k_s=0.35$)

Nominal Area mm ²	Cost Delta (%)				Most Cost Effective Design
	Air / CU	AL / CU			
		\$Cu/\$Al = 2X	\$Cu/\$Al = 3X	\$Cu/\$Al = 4X	
800	-5.2%	-5.2%	-5.2%	-5.2%	Mixed
1000	0.0%	0.0%	0.0%	0.0%	Mixed
1200	3.2%	1.8%	1.5%	1.4%	Segmented
1400	4.9%	1.7%	1.0%	0.7%	Segmented
1600	5.7%	2.0%	1.0%	0.5%	Segmented
2000	5.9%	4.8%	3.0%	2.1%	Segmented
2500	4.4%	9.2%	6.6%	5.3%	Segmented
3000	2.0%	11.7%	8.4%	6.8%	Segmented

TABLE 6-61 summarizes all of the preceding tables. In TABLE 6-61 some cells color coded yellow. In this case segmented or a bi-media conductor may be most cost effective, depending on the operating temperature and frequency. When “Mixed” is seen it indicates the most cost effective design is that of a bi-media conductor, but it may be either Air / CU or AL / CU depending on temperature and frequency.

TABLE 6-61: Cost deltas summary table

Nominal Area	Most Cost Effective Design			
	$k_s = 0.8$	$k_s = 0.62$	$k_s = 0.435$	$k_s = 0.35$
800	Segmented	Segmented	Segmented	Mixed
1000	Segmented	Segmented	Segmented	Segmented
1200	Segmented	Segmented	Segmented	Segmented
1400	AL / CU	Segmented	Segmented	Segmented
1600	AL / CU	Segmented	Segmented	Segmented
2000	AL / CU	Mixed	Segmented	Segmented
2500	Mixed	Mixed	Segmented	Segmented
3000	Mixed	Air / CU	Segmented	Mixed

From this it can be observed that generally bi-media conductors have an application range that becomes viable at a certain cross-sectional area. Additionally, the range when this happens is higher the lower the k_s value. It is also interesting that due to the large expense of enameled copper wires, enameled segmented conductors are never the most economical. Note that there is also the question of practical constructability that varies between the capabilities of different manufacturers. These tables indicate what design is most cost effective, but the individual manufacturer has to be able to implement it.

To demonstrate the simple usage of designing a bi-media conductor an example is now presented. First, what would be the AC resistance at a full operating temperature of 105°C of optimally designed nominal cross-sectional area 2000 mm² bi-media conductors (i.e. designs that minimize AC resistance) at 50 Hz? Since standardized tables have been presented the cross-sectional areas, DC resistance at 20°C, and radii can all be directly looked up. However, this is done as an example using the equations to demonstrate the process. This process applies to any sized conductor, but by using a standardized value the accuracy can be checked versus a known and already tabulated solution found using the analytical equations derived for bi-media. Note that due to the error of the polynomial

equations results differ from table values very slightly. Recall that the true area calculated based on DC resistance of a nominal 2000 mm² conductor is 1915.7 mm². Using this first in the equation of the Air / CU conductor at 105°C and 50 Hz to get the area of the air core yields:

$$\begin{aligned}
 A_{Air} = & 1.07063579005418E - 18 * (1915.7)^6 - 1.76945120426135E - 14 * (1915.7)^5 + \\
 & 1.20191876945413E - 10 * (1915.7)^4 - 4.30018744773316E - 07 * (1915.7)^3 + \\
 & 1.13414127335248E - 03 * (1915.7)^2 - 1.41003447701232E + 00 * (1915.7) + \\
 & 5.93785727623285E + 02 = 246.71 \text{ mm}^2
 \end{aligned} \tag{151}$$

Using the areas, the solid conductor radii can be calculated as:

$$r_1 = \sqrt{\frac{A_{Air}}{\pi}} = \sqrt{\frac{246.71}{\pi}} = 8.86 \text{ mm} \tag{152}$$

$$r_2 = \sqrt{\frac{A_{Air} + A_{CU}}{\pi}} = \sqrt{\frac{246.71 + 1915.7}{\pi}} = 26.24 \text{ mm} \tag{153}$$

Using the copper area the DC resistance of the conductor at 20°C is:

$$R_0 = \frac{\rho L}{A_{CU}} = \frac{1.7241 \times 10^{-8} \times 1}{1915.7 \times 10^{-6}} = 9 \times 10^{-6} \text{ ohm/m} \tag{154}$$

Therefore, the DC resistance of the conductor 105°C is:

$$\begin{aligned}
 R_{dc} &= R_0 [1 + \alpha_{20}(\theta - 20)] = R_0 [1 + 0.00393(105 - 20)] \\
 &= 1.2006 \times 10^{-5} \text{ ohm/m}
 \end{aligned} \tag{155}$$

The skin effect coefficient for this conductor is:

$$k_s = \left(\frac{d'_c - d_i}{d'_c + d_i} \right) \left(\frac{d'_c + 2d_i}{d'_c + d_i} \right)^2 = \tag{156}$$

$$\left(\frac{2 * 26.24 - 2 * 8.86}{2 * 26.24 + 2 * 8.86}\right) \left(\frac{2 * 26.24 + 2 * 2 * 8.86}{2 * 26.24 + 2 * 8.86}\right)^2 = 0.7767$$

The Bessel input argument is:

$$x_s = \sqrt{\frac{8\pi f}{R_{dc}} 10^{-7} k_s} = \sqrt{\frac{8\pi \cdot 50}{1.2006 \times 10^{-5}} 10^{-7} \cdot 0.7767} = 2.851 \quad (157)$$

Since $2.8 < x_s \leq 3.8$:

$$\begin{aligned} y_s &= -0.136 - 0.0177x_s + 0.0563x_s^2 = \\ &-0.136 - 0.0177 \cdot 2.851 + 0.0563 \cdot (2.851)^2 = 0.271 \end{aligned} \quad (158)$$

And therefore the AC resistance at 105°C is:

$$\begin{aligned} R_{ac} &= R_{dc}(1 + y_s + y_p) = 1.2006 \times 10^{-5} (1 + 0.271 + 0) \\ &= 1.526 \times 10^{-5} \text{ ohm/m} \end{aligned} \quad (159)$$

Note that the proximity effect is ignored here, and thus proximity effect factor is zero. This nearly identical method is also followed for the AL / CU conductor. At 105°C and 50 Hz to get the area of the aluminum core:

$$\begin{aligned} A_{AL} &= 2.52383039735396E - 19 * (1915.7)^6 - 6.28922567091373E - 15 * (1915.7)^5 + \\ &6.34365358862712E - 11 * (1915.7)^4 - 3.29729679547230E - 07 * (1915.7)^3 + \\ &9.42277611614648E - 04 * (1915.7)^2 - 9.28339573389156E - 01 * (1915.7) + \\ &2.07521460458207E + 02 = 273.61 \text{ mm}^2 \end{aligned} \quad (160)$$

In this case the copper area is:

$$A_{CU} = A_T - A_{AL} = 1915.7 - 273.61 = 1642.1 \text{ mm}^2 \quad (161)$$

It can be seen that in both cases of the Air / CU and AL / CU the total cross-sectional area of the conductor is 1915.7 mm^2 , which corresponds to the true area of a nominal 2000 mm^2 conductor. Using the areas, the solid conductor radii can be calculated as:

$$r_1 = \sqrt{\frac{A_{AL}}{\pi}} = \sqrt{\frac{273.61}{\pi}} = 9.33 \text{ mm} \quad (162)$$

$$r_2 = \sqrt{\frac{A_{AL} + A_{CU}}{\pi}} = \sqrt{\frac{273.61 + 1642.1}{\pi}} = 24.69 \text{ mm} \quad (163)$$

Using the copper area the copper DC resistance of the conductor at 20°C is:

$$R_{02} = \frac{\rho L}{A_{CU}} = \frac{1.7241 \times 10^{-8} \times 1}{1642.1 \times 10^{-6}} = 1.0499 \times 10^{-5} \text{ ohm/m} \quad (164)$$

Therefore, the copper DC resistance of the conductor 105°C is:

$$\begin{aligned} R_{dc2} &= R_{02}[1 + \alpha_{20}(\theta - 20)] = R_0[1 + 0.00393(105 - 20)] \\ &= 1.4007 \times 10^{-5} \text{ ohm/m} \end{aligned} \quad (165)$$

Using the aluminum area the aluminum DC resistance of the conductor at 20°C is:

$$R_{01} = \frac{\rho L}{A_{AL}} = \frac{2.8264 \times 10^{-8} \times 1}{273.61 \times 10^{-6}} = 1.033 \times 10^{-4} \text{ ohm/m} \quad (166)$$

Therefore, the aluminum DC resistance of the conductor 105°C is:

$$\begin{aligned} R_{dc1} &= R_{01}[1 + \alpha_{20}(\theta - 20)] = R_0[1 + 0.00403(105 - 20)] \\ &= 1.3869 \times 10^{-4} \text{ ohm/m} \end{aligned} \quad (167)$$

Therefore, the total conductor DC resistance at 105°C is:

$$R_{dc} = \frac{1}{\frac{1}{R_{dc1}} + \frac{1}{R_{dc2}}} = 1.2722 \times 10^{-5} \text{ ohm/m} \quad (168)$$

The skin effect coefficient for the AL / CU conductor is always one. Therefore, the Bessel input argument is:

$$x_s = \sqrt{\frac{8\pi f}{R_{dc}} 10^{-7} k_s} = \sqrt{\frac{8\pi \cdot 50}{1.2722 \times 10^{-5}} 10^{-7} \cdot 1} = 3.1429 \quad (169)$$

Using the newly derived skin effect factor equations, for $x_s \geq 2.7$:

$$\begin{aligned} y_s &= -0.01516x_s^3 + 0.20012x_s^2 - 0.57637x_s + 0.61188 \\ &= -0.01516 \cdot (3.1429)^3 + 0.20012 \cdot (3.1429)^2 - \\ &\quad 0.57637 \cdot (3.1429) + 0.61188 = 0.3065 \end{aligned} \quad (170)$$

And therefore the AC resistance at 105°C is:

$$\begin{aligned} R_{ac} &= R_{dc}(1 + y_s + y_p) = 1.2722 \times 10^{-5}(1 + 0.3065 + 0) \\ &= 1.6621 \times 10^{-5} \text{ ohm/m} \end{aligned} \quad (171)$$

Thus, at 50 Hz and 105°C the Air / CU conductor has a lower resistance and therefore higher ampacity than the AL / CU conductor. However, the total cross-sectional areas in both designs is the same. This means that the AL / CU conductor always must be less expensive, assuming the cost of copper is more than aluminum. Therefore, cost effectiveness this does not tell the whole story. This is also why the tables were generated for bi-media conductors with equal AC resistance to segmented conductors for all skin effect coefficients influencing their AC resistance. This allows for a true apples to apples comparison in terms of material costs.

To implement this the easiest way is to setup the equations in either a spreadsheet (e.g. Microsoft® Excel) or a programming software (e.g. MATLAB). After calculating the AC resistance of the segmented copper conductor following the methods of the industry

standards, an iterative approach can be used to programmatically find the correct cross-sectional area of the copper in the Air / CU conductors or total area required in the AL / CU conductors. Excel even has a goal seek function built in for this commonly sought after approach. In this case one would goal seek the desired AC resistance (i.e. that of the segmented copper conductor) by changing either the area of the copper in the Air / CU conductors or total area required in the AL / CU conductors. These were the values used as inputs in the example solved above, but by iteratively changing this input a desired output can be achieved instead.

A second example is now presented using this iterative technique to find the most cost effective design, and possible replacement of a 2500 mm² segmented copper conductor. It is assumed here that any non-standardized sized conductor is acceptable for the design. It is further assumed the segmented conductor is bi-directionally stranded and operating at 90°C and 60 Hz. First is to find the AC resistance of the segmented copper conductor. The DC resistance at 20°C is already provided in the standards [92], therefore the DC resistance of the conductor 90°C is:

$$\begin{aligned} R_{dc} &= R_0[1 + \alpha_{20}(\theta - 20)] = 7.2 \times 10^{-6}[1 + 0.00393(90 - 20)] \\ &= 9.1807 \times 10^{-6} \text{ ohm/m} \end{aligned} \quad (172)$$

The skin effect coefficient provided in the standards for this design is $k_s = 0.8$ [15].

Therefore, the Bessel input argument is:

$$x_s = \sqrt{\frac{8\pi f}{R_{dc}} 10^{-7} k_s} = \sqrt{\frac{8\pi \cdot 60}{9.1807 \times 10^{-6}} 10^{-7} \cdot 0.8} = 3.625 \quad (173)$$

Since $2.8 < x_s \leq 3.8$:

$$\begin{aligned}
 y_s &= -0.136 - 0.0177x_s + 0.0563x_s^2 = \\
 &-0.136 - 0.0177 \cdot 3.625 + 0.0563 \cdot (3.625)^2 = 0.54
 \end{aligned} \tag{174}$$

And therefore the AC resistance at 90°C is:

$$R_{ac} = R_{dc}(1 + y_s + y_p) = 9.1807 \times 10^{-6}(1 + 0.54 + 0) = 1.4135 \times 10^{-5} \tag{175}$$

To match this AC resistance, the iterative method described above was implemented simply in Microsoft® Excel. This resulted in a cross-sectional area of 567.9 / 2032.6 mm² for the Air / CU design and 814.1 / 1937 mm² for the AL / CU design. Note that these vary from the table values found using the analytical solution by 0.05% to 0.53%, which by the time the AC resistance is calculated the error range is only 0.06% to 0.14%. Therefore, the polynomial approximations are very accurate. In order to compare the cost effectiveness the weights of the materials need to be calculated. Therefore, metal weight of the copper used in the segmented copper conductor is (recalling the true area of a nominal 2500 mm² copper conductor is 2394.6 mm²):

$$W_{S_{Cu}} = 8.93 \cdot 2394.6 \cdot 0.001 = 21.38 \text{ kg/m} \tag{176}$$

The metal weight of the copper used in the Air / CU conductor is:

$$W_{AirCu_{Cu}} = 8.93 \cdot 2032.6 \cdot 0.001 = 18.15 \text{ kg/m} \tag{177}$$

The metal weights of the aluminum and copper used in the AL / CU conductor is:

$$W_{AlCu_{Al}} = 2.7 \cdot 814.1 \cdot 0.001 = 2.2 \text{ kg/m} \tag{178}$$

$$W_{AlCu_{Cu}} = 8.93 \cdot 1937 \cdot 0.001 = 17.3 \text{ kg/m} \tag{179}$$

From these results it can be immediately seen that both bi-media designs have less copper and therefore a lower weight of copper material usage. Therefore, the Air / CU

conductor must always be less expensive than the segmented copper conductor. The cost effectiveness of the AL / CU conductor depends on the price ratio of copper to aluminum. The weight of the copper in the AL / CU design is less than that of the segmented copper conductor, so the only way the segmented conductor could be more cost effective is if the price of aluminum were more than that of copper. The cost ratio can be found using the weights of the materials, but these are also provided on the tables detailing the replacement of segmented copper conductors with bi-media conductors of equal AC resistance. The calculation of the ratio where the material price of the segmented copper and AL / CU conductor is equal is shown here:

$$\frac{\$Cu}{\$Al} = \frac{W_{ALCu_Al}}{W_{S_Cu} - W_{ALCu_Cu}} = \frac{2.2}{21.38 - 17.3} = 0.5392 \quad (180)$$

Assuming a price ratio of three, which is closest to present day pricing, the cost deltas calculated next. The cost delta for the Air / Cu compared to the all segmented copper is:

$$CD = 100 \times \frac{W_{AirCu_Cu} - W_{S_Cu}}{W_{S_Cu}} = \frac{18.15 - 21.38}{21.38} = -15.1\% \quad (181)$$

Thus, the Air / CU design uses 15.1% less copper than the segmented copper design and is therefore -15.1% less expensive in terms of materials. Finally, the AL / CU conductor cost delta compared to the all segmented copper is:

$$CD = 100 \times \frac{W_{ALCu_Cu} + \frac{W_{ALCu_Al}}{\$Cu/\$Al} - W_{S_Cu}}{W_{S_Cu}} = \frac{17.3 + \frac{2.2}{3} - 21.38}{21.38} = -15.7\% \quad (182)$$

Thus, the AL / CU design is 15.7% less expensive in terms of materials. Therefore, overall the most cost effect choice for a conductor operating at 60 Hz and 90°C is the AL / CU conductor design.

CHAPTER 7: CONCLUSIONS

7.1 Overview

This chapter concludes the dissertation. It begins with a recap of the major contributions that were made within this document. There is also some commentary on these contributions, for example about their accuracy, assumption or range of applicability. The chapter is concluded with a look ahead through the doors that have been opened up as a result of the contributions made. Some recommendations for future work are proposed, for the vision of where this author sees developments within the realm of large power conductors. However, it should always be kept in mind that the theory of bi-media conductors holds true across the entire gamut of frequencies. Therefore, endless possibilities may open up as other technologies improve. For example, high frequencies are used in technologies such as radio and communications, but more of an overdesign approach is taken due to limitations in manufacturing (e.g. plating). However, as technology and manufacturing evolve the theory holds true and allows for minimizing waste by optimizing designs at all frequencies, relative to the properties of the materials used.

7.2 Summary of Contributions

The major contribution of this research was the development of the bi-media conductor AC resistance model. Although focused on large power conductors, this theory is true for all frequencies provided that the assumptions described throughout the

dissertation are maintained. Namely, the material is assumed to be linear, isotropic, homogeneous, isothermal and non-ferrous. Furthermore, as the solution can only be derived in cylindrical coordinates the shape must be round. The solution was derived for skin effect, and therefore also AC resistance and inductance of a round bi-media conductor carrying AC current. The analytical solution was derived using current density. The presented solution transcends the three major categories of research in skin effect: design, measurement, and approximation. The design goal was achieved by formulation of the closed-form mathematical solution for calculating skin effect in bi-media conductors, and the analysis into their optimization through the minima of their AC resistance. Whereas this design does exist there was no theory available for calculating skin effect for it. Furthermore, there was no study into the optimization of such designs and the AL / CU conductor design was optimized such that it minimizes AC resistance. The design for the Air / CU conductor had an existing solution, which is a specific case of the more general solution used in the AL / CU conductor. This solution, in general, is applicable to any two media so long as they meet the assumptions listed above. Although the Air / CU solution did exist, it also did not have a study into the analysis of optimizing the conductor based on the minima of the AC resistance.

For the measurement aspect of the contribution two samples were made: a solid conductor and a stranded conductor. Measurements have been made in the past on solid metal, stranded metal, and Air / CU designs. All have confirmed the existing theory of skin effect in such conductors. The measurements here were performed on bi-media AL / CU conductors. The solid AL / CU conductor confirmed the theory on frequencies up to 2 kHz when enough samples per cycle produced accurate results, but it was only able to be

manufactured on a smaller scale. Therefore, higher frequencies were used during testing. A large stranded conductor was also manufactured that is in an ideal size range of applicability of replacement of segmented copper conductors. Additionally, because it was stranded it also confirmed the stranded bi-media conductors behave in the same fashion as single medium stranded conductors. Specifically, stranded conductors have the same skin effect as solid conductors of the same cross-sectional areas.

The final portion of the contribution was in the approximation of the solution. To bring this solution to the industry it is imperative the solution is able to be implemented with more simple tools and equations. Tables were presented in two ways: ones to present standardized sizes of bi-media Air / CU and AL / CU conductors, and tables presented to give the designs of these bi-media conductors to replace segmented copper conductors by having the same AC resistance. Additionally, cost ratios of copper to aluminum were provided so one could know at any point of time if the solution were the most cost effective, depending on the price of copper and aluminum at that point in time. Aside from the table values, all the tools were also provided to design these bi-media conductors using simplified polynomial equations. This included the equations that define the cross-sectional area of the conductors, from which all other properties can be calculated. There is also a formula for calculating the skin effect factor for the AL / CU design. All designs presented in both tables and polynomial equations give results that are optimal designs, in that they represent the minima of the AC resistance possible with a bi-media design.

7.3 Future Vision

It has been shown that there are cost effective ranges for segmented copper conductors, Air / CU conductors, and AL / CU conductors. The bi-media conductors, as

can be seen through the theoretical knowledge developed in this document, hinge upon the behavior of the current density. Knowing this, if an insulating layer could be placed around each individual layer of strands the skin effect may be able to be reduced significantly. Understanding the current density behavior in segmented conductors will also be important to future work. Currently though, the theory has not been fully developed. A future application, once the current density of segmented conductor is more understood, is in hybrid bi-media segmented conductors. In understanding the behavior of the current density the size of the segments could be optimized, and well as the size or even inclusion of the center conductor. Additionally, perhaps a more optimal solution exists with the center of the individual segments being air, aluminum, or even both.

Another possible area of research this dissertation opens up is in more than two media being used. We know that the ideal design of the conductor has the more conductive medium on the outside, which can be replaced in an optimal way with a less conductive medium on the inside. This is because in single medium conductors the current density is always highest on the outside and decreases inward. In a bi-media conductor where a lower conductivity material were used on the outside, the current density also begins to decrease immediately moving radially inward. However, if the material were to switch to a higher conductivity material on the inside it is possible the current density would be higher than at any point on the outside. However, it is not optimal to use a higher conductivity material on the inside. This is because some attenuation of the EM wave has already taken place, so you cannot possibly get as much effectiveness out of the higher conductivity material had it been on the outside to begin with. Even if the high conductivity material were less expensive it would still make sense to use it on the outside to begin with. Especially then

in such a case. The only time it would make sense to use a lower conductivity material on the outside would be if it were only a thin layer for protection of the inner medium. As far as optimizing AC resistance though, it would never help. What is normally found in commonly used good conducting materials is that as conductivity decreases so does cost (e.g. in decreasing order: silver, copper, aluminum). Silver is generally expensive enough it is not worth using as a commonplace conductor. However, optimal designs could exist that are from the outside to inside of the conductor: copper, aluminum, air. To this effect, graded materials may be of research interest also. However, great care must be taken when working with these as they would no longer be homogeneous materials. In any case, a general solution for skin effect using n materials would be of great scientific interest.

Future research using the theory developed here would be interesting for overhead lines. In overhead lines a common design is ACSR conductors, which have a steel core. Therefore, the core is ferrous and additional research needs to be done to see how the magnetization of the core affects the skin effect and AC resistance of the conductor. This becomes a difficult question because the magnetization of the core is dependent upon the ampacity the conductor is carrying. All work done within the dissertation was able to assume the skin effect was independent of the current in the conductor because the media were non-ferrous. This research could also play into that of the general solution. Perhaps some optimal designs exist that use copper, aluminum and steel together in a single design.

The final interesting research note is on the hollow core. Hollow cores are not a new design concept, and have been used in the past for different applications. Some older applications include pumping insulating liquid or gas through the core as a means of insulating the conductor from ground. Other designs, such as super-conductors, have

hollow parts for pumping cooling liquids into. Extruded insulation has become the preferred design of cable, due to environmental and maintenance concerns. Therefore, while the hollow center may not be used for insulating liquid or gas, it may still be of use for cooling the conductor. This could allow for increasing future ampacity rating of the circuit, even if installed in present day as a hollow conductor alone. Another possible application for it would be the inclusion of a DTS fiber. Dynamic rating of conductors is a growing interest, and it hinges heavily upon knowing the temperature of the conductor at any point in time. Currently, the DTS is often placed in a layer of the design away from the conductor or even outside the entire cable design altogether. This leads to inaccurate results and a large time gap due to the high thermal time constant of the surrounding materials before changes of the conductor temperature can be reliably pinpointed at another location. Having the DTS inside the conductor greatly improves this dilemma and can lead to improvements in smart grid technology. This can be used to identify how much overload conductors can take and for how long in real time. This could even be used in conjunction with cooling should requirements of the grid demand the solution. In the end, in an Air / CU conductor the middle is just an empty hole. The possibilities of what can be done with it are only limited to imagination. Hopefully the work done here opens doors through which the creativity of others can work.

REFERENCES

- [1] J. C. Maxwell, "A treatise on electricity and magnetism," *Constable*, vol. 2, p. 692, 1873.
- [2] H. B. Dwight, "Skin effect in tubular and flat conductors," *AIEE Transactions*, vol. 37, pp. 1379-1403, 1918.
- [3] Cigré, "Technical brochure 345: alternating current (AC) resistance of helically stranded conductors," Working Group B2.12, 2008.
- [4] T. Sasaki, "Formation of ultra-fine copper grains in copper-clad aluminum wire," *Scripta Mater*, 2010.
- [5] G. Gaba and M. Abou-Dakka, "A simplified and accurate calculation of frequency dependence conductor impedance," in *Proceedings of the 8th International Conference on Harmonics and Quality of Power*, Athens, Greece, 1998.
- [6] G. Smith, "A simple derivation for the skin effect in a round wire," *European Journal of Physics*, vol. 35, 2014.
- [7] J. Fleming, "On some effects of alternating-current flow in circuits having capacity and self-induction," *Journal Institution of Electrical Engineers*, vol. XX, p. 471, 1891.
- [8] Z. Popovic and B. Popovic, *Introductory Electromagnetics*, Prentice Hall, 1999.
- [9] W. Burpee, "Skin effect current tracing," *IEEE Transactions on Industry Applications*, Vols. IA-13, no. 2, 1977.
- [10] S. Meliopoulos, *Power system grounding and transients*, Marcel Dekker, 1988.
- [11] M. Kosek, M. Truhlar and A. Richter, "Skin effect in massive conductors at technical frequencies," *Electrical Review*, vol. 87, no. 5, 2011.
- [12] C. Liu, S. Kamel and V. Cecchi, "Analysis of AC resistance in non-ferrous bimetallic solid conductors," in *Proceedings of the 2015 IEEE North American Power Symposium (NAPS 2015)*, Charlotte, NC, 2015.
- [13] J. Dahlquist, "DLAB - A downscaled distribution laboratory for education and research on intermittent earth faults," in *Seminar on Methods and Techniques for Earth Fault Detection, Indication and Location*, 2011.

- [14] D. T. Wood, D. Macpherson and S. Finney, "Ripple current propagation in bi-pole HVDC cables and applications to DC grids," *IEEE PES Transactions on Power Delivery*, 2013.
- [15] IEC, "International Standard 60287-1-1: Electric cables – calculation of the current rating – part 1: current rating equations (100% load factor) and calculation of losses – section 1: general," International Electrotechnical Commission, 2014.
- [16] L. F. Woodruff, *Electric power transmission and distribution*, John Wiley & Sons, 1925.
- [17] H. Forbes and L. Gorman, "Skin effect in rectangular conductors," *Electrical Engineering*, vol. 52, no. 9, 1933.
- [18] H. B. Dwight, "A precise method of calculation of skin effect in isolated tubes," *AIEE Transactions*, vol. 42, p. 827–831, 1923.
- [19] O. Coufal, "Current density in a long solitary tubular conductor," *Journal of Physics A: Mathematical and Theoretical*, vol. 41, 2008.
- [20] K. Simonyi, *Foundations of Electrical Engineering: Fields—Networks—Waves*, Elsevier, 2013.
- [21] O. Coufal, "Comments on skin effect in solitary solid tubular conductor," *Advances in Mathematical Physics*, 2011.
- [22] O. Gatous and J. Pissolato, "Frequency-dependent skin-effect formulation for resistance and internal inductance of a solid cylindrical conductor," *IEE Proceedings - Microwaves Antennas and Propagation*, vol. 151, no. 3, pp. 212–216, 2004.
- [23] J. Pissolato, "Simplified skin-effect formulation for power transmission lines," *IET Science, Measurement and Technology*, vol. 9, no. 2, pp. 47–53, 2014.
- [24] C. Balanis, *Advanced Engineering Electromagnetics*, Wiley, 1989.
- [25] V. T. Morgan, "The current distribution, resistance and internal inductance of linear power system conductors – a review of explicit equations," *IEEE Transactions on Power Delivery*, vol. 28, no. 3, pp. 1252–1262, 2013.
- [26] V. T. Morgan, "The thermal rating of overhead-line conductors. Part I, the steady-state thermal model," *Electric Power Systems Research*, vol. 5, p. 119–139, 1982.

- [27] D. Douglass and L. Kirkpatrick, "AC resistance of ACSR – magnetic and temperature effects," *IEEE Transactions on Power Apparatus and Systems*, Vols. PAS-104, no. 6, 1985.
- [28] A. Arnold, "Eddy current losses in multi-core paper-insulated lead-covered cables, armoured and unarmoured, carrying balanced three-phase current," *Journal of the Institute of Electrical and Electronics Engineers*, vol. 88, pp. 52-63, 1941.
- [29] Southwire, Overhead Conductor Manual, 2nd Ed., The Southwire Company, 2007.
- [30] H. B. Dwight, "Bessel functions for A.C. problems," *AIEE Transactions*, vol. 48, p. 812–820, 1929.
- [31] A. E. Kennelly, F. A. Laws and P. H. Pierce, "Experimental researches on skin effect in conductors," *AIEE Transactions*, vol. 34, pp. 1955-2021, 1915.
- [32] J. Zaborszky, "Skin and spiraling effect in stranded conductors," *AIEE Transactions*, vol. 72, p. 599–603, 1953.
- [33] Cigré, "Technical brochure 345: alternating current (AC) resistance of helically stranded conductors," WG B2.12, 2008.
- [34] L. Rayleigh, "The induction and resistance of straight conductors," *Philosophy Magazine*, vol. 21, pp. 381–394, 469, 1886.
- [35] A. Arnold, "The alternating current resistance of tubular conductors," *Journal of the Institute of Electrical and Electronics Engineers*, vol. 78, p. 580–593, 1936.
- [36] H. B. Dwight, "Skin effect and proximity effect in tubular conductors," *AIEE Transactions*, vol. 41, pp. 189-198, 1922.
- [37] V. T. Morgan, R. D. Findlay and S. Derrah, "New formula to calculate the skin effect in isolated tubular conductors at low frequencies," *IEE Proceedings - Science, Measurement and Technology*, vol. 147, no. 4, p. 169–171, 2000.
- [38] H. Goldenberg, "Some approximations to Arnold's formulae for skin effect and proximity effect factors for circular or shaped conductors," (British) Electrical Research Association, Rep. F/T 203, Leatherhead, U.K., 1961.
- [39] W. Mingli and F. Wu, "Numerical calculations of internal impedance of solid and tubular cylindrical conductors under large parameters," *Proceedings of IEE Generation, Transmission, and Distribution*, vol. 151, p. 67–72, 2004.

- [40] E. H. Salter, "Problems in the measurement of AC resistance and reactance of large conductors," *AIEE Transactions*, vol. 67, no. II, p. 1390–1397, 1948.
- [41] A. Arnold, "The alternating-current resistance of parallel conductors of circular cross-section," *Journal of the Institute of Electrical and Electronics Engineers*, vol. 77, p. 49–58, 1935.
- [42] F. Castelli, "Four-terminal impedance current transformer bridge with resistive ratio arm," *IEEE Transactions on Power Apparatus and Systems*, Vols. PAS-98, no. 3, p. 972–981, 1979.
- [43] P. E. Burke and R. T. H. Alden, "Current density probes," *IEEE Transactions on Power Apparatus and Systems*, vol. 88, no. 2, p. 181–185, 1969.
- [44] G. Schroder, J. Kaumanns and R. Plath, "Advanced measurement of AC resistance on skin-effect reduced large conductor power cables," in *8th International Conference on Insulated Power Cables*, Versailles, France, 2011.
- [45] G. Schroder, V. P. R. Waschk, R. Schuhmann and R. Suchantke, "Measures to reduce skin-effect losses in power cables with optimized conductor design and their evaluation by measurement," in *9th International Conference on Insulated Power Cables*, Versailles, France, 2015.
- [46] G. Schroder, D. Haring, A. Weinlein, A. Bossmann, R. Plath, M. Valtin and M. Majid, "AC resistance measurements on skin-effect reduced large conductor power cables with standard equipment," in *9th International Conference on Insulated Power Cables*, Versailles, France, 2011.
- [47] J. C. Maxwell, "A Treatise on Electricity and Magnetism Vol 2 3rd Ed.," Oxford University Press, Oxford, U.K., 1892.
- [48] T. J. Higgins, "The origins and developments of the concepts of inductance, skin effect and proximity effect," *American Journal of Physics*, vol. 9, pp. 337–346, 1941.
- [49] D. W. Jordan and D. E. Hughes, "Self-induction and the skin-effect," *Centaurus*, vol. 26, p. 123–53, 1982.
- [50] P. J. Nahin, "Oliver Heaviside: Sage in Solitude: the Life, Work, and Times of an Electrical Genius of the Victorian Age," IEEE Press, New York, NY, 1988.
- [51] B. J. Hunt, "The Maxwellians," Cornell University Press, Ithaca, NY, 1991.
- [52] I. Yavetz, "From Obscurity to Enigma: the Work of Oliver Heaviside," Birkhauser, Basel, 1995.

- [53] B. Mahon, "Oliver Heaviside maverick mastermind of electricity," IET Press, London, U.K., 2009.
- [54] J. W. Strutt, "On the self-induction and resistance of straight conductors," *Philosophy Magazine*, vol. 21, p. 381–94, 1886 .
- [55] O. Heaviside, "Electromagnetic induction and its propagation: 36. Resistance and self-induction of a round wire with current longitudinal. Ditto, with induction longitudinal. Their observation and measurement," *The Electrician*, vol. 18, p. 281–3, 1887.
- [56] O. Heaviside, "Electrical Papers vol 2, pp.97-101," Copley, Boston, MA, 1925.
- [57] W. Thomson, "President's address: ether, electricity, and ponderable matter," *Transactions of IEE*, vol. 18, p. 4–36, 1889 .
- [58] O. Heaviside, "Electromagnetic induction and its propagation: 27. The variable period in a round wire with a concentric tube at any distance from the return current," *The Electrician* , vol. 17, p. 88–9, 1886.
- [59] O. Heaviside, "Electrical Papers vol 2, pp.50-5," Copley, Boston, MA, 1925.
- [60] W. Thomson, "Mathematical and Physical Papers: Elasticity, Heat, Electro-Magnetism Vol 3," Clay, London, U.K., 1890.
- [61] A. Russell, "The effective resistance and inductance of a concentric main, and methods of computation for ber and bei and allied functions," *Philosophical Magazine*, vol. 17, p. 524–52, 1909.
- [62] H. Milliken, "Electrical Power Cable". United States Patent Office Patent 2.187.213, 16 January 1940.
- [63] H. Milliken, "Electrical cable". United States Patent Office Patent 1.904.162, 18 April 1933.
- [64] U. Fromm, "Optimized conductors for XLPE cables with a large cross-section," *European Transactions on Electrical Power*, vol. 15, pp. 109-121, 2005.
- [65] V. Vaisanen, J. Hiltunene, J. Nerg and P. Silventoinen, "AC resistance calculation methods and practical design considerations when using Litz wire," *Industrial Electronics Society, IECON 2013 - 39th Annual Conference of the IEEE*, pp. 368-375, 2013.
- [66] C. Katz, G. Eager and G. Seman, "Progress in the determination of A.C./D.C. resistance ratios of pipe-type cable systems," *IEEE Transactions*, vol. PAS 97, no. 6, 1978.

- [67] F. Young and S. Dudzinsky, "An a.c. bridge method to measure core loss," *IEEE Transactions on Communications Electronics*, vol. 69, 1963.
- [68] F. Castelli, L. Maciotta-Rolandin and P. Riner, "A new method of measuring the a.c. resistance of large cable conductors," *IEEE Transactions on Power Apparatus and Systems*, vol. PAS 96, 1977.
- [69] K. Sugiyama, "Development of Inter-layer insulated segmental conductor with low skin effect for power cables," *Electrical Engineering in Japan*, vol. 101, no. 6, 1981.
- [70] Cigré, "Technical brochure 272: large-cross sections and composite screens design," Working group B1.03, 2005.
- [71] D. Lovric, V. Boras and S. Vujevic, "Accuracy of approximate formulas for internal impedance of tubular cylindrical conductors for large parameters," *Progress in Electromagnetics Research*, vol. 16, pp. 171-184, 2011.
- [72] J. C. Maxwell, "On Physical Lines of Force," *Royal Astronomical Society*, 1861.
- [73] N. W. McLachlan, *Bessel functions for engineers*, 2nd Ed., Oxford University Press, 1961.
- [74] M. Kerker and E. Matijevic, "Scattering of electromagnetic waves from concentric infinite cylinders," *Journal of the Optical Society of America*, vol. 51, no. 5, 1961.
- [75] T. Worzyk, *Submarine power cables: design, installation, repair, environmental aspects*, Springer, 2009.
- [76] W. Stevenson, *Elements of power system analysis*, McGraw-Hill, 1955.
- [77] ICEA, "S-108-720-2012: standard for extruded insulation power cables rated above 46 through 345 kV," Insulated Cable Engineers Association, 2012.
- [78] P. N. Murgatroyd, "Calculation of proximity losses in multistranded conductor bunches," *IEE Proceedings*, vol. 136, pp. 115-120, 1989.
- [79] A. Arnold, "Eddy current losses in single-conductor paper-insulated lead-covered unarmoured cables of a single-phase system," *Journal of the Institute of Electrical and Electronics Engineers*, vol. 89, no. 12, 1942.
- [80] A. Arnold, *Journal of the Institution of Electrical Engineers*, vol. 76, p. 299, 1933.

- [81] A. Arnold, *Journal of the Institution of Electrical Engineers*, vol. 79, p. 595, 1936.
- [82] F. Ulaby, E. Michielssen and U. Ravaioli, *Fundamentals of Applied Electromagnetics*, 6th Ed., Prentice Hall, 2010.
- [83] W. Middleton and E. Davis, "Skin effect in large stranded conductors at low frequencies," *Journal of the American Institute of Electrical Engineers*, vol. 40, no. 9, pp. 757-763, 1921.
- [84] O. Heaviside, "Effective resistance and inductance of a round wire," *Electrical Papers*, Vols. 1,2, pp. 353, 429, 50, 97, 1884.
- [85] L. Kelvin, "Mathematical and Physical Papers," vol. 3, no. Cambridge University Press, p. 491-494, 1889.
- [86] E. B. Rosa, "The self and mutual inductances of linear conductors," (*US*) *Bureau of Standards*, vol. 4, no. 2, p. 300-344, 1908.
- [87] F. W. Grover, "Inductance calculations," Van Nostrand, New York, NY, 1946.
- [88] H. B. Dwight, "Electrical coils and conductors," McGraw- Hill, New York, NY, 1945.
- [89] L. J. Giacoletto, "Frequency- and time-domain analysis of skin effects," *IEEE Transactions Magazine*, vol. 35, no. 1, p. 223-232, 1996.
- [90] J. Miller, "Effective resistance and inductance of iron and bimetallic wires," (*US*) Bureau of Standards, Scientific Paper No. 252, 1915.
- [91] A. Arnold, "The alternating current resistance of non-magnetic conductors," Her Majesty's Stationery Office, London, U.K., 1946.
- [92] IEC, "International Standard 60228: conductors of insulated cables," International Electrotechnical Commission, 2004.
- [93] J. H. Neher and M. H. McGrath, "The calculation of the temperature rise and load capability of cable systems," *AIEE Transactions*, vol. 76, no. III, p. 752-772, 1957.
- [94] AESA, "Temperature and frequency effects on cable resistance," AESA Cortaillod, [Online]. Available: http://www.aesa-cortaillod.com/fileadmin/documents/knowledge/AN_150617_E_Snapshots_multimaterials.pdf. [Accessed 21 February 2016].

- [95] D. Couderc, "Development and testing of a 800-kV PPLP-insulated oil-filled cable and its accessories," in *Cigre 1996 Session Paper 21/22-04*, 1996.
- [96] Cigré, "Basic principles and practical methods to measure the AC and DC resistance of conductors of power cables and overhead lines," Working group D1.54, In progress.
- [97] W. Goch, "Overhead conductors (what's an arbutus)," Classic connectors, [Online]. Available: http://www.classicconnectors.com/downloads/overhead_conductor_arbutus.pdf. [Accessed 21 February 2016].
- [98] NFPA, NFPA 70: National Electrical Code, NFPA, 2014.
- [99] V. T. Morgan, B. Zhang and R. Findlay, "Effects of temperature and tensile stress on the magnetic properties of a steel core from an ACSR conductor," *IEEE Transactions on Power Delivery*, vol. 11, no. 4, pp. 1907–1913, , 1996.
- [100] V. T. Morgan, B. Zhang and R. D. Findlay, "Effect of magnetic induction in a steel-cored conductor on current distribution, resistance and power loss," *IEEE Transactions on Power Delivery*, vol. 12, no. 3, p. 1299–1306, 1997.
- [101] V. T. Morgan, R. D. Findlay and B. Zhang, "Distribution of current density in ACSR conductor," in *Proceedings of Canadian Conferences on Electrical and Computer Engineering*, Halifax, NS, Canada, 1994.
- [102] V. T. Morgan, "Effects of alternating and direct current, power frequency, temperature and tension on the electrical parameters of ACSR conductors," *IEEE Transactions on Power Delivery*, vol. 18, no. 3, p. 859–866, 2003.
- [103] V. T. Morgan, "The radial temperature distribution and effective radial thermal conductivity in bare solid and stranded conductors," *IEEE Transactions on Power Delivery*, vol. 5, no. 3, p. 1443–1452, 1990.
- [104] D. A. Douglass, "Radial and axial temperature gradients in bare stranded conductors," *IEEE Transactions on Power Delivery*, Vols. PWRD-1, no. 2, p. 7–15, 1986.
- [105] V. T. Morgan and D. K. Geddey, "Temperature distribution within ACSR conductors, paper 22-101," in *Cigre*, Paris, France, 1992.
- [106] D. E. Nevel, "Tables of kelvin functions and their derivatives, technical report 67," U.S. Army Snow Ice and Permafrost Research Establishment, 1959.

- [107] J. P. Donohoe, "Electromagnetic waves," Mississippi State University, [Online]. Available: www.ece.msstate.edu/~donohoe/ece3324notes10.pdf. [Accessed 21 February 2016].
- [108] General, "Wire and cable solutions," General cable, [Online]. Available: <http://www.generalcable.com/NR/rdonlyres/D7692D4A-F3A4-4023-B81F-DAE9DFA716E9/0/MingCblEngHdbk.pdf>. [Accessed 21 February 2016].
- [109] Comsol, "What is multiphysics?," Comsol, [Online]. Available: <https://www.comsol.com/multiphysics>. [Accessed 21 February 2016].
- [110] Comsol, "Finite element analysis (FEA) software," Comsol, [Online]. Available: <https://www.comsol.com/multiphysics/fea-software>. [Accessed 21 February 2016].
- [111] Comsol, "Finite element mesh refinement," Comsol, [Online]. Available: <https://www.comsol.com/multiphysics/mesh-refinement>. [Accessed 21 February 2016].
- [112] A. J. Yuffa and J. A. Scales, "Measuring the void: theoretical study of scattering by a cylindrical annulus," *Journal of Quantitative Spectroscopy and Radiative Transfer*, vol. 131, pp. 188-193, 2013.
- [113] L. Pincherle, "Refraction of plane non-uniform electromagnetic waves between absorbing medium," *Physical Review*, vol. 72, no. 3, pp. 232-235, 1947.
- [114] P. Silverster, "The accurate calculation of skin effect in conductors of complicated shape," *IEEE Transactions on Power Apparatus and Systems*, Vols. PAS-87, no. 3, 1968.
- [115] R. Jackson, "Measurement of skin and proximity effects in circular conductors," *Proceedings of IEE*, vol. 117, pp. 1435-1440, 1970.
- [116] Rydler, K.; Sjoberg, M.; Svahn, J., "A measuring system of conductor AC and DC resistance," in *Jicable'11: 8th International Conference on Insulated Power Cables*, Versailles, 2011.
- [117] Y. Zeroukhi, E. Juszczak, K. Komez, F. Morganti and G. Vega, "Identification of current flow depending on the mechanical deformation in a stranded cable," *The International Journal for Computation and Mathematics in Electrical and Electronic Engineering*, vol. 32, no. 4, pp. 1437-1450, 2013.
- [118] D. Bruyne and G. Mauron, "Effects of contact resistances in multi-stranded cables on linear-resistance measurements," *Wire Journal International*, pp. 144-147, May 2012.

- [119] D. Milz, "Conservation of raw materials in the production of power cable requires precise measurement of resistance and cross-section," *Wire & Cable Technology International*, pp. 64-66, November 2009.
- [120] E. H. Ball and G. Maschio, "The AC resistance of segmental conductors as used in power cables," *IEE Transactions on Power Apparatus and Systems*, vol. 87, pp. 1143-1148, 1968.

APPENDIX A: MATLAB CODE

```
% Derivative of Bessel function, first kind, zero order
function value = dJ0(x)
    n=0;
    value=0.5.*(besselj(n-1,x.*sqrt(li))-besselj(n+1,x.*sqrt(li)));
end

% Bessel - 2nd kind, 1st order
function value = Y1(x)
    value=bessely(1,x*sqrt(li));

% Derivative of Bessel function, second kind, zero order
function value = dY0(x)
    x=x+1e-100; % fixes discontinuity at x=0
    n=0;
    value=0.5.*(bessely(n-1,x.*sqrt(li))-bessely(n+1,x.*sqrt(li)));
end
```

```

% Hankel function - Bessel function of the 3rd kind, 0 order
function value = H0(x)
value=besselh(0,x*sqrt(1i));

% Hankel function - 1st kind, 1 order
function value = H1(x)
value=besselh(1,x*sqrt(1i));

% Bessel - modified 1st kind, 0 order
function value = I0(x)
value=besseli(0,x*sqrt(1i));

% Bessel - modified 1st kind, 1 order
function value = I1(x)
value=besseli(1,x*sqrt(1i));

% Bessel - 1st kind, 0 order
function value = J0(x)
value=besselj(0,x*sqrt(1i));

```

```

% Bessel - 1st kind, 1 order
function value = J1(x)
value=besselj(1,x*sqrt(1i));

% Bessel - modified 2nd kind, 0 order
function value = K0(x)
value=besselk(0,x*sqrt(1i));

% Bessel - modified 2nd kind, 1 order
function value = K1(x)
value=besselk(1,x*sqrt(1i));

% Bessel - 2nd kind, 0 order
function value = Y0(x)
value=bessely(0,x*sqrt(1i));

% Kelvin function, real part n-order
function value = kern(n,x)

```

```

value=real(besselk(n,x*sqrt(1i)));

% Bessel function, imaginary part 0-order
function value = bei(x)
n=0;
value=imag(-besselj(n,x*sqrt(1i)));

% Bessel function, imaginary part n-order
function value = bein(n,x)
value=imag(-besselj(n,x*sqrt(1i)));

% Bessel function, real part 0-order
function value = ber(x)
n=0;
value=real(besselj(n,x*sqrt(1i)));

% Bessel function, imaginary real n-order
function value = bern(n,x)

```

```

value=real(besselj(n,x*sqrt(1i)));

% Derivative of Bessel function, imaginary part 0-order
function value = Dbei(x)
n=0;
value=real((bern(n+1,x)-bein(n+1,x))./sqrt(2));

% Derivative of Bessel function, real part 0-order
function value = Dber(x)
n=0;
value=real(-(bern(n+1,x)+bein(n+1,x))./sqrt(2));

% Derivative of Kelvin function, imaginary part 0-order
function value = Dkei(x)
n=0;
for counter=1:1:length(x)
    if x(counter)==0
        x(counter)=x(counter)+1e-100; % fixes discontinuity at x=0
    end
end

```

```

end
value=real(-(+kern(n+1,x)+kein(n+1,x))./sqrt(2));

% Derivative of Kelvin function, real part 0-order
function value = Dker(x)
n=0;
for counter=1:length(x)
    if x(counter)==0
        x(counter)=x(counter)+1e-100; % fixes discontinuity at x=0
    end
end
value=real((-kern(n+1,x)+kein(n+1,x))./sqrt(2));

% Kelvin function, imaginary part 0-order
function value = kei(x)
n=0;
for counter=1:length(x)
    if x(counter)==0
        x(counter)=x(counter)+1e-100; % fixes discontinuity at x=0
    end
end

```

```

end
end
value=imag(besselk(n,x*sqrt(1i)));

% Kelvin function, imaginary part n-order
function value = kein(n,x)
value=imag(besselk(n,x*sqrt(1i)));

% Kelvin function, real part 0-order
function value = ker(x)
n=0;
TEMPvalue=real(besselk(n,x*sqrt(1i)));
for counter=1:length(x)
    if TEMPvalue(counter)==Inf
        TEMPvalue(counter)=1e+100; % fixes discontinuity at x=0
    end
end
value=TEMPvalue;

```

```

% Normalized data
function value = normalize(x,normalized_value)
value=x./normalized_value;

function value = VUC(Y,x,xstep,s_Ratio,di)
% Volume Under Curve (VUC) rotated about y-axis
% Y is Y-axis function (i.e. J)
% x is x-axis range (i.e. r)
% xstep is iterative value of x

if s_Ratio==1 % Calculate based on 1 metal
VolumeCylinder=pi.*max(x).^2.*max(y)-pi.*min(x).^2.*max(y);
VolumeUnderCurve=2.*pi.*(trapz(x.*y.*xstep,2));
kskVUC=VolumeCylinder/VolumeUnderCurve;
else % Calculate based on 2 metals
% Divide r and J into inner and outer boundaries
y1=y(1:di);
y2=y(di+1:length(y));
x1=x(1:di);

```

```

x2=x(di+1:length(x));
% Get cylinder volumes (note: both with height of curve 2)
VolumeCylinder1=pi.*max(x1).^2.*max(y2);
VolumeCylinder2=pi.*max(x2).^2.*max(y2)-pi.*min(x2).^2.*max(y2);
% Adjust inner cylinder volume to difference metal
VolumeCylinder1=VolumeCylinder1*s_Ratio;
% Get volume under each curve
VolumeUnderCurve1=2.*pi.*(trapz(x1.*y1.*xstep,2));
VolumeUnderCurve2=2.*pi.*(trapz(x2.*y2.*xstep,2));
% Get total volumes under both curves
VolumeCylinder=VolumeCylinder1+VolumeCylinder2;
VolumeUnderCurve=VolumeUnderCurve1+VolumeUnderCurve2;
% Get final ksk value
kskVUC=VolumeCylinder/VolumeUnderCurve;
end
% Return final value
value=kskVUC;
% Clear screen, set plot line width

```

```

clc; clear all; close all;

set(0,'defaultlinewidth',1.5)

% *****
% Variables
f=60; % frequency, Hz
T=90; % conductor temperature for calculations, degC
r_min=0; % first optimal bi-media point, mm
r_max=35; % last optimal bi-media point, mm
r_J_plot=20; % current density plot radius, mm
ks_seg=0.8; % segmented conductor skin effect coefficient
cost_en=1.3; % multiplier for enameling cost
cost_al_lb=0.75; % cost of aluminum, $/lb

% *****
% Constants
medium_out='CU'; % Copper
Tref=20; % conductor temperature for R0, degC
w=2*pi*f; % angular frequency, rad/sec

```

```

u0=4*pi*1e-7; % permeability of free space, H/m
rstep=0.000001; % ri (r) incremental counter, m
Z_pts=1000; % resolution for bi-media ksk plot, points from 0 to r_out
if strcmp(medium_out,'AL') % 800-3000mm2 Al DC resistance, ohm/m
    Rdc20_segmented=[3.67E-05 2.91E-05 2.47E-05 2.12E-05...
        1.86E-05 1.49E-05 1.19E-05 9.91E-06];
else % 800-3000mm2 Cu DC resistance, ohm/m
    Rdc20_segmented=[2.21E-05 1.76E-05 1.51E-05 1.29E-05...
        1.13E-05 9.00E-06 7.20E-06 6.00E-06];
end
% Nominal area of segmented conductors
area_segmented_nominal=[800 1000 1200 1400 1600 2000 2500 3000];
% True area of segmented CU conductors based on Rdc
area_segmented_true=[780.14 979.60 1141.79 1336.51 1525.75 1915.67 2394.58 2873.50];

for mediums=1:2
    if mediums==1
        Plot_J='Y';
        medium_in='Air'; % first loop is Air / CU

```

```

else
    Plot_J='Y';
    medium_in='AL'; % second loop is AL / CU
end
% *****
% Get basic data of inner and outer mediums
switch medium_in
case 'Air'
    p20_in=999; % resistivity, ohm meter @ 20C (IEC 60287-1-1)
    ur_in=1; % relative permeability of air
    a20_in=0; % temperature coefficient at 20C, 1/K
    SG_in=0; % specific gravity, g/cm3
case 'AL'
    p20_in=2.8264e-8; % resistivity, ohm meter @ 20C (IEC 60287-1-1)
    ur_in=1.00; % relative permeability of aluminum
    a20_in=0.00403; % temperature coefficient at 20C, 1/K
    SG_in=2.7; % specific gravity, g/cm3
case 'CU'
    p20_in=1.7241e-8; % resistivity, ohm meter @ 20C (IEC 60287-1-1)

```

```

ur_in=1.00; % relative permeability of copper
a20_in=0.00393; % temperature coefficient at 20C, 1/K
SG_in=8.93; % specific gravity, g/cm3

end

switch medium_out
case 'Air'
    p20_out=999; % resistivity, ohm meter @ 20C (IEC 60287-1-1)
    ur_out=1; % relative permeability of air
    a20_out=1; % temperature coefficient at 20C, 1/K
    SG_out=0; % specific gravity, g/cm3

case 'AL'
    p20_out=2.8264e-8; % resistivity, ohm meter @ 20C (IEC 60287-1-1)
    ur_out=1.00; % relative permeability of aluminum
    a20_out=0.00403; % temperature coefficient at 20C, 1/K
    SG_out=2.7; % specific gravity, g/cm3

case 'CU'
    p20_out=1.7241e-8; % resistivity, ohm meter @ 20C (IEC 60287-1-1)
    ur_out=1.00; % relative permeability of copper
    a20_out=0.00393; % temperature coefficient at 20C, 1/K

```

```

SG_out=8.93; % specific gravity, g/cm3

end

% *****
% Bessel Parameters calculated @ TdegC
p_in=p20_in.*(1+a20_in.*(T-Tref)); % convert inner rho @ 20C to (Tref)C, ohm-meter
p_out=p20_out.*(1+a20_out.*(T-Tref)); % convert outer rho @ 20C to (Tref)C, ohm-meter
u_in=u0*ur_in; % permeability of inner metal, H/m
u_out=u0*ur_out; % permeability of outer metal, H/m
m_in=sqrt(w*u_in/p_in); % Bessel input argument for inner medium
m_out=sqrt(w*u_out/p_out); % Bessel input argument for outer medium
d_in=sqrt(2*p_in/(w*u_in)); % skin depth (delta), m
d_out=sqrt(2*p_out/(w*u_out)); % skin depth (delta), m

% increment through conductor radius for all J and Z
for ri=1:Z_pts

% *****
% Set Conductor Radii & Calculate DC Resistance

```

```

r_out=0.001*r_max*ri/Z_pts; % increment up to r_max
r_in=linspace(1e-99,r_out,Z_pts); % span 0 to r_out: 1e-99 avoid singularity error
Rdc_in=p_in./(pi.*r_in.^2); % inner medium DC resistance, ohm/m
Rdc_out=p_out./(pi.*(r_out.^2-r_in.^2)); % outer medium DC resistance, ohm/m
Rdc=1./(1./Rdc_in+1./Rdc_out); % total DC resistance, ohm/m

% *****
% Skin Effect (Rac/Rdc) & Inductance Ratio (Lac/Ldc)

for ID=1:Z_pts
    if ID==1
        IsMixed='No'; % first point is all outer medium
        r=linspace(1e-99,r_out,Z_pts);
        J=J0(m_out.*r);
    elseif ID==Z_pts
        IsMixed='No'; % last point is all inner medium
        r=linspace(1e-99,r_out,Z_pts);
        J=J0(m_in.*r);
    else
        IsMixed='Yes';
    end
end

```

```

% Current density in outer medium
r2=linspace(r_in(ID),r_out,Z_pts-ID+1);
d=- (J1(m_in.*r_in(ID)).*J0(m_out.*r_in(ID))-
(m_out/m_in).*J0(m_in.*r_in(ID)).*J1(m_out.*r_in(ID)))/...
(J1(m_in.*r_in(ID)).*H0(m_out.*r_in(ID))-
(m_out/m_in).*J0(m_in.*r_in(ID)).*H1(m_out.*r_in(ID)));
J_out=J0(m_out.*r2)+d.*H0(m_out.*r2);
% Current density in inner medium
r1=linspace(1e-99,r_in(ID),ID);
J_in=J0(m_in.*r1); % current density of inner conductor
J_in=normalize(J_in,max(J_in)./(J_out(1)*(p_out/p_in))); % normalize inner start with outer

if length(r1)==1 % r and J composed only of outer metal
    J=J_out;
    r=r2;
elseif length(r2)==1 % r and J composed only of inner metal
    J=J_in;
    r=r1;
else % r and J composed of combination of inner and outer metal

```

```

end

```

```

J=[J_in,J_out];
r=[r1,r2];
    end
end
J=normalize(J,max(J)); % normalize current density
% Get skin effect with volume under curve function
if strcmp(IsMixed,'No') % volume under the curve (single medium)
    Z(ID)=VUC(J,r,r_out/Z_pts,1,ID);
else % volume under the curve (bi-media)
    Z(ID)=VUC(J,r,r_out/Z_pts,p_out/p_in,ID);
end
end
% Use skin effect calculate all AC resistance and inductance values
Rac=Rdc.*real(Z); % AC resistance, ohm/m
Rratio=Rac./Rdc; % AC/DC resistance ratio
Lac=Rdc.*imag(Z)./w; % AC inductance, H/m
Ldc=u_out./(8.*pi); % DC inductance, H/m
Lratio=Lac./Ldc; % AC/DC inductance ratio

```

```

% *****
% Get Rac minima (zero crossing of gradient)
Rac_slope=gradient(Rac); % slope of AC resistance
r_minima='None'; % set initial minima to 'None' in case no optimal solution
for x=1:Z_pts-1
    if Rac_slope(x)<0 && Rac_slope(x+1)>0 % locate minima when AC resistance slope changes sign
        % Approximate true minima radius with linear interpolation
        r_minima=r_in(x)+(r_in(x+1)-r_in(x))*(0-Rac_slope(x))/(Rac_slope(x+1)-Rac_slope(x));
        break
    end
end
% Record AC and DC resistance and ratios
% First value is single medium only (i.e. no inner medium)
Rac_solid(ri)=Rac(1); % ohm/m
Rdc_solid(ri)=Rdc(1); % ohm/m
kstk_solid(ri)=Rac(1)./Rdc(1);
if strcmp(r_minima,'None') % if Rac minima at ri doesn't exist
    r_optimal(ri)=0; % inner medium radius = 0 m
    Rac_optimal(ri)=Rac(1); % outer medium only Rac, ohm/m

```

```

Rdc_optimal(ri)=Rdc(1); % outer medium only Rdc, ohm/m
ksk_optimal(ri)=Rac(1)./Rdc(1); % outer medium only Rac/Rdc
else % if Rac minima at ri does exist
    if r_min==0 % record first optimal radius for plotting, m
        r_min=r_max*ri/Z_pts;
    end
    r_optimal(ri)=r_minima; % inner medium optimal radius, m
    Rac_optimal(ri)=Rac(x); % bi-media Rac at minima, ohm/m
    Rdc_optimal(ri)=Rdc(x); % bi-media Rdc at minima, ohm/m
    ksk_optimal(ri)=Rac(x)./Rdc(x); % bi-media Rac/Rdc at minima
end
% Save optimal radii for plot of J
if r_out>=r_J_plot*0.001
    if strcmp(Plot_J, 'Y')
        Plot_J='N';
        r_in_J=r_optimal(ri);
    end
end
% Save inner and outer mediums areas

```

```

area_in(ri)=pi.*r_optimal(ri).^2.*1e6; % inner, mm2
area_out(ri)=pi.*(r_out.^2-(r_optimal(ri)).^2).*1e6; % outer, mm2

% *****
% IEC Approximation (conductor only medium_out)
% Single medium design, solid conductor
ks=1;
xs=sqrt(8.*pi.*f.*10.^-7.*ks./Rdc_solid(ri));
if xs<=2.8
    ksk_solid_approx(ri)=1+xs^4/(192+0.8*xs^4);
elseif xs>2.8 && xs<=3.8
    ksk_solid_approx(ri)=1-0.136-0.0177*xs+0.0563*xs^2;
elseif xs>3.8
    ksk_solid_approx(ri)=1+0.354*xs-0.733;
end
% Bi-media design, Air / CU conductor
if strcmp(medium_in,'Air')
    % Use formula from IEC 60287 for ks
    dc=r_out;

```

```

di=r_optimal(ri);
ks=((dc-di)/(dc+di)).*((dc+2.*di)/(dc+di)).^2;
xs=sqrt(8.*pi.*f.*10.^-7.*ks./Rdc_optimal(ri));
if xs<=2.8
    ksk_optimal_approx(ri)=1+xs^4/(192+0.8*xs^4);
elseif xs>2.8 && xs<=3.8
    ksk_optimal_approx(ri)=1-0.136-0.0177*xs+0.0563*xs^2;
elseif xs>3.8
    ksk_optimal_approx(ri)=1+0.354*xs-0.733;
end
% Bi-media design, AL / CU conductor
elseif strcmp(medium_in,'AL')
    ks=1;
    xs=sqrt(8.*pi.*f.*10.^-7.*ks./Rdc_optimal(ri));
    if xs<=2.5
        ksk_optimal_approx(ri)=1+xs^4/(192+0.8*xs^4);
    elseif xs>2.5 && xs<2.7
        ksk_optimal_approx(ri)=1+1.6172*xs^3-12.8131*xs^2+34.0200*xs-30.0615;
    elseif xs>=2.7

```

```

ksk_optimal_approx(ri)=1-0.01516*xs^3+0.20012*xs^2-0.57637*xs+0.61188;

end

end

% Segmented design, outer medium only
xs=sqrt(8.*pi.*f.*10.^-7.*ks_seg./Rdc_solid(ri));

if xs<=2.8

ksk_segmented_approx(ri)=1+xs^4/(192+0.8*xs^4);

elseif xs>2.8 && xs<=3.8

ksk_segmented_approx(ri)=1-0.136-0.0177*xs+0.0563*xs^2;

elseif xs>3.8

ksk_segmented_approx(ri)=1+0.354*xs-0.733;

end

end

if strcmp(medium_in,'Air')

disp(sprintf(['=====']))
disp(sprintf(['===== AIR / CU RESULTS =====']))
disp(sprintf(['=====']))

else

```

```

disp(sprintf(['-----']))
disp(sprintf(['----- AL / CU RESULTS -----']))
disp(sprintf(['-----']))

end

% Check error of approximations & display results
Max_ksk_Solid_Error=(100*max(abs(ksk_solid_ksk_solid_approx)));
Max_ksk_Optimal_Error=(100*max(abs(ksk_optimal_ksk_optimal_approx)));
disp(sprintf(['-----']))

disp(['Max Rac/Rdc Approximation Error %0.2f',Max_ksk_Solid_Error) sprintf('% (Solid)')]
disp(['Max Rac/Rdc Approximation Error %0.2f',Max_ksk_Optimal_Error) sprintf('% (Mixed)')]

% *****
% Find Equivalent Design to Segmented
% *****
% *****
% Get IEC Approximate Rdc, ksk and Rac for nominal segmented designs
Rdc_segmented=Rdc20_segmented.*(1+a20_out.*(T-Tref));

```

```

for i=1:length(Rdc_segmented)
    xs=sqrt(8.*pi.*f.*10.^-7.*ks_seg./Rdc_segmented(i));
    if xs<=2.8
        ksk_segmented(i)=1+xs^4/(192+0.8*xs^4);
    elseif xs>2.8 && xs<=3.8
        ksk_segmented(i)=1-0.136-0.0177*xs+0.0563*xs^2;
    elseif xs>3.8
        ksk_segmented(i)=1+0.354*xs-0.733;
    end
end
end
Rac_segmented=Rdc_segmented.*ksk_segmented;
% Get Radius Where Rac Equal for Segmented & Bi-media
for i=1:length(Rac_segmented)
    for x=1:Z_pts
        if Rac_segmented(i)>Rac_optimal(x) % calculate radius with linear interpolation
            r_segmented(i)=r_in(x-1)+(r_in(x)-r_in(x-1))*(Rac_segmented(i)-Rac_optimal(x-
1))/(Rac_optimal(x)-Rac_optimal(x-1));
            break
        end
    end
end

```

```

end
end
area_segmented=1e6.*p_out./Rdc_segmented; % true mm2 area based on Rdc
% Get Bi-media Metal Area (mm2) Usage at Equal Rac Radius
for i=1:length(r_segmented)
    for x=1:Z_pts
        if r_segmented(i)<r_in(x) % calculate inner radius with linear interpolation
            r_out_mixed(i)=r_segmented(i);
            r_in_mixed(i)=r_optimal(x-1)+(r_optimal(x)-r_optimal(x-1))*(r_out_mixed(i)-r_in(x-
1))/(r_in(x)-r_in(x-1));
                break
            end
        end
    end
end
% Calculate inner and outer bi-media areas, mm2
area_in_mixed=pi.*r_in_mixed.^2.*1e6;
area_out_mixed=pi.*r_out_mixed.^2.*1e6-area_in_mixed;
area_mixed=area_in_mixed+area_out_mixed;
% Calculate metal weights (kg/m) usage for each design

```

```

weight_segmented=SG_out.*area_segmented./1000;
weight_in_mixed=SG_in.*area_in_mixed./1000;
weight_out_mixed=SG_out.*area_out_mixed./1000;
weight_mixed=weight_in_mixed+weight_out_mixed;
% Calculate metal costs ($/m)
cost_al_kg=cost_al_lb/0.45359237; % $/kg
if ks_seg>0.35
    cost_en=1; % no enamel markup on segmented conductor with ks <= 0.35
end
% Look at 2x, 3x, and 4x $Cu/$Al ratios
cost_cu_kg=2.*cost_al_kg;
cost_segmented_2=(cost_cu_kg*cost_en).*weight_segmented;
cost_mixed_2=cost_cu_kg.*weight_out_mixed+cost_al_kg.*weight_in_mixed;
cost_cu_kg=3.*cost_al_kg;
cost_segmented_3=(cost_cu_kg*cost_en).*weight_segmented;
cost_mixed_3=cost_cu_kg.*weight_out_mixed+cost_al_kg.*weight_in_mixed;
cost_cu_kg=4.*cost_al_kg;
cost_segmented_4=(cost_cu_kg*cost_en).*weight_segmented;
cost_mixed_4=cost_cu_kg.*weight_out_mixed+cost_al_kg.*weight_in_mixed;

```

```

% Calculate cost deltas
cost_delta_2=100.*(cost_mixed_2-cost_segmented_2)./cost_segmented_2;
cost_delta_3=100.*(cost_mixed_3-cost_segmented_3)./cost_segmented_3;
cost_delta_4=100.*(cost_mixed_4-cost_segmented_4)./cost_segmented_4;

% *****
% Plot bi-media optimal radii
if strcmp(medium_in, 'Air')
    figure(1);
else
    figure(3);
end
subplot(2,2,1);
plot(1000*r_in,1000*r_optimal, 'r-')
xlabel([medium_out ' Outer Radius (mm)']);
ylabel([medium_in ' Inner Radius (mm)']);
xlim([0 1000*r_out])
title(['Optimal Radii (' medium_in ' / ' medium_out ')']);

```

```

grid on;
% *****
% Plot AC & DC resistances
subplot(2,2,2);
plot(1000*r_in,Rac_solid,'r-',1000*r_in,Rac_optimal,'b--',1000*r_in,...
     Rdc_solid.*ksk_segmented_approx,'g-',1000*r_in,Rdc_solid,'k-',1000*r_in,Rdc_optimal,'m--')
legend('R_a_c: Solid CU','R_a_c: Air / CU',['R_a_c: Segmented CU (k_s=' num2str(ks_seg) ')],...
      'R_d_c: Air / CU','R_d_c: Solid/Segmented')
xlabel(['Outer Radius (mm)']);
ylabel('Resistance (ohm/m)');
xlim([r_min 1000*r_out])
title(['Resistance (f=' num2str(f) 'Hz,T=' num2str(T) 'C)']);
grid on;
% *****
% Plot bi-media optimal areas
subplot(2,2,3);
plot(1000*r_in,area_in,'r-',1000*r_in,area_out,'b-',1000*r_in,area_in+area_out,'k--')
legend(medium_in,medium_out,[medium_in '/' medium_out])
xlabel(['Outer Radius (mm)']);

```

```

ylabel('Area (mm^2)');
xlim([0 1000*r_out])
title(['Medium Areas ( ' medium_in ' / ' medium_out ')']);
grid on;
% *****
% Plot skin effect
subplot(2,2,4);
plot(1000.*r_in,ksk_solid,'k-',1000.*r_in,ksk_solid_approx,'r--',1000.*r_in,...
ksk_optimal,'m-',1000.*r_in,ksk_optimal_approx,'g--',1000.*r_in,ksk_segmented_approx,'c--')
legend('R_a_c/R_d_c: Solid CU (actual)', 'R_a_c/R_d_c: Solid CU (approx)', ...
'R_a_c/R_d_c: Mixed (actual)', 'R_a_c/R_d_c: Mixed (approx)', 'R_a_c/R_d_c: Segmented CU (approx)')
xlabel(['Outer Radius (mm)']);
ylabel('Rac / Rdc');
xlim([0 1000*r_out])
title(['Skin Effect ( ' medium_in ' / ' medium_out ')']);
grid on;
% *****
% Plot equal Rac areas

```

```

if strcmp(medium_in, 'Air')
    figure(2);
else
    figure(4);
end
subplot(2,2,1);
plot(area_segmented_nominal,area_segmented,'r-',area_segmented_nominal,area_mixed,'b-',...
area_segmented_nominal,area_out_mixed,'k--',area_segmented_nominal,area_in_mixed,'m--')
legend('CU: Segmented',[medium_in ' + ' medium_out],[medium_out ':' medium_in ' / ' medium_out],...
[medium_in ':' medium_in ' / ' medium_out])
xlabel(['Nominal Area (mm^2)']);
ylabel(['True Area (mm^2)']);
axis([0 3500 0 3500])
title(['Equal Rac Conductor Areas']);
grid on;
% *****
% Plot material consumption
subplot(2,2,2);
plot(area_segmented_nominal,weight_segmented,'r-',area_segmented_nominal,weight_mixed,'b-',...

```

```

area_segmented_nominal,weight_out_mixed,'k--',area_segmented_nominal,weight_in_mixed,'m--')
legend([medium_out ':' Segmented'],[medium_in ' + ' medium_out],...
[medium_out ':' medium_in ' / ' medium_out],...
[medium_in ':' medium_in ' / ' medium_out])
xlabel(['Nominal Area (mm^2)']);
ylabel(['Metal Weight (kg/m)']);
xlim([0 3500])
title(['Material Consumption']);
grid on;
% *****
% Plot conductor cost
subplot(2,2,3);
plot(area_segmented_nominal,cost_segmented_2,'r-',area_segmented_nominal,cost_mixed_2,'r--',...
area_segmented_nominal,cost_segmented_3,'b-',area_segmented_nominal,cost_mixed_3,'b--',...
area_segmented_nominal,cost_segmented_4,'m-',area_segmented_nominal,cost_mixed_4,'m--')
legend(['2x: Segmented ' medium_out],[ '2x: ' medium_in ' + ' medium_out],...
[ '3x: Segmented ' medium_out],[ '3x: ' medium_in ' + ' medium_out],...
[ '4x: Segmented ' medium_out],[ '4x: ' medium_in ' + ' medium_out])
xlabel(['Nominal Area (mm^2)']);

```

```

ylabel('$/m');
xlim([0 3500])
if strcmp(medium_in,'Air')
    if strcmp(medium_out,'AL')
        title(['Metal Cost (Al=$' num2str(cost_al_lb, '%.2f') '/lb)']);
    else
        title(['Metal Cost (Cu=$' num2str(2*cost_al_lb, '%.2f') '- ' num2str(4*cost_al_lb, '%.2f')
'/lb)']);
    end
else
    title(['Metal Cost (Al=$' num2str(cost_al_lb, '%.2f') '/lb, Cu=$' num2str(2*cost_al_lb, '%.2f') '- '
'/lb)']);
end
...
num2str(4*cost_al_lb, '%.2f') '/lb)'];
end
grid on;
% *****
% Plot cost delta from segmented to bi-media
subplot(2,2,4);
plot(area_segmented_nominal, cost_delta_2, 'r-', ...

```

```

area_segmented_nominal,cost_delta_3,'b-',...
area_segmented_nominal,cost_delta_4,'m-')
if strcmp(medium_in,'AL')
    legend('Cu/Al=2x','Cu/Al=3x','Cu/Al=4x')
end
xlabel(['Nominal Area (mm^2)']);
ylabel('Cost Delta (%)');
xlim([0 3500])
title(['Segmented to Bi-media Cost Delta']);
grid on;
% *****
% *****
% Current Density
% *****
if r_in_J=0 % if there is no optimal point (i.e. single medium)
    r=linspace(1e-99,r_J_plot*0.001,Z_pts);
    J=J0(m_out.*r);
else % if there is an optimal point (i.e. bi-media)

```

```

r2=linspace(r_in_J,r_J_plot*0.001,round(Z_pts*(1-1000*r_in_J/r_J_plot)));
d=- (J1(m_in.*r_in_J).*J0(m_out.*r_in_J)-(m_out/m_in).*J0(m_in.*r_in_J).*J1(m_out.*r_in_J))./...
    (J1(m_in.*r_in_J).*H0(m_out.*r_in_J)-(m_out/m_in).*J0(m_in.*r_in_J).*H1(m_out.*r_in_J));
J_out=J0(m_out.*r2)+d.*H0(m_out.*r2); % current density of outer conductor
r1=linspace(1e-99,r_in_J,Z_pts-round(Z_pts*(1-1000*r_in_J/r_J_plot)));
J_in=J0(m_in.*r1); % current density of inner conductor
J_in=normalize(J_in,max(J_in)./(J_out(1)*(p_out/p_in))); % normalize inner start with outer end
if length(r1)==1 % r and J composed only of outer metal
    J=J_out;
    r=r2;
elseif length(r2)==1 % r and J composed only of inner metal
    J=J_in;
    r=r1;
else % r and J composed of combination of inner and outer metal
    J=[J_in,J_out];
    r=[r1,r2];
end
end
J=normalize(J,max(J)); % normalize current density data

```

```

if strcmp(IsMixed, 'No')
    Z(ID)=VUC(J,r,r_J_plot*0.001/Z_pts,1,ID); % volume under the curve (bi-media)
else
    Z(ID)=VUC(J,r,r_J_plot*0.001/Z_pts,p_out/p_in,ID); % volume under the curve (bi-media)
end
% *****
if strcmp(medium_in, 'Air')
    figure(5);
else
    figure(6);
end
% Plot current density: real part (at specified J radius)
subplot(2,2,1)
plot(1000.*r,real(J), 'r-', [1000.*r_in_J,1000.*r_in_J], [min(real(J)),1], 'b--')
axis([1000*min(r) 1000*max(r) min(real(J)) 1])
legend('Density', 'Transition')
title('Current Density (Real)');
xlabel('Conductor Radius (mm)');
ylabel('Normalized Density');

```

```

grid on;
% Plot current density: all parts (at specified J radius)
subplot(2,2,2)
plot(1000.*r,real(J),'r-',1000.*r,imag(J),'m-',1000.*r,abs(J),'k-',[1000.*r_in_J,1000.*r_in_J],[-
1,1],'b--')
xlim([1000*min(r) 1000*max(r)])
legend('Density (Real)', 'Density (Imag)', 'Density (Abs)', 'Transition')
title('Current Density (All)');
xlabel('Conductor Radius (mm)');
ylabel('Normalized Density');
grid on;
Plot_J='N';
% Plot AC & DC resistance (0 to r_max)
subplot(2,2,3)
plot(1000.*r_in,Rac,'r-',1000.*r_in,Rdc,'b-')
title(['AC & DC Resistance (All ' medium_in ' Core Sizes)']);
xlabel([medium_in ' Inner Radius (mm)']);
ylabel('Resistance (ohm/m)');
xlim([0 r_max])

```

```

if strcmp(medium_in, 'Air')
    ylim([0.9*min(Rdc) 3*min(Rdc)])
end
grid on;
% Plot skin effect of bi-media (0 to r_max)
subplot(2,2,4)
plot(1000.*r_in,Rac./Rdc,'r-')
title(['Skin Effect (All ' medium_in ' Core Sizes)']);
xlabel([medium_in ' Inner Radius (mm)']);
ylabel(['R_a_c / R_d_c']);
grid on;
xlim([0 r_max])
Plot_J='N';

%% *****
% Optimal Design Data For Standardized Area @ T°C & f Hz
% *****
% Display heading of assumptions
disp(sprintf(['-----']))

```

```

disp(sprintf(['----- STANDARDIZED SIZES -----']))
disp(sprintf(['-----']))
disp(sprintf(['The following results are optimal for manufacturing designs']))
disp(sprintf(['of bi-media (' medium_in '/' medium_out ') conductors of standardized']))
disp(sprintf(['cross-sectional areas at ' num2str(T) '°C and ' num2str(f) ' Hz.']))
% Get outer radii, mm
if strcmp(medium_in,'Air') % for Air / CU design
    for i=1:length(area_segmented_true)
        for x=1:Z_pts
            if area_segmented_true(i)<area_out(x)
                % Calculate area, mm2
                area_in_MM(i)=area_in(x-1)+(area_in(x)-area_in(x-1))*...
                    (area_segmented_true(i)-area_out(x-1))/(area_out(x)-area_out(x-1));
                area_out_MM(i)=area_segmented_true(i);
                area_MM(i)=area_in_MM(i)+area_out_MM(i);
                % Calculate radii, mm
                r_in_MM(i)=sqrt((area_in_MM(i))./pi);
                r_out_MM(i)=sqrt(area_MM(i)./pi);
            break

```

```

end
end
% Error catching, no equal area found over 0 to r_max
if x==Z_pts
    r_in_MM(i)=Inf;
    r_out_MM(i)=Inf;
end
end
else % for AL / CU design
% Calculate radii, mm
r_out_MM=sqrt(area_segmented_true./pi);
for i=1:length(area_segmented_true)
    for x=1:Z_pts
        if r_out_MM(i)<1000.*r_in(x) % calculate inner radius with linear interpolation
            r_in_MM(i)=1000.*(r_optimal(x-1)+(r_optimal(x)-r_optimal(x-1))*...
                (r_out_MM(i)./1000-r_in(x-1))/(r_in(x)-r_in(x-1)));
            break
        end
    end
% Error catching, no equal area found over 0 to r_max

```

```

if x==Z_pts
    r_in_MM(i)=Inf;
end
end
% Calculate area, mm2
area_in_MM(i)=pi.*r_in_MM(i).^2;
area_out_MM(i)=pi.*(r_out_MM(i).^2-r_in_MM(i).^2);
area_MM(i)=area_in_MM(i)+area_out_MM(i);
end
end
% Calculate Rdc@20C, ohm/km
Rdc_in_MM=1e9.*p20_in./area_in_MM;
Rdc_out_MM=1e9.*p20_out./area_out_MM;
Rdc_MM=1./(1./Rdc_in_MM+1./Rdc_out_MM);
% Display results
for i=1:length(area_segmented_nominal)
    disp(sprintf(['-----']))
    disp(sprintf(['Results for ' num2str(area_segmented_nominal(i)) ' mm2:']))
    % Check if design is optimal

```

```

if r_in_MM(i)==0 || cost_delta_2(i)>0 || cost_delta_3(i)>0 || cost_delta_4(i)>0
    if r_in_MM(i)==0
        disp(sprintf(['Segmented is optimal (reason: bi-media not optimal)'])
    else
        disp(sprintf(['Segmented is optimal (reason: bi-media more expensive)']))
    end
    % Check if solution exists with outer radius < r_max
elseif r_out_MM(i)==Inf
    disp(sprintf(['Segmented is optimal (reason: outer radius > ' num2str(r_max) ' mm)']))
    % Display optimal design data
else
    disp(sprintf(['\t\t\tUnits\t\t' medium_in '\t\t\t' medium_out '\t\t\t' medium_in '/'
        medium_out]))
    % Areas, mm2
    if area_in_MM(i)<1000 % formatting for tabs
        if area_out_MM(i)<1000 % formatting for tabs
            if area_in_MM(i)<10 % formatting for tabs
                disp([sprintf('Area\t\tmm2\t\t\t%.1f', area_in_MM(i))...
                    sprintf('\t\t\t%.1f', area_out_MM(i)) sprintf('\t\t\t%.4g', area_MM(i))])
            end
        end
    end
end

```

```

else
    disp([sprintf('Area\t\tmm2\t\t%.1f', area_in_MM(i))...
          sprintf('\t\t%.1f', area_out_MM(i)) sprintf('\t\t%.4g', area_MM(i))])
    end
else
    disp([sprintf('Area\t\tmm2\t\t%.1f', area_in_MM(i))...
          sprintf('\t\t%.4g', area_out_MM(i)) sprintf('\t\t%.4g', area_MM(i))])
    end
end
else
    disp([sprintf('Area\t\tmm2\t\t%.0f', area_in_MM(i))...
          sprintf('\t\t%.4g', area_out_MM(i)) sprintf('\t\t%.4g', area_MM(i))])
    end
end
end
% Radii, mm
disp([sprintf('Radius\t\tmm\t\t%.2f', r_in_MM(i))...
      sprintf('\t\t%.2f', r_out_MM(i)) sprintf('\t\t%.2f', r_out_MM(i))])
% DC Resistance @ 20C, ohm/m
if strcmp(medium_in, 'Air')
    disp([sprintf('Rdc@20C\t\ttohm/km\t\tInf', Rdc_in_MM(i))...
          sprintf('\t\t%.4f', Rdc_out_MM(i)) sprintf('\t\t%.4f', Rdc_MM(i))])

```

```

else
    disp([sprintf('Rdc@20C\t\tohm/km\t\t%.4f',Rdc_in_MM(i))...
        sprintf('\t\t%.4f',Rdc_out_MM(i)) sprintf('\t\t%.4f',Rdc_MM(i))])
    end
end
end

% *****
% Optimal Design Data For Equal Segmented Rac @ T°C & f Hz
% *****
% Display heading of assumptions
disp(sprintf(['----- SEGMENTED REPLACEMENT -----']))
disp(sprintf(['----- SEGMENTED REPLACEMENT -----']))
disp(sprintf(['----- SEGMENTED REPLACEMENT -----']))
disp(sprintf(['The following results are optimal for replacing segmented']))
disp(sprintf(['with bi-media (' medium_in '/' medium_out ') conductors based on equal Rac']))
disp(sprintf(['at ' num2str(T) '°C and ' num2str(f) ' Hz.']))
for i=1:length(area_segmented_nominal)

```

```

% Get area (mm2) and radii (mm)
area_in_MM(i)=area_in_mixed(i);
area_out_MM(i)=area_out_mixed(i);
area_MM(i)=area_in_MM(i)+area_out_MM(i);
r_in_MM(i)=sqrt(area_in_MM(i)/pi);
r_out_MM(i)=sqrt(area_MM(i)/pi);
% Get inner and outer medium DC resistances, ohm/km
if strcmp(medium_in,'Air')
    Rdc_in_MM(i)=Inf;
else
    Rdc_in_MM(i)=1e9*p20_in./(pi.*r_in_MM(i).^2);
end
Rdc_out_MM(i)=1e9*p20_out./(pi.*(r_out_MM(i).^2-r_in_MM(i).^2));
Rdc_MM(i)=1./(1./Rdc_in_MM(i)+1./Rdc_out_MM(i));
disp(sprintf(['-----']))
disp(sprintf(['Results for ' num2str(area_segmented_nominal(i)) ' mm2:']))
% Check if design is optimal
if area_in_mixed(i)==0 || cost_delta_2(i)>0 || cost_delta_3(i)>0 || cost_delta_4(i)>0
    if area_in_mixed(i)==0

```



```

    sprintf('\t\t%.4g', area_out_MM(i)) sprintf('\t\t%.4g', area_MM(i))]
end
% Radii, mm
disp([sprintf('Radius\t\tmm\t\t%.2f', r_in_MM(i))...
      sprintf('\t\t%.2f', r_out_MM(i)) sprintf('\t\t%.2f', r_out_MM(i))])
% DC Resistance @ 20C, ohm/km
if strcmp(medium_in, 'Air')
    disp([sprintf('Rdc@20C\t\ttohm/km\t\t%.4f', Rdc_in_MM(i))...
          sprintf('\t\t%.4f', Rdc_out_MM(i)) sprintf('\t\t%.4f', Rdc_MM(i))])
else
    disp([sprintf('Rdc@20C\t\ttohm/km\t\t%.4f', Rdc_in_MM(i))...
          sprintf('\t\t%.4f', Rdc_out_MM(i)) sprintf('\t\t%.4f', Rdc_MM(i))])
end
end
end

% *****
% Compare replacement of segmented design
% *****

```

```

% Save results from each run
if strcmp(medium_in, 'Air') % Save Air / CU results
    cost_delta_2_Air=cost_delta_2;
    cost_delta_3_Air=cost_delta_3;
    cost_delta_4_Air=cost_delta_4;
    area_MM_Air=area_MM;
    area_in_MM_Air=area_in_MM;
    area_out_MM_Air=area_out_MM;
    r_in_MM_Air=r_in_MM;
    r_out_MM_Air=r_out_MM;
    Rdc_in_MM_Air=Rdc_in_MM;
    Rdc_out_MM_Air=Rdc_out_MM;
    Rdc_MM_Air=Rdc_MM;
else % Save AL / CU results
    cost_delta_2_AL=cost_delta_2;
    cost_delta_3_AL=cost_delta_3;
    cost_delta_4_AL=cost_delta_4;
    area_MM_AL=area_MM;
    area_in_MM_AL=area_in_MM;

```

```

area_out_MM_AL=area_out_MM;
r_in_MM_AL=r_in_MM;
r_out_MM_AL=r_out_MM;
Rdc_in_MM_AL=Rdc_in_MM;
Rdc_out_MM_AL=Rdc_out_MM;
Rdc_MM_AL=Rdc_MM;

end

end

% Get optimal design for each standard area
cost_delta_average_Air=(cost_delta_2_Air+cost_delta_3_Air+cost_delta_4_Air)/3;
cost_delta_average_AL=(cost_delta_2_AL+cost_delta_3_AL+cost_delta_4_AL)/3;
for i=1:length(area_segmented_nominal)
    % Check if bi-medias is not optimal
    if r_in_MM_Air(i)==0 && r_in_MM_AL(i)==0
        Rac_optimal_type{i}='Segment CU';
        Rac_optimal_note{i}='Mixed designs not optimal';
    % Check if cost is not optimal

```

```

elseif cost_delta_average_Air(i)>0 && cost_delta_average_AL(i)>0
    Rac_optimal_type{i}='Segment CU';
    Rac_optimal_note{i}='Mixed designs more costly';
elseif cost_delta_average_Air(i)>0
    Rac_optimal_type{i}='AL / CU';
    Rac_optimal_note{i}=['Cost Reduction: ' sprintf('%.1f', -cost_delta_average_AL(i)) '%'];
elseif cost_delta_average_AL(i)>0
    Rac_optimal_type{i}='Air / CU';
    Rac_optimal_note{i}=['Cost Reduction: ' sprintf('%.1f', -cost_delta_average_Air(i)) '%'];
% Check if Air or AL is optimal
elseif cost_delta_average_Air(i)>cost_delta_average_AL(i)
    Rac_optimal_type{i}='AL / CU';
    Rac_optimal_note{i}=['Cost Reduction: ' sprintf('%.1f', -cost_delta_average_AL(i)) '%'];
elseif cost_delta_average_Air(i)<=cost_delta_average_AL(i)
    Rac_optimal_type{i}='Air / CU';
    Rac_optimal_note{i}=['Cost Reduction: ' sprintf('%.1f', -cost_delta_average_Air(i)) '%'];
% Catch errors
else
    Rac_optimal_type{i}='ERR';

```

```

    Rac_optimal_note{i}=['Warning - An error occurred'];
end
end
% Display results of optimal Segmented CU, Air / CU, or AL / CU
disp(sprintf(['-----']))
disp(sprintf(['----- SEGMENTED REPLACEMENT SUMMARY -----']))
disp(sprintf(['-----']))
disp(sprintf(['The following results summarize the optimal deisgn in']))
disp(sprintf(['replacing segmented conductors with either an Air or ']))
disp(sprintf(['AL core, based on equal Rac at ' num2str(T) '°C and ' num2str(f) ' Hz.']))
disp(sprintf(['-----']))
disp(sprintf(['Area(mm2)\tType\t\tComment']))
for i=1:length(area_segmented_nominal)
    if area_segmented_nominal(i)<1000
        if strcmp(Rac_optimal_type{i}, 'AL / CU')
            disp([sprintf('%f', area_segmented_nominal(i)) sprintf('\t\t\t')...
                Rac_optimal_type{i} sprintf('\t\t\t') Rac_optimal_note{i}])
        else
            disp([sprintf('%f', area_segmented_nominal(i)) sprintf('\t\t\t')...

```

```

Rac_optimal_type{i} sprintf('\t\t') Rac_optimal_note{i}}

end

else

if strcmp(Rac_optimal_type{i}, 'AL / CU')

disp([num2str(area_segmented_nominal(i)) sprintf('\t\t')...

Rac_optimal_type{i} sprintf('\t\t') Rac_optimal_note{i}])

else

disp([num2str(area_segmented_nominal(i)) sprintf('\t\t')...

Rac_optimal_type{i} sprintf('\t\t') Rac_optimal_note{i}])

end

end

end

disp(sprintf(['-----']))

disp(sprintf(['Note: cost reduction of AL / CU is the average of two,']))

disp(sprintf(['three, and four times $Cu/$AL cost ratio']))

```